

DOCTORAL THESIS

Loading patterns in the intact limb of individuals with unilateral transtibial amputations and underpinning lower-limb joint mechanics

Moudy, Sarah

Award date:
2019

Awarding institution:
University of Roehampton

General rights

Copyright and moral rights for the publications made accessible in the public portal are retained by the authors and/or other copyright owners and it is a condition of accessing publications that users recognise and abide by the legal requirements associated with these rights.

- Users may download and print one copy of any publication from the public portal for the purpose of private study or research.
- You may not further distribute the material or use it for any profit-making activity or commercial gain
- You may freely distribute the URL identifying the publication in the public portal ?

Take down policy

If you believe that this document breaches copyright please contact us providing details, and we will remove access to the work immediately and investigate your claim.

**Loading patterns in the intact limb of individuals with
unilateral transtibial amputations and underpinning
lower-limb joint mechanics**

by

Sarah Catherine Moudy

A thesis submitted in partial fulfilment of the requirements for the
degree of PhD

Department of Life Sciences

University of Roehampton

April 2019

Abstract

Individuals with unilateral transtibial amputations (ITTAs) are at a greater risk of developing knee joint degenerative diseases in the intact limb compared to the general population. However, equivocal results from walking gait literature have found limited differences in load between the intact limb of ITTAs and control limbs. This thesis postulated that 1) data extraction of discrete points in loading signals are inconsistent; 2) other loading features, not previously considered, may more appropriately quantify load; and 3) overloading may be more prominent in tasks which have greater loading and joint movement demands. Therefore, this thesis aimed to determine if the intact limb of ITTAs had significantly different limb and knee joint loading patterns and underpinning mechanics compared to able-bodied controls during high loading activities. Eight ITTAs and twenty-two controls performed step descent and unilateral and bilateral drop landing tasks as experimental models to increase load. Loading waveforms were assessed using statistical parametric mapping as an alternative to discrete point analysis. Waveform analysis was able to identify loading rates (rather than peak magnitudes) as important measures of load and identify additional phases of interest when loading the limb. Anterior-posterior loading was also found to be an important feature in addition to the commonly examined loading features. The intact limb of ITTAs in this thesis was able to adapt to higher loading activities by adopting joint mechanics similar to controls despite reductions in quadriceps strength. Therefore, few differences were found in the whole-limb and knee joint loading patterns. This would suggest that high load in the intact limb compared to a control limb may not suggest an increased risk of knee joint degeneration but rather the asymmetry between prosthetic and intact limbs. Additionally, it is just as plausible to suggest that high limb loading is not the mechanism of injury in ITTAs.

Table of Contents

ABSTRACT	i
TABLE OF CONTENTS	ii
ACKNOWLEDGEMENTS	vii
DISSEMINATION OF RESEARCH	viii
LIST OF FIGURES	x
LIST OF TABLES	xix
CHAPTER 1. INTRODUCTION	1
CHAPTER 2. LITERATURE REVIEW & WAVEFORM ANALYSIS METHODOLOGY	5
PART ONE: LITERATURE REVIEW	
2.1. Loading Features	6
2.2. Compensatory Movement Strategies.....	11
2.2.1. Dynamic Walking Theory	12
2.2.2. ITTA Walking Gait.....	15
2.2.2.1. Temporal-Spatial Features	15
2.2.2.2. Kinematic and Kinetic Features	16
2.3. Joint Coordination	18
2.4. Step Descent.....	20
2.5. Drop Landing.....	25
PART TWO: WAVEFORM ANALYSIS METHODOLOGY	
2.6. Discrete versus Continuous Analysis.....	31
2.7. Statistical Parametric Mapping	32
2.8. Issues with Waveform Analysis	33
2.9. Landmark Registration	34
2.10. Other Approaches to Waveform Analysis	36
2.11. Summary and Thesis Aims.....	38
CHAPTER 3. METHODS.....	41
3.1. Ethical Approval and Participant Recruitment.....	41

3.2. Participant Populations.....	42
3.3. Equipment.....	44
3.3.1. Step Platform.....	44
3.3.2. Drop Landing Frame.....	46
3.3.3. Hardware.....	47
3.3.3.1. Vicon Motion Systems.....	47
3.3.3.2. Kistler Force Platforms.....	49
3.4. Data Collection Protocol.....	50
3.4.1. System Calibration.....	51
3.4.2. Anthropometric Measures.....	51
3.4.3. Marker Placement and Participant Calibration.....	52
3.4.3.1. Validation Test.....	54
3.4.4. Step Descent.....	55
3.4.5. Drop Landing.....	56
3.5. Data Processing.....	56
3.6. Data Analysis.....	58
3.6.1. Loading Features Extracted.....	58
3.6.2. Statistical Parametric Mapping Methods.....	59
3.6.3. Loading Waveform Pilot Studies.....	60
3.6.3.1. Pilot Study 1: Landmark Registration.....	60
3.6.3.2. Pilot Study 2: Level-Walking Gait Analysis.....	61
3.6.4. Movement Features Extracted.....	64
3.6.4.1. Calculation of Coupling Angles.....	65
CHAPTER 4. MECHANICS OF A STEP DESCENT IN ABLE-BODIED INDIVIDUALS.....	72
4.1. Introduction.....	72
4.2. Methods.....	75
4.2.1. Features Extracted.....	76
4.2.2. Statistical Analysis.....	79
4.3. Results.....	80
4.3.1. Loading Differences.....	80
4.3.2. Movement Differences.....	83
4.3.2.1. Leading Limb Features.....	84
4.3.2.2. Trailing Limb Features – Phase 1.....	87
4.3.2.3. Trailing Limb Features – Phase 2.....	89
4.4. Discussion.....	90

4.5. Conclusion	96
4.6. Further Work	96
CHAPTER 5. MECHANICS OF A STEP DESCENT IN AMPUTEES	97
5.1. Introduction	97
5.2. Methods	101
5.2.1. Statistical Analysis	101
5.3. Results	102
5.3.1. Loading Differences	102
5.3.2. Movement Differences	103
5.3.2.1. Leading Limb Features	105
5.3.2.2. Trailing Limb Features – Phase 1	107
5.3.2.3. Trailing Limb Features – Phase 2	108
5.4. Discussion.....	110
5.5. Conclusion	115
5.6. Further Work	116
CHAPTER 6. LOWER-LIMB MOVEMENT ASSOCIATED WITH HIGH LEAD LIMB LOADING DURING A STEP DESCENT	117
6.1. Introduction	117
6.2. Methods	120
6.2.1. Statistical Analyses	123
6.3. Results	123
6.4. Discussion.....	129
6.5. Conclusion	133
6.6. Further Work	134
CHAPTER 7. MECHANICS OF UNILATERAL DROP LANDINGS IN THE INTACT LIMB OF AMPUTEES.....	135
7.1. Introduction	135
7.2. Methods	139
7.2.1 . Strength Data Collection	139
7.2.1.1. Equipment	139
7.2.1.2. Protocol	140
7.2.2. Biomechanical Features Extracted.....	141
7.2.3. Statistical Analysis	142

7.3. Results	142
7.3.1. Strength Differences	143
7.3.2. Loading Differences	143
7.3.3. Movement Differences	144
7.3.4. Waveform Variability Sub-Analysis	146
7.3.4.1. vGRF	146
7.3.4.2. KAM	152
7.3.4.3. Stepwise Regression	153
7.4. Discussion	155
7.5. Conclusion	160
7.6. Further Work	160
CHAPTER 8. MECHANICS OF BILATERAL DROP LANDINGS IN THE INTACT LIMB OF AMPUTEES	162
8.1. Introduction	162
8.2. Methods	165
8.2.1. Statistical Analysis	166
8.3. Results	166
8.3.1. Loading Differences	166
8.3.2. Movement Differences	167
8.3.3. Variability Sub-Analysis	170
8.4. Discussion	176
8.5. Conclusion	178
8.6. Further Work	178
CHAPTER 9. CONCLUSION	179
9.1. Waveform Analysis	180
9.2. Intact Limb Loading	181
9.3. Joint Mechanics	183
9.4. Application for ITTAs	185
9.5. Limitations	186
9.6. Further Work	187

Appendix A. Participant Documentation.....	189
Appendix B. Pilot Study Results.....	204
Appendix C. Chapter 4 & 5 Landmark Registration Results	212
Appendix D. Lower-Limb Joint Angle and Power Waveforms	219
Appendix E. Discussion on Feature Selection for Chapter 6	224
Appendix F. Chapter 7 Additional Information.....	227
References	231

Acknowledgements

I would like to extend my sincere gratitude to my supervisors, Dr Siobhán Strike and Dr Neale Tillin, for their guidance and support, and for providing opportunities to enhance myself as a researcher throughout this process. In particular, I would like to thank Siobhán for her *incredible* patience, guidance, and interest in my work over the last three and a half years without which this thesis could not have been completed.

I would also like to extend a massive thank you to Amy Sibley. You kept me sane, provided laughter during those long days in the lab, and helped me greatly with the learning curve that is academic writing.

To Alison Carlisle, for her technical support and cheery disposition throughout the data collection process.

To all my colleagues and friends within the sport and exercise science department who provided support along the way.

To all the participants who gave up their time and effort to volunteer for this research.

And last, but not least, a massive thank you to my friends and family for their love and support every day. For those who *insisted* on the inclusion of their names, thank you Dad, Mom, Michelle, Mark, and Brendan. Without you all, I would not be where I am today.

Dissemination of Research

Publications

Moudy, S., Tillin, N.A., Sibley, A.R., Strike, S. 2019. Mechanisms to attenuate load in the intact limb of transtibial amputees when performing a unilateral drop landing. *Under Review with the Journal of Applied Biomechanics.*

Moudy, S., Richter, C., Strike, S. 2018. Landmark registering waveform data improves the ability to predict performance measures. *Journal of Biomechanics.* 78 pp.109-117.

Conference Proceedings

Oral Presentations

Moudy, S., Tillin, N.A., Sibley, A.R., Strike, S. (2018) *Limb loading is associated with underlying movement patterns during a step descent in transtibial amputees.* Presented at: World Congress of Biomechanics, Dublin, Ireland.

Moudy, S., Tillin, N.A., Sibley, A.R., Strike, S. (2018) *Movement pattern and loading differences between bilateral and unilateral drop landings in transtibial amputees.* Presented at: European Congress of Sport Science, Dublin, Ireland.

Poster Presentations

Moudy, S., Tillin, N.A., Sibley, A.R., Strike, S. (2018) *Limb loading differences of the leading limb during a step descent in transtibial amputees.* Presented at: World Congress of Biomechanics, Dublin, Ireland.

Moudy, S., Tillin, N.A., Sibley, A.R., Strike, S. (2017) *Lower-limb joint coupling during step descent in transtibial amputees*. Presented at: International Society of Prosthetics and Orthotics Annual Scientific Meeting, Cambridge University.

Other Oral Presentations

Moudy, S., Tillin, N.A., Sibley, A.R., Strike, S. (2018) *The mechanics of lower-limb motion in transtibial amputees and its association with intact limb loading*. Presented at: Southern Methodist University, Dallas, TX.

Moudy, S., Tillin, N.A., Sibley, A.R., Strike, S. (2018) *Landmark registration: application and clinical relevance*. Presented at: Sport Surgery Clinic, Dublin, Ireland.

Moudy, S., Tillin, N.A., Sibley, A.R., Strike, S. (2017) *Lower-limb loading in unilateral transtibial amputees and its relationship to movement patterns in various daily and exercise activities*. Presented at: Sport and Exercise Science Research Centre, University of Roehampton.

List of Figures

Figure 2.1. Definition of lead and trail limbs during a step descent with force platform placements noted	20
Figure 2.2. A) Time-normalised vGRF curves for the take-off phase of countermovement jumps for two subjects. The end of the eccentric phase is denoted by a red dot with solid vertical lines. B) The time-domain for each subject representing the time taken to complete the take-off phase.....	34
Figure 2.3. An illustration of three registration approaches performed on the time-domain of the take-off phase in a countermovement jump. These approaches include piecewise linear (red), piecewise spline (blue), and piecewise velocity (green) (Moudy et al., 2018, pg. 111).....	36
Figure 3.1. Dimensions of the step platform as seen from a A) side-view and B) top-view. Force platform (FP) positions relative to the end of the step platform are also depicted. The platform situated above FP1 was an independent structure from the rest of the platform.....	45
Figure 3.2. Drop landing frame with dimensions and safety features depicted	47
Figure 3.3. Origin of the global coordinate system as set by the Vicon Active Wand where positive values in each plane of motion are denoted by the direction of the red arrows.....	48
Figure 3.4. Marker placement as outlined by Davis et al. (1991) depicted by red dots and the extra SARA and SCoRE depicted by yellow dots.	53

Figure 3.5. A) vGRF and B) KAM loading waveforms for the intact limb of ITTAs (dashed line) and control limbs (solid line) during the absorption phase of habitual level-walking gait. †highlighted area represents the phase that became significant after covarying for speed with p-value noted..... 63

Figure 3.6. Loading waveforms for the intact limb of ITTAs (dashed line) and control limbs (solid line) during the absorption phase of habitual level-walking gait. †highlighted area represents the phase that became significant after covarying for speed with p-value noted..... 64

Figure 3.7. An example of an angle-angle plot for sagittal plane ankle and knee joint motion performed during a step descent for the absorption phase. Initial contact is denoted by the black circle. The coupling angle is represented by θ 65

Figure 3.8. Coupling angle calculated from ankle-knee angle-angle plot for a single participant performing an initial heel contact during step descent throughout the absorption phase. 67

Figure 3.9. Lower-limb joint pair coupling angle waveforms for the duration of the braking phase in the leading limb for the heel initial contact (black), toe initial contact (red), and intact limb of ITTAs (blue) groups. The vertical dashed line denotes the end of the double support phase. Three trials for each participant is presented..... 68

Figure 3.10. Trailing limb lower-limb joint pair coupling angle waveforms for the heel initial contact (black), toe initial contact (red), and intact limb of ITTAs (blue) groups. The vertical dashed line denotes the end of the single limb support phase. Three trials for each participant is presented. 69

Figure 3.11. Unilateral drop landing joint pair coupling angle waveforms for the intact

limb (IL) of ITTAs (blue) and dominant control limbs (DCL; black). The black vertical dashed line denotes the average time point at which peak vGRF occurred. All trials are presented for each participant. 70

Figure 3.12. Bilateral drop landing joint pair coupling angle waveforms for the intact limb (IL) of ITTAs (blue) and dominant control limbs (DCL; black). The black vertical dashed line denotes the average time point at which peak vGRF occurred. All trials are presented for each participant. 71

Figure 4.1. A) Depiction of the performance of a step descent with force platform placements noted and B) definition of step descent sub-phases for the leading limb (LL; dashed lines) and trailing limb (TL; solid lines) based on the vGRF and anterior-posterior GRF. 77

Figure 4.2. Leading limb A-C) GRF, D-F) knee moment, and G-I) intersegmental knee force waveforms for the initial heel contact group (HC; black solid line) and the initial toe contact group (TC; blue dashed line). The phases of significant difference are highlighted in grey with p-values noted. †Red highlighted areas represent phases that became significant or trended towards significance after covarying for speed. The black vertical dashed line represents the average time point at which the end of the double support phase occurred across all participant trials. 82

Figure 4.3. Leading limb (LL) and trailing limb (TL) A) individual joint features and B) coupling angles for all lower-limb joint pairs in the initial heel contact (HC; black) and initial toe contact (TC; grey) groups. *p < 0.05, **p < 0.001 between groups, †p < 0.05 remained significant after covarying for speed. IC = initial contact, TO = toe-off, ROM = range of motion, A-K = ankle-knee, K-H = knee-hip, H-A = hip-ankle..... 85

Figure 4.4. Lower-limb joint peak absorption and generation powers in the leading

limb (LL) and trailing limb (TL) during their respective phases of interest in the initial heel contact (HC; black) and initial toe contact (TC; grey) groups. *p < 0.05, **p < 0.001 between groups, †p < 0.05 differences that remained significant after covarying for speed. 86

Figure 4.5. A) Absolute joint work completed and B) percentage of total negative joint work contribution at the ankle (bottom), knee (middle), and hip (top) for the leading limb (LL) and trailing limb (TL) phases for the heel initial contact (HC) and toe initial contact (TC) groups. 88

Figure 5.1. The GRF (A,B,C), knee moment (D,E,F), and intersegmental knee force (G,H,I) loading waveforms' in the intact limb of ITTAs (red dashed line) and leading limb of the initial toe contact group (TC; black solid line) for the duration of the braking phase. The phase of significant difference is highlighted in grey whereas †red highlighted areas represent phases that became significant after covarying for speed. The black vertical dashed line represents the average time point at which the end of the double support phase occurred across all participant trials. 103

Figure 5.2. Leading limb and trailing limb A) joint angle features, and B) coupling angles for all lower-limb joint pairs. *p < 0.05, **p < 0.001 significant differences between groups, †p < 0.05 significantly different after covarying for speed. IC = initial contact, ROM = range of motion, TO = toe-off, A-K = ankle-knee, K-H = knee-hip, H-A = hip-ankle..... 106

Figure 5.3. Joint peak powers in the leading limb (LL) and trailing limb (TL) phase 1 and phase 2 for the ITTA (grey) and TC (black) groups. *p < 0.05, **p < 0.001 significant differences between groups, †p < 0.05 significantly different after covarying for speed 108

Figure 5.4. A) Absolute joint work completed and B) percentage joint contribution relative to the total joint work completed in the ankle (bottom), knee (middle), hip (top) joints during the leading limb (LL) and trailing limb (TL) phases of interest for the ITTA and toe initial contact (TC) groups. 109

Figure 6.1. Bivariate relationships of stepping speed with vGRF and KAM loading rates and average sustained midstance magnitudes, and KFx impact peak. Experimental groups are denoted as follows: heel initial contact control (HC, circle), toe initial contact control (TC, asterisk), and intact limb of ITTAs (square). 125

Figure 7.1. Each row presents the 3-dimensional loading waveforms for the A) GRFs, B) knee moments, and C) intersegmental knee forces (KF) in the intact limb (IL; red dashed) and dominant-control limb (DCL; black solid). Loading waveforms are presented for the duration of the absorption phase. 144

Figure 7.2. A) Joint angular position at touchdown (TD) and joint range of motion (ROM) in the sagittal and frontal plane, B) joint coordination coupling angle for the ankle-knee (AK), knee-hip (KH) and hip-ankle (HA), and C) peak joint absorption powers when landing at the ankle, knee, and hip joints in the intact limb (IL) and dominant control limb (DCL). 145

Figure 7.3. A) Individual joint work and B) joint percentage contribution of the total negative joint work performed in the ankle, knee, and hip joints for the intact limb (IL) and dominant control limb (DCL) during the absorption phase of landing 146

Figure 7.4. vGRF waveforms for participants with a longer time to peak magnitude (dashed line) and shorter time to peak magnitude (solid line) based on splitting the dataset by the time to peak vGRF as a percentage of the absorption phase. ITTA and control participants are present in both groups. 148

Figure 7.5. Early (grey) and late (black) groups A) Joint angular positions at touchdown (TD) and joint range of motion (ROM) in the sagittal and frontal plane, B) joint coordination coupling angle for the ankle-knee (AK), knee-hip (KH) and hip-ankle (HA), and C) peak joint absorption powers when landing at the ankle, knee, and hip joints. 150

Figure 7.6. Early and late group A) Individual joint work and B) joint percentage contribution of the total negative joint work performed in the ankle, knee, and hip joints during the absorption phase 154

Figure 7.7. KAM waveforms (mean and SD cloud) for participants with a longer time to peak magnitude (dashed line) and shorter time to peak magnitude (solid line) based on splitting the dataset by the A) time to peak vGRF and B) time to peak KAM as a percentage of the absorption phase. ITTA and control participants are present in both groups. 156

Figure 8.1. Each row presents the 3-dimensional loading waveforms for the A) GRFs, B) knee moments (KM), and C) intersegmental knee forces (KF) in the intact limb (IL; red dashed line) and dominant-control limb (DCL; black solid line). Loading waveforms are presented for the duration of the absorption phase. The highlighted red area represents the phase of significant difference between the IL and DCL with the p-value noted based on the SPM {t}-statistic results. 167

Figure 8.2. A) Joint angular position at touchdown (TD) and joint range of motion (ROM) in the sagittal and frontal plane, B) joint coordination coupling angle for the ankle-knee (AK), knee-hip (KH) and hip-ankle (HA) joint pairs, and C) peak joint absorption powers when landing at the ankle, knee, and hip joints in the intact limb (IL) and dominant control limb (DCL). *p < 0.05 between groups..... 169

Figure 8.3. A) The individual joint work completed and B) the percentage contribution of each joint relative to the total negative joint work performed in the ankle, knee, and hip joints for the intact limb (IL) and dominant control limb (DCL) during the absorption phase of landing 170

Figure 8.4. vGRF waveforms (mean and SD cloud) for the intact limb of ITTA participants with a higher peak magnitude (solid line) and lower peak magnitude (dashed line)..... 171

Figure 8.5. Individual mean trials for the A) high and B) low peak vGRF ITTA groups to illustrate variability in the vGRF waveform from ~20-30% of the absorption phase. Vertical black dashed lines indicate the average time at which peak vGRF occurred. The two dot-dashed lines in the low peak vGRF sub-group indicates the early peak participants. 173

Figure 8.6. A) Control low_c (dashed line) and high_c (solid line) sub-groups mean and standard deviation clouds. Individual trials for B) high_c and C) low_c sub-group and participants with the earlier time to peak vGRF represented by a dashed line. 174

Figure B2.1. A) Configuration of the rigid frame, showing rod and marker positions. B) Base plate dimensions from rod centre to rod centre. Neither diagram to scale. 207

Figure B3.1. Dynamic walking gait force and knee moment waveforms for full-platform and cross-platform strikes 209

Figure C1.1. GRF landmark registered magnitude-domain (top row), time-domain (middle row), and warping function (bottom row) with significant differences highlighted in grey between heel initial contact (HC: black) and toe initial contact (TC:

blue) descent strategies. The vertical dashed line represents the end of the double support phase..... 213

Figure C1.2. The knee intersegmental forces (KF) landmark registered magnitude-domain (top row), time-domain (middle row), and warping function (bottom row) with significant differences highlighted in grey between heel initial contact (black) and toe initial contact (blue) descent strategies. The vertical dashed line represents the end of the double support phase. 214

Figure C1.3. Knee moment landmark registered magnitude-domain (top row), time-domain (middle row), and warping function (bottom row) with significant differences highlighted in grey between heel initial contact (black) and toe initial contact (blue) descent strategies. The vertical dashed line represents the end of the double support phase..... 215

Figure C2.1. GRF landmark registered magnitude-domain (top row), time-domain (middle row), and warping function (bottom row) with significant differences highlighted in grey between the intact limb of TTAs (red) and toe initial contact (TC: black) control limb. The vertical dashed line represents the end of the double support phase..... 216

Figure C2.2. The knee intersegmental forces (KF) landmark registered magnitude-domain (top row), time-domain (middle row), and warping function (bottom row) for the intact limb of TTAs (red) and toe initial contact (black) control limb. The vertical dashed line represents the end of the double support phase. 217

Figure C2.3. Knee moment landmark registered magnitude-domain (top row), time-domain (middle row), and warping function (bottom row) for the intact limb of ITTAs

(red) and toe initial contact (black) control limb. The vertical dashed line represents the end of the double support phase..... 218

Figure D1.1. Leading limb sagittal plane joint angle and power waveforms for the ankle, knee, and hip during a step descent for the heel initial contact (HC) controls (black), toe initial contact (TC) controls (blue), and intact limb of ITTAs (red). Calculation of joint range of motion (ROM) and *peak powers are denoted on their respective figures..... 220

Figure D1.2. Trailing limb sagittal plane joint angle and power waveforms for the ankle, knee, and hip during a step descent for the heel initial contact (HC) controls (black), toe initial contact (TC) controls (blue), and prosthetic limb (PL) of ITTAs (red). Calculation of joint range of motion (ROM) and *peak powers are denoted on their respective figures. The vertical black dashed line represents initial contact of the leading limb. 221

Figure D2.1. Unilateral drop landing sagittal plane joint angle and power waveforms for the ankle, knee, and hip when landing on the intact limb (IL) of ITTAs (red) and dominant control limb (DCL; black). 222

Figure D2.2. Bilateral drop landing sagittal plane joint angle and power waveforms for the ankle, knee, and hip when landing on the intact limb (IL) of ITTAs (red) and dominant control limb (DCL; black). 223

Figure F1.1. Depiction of the middle group (blue) relative to the early (solid black) and late (dashed black) groups..... 229

Figure F1.2. Representative trials for participants in the early and late groups in their original temporal format. The figure depicts the shorter duration of the absorption phase with a longer time to peak vGRF. 229

List of Tables

Table 2.1. First peak knee external adduction moment (KAM) and vertical ground reaction force (vGRF) and the vGRF and KAM loading rates (mean \pm SD) for the intact limb of ITTAs and control limb.	8
Table 2.2. Temporal-spatial characteristics for the intact and prosthetic limbs of unilateral transtibial amputees and between-limb averages for able-bodied controls	16
Table 3.1. Amputee and matched able-bodied control participant characteristics and amputee prosthetic components	42
Table 3.2. Discrete loading features (mean \pm SD) during habitual level-walking gait for the intact limb of ITTAs and control limbs	62
Table 4.1. Participant demographics and stepping speed presented as the mean \pm SD for the initial heel contact (HC) and initial toe contact (TC) groups	80
Table 4.2. Whole-body features (mean \pm SD) presented for the heel initial contact (HC) and toe initial contact (TC) groups	83
Table 5.1. Participant demographics and stepping speed (mean \pm SD) for the ITTA and initial toe contact (TC) groups	102
Table 5.2. Mean \pm SD of the whole-body features for the ITTA and initial toe contact (TC) control groups	104
Table 6.1. Cohort demographics and discrete loading features (mean \pm SD)	124

Table 6.2. Pearson's product-moment bivariate correlations (<i>r</i> -values) for discrete vGRF (<i>n</i> = 30), KAM (<i>n</i> = 29), and KFx (<i>n</i> = 30) loading features with temporal-spatial, leading limb (LL) and trailing limb (TL) movement features.....	126
Table 6.3. Multiple linear regression of discrete vGRF and KAM loading features with all movement features forced into the regression model. The values denoted are the β -coefficient values (standard error).	127
Table 7.1. Participant demographics and whole-body features (mean \pm SD) for the intact limb of ITTAs and dominant control limbs.....	143
Table 7.2. Maximal voluntary isometric torque (MVT) and peak rate of torque development (RTD) mean \pm SD for the intact limb of ITTAs and dominant control limb	143
Table 7.3. Early and late group temporal features and group composition characteristics.....	149
Table 7.4. Stepwise linear regression in the order added into the model. Values are denoted are the β -coefficient (standard error) with their respective adjusted R^2 contribution to the total adjusted R^2	155
Table 8.1. Whole-body features (mean \pm SD) for the ITTA and control groups....	168
Table B1.1. Static variability and accuracy measures for the standard force platform position output (FP1) and with the addition of the step platform output (step) for three different masses	205
Table B1.2. Bland-Altman 95% limits of agreement (LOA) between the standard force platform output and the step platform force output for three different masses.....	206

Table B1.3. Mean (SD) and p -values presented for discrete dynamic walking features for both force platform conditions	206
Table B2.1. Static frame variability between trials	207
Table B3.1. Static vertical ground reaction force (N) reliability and accuracy of both full-plate and cross-plate strikes for three different known masses.	208
Table B4.1. Within-day repeatability of marker placement for two participants	211
Table E1.1. Variance inflation factors (VIF) and absolute r -values for the movement features included in the step descent regression model.....	224
Table F1.1. Individual participant time to peak vGRF difference from the mean across all participants as a percentage of the absorption phase and in seconds	228
Table F2.1. Variance inflation factors (VIF) and Pearson's correlation coefficients between all movement features	229

Chapter 1.

Introduction

Individuals with unilateral transtibial amputations (ITTAs) have undergone the surgical removal of the lower leg on one side resulting in the loss of the ankle joint and surrounding musculature (Neptune et al., 2001, Silverman et al., 2008). ITTAs perform altered movement patterns compared to able-bodied individuals due to the decreased capacity of the prosthetic limb to mimic the functionality of the intact ankle joint (Hurley et al., 1990). This possibly results in higher loading experienced in the intact limb (Gailey et al., 2008). Mechanical loading of a joint is necessary for the maintenance of cellular homeostasis in healthy joint cartilage (Farrokhi et al., 2016); however, excessive loading is thought to place joints at risk of developing loading related diseases, such as osteoarthritis (Griffin & Guilak, 2005, Egloff et al., 2012). As the intact limb of ITTAs is at a 25-28% greater risk of developing knee pain and subsequent degenerative conditions than able-bodied individuals (Struyf et al., 2009, Norvell et al., 2005, Melzer et al., 2001), it would be expected that greater intact limb loading would be present compared to a control limb. However, equivocal results have been found in level-walking gait when comparing the load experienced in an intact ITTA limb to a control limb. For example, peak knee external adduction moment (KAM; a common measure of medial knee joint loading) has been found to be greater in the intact limb of some studies (Royer & Koenig, 2005, Grabowski & D'Andrea, 2013, Lloyd et al., 2010) and lower in other studies (Esposito & Wilken, 2014, Rueda et al., 2013). None of these studies found significant differences between ITTAs and their control cohorts.

Ambiguity related to the presence of overloading in the intact limb of ITTAs may be due to the reduction of loading waveforms to discrete points (e.g., peak magnitude), which are assumed to best represent the waveform. Reducing highly multivariate datasets to discrete points may result in the loss of valuable information (Pataky et al., 2013). An alternative method to discrete point analysis, and one which has been growing in popularity in the field of biomechanics, is waveform analysis. This approach has been demonstrated to provide greater insight into the task mechanisms beyond that which is examined by discrete point analysis (Ramsay & Silverman, 2002, Warmenhoven et al., 2018, Richter et al., 2014b, Godwin et al., 2010). Statistical parametric mapping is a type of waveform analysis used for hypothesis-driven testing to capture phases of covariance between multivariate datasets (Robinson et al., 2015). Statistical parametric mapping of the waveforms which hold the currently established discrete loading features may indicate more appropriate phases of overloading that could indicate an increased risk of developing degenerative diseases in ITTAs. Further, limb and joint loading are most commonly assessed through the vertical ground reaction force and KAM. Recent research has suggested that other loading features, such as the knee external flexor moment and joint intersegmental forces, may contribute to joint degeneration (Creaby, 2015, Silverman & Neptune, 2014, Walter et al., 2010).

Altered movement strategies that are adopted following amputation (Burke et al., 1978, Nolan et al., 2003, Sadeghi et al., 1997) have been thought to influence the loading patterns in the intact limb of ITTAs (Gailey et al., 2008, Radin & Paul, 1971). These alterations are postulated to result in the increased risk of joint degeneration. Thus, ITTAs are an ideal model for understanding the pathogenesis of degenerative diseases. Typically, movement patterns are assessed through individual joint motion in the limb of interest, yet movement is produced through the coordination of joints and limbs. Coordination can represent a measure of the interaction between joints

which may provide in-depth knowledge on the mechanisms underpinning high limb loading (van Emmerik et al., 2016, Chiu & Chou, 2012, Nematollahi et al., 2016). Further, the dynamic walking theory introduces the concept of a between-limb influence (Kuo, 2007). In ITTAs, reduced prosthetic limb push-off work at the ankle joint has been associated with increased peak KAM in the contralateral intact limb (Morgenroth et al., 2011). However, this theory has only been applied to level-walking gait and it is unclear if this exists in other continuous anti-phase tasks such as step descent.

It is also possible that ITTAs do not experience overloading in the intact limb compared to able-bodied controls during walking gait. Tasks other than level-walking, such as step descent, have indicated greater vertical ground reaction forces are experienced and require greater joint motion to complete the task (Christina & Cavanagh, 2002) and, therefore, may require investigation. It is plausible to suggest that overloading, associated with an increased risk of degenerative conditions, may be present when performing higher impact activities. Step descent is an extension of level-walking gait and is a functional task performed daily, yet the development of load and movement strategies utilised in established ITTAs have not been examined. Compensatory joint mechanics that may underpin high load in the intact limb when leading during a step descent could indicate areas of focus for rehabilitation and exercise protocols.

One approach that may improve our understanding of the loading patterns in the intact limb of ITTAs is through the assessment of drop landings. Unilateral drop landings provide a controlled task in which the effects from the altered joint mechanics of the prosthetic limb and requirements for forward progression are absent. Removal of these influences could suggest if inherent deficiencies exist in the intact limb post-amputation. In this high impact activity, deficiencies in muscle strength of the knee extensors may also influence load attenuation. Drop landings are, therefore, a good

model to assess the influence of muscle strength when other influences are controlled. Two key measures of muscle strength are maximal and explosive force production. Decreased maximum muscle strength has been suggested as an indication of increased limb loading (Egloff et al., 2012, Lloyd et al., 2010) and has been associated with alterations in movement patterns in the trunk and lower-limbs that may increase the risk of injury (Blackburn & Padua, 2008, Blackburn & Padua, 2009, Hewett et al., 2005, Markolf et al., 1978). Generation of rapid muscle force (i.e. explosive strength) is important for stabilisation of the lower-limb joints (Tillin et al., 2013, Andersen & Aagaard, 2006, Aagaard et al., 2002) as dynamic actions, such as landing from a jump, involve shorter contraction times (<50 ms) than it typically takes to generate maximal force (~300 ms) (Buckthorpe & Roi, 2017). The inability to develop muscular force rapidly, as required when landing from a jump, can additionally lead to various injuries including joint degeneration and non-specific knee pain (Aerts et al., 2013). Additionally, bilateral landings are present in many sporting activities (e.g. basketball, volleyball) where between-limb influences may impact the magnitude and rate of load experienced in the intact limb further leading to injury. For this reason, ITTAs are commonly encouraged to participate in sitting or wheelchair adapted sports which could limit the cardiovascular benefits of exercise (Chapman, 2008, Sanderson & Martin, 1996). However, there is limited evidence to suggest that ITTAs experience increased forces during landings compared to able-bodied controls.

The purpose of this thesis was, therefore, to 1) provide a greater understanding of the loading patterns experienced in the intact limb of ITTAs during step descent and drop landing tasks by utilising waveform analysis and 2) examine the joint mechanics, including joint coordination, that could influence these loading patterns. Insight into the joint mechanics utilised to attenuate load could provide information to clinicians for development of rehabilitation and exercise protocols.

Chapter 2.

Literature Review & Waveform

Analysis Methodology

Part One: Literature Review

This literature review will discuss the previously researched features of limb and joint loading and the limitations of these features in relation to individuals with transtibial amputations (ITTAs). Forces (load) acting on the body can be mediated by segment motion and muscular contractions. Therefore, a review of the movement mechanics adopted by ITTAs during walking gait will highlight possible compensatory strategies that could be expected in the analysis of a step descent. Finally, the joint mechanics of step descent and drop landing movements will be examined to aid in the interpretation of the results in the experimental chapters.

The articles in this literature review were included based on a systematic search strategy. The following databases were searched: Cochrane Library, PubMed, Science Direct, and Google Scholar. Each database was searched using the following keyword phrases (and synonyms): amputees, osteoarthritis, knee joint, loading, step descent, landing, and quadriceps strength. Able-bodied articles were included to aid in comparisons. Articles were excluded from the final literature review if they were non-English full text. It is possible that the findings from this literature review are subject to publication bias.

2.1. Loading Features

Mechanical loading of a joint is necessary for the maintenance of healthy joint cartilage (Farrokhi et al., 2016); however, too much loading can place joints at risk of developing loading related diseases (Radin & Paul, 1971). Loading is broadly defined as the forces acting on the body or joint where injuries can occur when these forces exceed certain limits on any one element in the kinematic chain. The knee joint, in particular, is at a higher risk of injury as it is subject to greater translation forces in dynamic movement compared to the hip and ankle joints (Egloff et al., 2012). Many studies exploring knee joint loading focus on the medial knee compartment as 60-80% of total knee joint loading is transmitted across the medial side of the knee (Erhart et al., 2010). There is a wide base of research that provides robust, well-evidence loading features to represent medial compartment knee joint loading in both able-bodied (Miyazaki et al., 2002, Egloff et al., 2012) and other injury populations (Øiestad et al., 2009, Levinger et al., 2008). Loading features that have been linked to the onset and progression of medial compartment joint degeneration are the knee external adduction moment (KAM) and vertical ground reaction force (vGRF) (Egloff et al., 2012, Henriksen et al., 2006, Gailey et al., 2008, Morgenroth et al., 2014).

KAM is commonly used to estimate medial knee joint loading as it has been associated with the severity of joint degeneration, rate of progression, and treatment outcomes (Miyazaki et al., 2002, Vanwanseele et al., 2010, Thorp et al., 2006, Sharma et al., 2003). It was found that for every unit increase in peak KAM, there was a 6.5-unit increase in the risk of developing knee joint comorbidities (Miyazaki et al., 2002, Egloff et al., 2012). This occurred independent of bodyweight and static misalignment contributions which have also been suggested as indicators for an increased risk of joint degeneration. A meta-analysis performed by Henriksen et al. (2006) on five able-bodied studies, further found a positive relationship between peak KAM and osteoarthritis progression. Not specific to the knee joint, vGRF is a whole-

body measure of force where higher forces have been associated with knee pain (de Oliveira Silva et al., 2015) and various knee joint injuries (Mündermann et al., 2005, Hunt et al., 2006, Hunt et al., 2010). These studies denote the importance of examining KAM and vGRF as potential indicators for the onset and progression of knee joint degeneration.

KAM and vGRF waveforms are commonly reduced to discrete features (peak magnitude and loading rate) when assessing populations with joint degenerative diseases. Peak magnitudes represent the maximal load experienced. Loading rates provide an ability to measure how quickly the load is delivered to the body over a certain time phase (Cheung & Rainbow, 2014). It has been suggested that loading rates may be a more relevant measure than peak magnitudes in assessing joint loading and injury occurrence (Morgenroth et al., 2014). In a study conducted on rabbits *in vivo*, higher loading rates led to greater cartilage degeneration than with lower loading rates, even when the latter had a higher peak magnitude of load (Boyd et al., 1991). Mündermann et al. (2005) found able-bodied the vGRF loading rate was 50.1% greater in those with knee osteoarthritis than matched controls while peak vGRF was not significantly different. This could suggest that temporal-spatial patterns in the loading waveforms are important and should be further examined.

In ITTAs, however, both peak magnitudes and loading rates during level-walking gait have provided inconclusive evidence that overloading is occurring in the intact limb compared to able-bodied controls (Table 2.1). This is unexpected given the increased risk of developing loading comorbidities in the intact limb of ITTAs (Struyf et al., 2009, Norvell et al., 2005, Melzer et al., 2001). Table 2.1 presents the commonly researched discrete loading features from the few ITTA studies that examined the differences between intact and control limbs when walking at similar speeds (1.2 - 1.3 m/s). For peak magnitudes, only one study found a significantly greater peak vGRF in the intact limb (Grabowski & D'Andrea, 2013). The other studies found no significant differences

for peak vGRF or KAM. Interestingly, two of the six studies (Esposito & Wilken, 2014, Rueda et al., 2013) found peak KAM to be lower in the intact limb than the control limb, and one study (Sanderson & Martin, 1997) found peak vGRF to be lower in the intact limb. These results were not statistically significant. This further suggests that peak magnitudes may not best represent any overloading that may be occurring in the intact limb of ITTAs, if it is a mechanism of joint degeneration in this population.

There have been limited studies exploring loading rates in the amputee population (Table 2.1). Grabowski & D'Andrea (2013) found significantly higher vGRF loading rates in the intact limb compared to a control limb. The other studies found no significant differences for either vGRF or KAM loading rates. Although not significant, all except one study (Esposito & Wilken, 2014) found the intact limb to experience a higher rate of load than the control limb for both vGRF and KAM. The study conducted by Esposito & Wilken (2014) found a non-significant lower vGRF loading rate in the intact limb compared to the control limb yet a non-significant greater peak vGRF. Morgenroth et al. (2014) conducted a study on the relationship between joint loading risk factors and cartilage degeneration in the intact limb of transfemoral amputees. A direct relationship to cartilage degeneration with peak KAM (linear regression slope = 0.42 [SE = 0.20], $p = 0.037$) and KAM loading rate (linear regression slope = 12.3 [SE = 3.2], $p = 0.0004$) was found. However, peak KAM was no longer related to cartilage degeneration when the regression considered KAM loading rate as an independent covariate. This suggests that the rate at which load is absorbed (i.e. temporal-spatial characteristics) is an important factor in the development of loading related diseases.

Table 2.1. First peak knee external adduction moment (KAM) and vertical ground reaction force (vGRF) and the vGRF and KAM loading rates (mean \pm SD) for the intact limb of ITTAs and control limb.

Reference	Peak KAM (Nm/kg)		KAM Loading Rate (Nm/kg/s)		Peak vGRF (N/kg)		vGRF Loading Rate (N/kg/s)	
	Intact	Control	Intact	Control	Intact	Control	Intact	Control
Royer & Keonig (2005)	0.48	0.38	--	--	No value provided; IL was 7% greater than CL	--	--	--
Grabowski & D'Andrea (2013)	0.50 \pm 0.14	0.38 \pm 0.11	3.89 \pm 1.4 ^A	2.64 \pm 1.15 ^A	11.3 \pm 0.67 [*]	10.6 \pm 0.39	118 \pm 42 ^{A*}	79.6 \pm 7.4 ^A
Esposito & Wilken (2014)	0.35 \pm 0.11	0.43 \pm 0.10	--	--	10.7 \pm 0.58 [†]	10.3 \pm 0.29 [†]	56.8 \pm 9.2 ^A (BW/s)	60.8 \pm 10.2 ^A (BW/s)
Rueda et al. (2013)	0.55 \pm 0.26	0.61 \pm 0.12	--	--	--	--	--	--
Sanderson & Martin (1997)	0.39 [†]	0.29 [†]	--	--	103 \pm 7 (%BW)	104 \pm 4 (%BW)	--	--
Lloyd et al. (2010)	0.24 \pm 0.10	0.22 \pm 0.10	4.80 \pm 2.1 ^{IN}	3.58 \pm 1.1 ^{IN}	11.6 [†]	11.2 [†]	19.9 \pm 3.9 ^{IN} (BW/s)	14.6 \pm 3.0 ^{IN} (BW/s)

^{*}*p* < 0.05 between intact and control limbs, [†]BW values converted to kg, ^AAverage loading rate, ^{IN}Instantaneous loading rate, ^{IL} = intact limb, ^{CL} = control limb. Both ITTA and control groups walked at speeds between 1.2 and 1.3 m/s. Those studies with no standard deviation denote that values were estimated from graphs.

The results from previous walking gait research on lower-limb amputees demonstrate ambiguity amongst the commonly researched discrete loading features on if overloading occurs in the intact limb of ITTAs. Thus, it is possible that these discrete loading features may not be the best reductions of the loading waveforms. Further, it is possible that overloading may be present in other measures of medial knee joint compartment loading such as intersegmental knee joint contact forces. Joint intersegmental forces are not widely assessed in the literature yet have been considered in ITTAs given the ambiguity in vGRF and KAM features in this population (Fey & Neptune, 2012, Silverman & Neptune, 2014, Karimi et al., 2017). Fey & Neptune (2012) and Karimi et al. (2017) found no significant differences in peak knee joint contact forces between intact and control limbs in the anterior, medial, and vertical (compressive) directions. In contrast, Silverman & Neptune (2014) found peak knee joint contact forces in the intact limb to be greater compared to both control and prosthetic limbs. They also found that the anterior and medial knee impulse forces during stance were greater in the intact limb compared to a control limb. However, the compressive knee force impulse was greater in the control limb. As the duration of the stance phase was similar between the intact and control limbs (0.82 s vs 0.80 s, respectively), the overall magnitude of the compressive knee force was greater in the control limb. This indicates that the waveform pattern may be important when assessing the intersegmental knee forces. Furthermore, these studies have indicated conflicting results on the presence of overloading in the intact limb when assessing knee joint contact forces in walking gait. It could be suggested that overloading may not be present during level-walking gait but rather in other high impact activities.

When the quadriceps are activated during walking gait, they produce an internal knee extension moment in response to the external knee flexion moment (KFM). Quadriceps activation imparts a compressive force at the knee joint which is postulated to be associated with medial knee compartment loading (Creaby, 2015).

Manal et al. (2015) found that peak KAM alone could account for 63% of the variance in medial knee forces, while inclusion of peak KFM increased the prediction power by 22%. They additionally investigated the force patterns of individual participants and found that when medial knee forces were similar there could be a different contribution from KAM and KFM. In some instances, peak KFM contributed to the medial knee forces to a greater extent than peak KAM. Walter et al. (2010) investigated gait modification strategies that have been demonstrated to reduce the magnitude of peak KAM to determine their influence of medial contact forces. While decreases in peak KAM were present, there was a corresponding increase in peak KFM. Therefore, peak medial contact forces were not reduced. These studies suggest that KFM is an important feature to examine in the development of joint degeneration and should be considered to provide more accurate representations of any changes in medial knee compartment loading (Creaby, 2015, Richards et al., 2018). KFM has not been investigated as a feature of high load in the ITTA population.

Inconclusive results from the limited amputee studies examining intact limb loading compared to controls suggest that 1) the reduction of loading waveforms to discrete points may ignore other phases of interest in the loading waveforms, 2) other measures of load (e.g. KFM) could indicate overloading in the intact limb, and 3) overloading may occur in high impact activities rather than level-walking gait.

2.2. Compensatory Movement Strategies

Through the impulse-momentum relationship, the magnitude of the vertical impulse absorbed when loading a limb can be mediated by changes in momentum. The downward-forward momentum of the centre of mass (CoM) during initial loading of a limb is controlled through joint/segment motion and muscular contraction. In running and landing tasks, the lower-limbs can be viewed as a simple spring-mass model with the joints of the limb contributing to the deformation of the spring (Blickhan, 1989). As greater forces are absorbed by the body, greater resistance (stiffness) from the joints

is required to produce controlled movements. While some level of stiffness is necessary in the performance of a task, too much stiffness may result in injury (Butler et al., 2003). Stiffness is broadly examined through the applied force and displacement of the joint. Thus, greater stiffness is associated with increased peak forces and reduced joint flexion and range of motion (ROM) (McMahon & Cheng, 1990) which is thought to lead to joint degeneration. Eccentric muscular contraction of the knee extensors also acts as a shock absorption mechanism to absorb the negative mechanical work done during the loading response phase of stance (LaStayo et al., 2003, Zhang et al., 2000). Muscle force produced by the knee extensors can increase the duration of absorption phase (Rudenko et al., 2016) providing greater time for joint flexion to occur and reducing peak forces and joint power. A spring-mass model is a useful model to indicate the shock absorption mechanisms of a limb. However, a spring-mass model is not applicable to walking gait as this task is not a conserved system. Thus, the dynamic walking theory was developed to examine the energy transfer between-limbs.

2.2.1. Dynamic Walking Theory

Dynamic walking theory builds on the basic premise of the passive inverted pendulum model (Cavagna et al., 1976) and the six determinants of gait model (Saunders et al., 1953) by examining the phase where energy is expended. In the inverted pendulum model, the CoM moves in an arc-like trajectory over a straight stance leg using gravitational potential energy for forward progression. By utilising an extended knee during single support, the muscle force needed to support body weight is reduced thereby theoretically requiring no mechanical work (Kuo & Donelan, 2010). According to the model, if the CoM moves like a pendulum, there should be no energy cost at all. However, the inverted pendulum model fails as some energy is expended during walking in order to maintain forward progression (Kuo et al., 2005). This energy cost has been associated with the double support phase, the 'step-to-step transition', when

the legs cannot function as a true pendulum (Kuo, 2007). The goal of the step-to-step transition is to change the direction of the CoM velocity from a downward-forward to an upward-forward trajectory to continue horizontal progression at a consistent speed. This redirection can be viewed by the vGRF impulse (the force-time integral) interaction between push-off from the trailing limb and braking of the leading limb (Adamczyk & Kuo, 2009, Gard & Childress, 1999, Morgenroth et al., 2011). Dynamic walking models show that a reduced push-off impulse from the trailing limb leads to an increased leading limb impulse (Kuo & Donelan, 2010, Kuo et al., 2005, Donelan et al., 2002a, Morgenroth et al., 2011, Adamczyk & Kuo, 2009).

In these models, a theoretical link was made between trailing limb impulse and lead limb loading (Kuo, 2007, Vanderpool et al., 2008). Morgenroth et al. (2011) was one of the first studies to explore the between-limb influence in the ITTA population. ITTAs were utilised as this group has been shown in previous literature to have a reduced push-off capacity from the prosthetic trailing limb and higher limb loading on the leading intact limb compared to the prosthetic limb. This study firstly confirmed the negative relationship between trailing limb impulse and leading limb impulse (slope = -0.34 [SE = 0.14], $p = 0.001$) validating this aspect of the dynamic walking models. Secondly, there was a significant relationship between trailing limb prosthetic push-off work and peak KAM in the leading limb (slope = -0.72 [SE = 0.22], $p = 0.011$). This suggests that increasing the push-off capacity of the prosthetic ankle joint could lower the magnitude of intact limb loading. These results were compared with a powered dynamic elastic response prosthetic which utilises motorised components to provide additional energy in propulsion. A 68% increase in push-off work on the prosthetic limb was found, with only a 10% reduction in peak KAM on the intact limb. Similar results were found in other amputee studies utilising a powered dynamic elastic response prosthetic (Grabowski & D'Andrea, 2013, Esposito & Wilken, 2014). Esposito & Wilken (2014) found a significant 6.4% reduction in peak vGRF and 23%

reduction in vGRF loading rate compared to prostheses without motorised components when walking at similar speeds to the Morgenroth et al. (2011) study (1.25 m/s vs 1.14 m/s, respectively). Grabowski & D'Andrea (2013) also found a significant 7.2% reduction in peak vGRF when walking at 1.25 m/s. Both Esposito & Wilken (2014) and Grabowski & D'Andrea (2013) only found significant reductions in peak KAM when walking speeds were between 1.5 - 1.75 m/s which requires increased propulsion to maintain greater speeds. These studies indicate that propulsion from the ankle joint is associated with contralateral limb loading, however, speed and joint mechanics beyond that of the ankle may additionally play a role in contralateral load reduction.

The step-to-step transition has been defined as the phase in which energy is expended, thus, research has focused on the double support phase (Kuo, 2007). While much of the energy transfer between limbs to continue forward progression does occur during double support, further research has suggested that energy is expended prior to and after double support (Adamczyk & Kuo, 2009). Energy expenditure can occur for up to 20-27% of stance. This was determined based on the beginning of trailing limb push-off work and end of lead limb collision work. Donelan et al. (2002b) also indicated that in certain individuals the negative work done in the leading limb continued to occur after double support ended. These studies suggest that between-limb influences can occur outside of the double support phase.

While the dynamic walking theory is related to the energetic cost of walking, the underlying principle states there is a between-limb influence in order to produce movement efficiently. Therefore, this theory can be applied to kinematic and kinetic features to examine the influence of movement strategies on loading patterns. In the ITTA population, research has suggested the importance of the influence from the reduced prosthetic ankle joint propulsion on intact limb loading (Morgenroth et al., 2011, Kuo, 2007). However, the dynamic walking theory has yet to be applied to other

joints on the prosthetic limb or to any joint motion occurring on the intact limb when loading the limb. This could provide additional information on the involvement of movement patterns associated with high limb loading beyond that of the ankle joint.

2.2.2. ITTA Walking Gait

Previous ITTA research has suggested greater intact limb loading stems from altered movement patterns due to the functional loss of the ankle plantarflexors following amputation (Morgenroth et al., 2011, Nolan & Lees, 2000). As limited research has assessed both step descent and drop landing movement strategies in the ITTA population, compensatory strategies presented in walking gait literature can aid in the development of hypotheses. ITTAs perform compensatory movement patterns during the step-to-step transition of the walking gait cycle in order to load the limb and continue forward progression at a consistent speed. These compensations can be examined by comparing joint mechanics of ITTAs to those performed by able-bodied individuals and may aid in understanding the influence of joint mechanics on limb loading. Typically, in biomechanics, movement patterns are assessed from a combination of temporal-spatial features (e.g., walking speed), kinematics (e.g., individual joint angular motion), and kinetics (e.g., joint power).

2.2.2.1. Temporal-Spatial Features

Table 2.2 presents temporal-spatial characteristics for ITTAs and able-bodied controls. In ITTAs, between-limb asymmetries are found where the intact limb, as compared to the prosthetic limb, has a shorter step length (Howard et al., 2013, Sanderson & Martin, 1997, de Cerqueira Soares et al., 2009) and increased stance, single limb support and double limb support duration (Isakov et al., 2000, Mattes et al., 2000, Kovač et al., 2010). Able bodied individuals are found to have 98% between-limb symmetry in step length and 90-96% symmetry in single support and double support stance duration, respectively (Oberg et al., 1993, Hirokawa, 1989, Kovač et al., 2010).

Table 2.2. Temporal-spatial characteristics for the intact and prosthetic limbs of unilateral transtibial amputees and between-limb averages for able-bodied controls

	Intact	Prosthetic	Control
Step Length (m)	0.64 – 0.69	0.69 – 0.74	0.64
Stance Duration (s)	0.71 – 0.74	0.68 – 0.71	0.68
Single Support (s)	0.44 – 0.58	0.41 – 0.55	0.55
Double Support (s)	0.13	0.12	0.13
Walking Speed (m/s)		1.25	1.4

The range of data presented in Table 2.2 for ITTAs is possibly due to differences in prosthetic components, length of time since amputation, activity level and/or walking speed. ITTAs are found to have an overall slower habitual walking speed compared to able-bodied individuals (Sanderson & Martin, 1997, Oberg et al., 1993). This is consistent with significant differences found in cadence between ITTAs (105 ± 7.5 steps/min) and able-bodied individuals (110-120 steps/min; Kovač et al., 2010). As walking speed increases, step length increases while the stance phase duration shortens. Previous research in ITTAs has suggested temporal-spatial between-limb asymmetry remains the same regardless of overall walking speed (Isakov et al., 1996, Nolan et al., 2003). This indicates that temporal-spatial changes with speed occur to the same magnitude in both limbs.

2.2.2.2. Kinematic and Kinetic Features

The most notable difference between ITTAs and able-bodied individuals is within the sagittal plane ankle joint motion of the prosthetic limb. When loading the limb, an able-bodied ankle joint undergoes approximately 10° of plantarflexion controlled by a small internal ankle dorsiflexor moment to bring the foot flat with the ground. The ankle joint also plays a crucial role in producing the propulsive power (A2S power generation burst) required to continue forward progression (Winter & Sienko, 1988, Sanderson & Martin, 1997). Winter (1983) noted that the ankle plantarflexors produce over 80%

of the mechanical power generated to enable forward progression. In able-bodied individuals, rapid plantarflexion of $\sim 20^\circ$ unloads the ipsilateral limb and transfers the load to the contralateral limb (Brockett & Chapman, 2016). The prosthetic ankle joint motion and propulsive capacity is dependent on the prosthetic components, but typically has a reduced ROM compared to an intact ankle joint (Sanderson & Martin, 1997). Reduced propulsion has been associated with a shorter step length which is consistent with that exhibited by ITTAs (Browne & Franz, 2017a). To compensate for reduced prosthetic ankle joint propulsion, Nolan & Lees (2000) found the intact limb ankle joint moved through a greater average ROM (26°) when loading the limb than the prosthetic limb (20°) and able-bodied individuals (21°). It was additionally found that the intact ankle joint motion during loading increased as the prosthetic ankle ROM decreased during propulsion.

Beyond the ankle joint, additional work is completed by the prosthetic hip joint to compensate for reduced ankle joint propulsion. In able-bodied persons, the hip performs positive work during late push-off and early swing (Donelan et al., 2002a, Neptune et al., 2001). ITTAs are characterised with greater hip joint power in the prosthetic limb, compared to the intact limb and control limbs, in the attempt to increase step-frequency to maintain speed (Ventura et al., 2011, Silverman et al., 2008). This also tends to shorten the step length of the intact limb which is indicative of the asymmetrical walking gait seen in ITTAs, possibly leading to increased and faster loading of the intact limb (de Cerqueira Soares et al., 2009).

The intact limb hip joint reaches similar magnitudes of peak flexion as the prosthetic and able-bodied limbs (40°); however, this peak was found to occur at 8% of the gait cycle (loading response) in the intact limb as compared to 92% of the gait cycle (during swing prior to initial contact) in the other two limbs (Grumillier et al., 2008). The H1S work done has, therefore, been found to be greater in the intact limb compared to able-bodied controls during loading response to ensure the completion

of the step-to-step transition (Grumillier et al., 2008). The intact knee joint also undergoes greater maximal flexion compared to a control limb during loading response (24° and 19°, respectively; Bayaert et al., 2008, Sanderson & Martin, 1997). As such, increased work is done during the K1S absorption power burst phase compared to able-bodied individuals (Beyaert et al., 2008). Both the intact knee and hip joints have increased internal extensor moments compared to controls to control the increased joint flexion and prevent buckling (Nolan & Lees, 2000, Beyaert et al., 2008, Grumillier et al., 2008). The mechanics at the intact knee and hip joints are possible compensatory movement patterns to enable progression in response to the altered prosthetic limb motion.

Compensatory strategies undertaken by ITTAs have been examined extensively in walking gait and can provide indications of altered mechanics that are likely to be adopted in other cyclical movement patterns (e.g. step descent). Movement strategies in both the intact and prosthetic limbs may play a role in the magnitude and rate of intact whole-limb and joint loading based on the impulse-momentum theorem and dynamic walking theory.

2.3. Joint Coordination

Biomechanical analysis of human movement typically assesses individual joint motion. However, analysis of individual joint motion is unable to fully encompass the dynamic nature of movement as only inferences can be made regarding the influence of one limb or joint on another. Coordination between joints can provide a measure of the self-organisation utilised for the production of movement patterns. Coordination is defined as the ability of the system to functionally control a series of joints or segments in time and in sequence to produce a functional movement pattern (Byrne et al., 2002). Essential to this definition, is that failure of one of the joints in the series can be compensated for at another joint to complete the movement task (Bernstein, 1967). The inability or inconsistency in the development of self-organised

coordination patterns may result in pathological gait, such as that seen in amputees. For example, ITTAs, in the prosthetic limb, utilise the hip joint to provide 'pull-off' power in compensation for reduced 'push-off' power from the ankle joint. Under this assumption, it is therefore plausible to state that amputees, from the loss of the ankle joint, produce a different coordination pattern that elicits the same movement outcome (e.g. forward progression) as able-bodied individuals. It is possible that the coordination patterns adopted may provide additional information on the relationship between movement patterns and limb and joint loading than that which can be depicted by individual joint motion alone.

Limited, if any, coordination research has been conducted in the ITTA population, yet can provide valuable insight into the strategies utilised to achieve a task goal. Elderly individuals tend to exhibit similar gait characteristics as ITTAs (e.g. slower walking speeds, smaller step lengths, balance recovery issues following perturbations). Chiu & Chou (2012) found that as walking speeds increased, elderly individuals did not adapt their knee-hip coordination strategies. In contrast, younger individuals modified their coordination patterns with increases in walking speed to complete the task and ensure stability when walking. It is possible that ITTAs, similar to elderly populations, may not be able to adapt their coordination strategies when performing more demanding movement tasks. Patients who have undergone anterior cruciate ligament reconstructive surgery tend to perform compensatory strategies that are associated with risk factors for joint degeneration. Segment coordination in anterior cruciate ligament reconstructive patients have been found to differ significantly compared to a matched control group (Nematollahi et al., 2016). This was despite no significant differences in the individual joint motion. This suggests that it is the way in which joints coordinate to produce functional movement patterns that may be related to injury (Hughes & Watkins, 2008, Doherty et al., 2014). No research has investigated the role of joint coordination in relation with limb and joint loading in the ITTA population.

2.4. Step Descent

It has been postulated in this thesis that overloading of the intact limb, if it exists as a mechanism in the development of joint degeneration in this population, could be present in tasks other than level-walking. A step descent, similar to stepping off a kerb, is an important functional task regularly performed in daily living. Step descent is a functionally demanding extension of level-walking gait that requires increased joint motion and mechanical work to attenuate higher loads relative to level-walking gait (Jones et al., 2006, van Dieën et al., 2007, Barnett et al., 2014, van Dieën et al., 2008, Christina & Cavanagh, 2002, Novak & Brouwer, 2011). Limited research has assessed loading patterns during a step descent and the movement strategies performed by established ITTAs is currently unknown.

To perform a step descent, the leading limb must absorb the kinetic energy generated from the vertical displacement of the CoM and aid in transferring the weight from the trailing limb (Figure 2.1). The trailing limb must safely control the lowering of the CoM through increased eccentric control of the quadriceps and plantarflexors compared to level-walking gait and subsequently propel the CoM to continue forward progression.

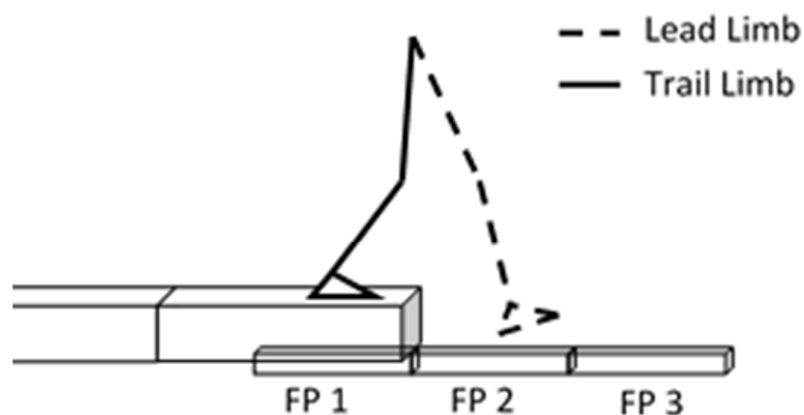


Figure 2.1. Definition of lead and trail limbs during a step descent with force platform placements noted

The phases of a step descent have not been clearly established in the literature. Step and stair descent require similar mechanics to accomplish the task, thus, phases of stair descent can be used to help inform the phases of a step descent. Stair descent literature has identified three distinct phases during stance: 1) weight acceptance (i.e., absorption of load during double support), 2) forward progression during the first half of single support, and 3) controlled lowering during the second half of single support and continuing throughout the entire double support phase as the contralateral limb undergoes phase 1 (Zachazewski et al., 1993, Buckley et al., 2013). Both stair and step descent tasks require the leading limb to absorb the load from the descending CoM and is similarly defined as the loading response phase (Stair: Spanjaard et al., 2009, Zachazewski et al., 1993, Buckley et al., 2013, Schmalz et al., 2007; Step: van Dieën et al., 2008, van Dieën et al., 2007, Jones et al., 2006). Unlike stair descent, a single step descent requires the ability to transition to level-walking gait and continue forward progression immediately. The majority of the propulsion required during step descent occurs in the trailing limb during the period of double support while the leading limb concurrently absorbs load. This differs from stair descent when forward progression occurs in single support. Limited research has examined the trailing limb during a step descent and, as such, the trailing limb sub-phases of a single step negotiation have not been adequately defined.

Of the few step descent studies investigating the mechanics of the trailing limb, analysis consisted of the entire trail limb stance phase (van Dieën et al., 2007), the single support phase of the trail limb to assess the lowering of the CoM (Selfe et al., 2008), and the propulsive phase defined as the double support phase (van Dieën et al., 2008). When analysing the entire trailing limb stance phase, van Dieën et al. (2007) did not define specific trail limb sub-phases. However, discussion of the results in the study separated the trailing limb mechanics between those that were utilised to lower the CoM during single support and those required to propel the CoM forward

during double support. The inclusion of analysing the mechanics during single support is necessary as between-limb influences could occur outside of the double-support phase as depicted by the step-to-step transition. Differences could occur when lowering the CoM as controlled eccentric contractions from the trailing limb are necessary to resist the effect of gravity and prevent collapse of the knee joint. A reduction in the joint flexion to lower the CoM could result in less work done by the trailing limb. As a consequence, the forward and vertical momentum not controlled by the trailing limb could potentially lead to higher load in the leading limb as a greater impulse must be generated to lower the CoM and continue forward progression (Donelan et al., 2002a). No research has examined these sub-phases in ITTAs where compensations due to the loss of the ankle joint could result in a combination of these two sub-phases (i.e. no distinct sub-phases).

There are two descent strategies that have been identified by previous research based on the contact area of the foot (Freedman & Kent, 1987). Initial contact of the leading limb is made with either the heel or toe. The effect of descent strategy on the development of load is not well understood. van Dieën et al. (2008) examined peak vGRF and found that utilising a toe contact (TC) strategy resulted in significantly reduced peak magnitude compared to a heel contact strategy. However, this study and other step and stair descent studies attribute the preference for a TC strategy to aid in whole-body stability rather than to reduce the load experienced (van Dieën et al., 2008, Spanjaard et al., 2009, Jones et al., 2006). In elderly individuals, it is well established that muscular strength is lost first in the ankle musculature (Kerrigan et al., 1998, Judge et al., 1996). A TC strategy, compared to a heel contact (HC) strategy, is mechanically more demanding at the ankle joint as it requires greater work and absorption power (Gerstle et al., 2018). It is, therefore, unexpected that elderly individuals would prefer to utilise a TC strategy independent of step height and walking speed (van Dieën & Pijnappels, 2009). This would suggest that the

preference of a TC strategy in elderly individuals may be to minimise forces in the limb. As high load is thought to be associated with joint degeneration, it is important to understand the effect of the descent strategy on the development of load.

Previous research has indicated that the choice of descent strategy can be influenced by a number of factors including step height (van Dieën & Pijnappels, 2009, Gerstle et al., 2017), stepping speed (van Dieën et al., 2008, Gerstle et al., 2017), age (van Dieën & Pijnappels, 2009), and stability (van Dieën & Pijnappels, 2009, Gerstle et al., 2018). A TC strategy is more commonly performed at higher step heights (van Dieën & Pijnappels, 2009, Gerstle et al., 2017). The lengthened leading limb can aid in reducing the vertical velocity at initial contact as the CoM is higher. The ankle joint can also be utilised to absorb the greater velocity from the higher step height through increased eccentric activation from the ankle plantarflexors. As step height increases from 5 to 10 cm, the probability of a heel strike to occur in young able-bodied individuals decreases by ~43-63% dependent on the walking speed (van Dieën & Pijnappels, 2009). Again, when increasing the step height from 10 to 15 cm, heel strike preference decreases by ~7-26%. These decreases were smaller in elderly individuals (72.5 ± 5 years) who prefer to perform a TC strategy more often than young individuals (23 ± 1 years) independent of step height or stepping speed. van Dieën et al. (2008) also suggested, based on pilot work, that 10 cm was the height at which the descent strategy begins to alternate between toe and heel contact. Gerstle et al. (2017) found that at 5 and 15 cm step heights the descent preference was a HC strategy (95% and 59%, respectively). At 25 cm, however, the preference transitioned to a TC strategy (77%). These studies suggest that between 10 and 20 cm is the height about which descent strategy preference is unclear. Descending from a step within this range may help to indicate other factors that could influence descent preference, such as reducing impact forces.

At a step height of 15 cm, the influence of stepping speed on the choice of the descent strategy performed is unclear. van Dieën et al. (2008) found that speed was reduced when utilising a TC strategy compared to a HC strategy despite controlling for overall walking speed. In another study, van Dieën & Pijnappels (2009) asked able-bodied participants to walk at various controlled walking speeds. It was found that the preference for a TC strategy reduced as speed increased in both young and elderly populations. However, this is in contrast to Gerstle et al. (2017) who found that participants that performed a TC strategy actually maintained faster walking speeds. The differences across studies possible occurred as van Dieën and colleagues (2008, 2009) controlled walking speed, while Gerstle et al. (2017) allowed participants to walk at their self-selected pace. In a study assessing the descent preferences of ITTAs within 6-months post-amputation, speed was independent of the descent strategy chosen. As these ITTAs had not established their joint mechanics, the descent strategy changed between HC and TC strategies when leading with the intact limb at each visit to lab (1-, 3-, and 6-months), while walking speed plateaued at the 3- and 6-month visits (0.96 and 0.98 m/s, respectively). This may suggest that walking at preferred speeds may provide greater insight into the natural mechanics performed and/or that stepping speed is independent of the chosen descent strategy.

The role of the trailing limb in relation to the descent strategy has not been fully explored. It is plausible that descent strategy preferences could be due to inhibition from the trailing limb to accommodate for the increased demand of the task. The trailing limb may be unable to produce the ROM or eccentrically control the vertical displacement of the CoM to necessitate changes in step height or walking speeds. van Dieën et al. (2008) is the only study to examine the trailing limb mechanics (peak power and work done at each lower-limb joint) in both HC and TC strategies. No significant differences were found between strategies ($p > 0.244$). The study, however, only assessed the propulsive phase and controlled for walking speed

suggesting similar propulsion was required to continue forward progression. Additionally, participants were instructed to perform both descent strategies. Insight into the effects of the trailing limb mechanics on the descent strategy (and subsequent development of lead limb loading) could be informed by examining step descent strategies from a step height about which strategy preferences are unclear (10-20 cm) and when performed at habitual walking speeds.

While numerous studies have examined the movement strategies adopted by ITTAs during level-walking gait, there is a paucity of research in higher demanding tasks such as step descent. One study in ITTAs assessed the mechanics when leading with the intact limb (Barnett et al., 2014), another study examined only the mechanics of the prosthetic limb leading (Jones et al., 2006), and the last study in ITTAs examined only the trailing limb mechanics utilised to lower the CoM (Murray et al., 2017). These studies did not include comparisons to a control population. Thus, it is unclear how the joint mechanics of the intact limb may compensate compared to a 'normal' descent strategy. It is possible that ITTAs may choose to descend a step leading with the prosthetic limb in order to utilise the functionality of the intact limb to control the downward-forward momentum and provide stability (van Dieën et al., 2008, Spanjaard et al., 2009, Jones et al., 2006). However, Barnett et al. (2014) observed that a lead limb preference of the prosthetic limb was reduced from 90.8% at 1-month post-discharge to 52.6% at 6-months. This would suggest that there is no lead limb preference consistent across established ITTA individuals. This further indicates the importance of examining the loading patterns and underpinning joint mechanics when leading with the intact limb during a step descent.

2.5. Drop Landing

Drop landing was chosen as an experimental model to further examine the loading patterns and joint mechanics of the intact limb when contributions from the prosthetic limb and requirements of task demands (e.g. horizontal progression) are controlled.

It is additionally a task in which the vertical momentum is reduced by the same amount across all participants, thus, making comparisons equivalent. Further, the quickly applied forces that occur during landings have been associated with various knee injuries, including osteoarthritis and non-specific knee pain (Murphy et al., 2003). When modelling the limb as a spring, absorption of forces can be mediated by changes in the displacement of joints (Farley & Morgenroth, 1999). Unilateral landings on the intact limb of ITTAs could indicate the inherent joint mechanistic approach utilised in this limb to mediate forces independent of influencing factors (i.e. task demands and effects from the prosthetic limb). Additionally, the compensatory strategies performed in the intact limb of ITTAs in response to the limited capacity of the prosthetic limb are unknown when landing from a jump. It is unclear if compensations are indicative of risk factors associated with joint degeneration. Thus, ITTAs are encouraged to participate in sports adapted to either sitting or wheelchair versions to reduce repetitive high impact loading, however, this can limit the cardiovascular benefits of exercise (Chapman, 2008, Sanderson & Martin, 1996).

During bilateral landing, rapid impact forces are typically dissipated by near synchronous joint flexion of both limbs and eccentric work of the quadriceps muscles. The ankle joint is the first joint where shock absorption occurs in the lower-limbs and is thought to be the main contributor to limb stiffness (Farley & Morgenroth, 1999). An optimal ankle plantarflexion angle at initial contact between 20-30° has been associated with reduced peak vGRF and vGRF loading rates (Rowley & Richards, 2015). This 'optimal' angle was also associated with equivalent contributions to the total support moment from the knee and hip joints. Plantarflexion angles smaller than 20° resulted in increased peak vGRF and vGRF loading rate and a greater reliance on the hip joint to attenuate load. Larger plantarflexion angles resulted in overall minor decreases in vGRF, however, this was not consistent across participants where increases in vGRFs could occur with larger than 30° plantarflexion angles at initial

contact. Previous research has determined that greater joint flexion from all lower-limb joints is associated with reduced peak vertical forces as the duration of the absorption phase increases (DeVita & Skelly, 1992, Zhang et al., 2000, Norcross et al., 2010). Whereas, individuals who perform a more extended landing strategy tend to have higher peak forces as the greatest joint flexion ROM occurs at the ankle joint and less joint flexion at the knee and hip joints. Greater utilisation of the ankle joint power compared to the knee and hip joints, can also lead to reductions in the hip joint power contribution to dissipating the kinetic energy at touchdown (Zhang et al., 2000, Norcross et al., 2013, DeVita & Skelly, 1992). Thus, a more extended landing strategy could place these individuals at a greater risk of injury. Taken together, these studies suggest that in-phase flexion coordination of the lower-limb joints may be an important factor in mediating forces upon landing (Aerts et al., 2013).

ITTAs have limited ROM at the prosthetic ankle and, therefore, will compensate elsewhere in the kinematic chain. Only one study has previously assessed landings in the amputee population (Schoeman et al., 2013). A quasi-unilateral landing was performed by the ITTAs following a maximal vertical jump in which the intact limb touched down earlier than the prosthetic limb. This places a greater demand on the intact limb to attenuate the impact forces. Schoeman et al. (2013) found that the intact limb of ITTAs experienced a greater peak vGRF and performed reduced joint ROM compared to the matched control limbs. This would suggest that ITTAs perform a more extended landing strategy. However, this study examined voluntary maximal jump efforts in which the ITTAs achieved maximal jump heights of half that of the able-bodied controls (15 ± 6 cm vs 30 ± 4 cm). This makes comparisons between the two groups difficult as significant differences in the joint mechanics may have been the result of different vertical velocities at initial contact (Yeow et al., 2009a, Yeow et al., 2009b, Yeow et al., 2010). Between-limb influences have been demonstrated to occur in walking gait (Morgenroth et al., 2011), yet have not been examined in

discrete in-phase tasks such as drop landings. It is possible that the intact limb may be able to perform a more flexed landing strategy, associated with reduced risk of knee pain, without the possible influence from the prosthetic limb.

The extended landing strategy that was possibly performed by the intact limb in the Schoeman et al. (2013) study could have been a compensatory strategy performed in response to reduced quadriceps strength. The intact limb of ITTAs has been found to have substantial deficits in maximal quadriceps strength of up to 39% compared to controls (Lloyd et al., 2010, Pedrinelli et al., 2002). Reduced flexion at all lower-limb joints could limit the eccentric work required from the quadriceps muscles (Bisseling et al., 2007). However, this could lead to greater load and a transfer of this load to the surrounding joint tissue rather than dissipating through the larger muscle groups (DeVita & Skelly, 1992). A possible strategy to overcome reduced quadriceps strength while decreasing the risk of injury is through increasing trunk flexion. Greater trunk flexion during landings has been associated with greater flexion at all lower-limb joints and reduces the reliance on the eccentric contraction of the quadriceps muscles to arrest the downward momentum (Blackburn & Padua, 2008, Blackburn & Padua, 2009).

A more extended landing strategy and decreased quadriceps muscle force can also alter the joint mechanics in the frontal plane (Hewett et al., 2005, Markolf et al., 1978). Knee valgus motion is an established feature associated with the occurrence of non-descriptive knee pain and anterior cruciate ligament injuries (Miyazaki et al., 2002). Individuals who landed with increased knee valgus have also been found to exhibit hip adduction angles and internal rotation coupled with tibial external rotation and foot eversion (Kobayashi et al., 2013, Yasuda et al., 2016). This research has indicated that the multi-planar motion at the hip joint, rather than the ankle joint, may have a greater influence on knee loading (Powers, 2010, Kobayashi et al., 2013). However, current research has found conflicting evidence on the relationship between hip

strength and knee valgus motion (Chaudhari & Andriacchi, 2006, Sigward & Powers, 2007, Geiser et al., 2010, Hughes, 2014). Additionally, studies assessing ankle and hip frontal plane features have only been able to explain 16-49% of the variation in knee valgus motion (Sigward & Powers, 2007, Sigward et al., 2008). The remaining variance is most likely explained by the sagittal plane joint motion (Pollard et al., 2010), trunk flexion (Blackburn & Padua, 2008), and quadriceps strength (Kuenze et al., 2015, Ward et al., 2018) which will be explored in this thesis.

The compensatory strategies performed by established ITTAs when landing from a jump are unclear. It is possible that deficiencies in the intact limb post-amputation may contribute to high load in this limb, if high load is a mechanism of joint degeneration in this population. Unilateral drop landings could possibly provide information regarding these deficiencies. Additionally, bilateral drop landings can indicate the effects from the prosthetic limb on the intact limb joint mechanics and loading patterns. Rehabilitation and exercise protocols for ITTAs could be enhanced by utilising unilateral and bilateral drop landings yet the occurrence of high load in the intact limb loading is unknown.

This literature review has highlighted the lack of research on the loading patterns in lower-limb amputees and how the joints act to mediate these loads. Step descent and drop landing tasks are ideal to investigate the load on the intact limb of ITTAs and how the joint mechanics of the intact and prosthetic limbs interact in the development of this load. Step descent, an out-of-phase asymmetrical task, requires a step-to-step transition where the reduced joint motion and propulsive power of the prosthetic ankle joint may influence the development of lead limb loading and performance of the task. The discrete in-phase symmetrical drop landing task can remove the effects of the prosthetic limb and the requirements to continue forward progression to investigate deficiencies in the intact limb. Additionally, drop landing tasks could indicate if the effects from the prosthetic limb influence the development of load on the intact limb.

This literature review has also highlighted the inconclusive results from walking gait research in which it is unclear if high load exists in the intact limb of ITTAs as compared to controls. It was postulated that these results may be due to issues surrounding discrete point analysis.

Part Two: Waveform Analysis Methodology

This section will discuss the current issues with discrete point analysis and methods that have been performed in previous research to solve these problems, such as waveform analysis.

2.6. Discrete versus Continuous Analysis

A potential reason for the inconclusive results when assessing intact limb overloading is that the commonly researched loading features are discrete points extracted from a continuous waveform. Discrete point analysis (DPA) reduces a waveform to a single time-dependent point which is assumed to capture the underlying function of the signal. DPA is prevalent in biomechanical literature as it is an efficient and convenient way to reduce and analyse the complex nature of movement; however, DPA is unable to encompass the dynamic mechanics of movement and has three significant limitations. First, the 'key' discrete features analysed are determined from previous literature and can fail to detect important information elsewhere in the waveform (Dona et al., 2009, Donoghue et al., 2008). This *ad hoc* approach can be biased as the discrete features are typically chosen based on unjustified positional values (e.g. peaks or troughs) and/or temporal windows where limited evidence has suggested that these features are physiologically meaningful (Pataky et al., 2014). This approach allows only what is expected by researchers to be detected (Schöllhorn et al., 2002). Second, 'key' features may occur at different time positions in the waveform (Richter et al., 2014b). For example, in bi-modal waveforms, the peak may occur at either the first or second maximum; DPA may, therefore, compare non-related neuromuscular measures. Lastly, DPA is unable to examine how features develop over a phase of movement. Reducing highly multivariate datasets to discrete points may result in the loss of valuable information (Pataky et al., 2013) as the majority of the waveform is not considered. Based on the number of discrete features chosen for analysis and assuming that each waveform consists of 101 points, one study estimated that only

0.5-1.4% of the data is examined within a study (Richter, 2014a). One way to overcome these limitations is by utilising continuous waveform analysis.

It should be emphasised that DPA is a useful way to reduce waveform data when working with such large datasets as are common in the field of biomechanics. Indeed, it may be found that the results from waveform analysis suggest those 'key' discrete features that are often assessed are a sufficient and appropriate way to reduce waveform data. Waveform analysis should be utilised to reduce bias in the features selected, especially when previous research provides inconclusive results when analysing the *ad hoc* 'key' features.

2.7. Statistical Parametric Mapping

Statistical parametric mapping (SPM) is one type of waveform analysis that allows for testing of biomechanical variables in their original temporal-spatial context. It does this by capturing phases of covariance between multivariate datasets (Pataky, 2012). SPM was originally developed by Karl Friston (Friston et al., 1991) to examine three-dimensional differences in brain activity. It has been adapted to analyse biomechanical waveform data by Pataky and colleagues (Pataky et al., 2013). In essence, it is a technique that extends zero-dimensional (discrete) statistical processes through time.

Both discrete and SPM approaches utilise *t*-distributions (associated with *t*-tests) or *F*-distributions (associated with ANOVAs). The other aspect of performing a statistical analysis is determining the *p*-value threshold. This threshold (also called the alpha threshold) describes the behaviour of random data across infinite sets of experiments. It represents the likelihood of a false positive and is most commonly set at 0.05; i.e. one false positive will occur for every 20 times the experiment is repeated. The typical Bonferroni correction of the alpha threshold to account for multiplicity (multiple comparisons using the same data) is in most cases too conservative. With Bonferroni correction, the alpha threshold is most commonly set as alpha/ number of

comparisons. The t - and F-distribution values that are above the alpha threshold represent the data points that have a 95% probability of being significantly different over an infinite number of experiments. However, a Bonferroni correction assumes all data points are independent. The main difference of one-dimensional (continuous) analyses from DPA is the use of random field theory (RFT). RFT accounts for the multiple comparison problem as one-dimensional continuous data points are not independent because the waveform develops over time and each datum will be related to those before and after. RFT is similar to a Bonferroni correction, except that RFT controls for false positives within regions rather than for single datum. The threshold for RFT in SPM one-dimensional analyses is determined by using the classical height-threshold cluster-breadth procedure (Pataky, 2012). The mathematical calculations and approaches for estimating the RFT thresholds are described in full for all multivariate statistical tests in the Friston et al. (1994) and Worsley et al. (2004) papers. For the purposes of this thesis, these calculations will not be presented in text.

2.8. Issues with Waveform Analysis

One issue with waveform analysis is the inherent timing/phase variability that is present within and between participants. This can limit direct magnitude comparisons of physiological events (Chau et al., 2005, Godwin et al., 2010) where significant findings may not reflect the movement physiology (Sadeghi et al., 2000). The main approach to limit variability is to linearly time-normalise the data (Page & Epifanio, 2007). However, timing/phase variability can still exist after time-normalisation (Buzzi et al., 2003). For example, Figure 2.2A depicts the time-normalised vGRF curves for two different participants during the take-off phase of a countermovement jump. The physiological event, denoted by the asterisk, represents the end of the eccentric phase which differs between participants even after time-normalisation. Waveform analysis following time-normalisation could possibly result in magnitude comparisons

across different phases of the movement. Therefore, results could be wrongly interpreted as magnitude differences rather than as a result of comparing different physiological phases due to timing differences between participants.

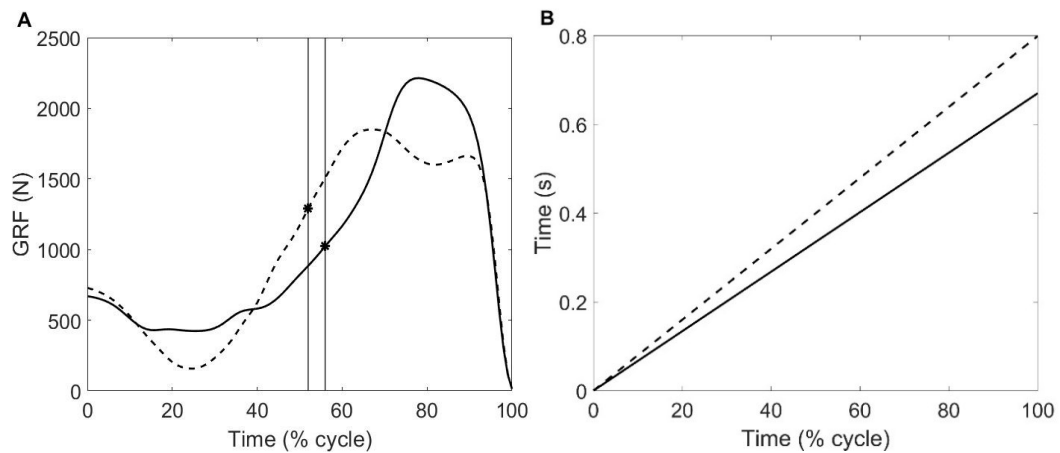


Figure 2.2. A) Time-normalised vGRF curves for the take-off phase of countermovement jumps for two subjects. The end of the eccentric phase is denoted by a red dot with solid vertical lines. B) The time-domain for each subject representing the time taken to complete the take-off phase.

An additional issue with time-normalisation is the warping of the original timing of events in the waveform which could be important in assessing the efficiency of a movement or the risk of injury. Previous research has suggested that the difference in the timing of events is as important as magnitude differences (Levitin et al., 2007). One way to examine the timing of events after time-normalisation and any other methods of time-warping is through the extraction of the time-domain (Figure 2.2B). The time-domain represents the time taken to complete the movement or phase of the movement and can be assessed in the same manner as the magnitude-domain.

2.9. Landmark Registration

Landmark registration is one possible solution to account for timing/phase variability in waveforms after time-normalisation by registering the signal to meaningful events inherent within the movement task. Landmark registration is a technique that 'stretches' or 'shortens' phases of a task that occur between specified landmarks (i.e.

events) while maintaining each waveform's individual shape and amplitude (Crane et al., 2010, Levitin et al., 2007). Aligning to specified landmarks, such as the end of the eccentric phase in a countermovement jump, may allow for more valid waveform magnitude analyses by aligning distinct physiological events. Landmark registration can be applied to any waveform including the time-domain to ensure that differences in timing between events are maintained for subsequent analyses. The ability of landmark registration to reduce the inherent timing/phase variability was assessed in a pilot study of this thesis (Section 3.6.3.1).

To perform landmark registration, the landmark must first be identified. A landmark is defined as a point that is identifiable in every waveform and is typically a maximum, minimum or zero crossing. The average time point at which the landmark occurs is calculated across all the waveforms. The time of each waveform is then warped so that the individual waveform landmark occurs at the average time point. To register each curve to the specified landmarks, a warping function is created that determines whether the phase between two successive landmarks should be 'stretched' or 'shortened'. The warping function contains the information about how the phases in a waveform are adjusted. Once the warping function is created, it is then applied to any waveform of interest to answer the specified research questions.

There are different approaches in the calculation of the warping function. The warping function applied in this thesis was based on adjusting the differentiation of time using a piecewise velocity registration. Unlike time-normalisation, this registration is a non-linear approach. Alternative approaches to creating a warping function include piecewise linear and spline registrations (Ramsay, 2006, Page et al., 2006); however, these approaches can result in sharp corners at the landmarks and "backward flowing" time, respectively (Figure 2.3, adapted from Moudy et al., 2018). The piecewise velocity approach utilised in this thesis allows for alterations of the differentiation of time within set phases between landmarks.

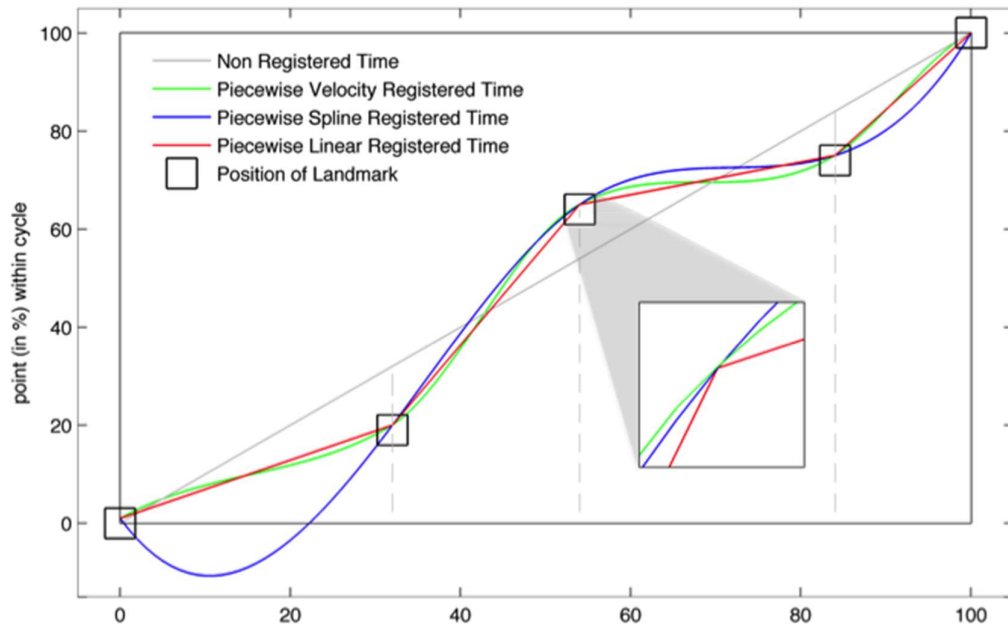


Figure 2.3. An illustration of three registration approaches performed on the time-domain of the take-off phase in a countermovement jump. These approaches include piecewise linear (red), piecewise spline (blue), and piecewise velocity (green) (Moudy et al., 2018, pg. 111).

There are two main factors that could influence waveform analysis after landmark registration: the landmarks (i.e. key events) themselves and the number of landmarks chosen. However, there has been no research to date to examine these key issues. A pilot study of this thesis was performed to investigate different landmark positions and the optimal number of landmarks to avoid over-registration of the signal (Section 3.6.3.1)

2.10. Other Approaches to Waveform Analysis

In addition to SPM, principal component analysis (PCA) and analysis of characterising phases (ACP) are approaches that have been used in previous research to examine waveform data. PCA is a dimensionality reduction technique where large data sets can be reduced to few dominant dimensions (Wold et al., 1987). This approach works under the assumption that large data sets have correlated features and, therefore, redundant information is present. A linear transformation is performed on the data to

create a set of uncorrelated principal components that contain the greatest amount of variation. The first principal component explains the greatest amount of variation with each subsequent principal component explaining less than the previous. The features that make up the principal components are also rated by importance by the amount of variance explained. This approach is able to identify which features could be the most important for task completion, injury assessment, or group identification (Deluzio et al., 1997, Mantovani et al., 2011, Deluzio & Astephen, 2007). Functional PCA is the specific branch of PCA that analyses waveforms rather than specific discrete time points within the waveform. There are limited differences between PCA and functional PCA other than that principal components of functional PCA describe the 'typical' shape of the input waveforms (Epifanio et al., 2008). Functional PCA identifies the greatest phases of variation and the features which can explain the variance of these phases. Warmenhoven et al. (2018) examined the results of functional data analysis and SPM *t*-tests and found that both approaches identified similar phases of significant difference. While functional PCA for waveform analysis has grown in popularity over the recent years, PCA is an exploratory approach to data analysis to assess large datasets when a clear hypothesis is not possible. This is the opposite approach to that of SPM which is used to analyse specific hypotheses. It was also suggested by Warmenhoven et al. (2018) that SPM would be more suitable for waveform analysis on specific regions of interest (i.e. step-to-step transition).

ACP is not a statistical approach to analysing waveform data, but rather a method that reduces waveform data to discrete points (Richter et al., 2014c). This approach was developed in the attempt to deal with the issues surrounding DPA (Section 2.6.). ACP first utilises PCA to identify phases of variation within a single waveform. Within the phase of variation identified by PCA, the average magnitude value is calculated to provide a discrete point for further analysis. This approach removes the issues surrounding waveform analysis and allows the waveform data to provide the

'key' discrete points of interest. ACP has been demonstrated to be more effective in identifying performance related features compared to DPA (99% vs 21%, respectively) (Richter et al., 2014c). However, the main problem with this approach is the manner in which the waveform phase of interest is reduced. It is possible that differences between groups that are detected through PCA may no longer be significantly different when reduced to this average discrete point. For example, when the magnitude of a feature increases or decreases quickly, such as loading rates or dynamic joint movement, the average value of the magnitude may not appropriately reflect the waveform data. Therefore, SPM was utilised in this thesis to perform waveform analysis based on a hypothesis-driven approach.

2.11. Summary and Thesis Aims

It is thought that greater than normal loading is a determinant of the onset and progression of joint degeneration. The intact limb of ITTAs is at a greater risk of developing knee joint degenerative diseases, yet the current literature is unclear if high load, as a mechanism of the disease, occurs in the intact limb compared to able-bodied controls. It is possible that these inconclusive results could be, in part, that: 1) commonly research loading features are discrete in nature, 2) overloading may possibly occur in other non-established loading features (e.g. KFM), and 3) overloading may occur in tasks outside of level-walking gait that have greater load and joint movement demands. Identification of the phases in which overloading occurs and those strategies that may be utilised to reduce load are important in decreasing the risk of developing degenerative diseases in the amputee population. Before implementation of intervention strategies, the influential and key mechanics on the development of load must be understood.

There are two distinct step descent strategies that have been demonstrated in the literature: an initial toe contact or an initial heel contact of the leading limb. The extent to which these descent strategies may influence the development of load in the

leading limb has not been examined. Thus, **the first main aim of this thesis was to 1) examine the limb and joint loading patterns in the leading limb and 2) determine any differences in the joint mechanics of the leading and trailing limbs when *able-bodied controls* performed a step descent (Chapter 4).** The descent strategy and compensatory joint mechanics utilised by established ITTAs when leading with the intact limb is unclear. Therefore, **the second main aim of this thesis was to examine the loading patterns in the intact leading limb and joint mechanics utilised in both limbs to perform a step descent compared to able-bodied controls (Chapter 5).** To provide clinical application for rehabilitation protocols and gait modification strategies, **the third main aim of this thesis was to identify key movement features in both the leading and trailing limbs that were associated with high load during a step descent (Chapter 6).**

Dynamic walking theory models have provided evidence that between-limb influences are present in walking gait. Reduced propulsion from the trailing limb can consequently increase the magnitude and rate of load experienced on the leading limb. It is currently unknown if the intact limb, post-amputation, is able to attenuate load independent of any between-limb influences from the prosthetic limb and/or the requirement to continue forward progression. This could provide indications of deficiencies in the intact limb which may be useful for informing rehabilitation protocols. **The fourth main aim of this thesis was, therefore, to assess the shock absorption mechanics of the intact limb when attenuating load independent of the effects from the prosthetic limb or task demands by examining a unilateral drop landing (Chapter 7).**

ITTAs are encouraged to participate in sport and exercise yet are discouraged from participating in sports involving jumping. It is possible that influences from the prosthetic limb on the intact limb's absorption mechanics may be present when performing a bilateral landing. This could place ITTAs at a greater risk of joint

degeneration. However, there is limited evidence to suggest that a greater than normal load is experienced in the intact limb of ITTAs compared to able-bodied controls when landing from a jump. Additionally, it is unknown if between-limb influences occur during discrete in-phase tasks such as jump landings. Thus, **the fifth and final aim of this thesis, was to examine the load experienced in the intact limb during a bilateral drop landing to provide a greater understanding of the influence from the altered mechanics of prosthetic limb on the absorption mechanics of the intact limb (Chapter 8).**

Chapter 3.

Methods

This chapter presents the methods completed in preparation for data collection, the data collection protocol, and the data processing and analysis conducted for step descent and drop landing tasks.

3.1. Ethical Approval and Participant Recruitment

The research for this project was submitted for ethics consideration under the reference LSC 16/ 176 in the Department of Life Sciences and was approved under the procedures of the University of Roehampton's Ethics Committee on 11/07/16 (Appendix A1). Recruitment for two groups of participants (one for individuals with a transtibial amputation (ITTA) and the second for able-bodied individuals) was completed through posters and word-of-mouth. Additionally, amputees were approached at multiple amputee charities and through prosthetic companies including, but not limited to, LimbPower, Blatchford Prosthetics, Douglas Bader Foundation, Help for Heroes, BLESMA, and the Tennis Foundation. Due to limited response from ITTA participants, an ethical application was submitted and approved by the National Health Services (NHS) Health Research Authority under the reference number 17/NW/0566 (Appendix A2). Two NHS limb-fitting centres agreed to facilitate recruitment through identification of potential ITTA participants. Each NHS site was provided with flyers and posters to distribute and display. Additionally, the sites were provided a 'consent to contact' form (Appendix A3) for those potential participants that wanted to receive additional information regarding the project.

All potential participants were provided an information sheet (Appendix A4) informing them of the purpose of the study, the protocol to be used including any risk involved, and their right to withdraw from all or parts of the study at any time without needing to provide a reason. Participants provided written informed consent (Appendix A5 & A6) upon their first visit to the biomechanics laboratory at the University of Roehampton. Participants were compensated £10 in cash per session (£30 in total) for their time and effort (Appendix A7). Amputee participants were provided up to an additional £20 per session to cover travel expenses upon providing a ticket receipt or details of distance driven (reimbursed at £0.45/mile; Appendix A8).

3.2. Participant Populations

Inclusion criteria required all participants to be between the ages of 20-50 years and partaking in moderate physical activity a minimum of 2-3 days per week. Moderate physical activity was defined by the international physical activity questionnaire as any activity that makes you breathe somewhat harder than normal. Amputee inclusion criteria for this study were individuals with a unilateral transtibial amputation where amputations were as a result of traumatic incidence (e.g., auto accident). Additionally, ITTA participants included in the study had a grading of K3/K4 which denotes that an amputee “has the ability or potential for ambulation with variable cadence and to negotiate environmental barriers outside the home” and “has the ability or potential for prosthetic ambulation that exceeds basic ambulation skills, exhibiting high impact, stress, or energy levels” (Orendurff et al., 2016). This K-level was deemed necessary to ensure those ITTAs participating in the study would be able to safely perform high impact tasks such as drop landing. Participants were excluded if they had sustained a musculoskeletal injury in the six months prior to participation in the research study. Amputee participants had to be at least six months’ post-amputation and were excluded if they experienced any pain or discomfort in the residual limb whilst using their prosthesis that affected their mobility.

Table 3.1. Amputee and matched able-bodied control participant characteristics and amputee prosthetic components

Participant	Age (years)	Mass (kg)	Height (cm)	Amputated Limb (R/L)	Time Since Amputation (years)	Prosthetic Components
1	29	82.3	174.6	R	5	Össur Re-flex Shock; TSB
2	48	81.5	179.7	L	29	Ottobock; TSB
3	38	114.4	184.5	L	16	Ottobock; TSB
4	48	83.4	183.7	R	2	RUSH HiPro; TSB
5	45	105.9	185.7	R	DNA	DNA; PTB
6	45	76.5	175.5	R	26	Össur Re-flex Shock; PTB
7	24	78.8	169.8	R	1.5	Endolite Blade XT; TSB
8	43	54.6	165.2	R	6	Endolite Elite VT; PTB
Mean (SD)	40.0 ± 9.0	84.5 ± 17.9	177.4 ± 7.4		12.2 ± 11.5	
Control (n = 22)	34.0 ± 6.5	83.4 ± 11.4	179.3 ± 6.2			

DNA = did not answer, TSB = total surface bearing socket, PTB = patellar tendon bearing socket

There were no gender exclusion criteria, however, all ITTA participants who volunteered were male, therefore, in order to match the two groups, only males were recruited to the able-bodied cohort. Recruitment provided eight ITTAs to participate in the research study. Table 3.1 presents the amputee physical characteristics and prosthetic components. All ITTA participants wore dynamic elastic response type prosthetics during testing. Additionally, a total of twenty-two able-bodied controls completed the study. No significant differences in age, height, or mass were found between the ITTA and control groups.

3.3. Equipment

3.3.1. Step Platform

Prior to data collection, a custom raised-surface walkway was constructed (Figure 3.1). Five square wooden boxes (100 cm width x 100 cm length) were constructed to create a 5 m long walkway. Previous research found that a 5 m walkway would allow enough space for participants to reach habitual walking speeds prior to any change in mechanics being made to perform a step descent (Barnett et al., 2014, Begg & Sparrow, 2000). The 100 cm width of the platform was chosen as the average width used in both step (Begg & Sparrow, 2000, Barnett et al., 2014, Delbaere et al., 2009) and stair negotiation studies (Buckley et al., 2013, Reeves et al., 2008, Mian et al., 2007). Lastly, the platform was constructed with a step height of 14 cm representing standard kerb height (Department of Transport, 2005).

The step platform was placed in the middle of a 10 m walkway with force platform (FP) placement as depicted in Figure 3.1. The step platform was constructed to allow for force data to be collected from both the trailing limb on the step platform and the leading limb on the ground in front of the step platform. To ensure clean force data with no interference from the step platform, the final wooden box (labelled Box A and B in Figure 3.1B) situated over the first FP (FP1) was constructed in two pieces (Lythgo et al., 2007). A separate wooden box (Box A) the same size as the FP (40

cm width x 60 cm length) was built to fit directly over FP1. This separate structure was built to be screwed into FP1 to ensure that no movement of the step platform occurred relative to the FP as participants stepped on the structure. Box B was then placed around the separate structure leaving a gap of 1 cm to ensure no interference in the capture of force data. The second and third FP (FP2 and FP3) were placed directly after FP1 to accommodate for differing step lengths between the ITTA and able-bodied populations.

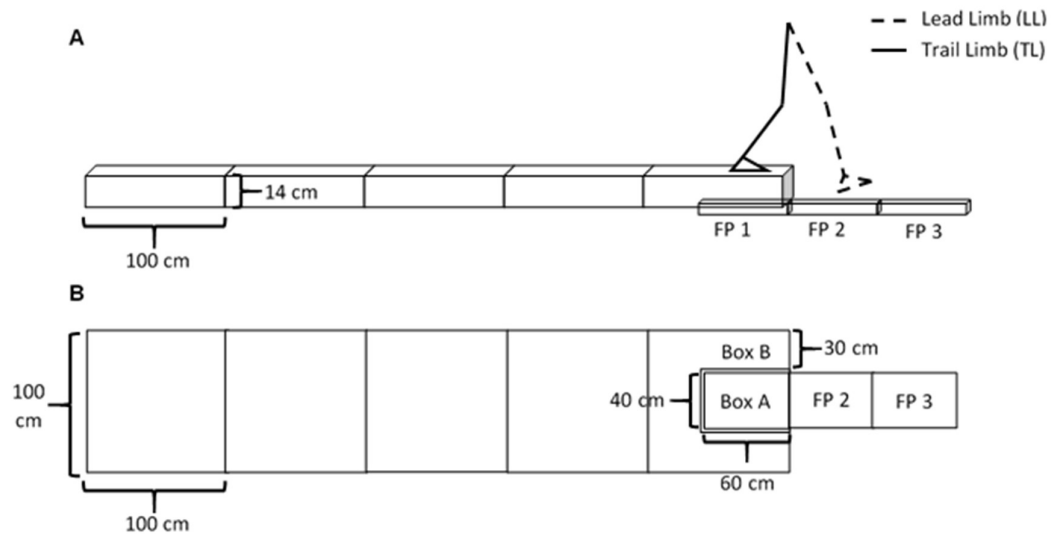


Figure 3.1. Dimensions of the step platform as seen from a A) side-view and B) top-view. Force platform (FP) positions relative to the end of the step platform are also depicted. The platform situated above FP1 was an independent structure from the rest of the platform.

To determine the accuracy of step platform force data, static vertical ground reaction force (vGRF) data were collected for three different increasing masses (~20, ~30, and ~40 kg) and compared to the FP1 force output without the step platform. Results from the static validation test are included in Appendix B1. The mean absolute error between the force output and the actual mass was similar with and without the step platform (step: 2.45 - 2.81N, no step: 2.26 - 3.21N; Table B1.1). The average difference in force (Table B1.2) between FP1 and FP1 with the step platform attached for ~20 kg mass was -4.50N, ~30 kg mass was -5.37N, and ~40 kg mass was -5.84N. Previous research has suggested that greater than 5N difference between FPs can

result in cumulative error in higher-order calculations (Rist et al., 2014, Wong et al., 2010). To address this, dynamic walking peak forces and impulses in the vertical and anterior-posterior directions during the braking phase of level-walking and peak knee external adduction moment data were captured from three participants as they walked across FP1 with and without the step platform. Results from dependent *t*-tests found no differences between conditions for any of the discrete dynamic walking features (Table B1.3). Both static and dynamic results found the constructed step platform provided accurate and reliable force data.

3.3.2. Drop Landing Frame

Traditionally, drop landing is performed by rolling off a box from a standardised height and landing in front of the box (Pappas et al., 2007a, Orishimo et al., 2009, Yeow, Lee et al., 2009a, Jones et al., 2014). There are three limitations associated with this technique: 1) participants can jump slightly raising the centre of mass which will change the vertical velocity at touchdown, 2) a horizontal velocity is introduced as participants are required to land in front of the box, and 3) ITTAs may find rolling off the edge of a box to be a difficult task to perform due to the constraints from the prosthesis. To address these issues, a metal drop landing frame was constructed. This frame allows for vertical adjustment of a hanging bar to ensure all participants drop the same distance to the ground (Figure 3.2). The hanging bar can be adjusted to the nearest centimetre by using a clamp to tighten the adjustment leg in place. As a safety feature, holes are positioned every 5 cm where a plunger bolt can hold the frame in place without the clamps. During data collection, the plunger was prepared to catch the frame in case the adjustment leg slipped allowing a maximum drop of up to 4 cm. To collect force data from both limbs individually, the width of the frame was built to encompass two FPs. Additionally, to ensure no interference of the drop landing frame with the force data, the leg stands were built 60 cm in depth to encompass either side of the FPs.

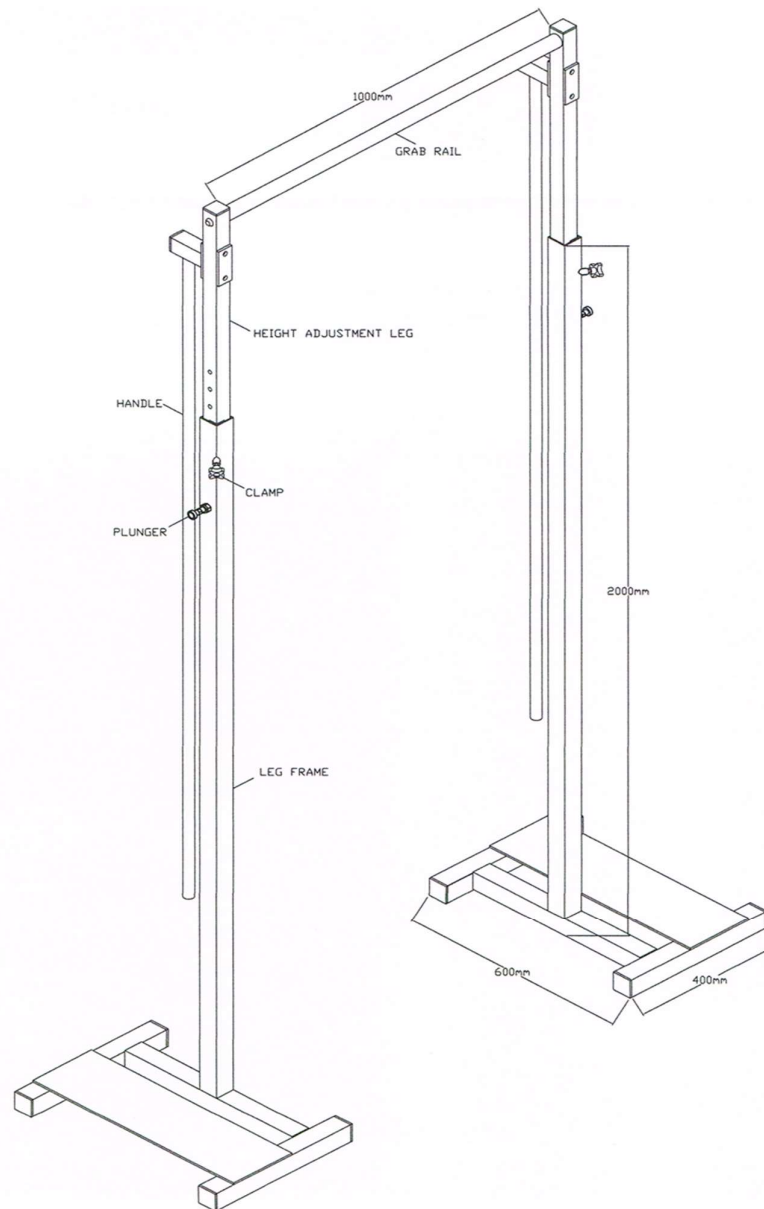


Figure 3.2. Drop landing frame with dimensions and safety features depicted

3.3.3. Hardware

3.3.3.1. Vicon Motion Systems

Kinematic data were collected using twelve Vicon Vantage V5 (Vicon Motion Systems Ltd.; Oxford, UK) motion capture cameras positioned above the area of movement mounted on a non-movable metal frame. The passive optical system tracks retroreflective markers to capture the spatial positioning of each marker. The markers

reflect light that is generated near the camera's lens. If a minimum of two cameras can capture the position of a marker during the same time point, a three-dimensional fix of the marker within the global coordinate system (GCS) can be obtained. The GCS is oriented based on the origin of the laboratory and was set between FP2 and FP3 defining 'z' as vertical, and 'x' along the short axis of the FP and 'y' along its length which corresponds with mediolateral and anterior-posterior directions in walking, respectively (Figure 3.3). Kinematic data were captured at 200Hz as a higher data collection frequency allows for more accurate event detection during tasks that happen quickly (i.e., drop landing).

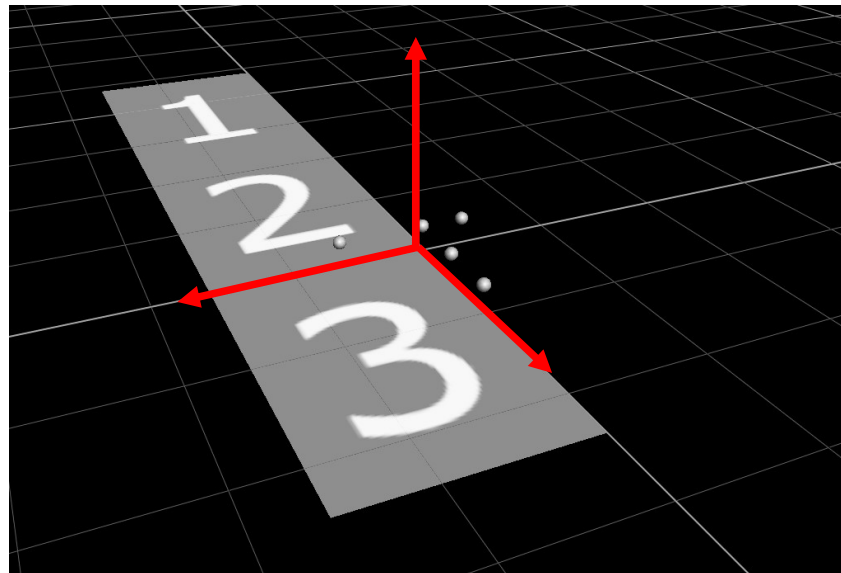


Figure 3.3. Origin of the global coordinate system as set by the Vicon Active Wand where positive values in each plane of motion are denoted by the direction of the red arrows

Before the commencement of data collection, the reliability and accuracy of the Vicon system was assessed. Static trials were collected using a rigid frame with markers attached at known distances from each other for ~10s (Figure B2.1). The average, standard deviation, and standard error of the mean (SEM) for the distance between markers in each direction were calculated across 5 trials. The maximum standard

deviation was 0.1 mm and maximum SEM was 0.9 mm (Table B2.1). System accuracy results are presented in full in Appendix B2.

The Vicon Nexus 2.6.1. system interface allows the integration of external devices such as the Kistler FPs (Type 9281c; Kistler Instruments Ltd., Hampshire, UK) in order to temporally align kinematic and kinetic data. System calibration, data collection and data processing were completed using this software.

3.3.3.2. Kistler Force Platforms

Three Kistler FPs were used to collect force data at a sampling frequency of 1000 Hz and aligned sequentially to best capture all movement phases of interest. Kistler FP use four built-in piezoelectric force sensors located in the corners of each platform to measure applied force. Each force sensor has three compartments holding quartz crystals to collect force data in all three planes of motion. As mechanical force is applied to the crystal, the force is transformed into electrical charge. This charge is transferred as analogue data where it is converted to digital data through an analogue to digital convertor.

Vicon Motion Capture Systems recently added the ability to collect cross-platform strikes, i.e. where a single foot crosses two FPs in a single stance phase. The forces are summed across both FPs, while moments are combined by referring the secondary platform moment back to the origin of the primary plate (Vicon Nexus 2.5 Documentation). This feature limits the amount of time and effort on the participants and researchers to obtain successful trials. However, there are limited studies on the validity of cross-platform strikes (Exell et al., 2012). To determine the validity of cross-platform strikes, comparisons of force output and joint moments in both static and dynamic conditions were performed between strike conditions (Appendix B3). Static trials found standard deviation of the signal ranged from 1.54 – 2.44N and a mean absolute error from 1.56N – 4.69N (both maximums occurring in the cross-platform condition; Table B3.1). Dynamic walking trials were completed for one participant

performing three trials for each FP condition (full-platform: FP1, FP2, FP3 and cross-platform: FP1 & 2 and FP2 & 3). Statistical parametric mapping one-way ANOVAs were performed for vGRF, anterior-posterior GRF, and KAM waveforms (Figure B3.1). Results found no significant differences between full- and cross-platform strikes. Cross-platform foot strikes were still counted as invalid if both feet were in contact with the same FP at the same time.

3.4. Data Collection Protocol

The overall project was run in conjunction with another PhD student which involved three data collection sessions in total. The first two sessions undertaken by all participants involved muscle function testing in which participants visited the laboratory for two-three hours on two separate occasions that were 3-7 days apart. The first session was to familiarise the participants with the strength testing procedures. Familiarisation of the strength testing procedures is necessary to improve reliability of the strength data and remove the effects of learning (Maffiuletti et al., 2016). The second session collected the data for the strength measures. Strength data collection methods related to this thesis are presented in Chapter 7 Section 7.2.1. The procedure outlined below was the third session when data for the experimental chapters included in the thesis were captured. This methods chapter will only discuss the procedures for the collection of step descent and drop landing data, however, it should be noted that participants were also asked to complete walking, running, and countermovement jump tasks. The biomechanical testing procedure was performed in the following order: step descent/ascent, habitual and fast walking, jogging, running, bilateral and unilateral countermovement jumps, and bilateral and unilateral drop landings. Participants were provided rest between each change in task/task demand to ensure limited to no effects of fatigue on subsequent activities.

Participants were instructed to bring/wear shorts no longer than mid-thigh. For those

shorts that were too long and occluded marker detection, the shorts were taped up. To ensure no occlusion of upper body markers, participants did not wear a shirt throughout data collection.

3.4.1. System Calibration

Prior to the arrival of the participant, the Vicon cameras were turned on for a minimum of 20 minutes before system calibration was completed. First, a dynamic calibration was performed using the Vicon Active Wand. The Vicon Active Wand contains five light-emitting diodes (LED) to calibrate the relative position of each camera according to the other cameras. The wand was moved through the anticipated data capture volume producing a 'cloud' of markers. When a minimum of two cameras detected an LED, the 3D position of the LED was reconstructed, and the location of the cameras position relative to the other was determined. Dynamic calibration was deemed successful when the image error rates were ≤ 1.5 mm indicating a good accuracy of the 3D spatial reconstruction of the LEDs. Following dynamic calibration, the Vicon Active Wand was used for the static calibration to set the cameras relative to the GCS. FPs were calibrated in an unloaded state by setting the zero level. When the step descent platform was attached, FP1 was re-zeroed. FPs were considered functioning correctly when the Newton difference between all FPs was ≤ 5 N. The FPs were re-calibrated between each change of task conditions to ensure accuracy of the data collected. Force data were collected at 1000Hz to accurately capture the movement of faster tasks such as drop landings.

3.4.2. Anthropometric Measures

Body mass and height were taken first. A second height measure was taken with arms stretched reaching to the ceiling with the feet flat on the ground. This measurement was used to prepare the drop landing frame for later in the session. The following measures were taken bilaterally using a sliding calliper:

Ankle Width:	distance between the medial and lateral malleolus of the tibia and fibula, respectively
Knee Width:	distance between the medial and lateral epicondyle of the femur
Leg Length:	distance from the most prominent portion of the anterior superior iliac spine to the medial malleolus of the tibia
Elbow Width:	distance between the medial and lateral epicondyle of the humerus
Wrist Width:	distance between the radial and ulnar styloid processes
Hand Thickness:	distance between the dorsal and palmar surfaces of the hand taken at the point of flexion of the second metacarpal joint
Shoulder Offset:	vertical distance from the acromion clavicular joint to the centre of the glenohumeral joint

This sequence of measurements was performed twice. If the difference between the two values for a given measure was greater than 2 mm, a third measurement was taken. An average of two measurements that were within 2 mm of each other was used as the input to the Plug-In Gait model in Vicon Nexus 2.6.1.

3.4.3. Marker Placement and Participant Calibration

Forty-three retroreflective markers (diameter: 14 mm) in total were attached directly to the skin using double-sided tape. Thirty-nine of these markers were placed in accordance with the full-body marker set outlined by Davis et al. (1991) (Figure 3.4). Four markers were placed bilaterally on the anterior aspects of the thigh and tibia to allow for the Symmetrical Axis of Rotation Approach (SARA) and Symmetrical Centre

of Rotation Estimation (SCoRE) model calibration. The prosthetic limb markers were placed on corresponding positions as the intact limb (Rusaw, D. & Ramstrand, 2011, Rusaw, David & Ramstrand, 2010, Kent & Franklyn-Miller, 2011).

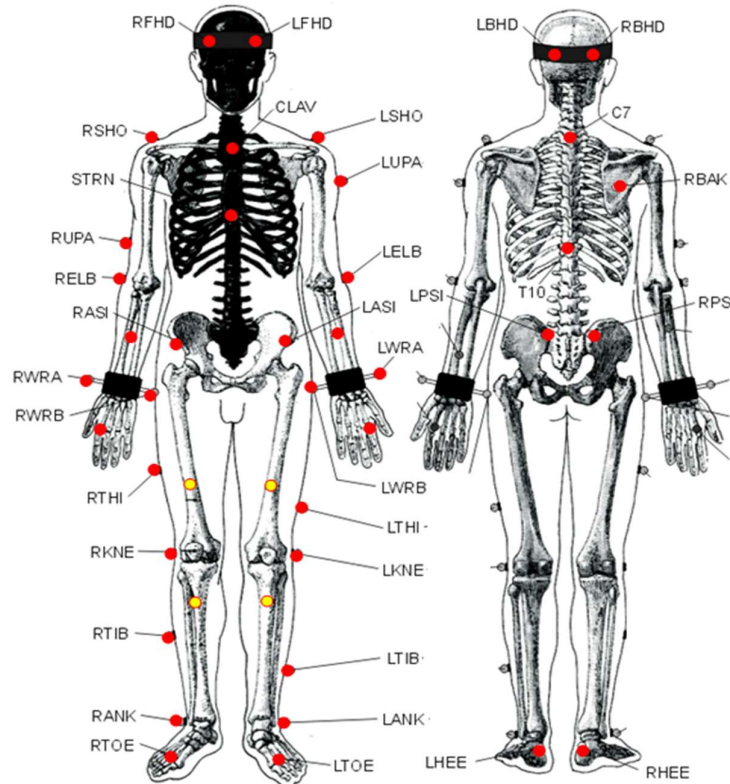


Figure 3.4. Marker placement as outlined by Davis et al. (1991) depicted by red dots and the extra SARA and SCoRE depicted by yellow dots.

Following marker placement, participant calibration (i.e. static trial) was performed to obtain participant specific reference locations for the markers to be used in data processing. Participants were asked to stand with their feet shoulder width apart, knees slightly bent, arms parallel with the floor, and elbows bent at a 90° angle. They were asked to hold this position looking straight ahead for 2 seconds. The static trial was then checked to ensure all markers were present and were clearly seen by the cameras.

3.4.3.1. Validation Test

An essential prerequisite to reliable determination of kinetic and kinematic data is the accurate assessment of skeletal joint centres. Biomechanical modelling software uses real marker trajectories and generates 'virtual' marker trajectories to represent joint centres. The Vicon Nexus model (Plug-in Gait, PiG) uses the Newington-Gage model to determine the hip joint centres (HJC) based on marker trajectories and anthropometric measures. The knee and ankle joint centres are calculated using a modified chord function.

Accurate calculations of joint centres highly depend on both reliable marker placement and anthropometric measures (Sinclair et al., 2012, Tsushima et al., 2003). To minimise this error prior to the commencement of data collection, the reliability of marker placement was investigated (Appendix B4). A within-day test-retest design was used. The inter-ASIS, ASIS to knee, and knee to ankle distances on both limbs were extracted during a 2-second capture of a static trial. The test-retest SEM for the average distance between markers on both limbs ranged from 0.02 – 0.17 mm with the greatest error occurring between the right ASIS and the knee joint marker position (0.17 mm) followed by the distance between the right knee and ankle joint markers (0.14 mm; Table B4.1). Results suggest that detection of anatomical landmarks and marker placement were reliable.

In recent years, a new modelling technique has been implemented by Vicon to address concerns regarding the accuracy of the knee and hip joint centre locations using the PiG model calculations. The optimum common shape technique (OCST) is a functional approach in identifying joint centres thought to provide more reliable kinematic outputs by reducing systematic errors, such as marker placement and skin movement artefacts (Taylor et al., 2010). The main purpose of SCoRE is to provide a more repeatable hip joint centre calculations (Ehrig et al., 2006), while SARA provides more repeatable knee joint centre calculations (Ehrig et al., 2007). In a study

that assessed the reliability of the OCST functional technique, intra-class correlation results both between-days and between investigators found the OCST functional technique to be more reliable than the standard regression technique implemented by Vicon (Taylor et al., 2010). However, both techniques had intra-class correlation scores great than 0.88, indicating excellent reliability. The SARA and SCoRE functional techniques were developed for clinical laboratories to reduce the systematic error associated with long-term studies. Due to the similarity in reliability, greater processing time required for OCST modelling, and that the current study was performed on a single day for a single session, the functional approach was not utilised in the current study.

3.4.4. Step Descent

To acclimate to the step platform, participants first performed a warm-up by walking the length of the lab (25 m) and stepped up and down as they reached the platform on either end. Participants walked at a self-selected pace until they felt comfortable negotiating the step platform. Once acclimated, data were collected while participants walked the length of the platform, stepped-down and continued to the end of the laboratory (10 m). Participants walked at a self-selected habitual pace and were given no instructions on which limb to lead with during the step descent. The dominant limb for the able-bodied control participants was determined as the first limb chosen to lead during descent. A minimum of five trials were collected for each limb leading (i.e., intact, prosthetic, dominant, and non-dominant). Once five trials were collected for the preferred/dominant leading limb, participants were then instructed to take their first step with the other limb. A trial was successful if the trailing limb foot was placed fully on the step platform and a successful strike was performed from the leading limb (e.g., no double hits on a single FP). A cross-platform strike was considered a successful strike for the leading limb in order to capture the natural performance of the task without restriction. When all step descent trials were collected, participants

were given a five-minute break while the step platform was removed.

3.4.5. Drop Landing

To remove the influence of jump height on landing techniques, drop landing was additionally performed both bilaterally and unilaterally. The ITTA population only performed the unilateral drop landing on the intact limb. Amputees were unable or chose not to perform a unilateral drop landing on to the prosthetic limb due to either balance issues or worries of pain upon impact in the residual limb. The drop landing frame was placed around two of the FPs to gather data from both limbs individually during the bilateral drop landing. The hanging bar was adjusted so that the participants were 30 cm off the ground as measured from the heel while hanging. This drop height was chosen as the typical drop height across multiple studies (Pappas et al., 2007a, Orishimo et al., 2009, Yeow et al., 2009a, Jones et al., 2014, Durall et al., 2011, Doherty et al., 2014, Ford et al., 2003). Following a demonstration, participants climbed a small step ladder (3 steps), held onto the hanging bar and slowly lowered themselves to a hanging position. An investigator was nearby to stabilise the participant once hanging. Participants were instructed to hold for one second after the investigator let go before dropping. On the first trial, participants were asked to hang for 2-3 seconds to check they were 30 cm off the ground by measuring the distance with a ruler from the ground to the bottom of the heel. Adjustments to the hanging bar were made, if necessary, and the heel height off the ground was checked in the next trial. This continued until the participants were 30 cm off the ground and typically only required 1-2 checks. Three successful trials were captured for both bilateral and unilateral drop landings. Trials were deemed unsuccessful if participants pulled themselves up before dropping, did not land with each foot on their individual FPs, or were unable to stabilise themselves from landing through to recovery.

3.5. Data Processing

Vicon Nexus 2.6.1. was used for data processing. First, the static trial was processed

to enable automatic detection of markers in the dynamic trials. Any gaps were filled (discussed below), and the Plug-In Gait static pipeline was used. Dynamic trial markers were then automatically labelled based on the static trial configuration and checked for accuracy.

If 2 or fewer cameras were able to detect a marker at any given time during dynamic trials, marker data for the duration of the time undetected was not captured. These marker trajectories were gap filled first using a cubic spline interpolation for all gaps less than 10 frames. In Vicon Nexus, the spline fill requires a minimum of 5 valid frames before and after the gap. For gaps larger than 10 frames, judgement was used to determine if spline fill appropriately matched the movement pattern. Any trials that had larger than 40 frame gaps were excluded from further analysis.

Raw marker trajectories and analogue force data were filtered using a low-pass zero-lag fourth-order Butterworth filter. This type of filter is the most commonly used in biomechanics as it effectively reduces random noise while ensuring no time phase shifting of the signal (Yu et al., 1999). Kinematic cut-off frequencies were 10Hz for step descent and 15 Hz for drop landings. Force data were filtered with a cut-off frequency of 200Hz. Cut-off frequencies were determined through both a residual analysis and based on previous literature for the respective tasks to determine the optimum signal to noise ratio (Winter, 2009, Robertson et al., 2013). Kinematic and kinetic cut-off frequencies were set at different levels to ensure no loss of physiologically meaningful data in the GRF signal (Roewer et al., 2014).

Three trials were used for all tasks in subsequent analysis (Diss, 2001). If more than three successful trials collected were processed fully with no issues, the best three step descent trials were picked based on two criteria: 1) remove leading limb cross-platform strike trials, and 2) include trials with the closest performed walking speeds. Three drop landing trials were collected, and all three were utilised for further analysis. These selected trials were exported as C3D files and averaged for subsequent data

analysis in all tasks.

3.6. Data Analysis

All data extraction and statistical analyses were performed in MatLab (R2017a, The Mathworks Inc, Natick, MA) using both custom-written code and open-source spm1d code (v.M0.4.5, www.spm1d.org). Each experimental chapter underwent similar extraction and analysis procedures. All data were normally distributed as determined by the Shapiro-Wilk test of normality for the discrete features ($p > 0.05$) and based on normality tests in SPM for loading waveform features ($p > 0.05$).

3.6.1. Loading Features Extracted

The loading waveforms extracted were the same for both tasks. The loading waveforms extracted for analysis include the GRF, external knee moments, and intersegmental knee forces in all three planes of motion for a total of 9 waveforms.

Vicon Motion Capture defines the planes of each loading feature as:

GRF	X	Lateral-Medial
	Y	Anterior-Posterior
	Z	Vertical
Knee Moment	X	Flexion-Extension
	Y	Adduction-Abduction
	Z	Internal-External Rotation
Intersegmental Knee Forces	X	Anterior-Posterior
	Y	Lateral-Medial
	Z	Tension-Compression

where the first direction represents positive values.

These loading features were analysed as they have either been found to directly relate to cartilage degeneration in the knee joint or represent key features to assess medial compartment knee joint loading. All loading features were extracted from the intact limb of ITTAs and the dominant limb of control group(s). Step descent dominance was determined as the limb that was chosen to lead first with no instruction from the investigators. Drop landing control limb dominance was defined as the limb chosen first to perform a unilateral landing. Limb dominance was the same for both tasks for all except two control participants.

All waveforms were extracted from initial contact to the end of the braking/absorption phase which represents the step-to-step transition. Initial contact was determined based on a 20 N threshold of the raw vGRF data sampled at 1000Hz. Initial contact for those data sampled at 200Hz (i.e. joint moments) were determined as the nearest time frame after dividing the time point of initial contact of the raw vGRF data by 5. The end of the braking/absorption phase was determined as the last negative value in the anterior-posterior GRF for step descent, and the time point of maximum knee flexion for drop landing. All waveform data were time normalised to 100% based on the average length of the braking/absorption phase across all participants to avoid over-stretching or -shrinking of the data (Page & Epifanio, 2007). Step descent had an average braking phase length of 60 frames, whereas drop landing had an average absorption phase length of 40 frames.

3.6.2. Statistical Parametric Mapping Methods

Pataky and colleagues developed a free open-source software package in MatLab, statistical parametric mapping (SPM), for the testing of waveform data including a wide range of statistical tests. The statistical functions can be implemented into custom-written code and are performed following data processing and extraction of data. Waveform data must be time-normalised to align all trials to the same length prior to input into the analysis. Time-normalisation matches the length of different

trials by linearly converting the time-domain (frames or seconds) to a percentage of time (0-100%). Waveform analyses through SPM are then performed in the same manner as any other statistical software and is dependent on the research questions and hypotheses.

3.6.3. Loading Waveform Pilot Studies

3.6.3.1. Pilot Study 1: Landmark Registration

This pilot study was conducted to determine if landmark registration improves the ability to predict performance measures. This method could reduce the inherent waveform timing/phase variability. To assess this, the vGRF waveform during the take-off phase of a countermovement jump was utilised as an experimental model. The countermovement jump was chosen as it has a good performance indicator (jump height) and the vGRF waveform theoretically holds all the information necessary to describe jump height based on the impulse-momentum relationship. The results from this pilot study, which was subsequently published in the *Journal of Biomechanics* (Moudy et al., 2018), found that a landmark registered waveform was able to increase the prediction power to jump height by up to 21% as compared to a time-normalised waveform. This suggests that landmark registration is able to reduce the timing/phase variability and can increase the physiological validity of waveform analyses.

A secondary aim of this pilot study was to investigate two key issues that could impact the analysis of waveforms after employing landmark registration: the position of the landmark (i.e. key events) and the number of landmarks chosen. It is difficult to determine the optimal landmark positions as these can change based on the movement task demands and research questions. When assessing a specific phase of interest, landmark registration may not be necessary. For example, the prediction power to jump height was 87% when assessing vGRF in the concentric phase only. When assessing the vGRF over the entire take-off phase and registering to the beginning of the concentric phase, 86% of the variation in jump height was predicted

(Moudy et al., 2018). This suggests that, when aligned with the research questions, analysis of the specific phase of interest can be just as powerful without registration.

The second key issue addressed was determining the optimal number of landmarks for the creation of the time-warping function. This pilot study found that one landmark provided the greatest ability to align phases of the waveform without the risk of over-registration. When an additional landmark was added, the ability to predict a performance measure reduced by 15% suggesting that over-registration of the waveform had occurred. Each subsequent addition of landmarks, up to 4 landmarks, were unable to return the prediction power to that performed by one landmark. Over-registration can occur when the physiological features of a waveform are warped too much. This can result in features that are important to the neuromuscular requirements of the task to be undetected during waveform analysis. Thus, the results from this pilot study denote that the use of landmark registration should be made on a case-by-case basis (Crane et al., 2010) with consideration of the above issues.

3.6.3.2. Pilot Study 2: Level-Walking Gait Analysis

This thesis postulates that the ambiguity in the commonly researched vGRF and KAM loading features in previous amputee walking gait studies is possibly due to their discrete nature (e.g., peak magnitudes). This pilot study aimed to examine if the ITTA population who participated in the current thesis exhibited increased load in the vGRF and KAM discrete features. This pilot study also aimed to determine if waveform analysis could detect any high load that was not detected by discrete point analysis (DPA). vGRF and KAM loading waveforms and commonly researched discrete loading features (loading rates and peak magnitudes) were extracted from the intact limb of ITTAs ($n = 8$) and able-bodied control limbs ($n = 22$) during habitual level-walking gait. Waveforms were extracted from initial contact, based on a 20 N threshold of the vGRF, to the end of the braking phase. The end of the braking phase was determined as the last negative point in the anterior-posterior GRF. Loading rates

were calculated by dividing peak magnitude by the time taken to reach peak magnitude from initial contact. Independent *t*-tests were performed to determine differences between the intact limb of ITTAs and able-bodied control limbs. SPM was used to assess the loading waveforms. Analyses of covariance (ANCOVA) were used to account for differences in walking speed ($p = 0.031$; ITTA: 1.37 ± 0.17 m/s, Control: 1.53 ± 0.17 m/s).

No significant differences between groups were found for either discrete features (Table 3.2) or loading waveforms (Figure 3.5). After covarying for speed, the intact limb had significantly greater peak vGRF ($p < 0.001$) and vGRF loading rates ($p = 0.022$). Waveform analysis, after point-by-point ANCOVA, indicated significantly greater vGRF from 21-55% of the absorption phase ($p = 0.010$; †highlighted phase denoted in Figure 3.5). The phase of interest included both the loading rate and peak vGRF. This confirms that waveform analysis can detect significant differences similarly to DPA. Additionally, slower walking speeds may be a compensatory mechanism utilised in level-walking gait to reduce load. While waveform analysis did not indicate differences beyond those that were detected by DPA in level-walking gait, it is possible that waveform analysis will be able to detect differences in other tasks such as step descent when the load demand is increased.

Table 3.2. Discrete loading features (mean \pm SD) during habitual level-walking gait for the intact limb of ITTAs and control limbs

	ITTA	Control	<i>p</i> -value
vGRF			
<i>Peak (N/kg)</i>	12.3 \pm 1.4	12.0 \pm 1.2	0.489
<i>Loading Rate (N/kg/s)</i>	81.7 \pm 21	83.5 \pm 15	0.804
KAM			
<i>Peak (Nm/kg)</i>	0.63 \pm 0.3	0.74 \pm 0.3	0.436
<i>Loading Rate (Nm/kg/s)</i>	4.93 \pm 1.4	5.72 \pm 1.8	0.271

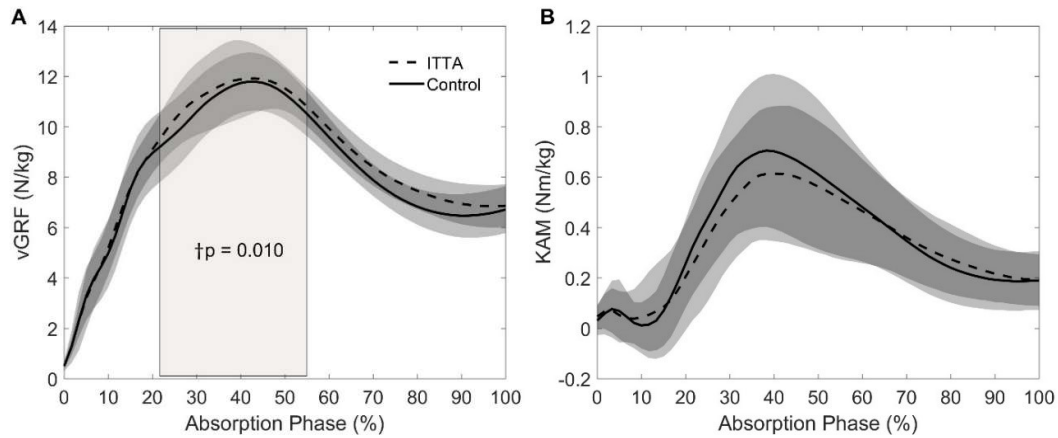


Figure 3.5. A) vGRF and B) KAM loading waveforms for the intact limb of ITTAs (dashed line; $n = 8$) and control limbs (solid line, $n = 22$) during the absorption phase of habitual level-walking gait. †highlighted area represents the phase that became significant after covarying for speed with p -value noted. Each group's waveform data represents the mean of each participant's mean data.

This thesis and previous literature have also postulated that loading features outside of those typically examined (e.g. knee flexor moment, intersegmental knee forces) could indicate overloading in walking gait. Waveform analysis was additionally performed on the anterior-posterior and medial-lateral GRF; knee flexor and rotational moments; and the anterior, medial, and compressive intersegmental knee forces. DPA was not conducted on these loading waveforms given the lack of past research to identify *a priori* appropriate features which could be extracted for a DPA and results from the above analysis indicated that DPA and waveform analysis detect similar significant differences. No significant differences were present between the intact limb of ITTAs and controls limbs for any loading waveform (Figure 3.6). After covarying for speed, the compressive knee force was significantly greater in the intact limb from 23-55% of the braking phase ($p = 0.007$). This phase corresponds with the significant phase from the vGRF after covarying for speed. This suggests that there is an indication of overloading occurring in level-walking gait in features other than vGRF and KAM, yet this overloading is being reduced by decreases in walking speed. Given the limited significant differences and the increased risk of joint degeneration in the

intact limb of ITTAs, it is possible that overloading, if it is a mechanism of joint degeneration in this population, may be more prominent in other high impact activities that have greater load demand, such as step descent.

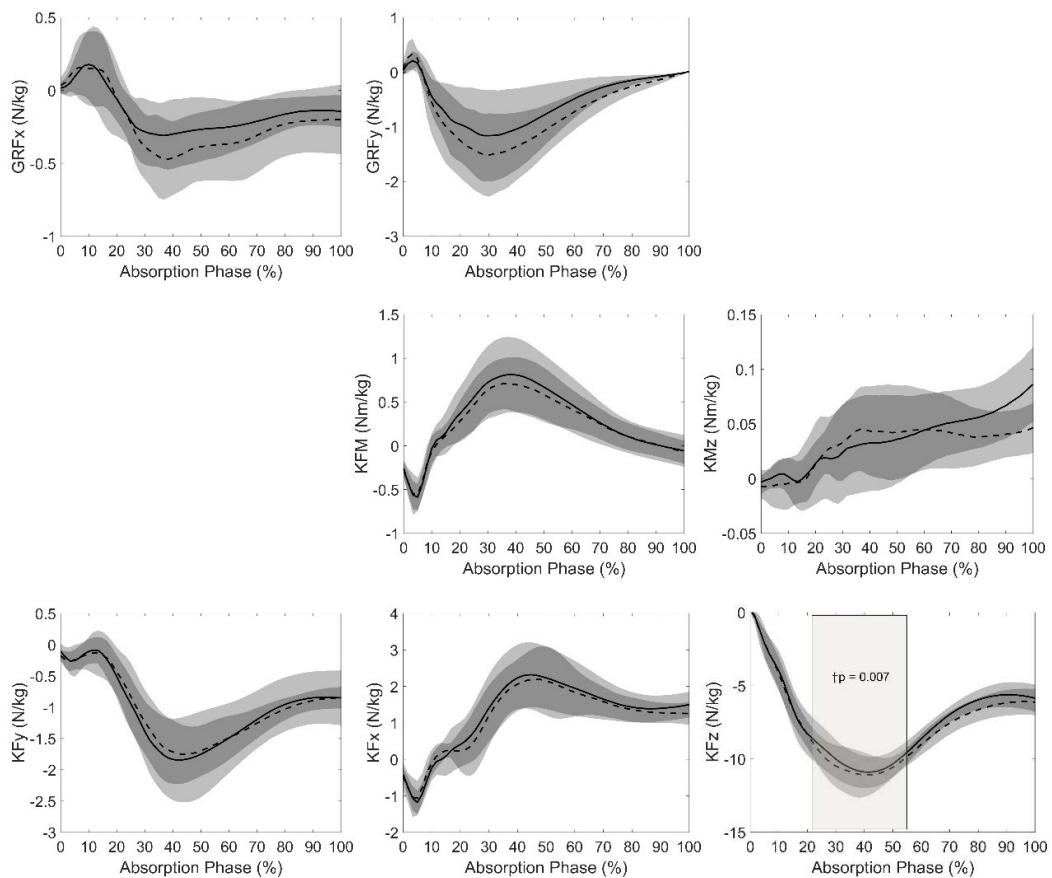


Figure 3.6. Loading waveforms for the intact limb of ITTAs (dashed line; $n = 8$) and control limbs (solid line; $n = 22$) during the absorption phase of habitual level-walking gait. [†]highlighted area represents the phase that became significant after covarying for speed with p -value noted. Each group's waveform data represents the mean of each participant's mean data.

3.6.4. Movement Features Extracted

The specific joint mechanic features extracted for each high impact task are discussed in detail within each experimental chapter methods sections. These movement features included joint angles, ROM, lower-limb joint coordination, powers, and work done as measures of shock absorption. These features have been previously shown to be 1) important in the performance of a step descent (van Dieën

et al., 2008, Barnett et al., 2014), 2) measures of shock absorption in other activities (DeVita & Skelly, 1992, Pollard et al., 2010, Blackburn & Padua, 2009, Norcross et al., 2010), and 3) representations of the spring-mass model and how the body attenuates a force (McGowan et al., 2012, Blickhan, 1989, Butler et al., 2003).

In this thesis, joint coordination was calculated by determining coupling angles as a simple approach to quantify joint coordination. This approach does not require a greater amount of data manipulation than that required to calculate joint angles (Hamill et al., 2000). Additionally, coupling angles provide an easy interpretation of the joint coupling mechanisms during dynamic movement that is lost when utilising other measures of coordination (e.g. continuous relative phasing).

3.6.4.1. Calculation of Coupling Angles

Coupling angles are calculated from an angle-angle plot. An angle-angle plot is simply the relation of one joint motion relative to a secondary joint motion over time (Figure 3.7).

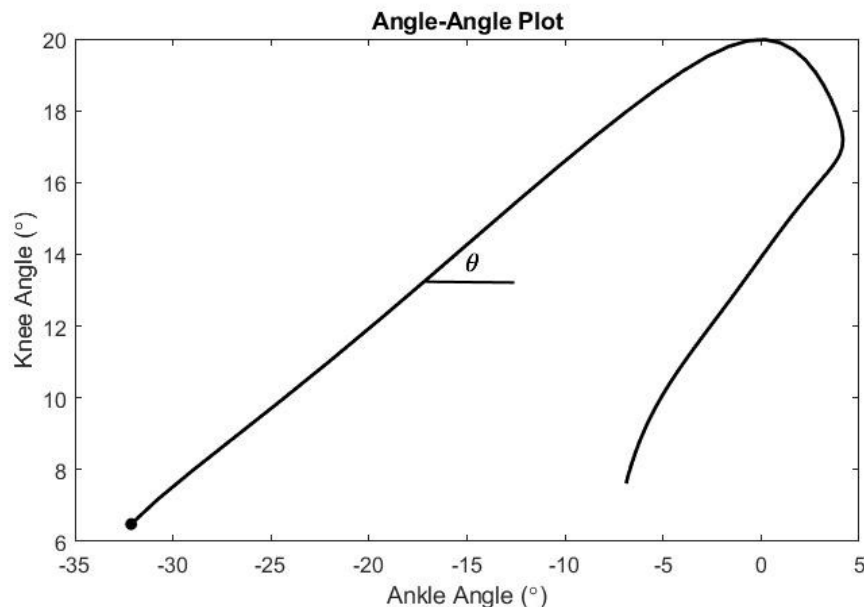


Figure 3.7. An example of an angle-angle plot for sagittal plane ankle and knee joint motion performed in the leading limb during a step descent for the braking phase. Initial contact is denoted by the black circle. The coupling angle is represented by θ .

The coupling angle (θ) is calculated as the angular orientation between two adjacent points relative to the right horizontal (Sparrow et al., 1987, Tepavac & Field-Fote, 2001, Chang et al., 2008). The coupling angle is calculated by using the following equations:

$$\theta_t = \tan^{-1} \left(\frac{Y_{t+1} - Y_t}{X_{t+1} - X_t} \right), \text{ where } t = \text{time points}$$

Y represents the distal joint angular position, and X represents the proximal joint angular position.

if $\theta < 0$

$$\theta_t = \theta_t + 2\pi$$

The output from the above calculations represent the coupling angle in radians and can be converted to degrees by the following:

$$\theta = \frac{180^\circ}{\theta\pi}$$

This results in a range of coupling angle values from 0° to 360° (Figure 3.8). Coupling angles of 0° , 90° , 180° , and 270° represent single joint movement and 45° , 135° , 225° , and 315° indicate equal motion between the two joints (Hamill et al., 2000). When the proximal joint is moving individually, the coupling angle is 0° or 180° whereas 90° and 270° represents distal joint motion. When the two joints are moving equally in the same direction (in-phase strategy), the values are 45° and 225° . Equal, but opposite joint movement (anti-phase strategy), occurs at 135° and 315° . The discontinuity seen in Figure 3.8 at $\sim 20\%$ of the absorption phase represents a redundancy in the coupling angles (i.e., 0° and 360° represent the same joint motion).

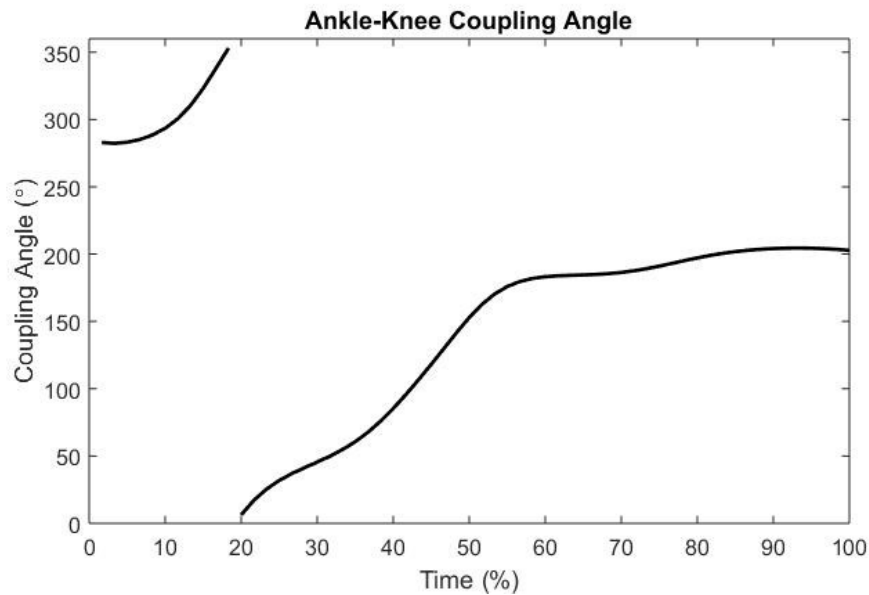


Figure 3.8. Coupling angle calculated from ankle-knee angle-angle plot for a single participant performing an initial heel contact during step descent throughout the braking phase.

After calculating the coupling angles, these values can be used similar to any other movement feature extracted and can be input into traditional statistical analyses. Waveform analysis of the coupling angles was not possible due to the issues surrounding the $0^{\circ}/360^{\circ}$ position. These values denote the same coordination approach yet can result in 'cliffs' making waveform analysis results difficult to interpret (Figure 3.11). Therefore, an appropriate reduction of the waveforms was necessary for further comparisons between ITTAs and able-bodied controls in both step descent and drop landing tasks.

In the leading limb during step descent, 'cliffs' were predominant in the initial heel contact (HC) group (Figure 3.9). Therefore, the leading limb average coupling angle was calculated for the duration of the double support phase (denoted by vertical dashed line). This approach was deemed appropriate as the waveform was relatively flat during the double support phase for ITTAs and controls performing a toe contact strategy (TC), the majority of differences occurred in this phase between groups, and

after double support ended there were limited differences present between groups. As the double support phase concluded after the ‘cliffs’ appeared for the HC group, the values after the ‘cliff’ were continued upwards past 360° . This was done to ensure that values close to 360° were not being averaged with values close to 0° which would result in average values of $\sim 180^\circ$ that are not indicative of the coordination strategy performed. If average values were above 360° , this would denote a coupling angle value of slightly above 0° . However, this did not occur as all average values for the HC group were below 360° .

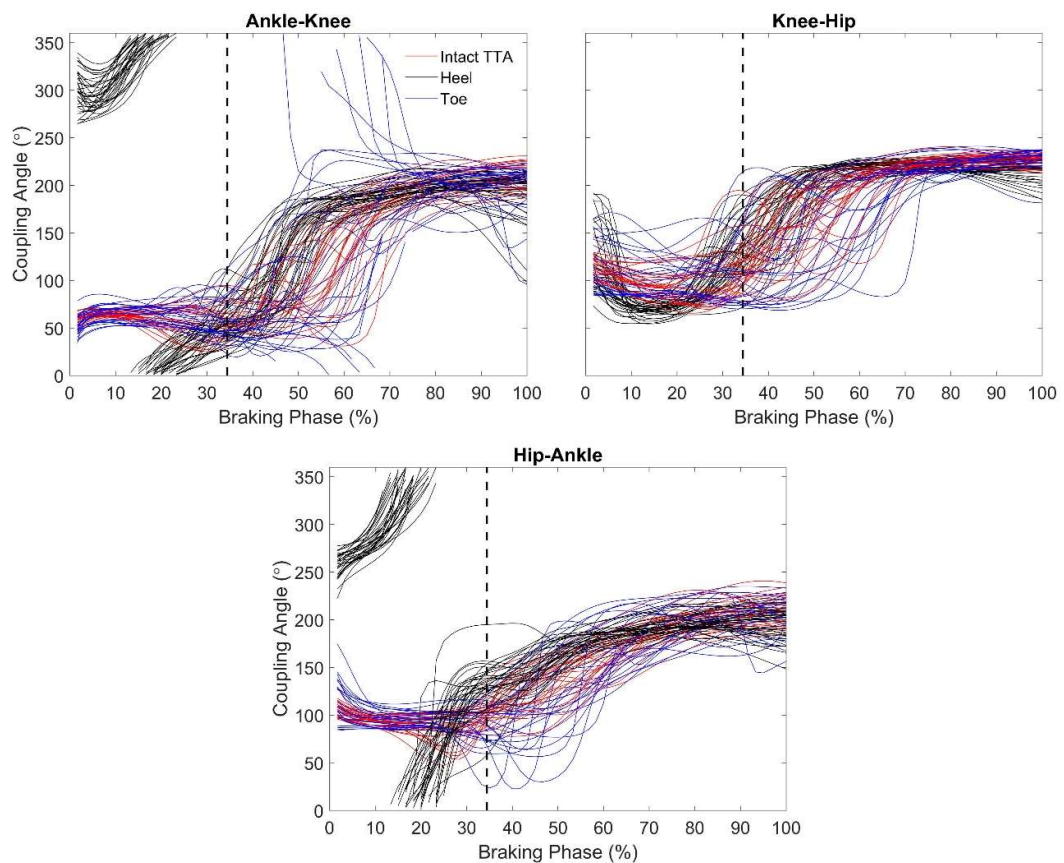


Figure 3.9. Lower-limb joint pair coupling angle waveforms for the duration of the braking phase in the leading limb for the heel initial contact (black), toe initial contact (red), and intact limb of ITTAs (blue) groups. The vertical dashed line denotes the end of the double support phase. Three trials for each participant is presented.

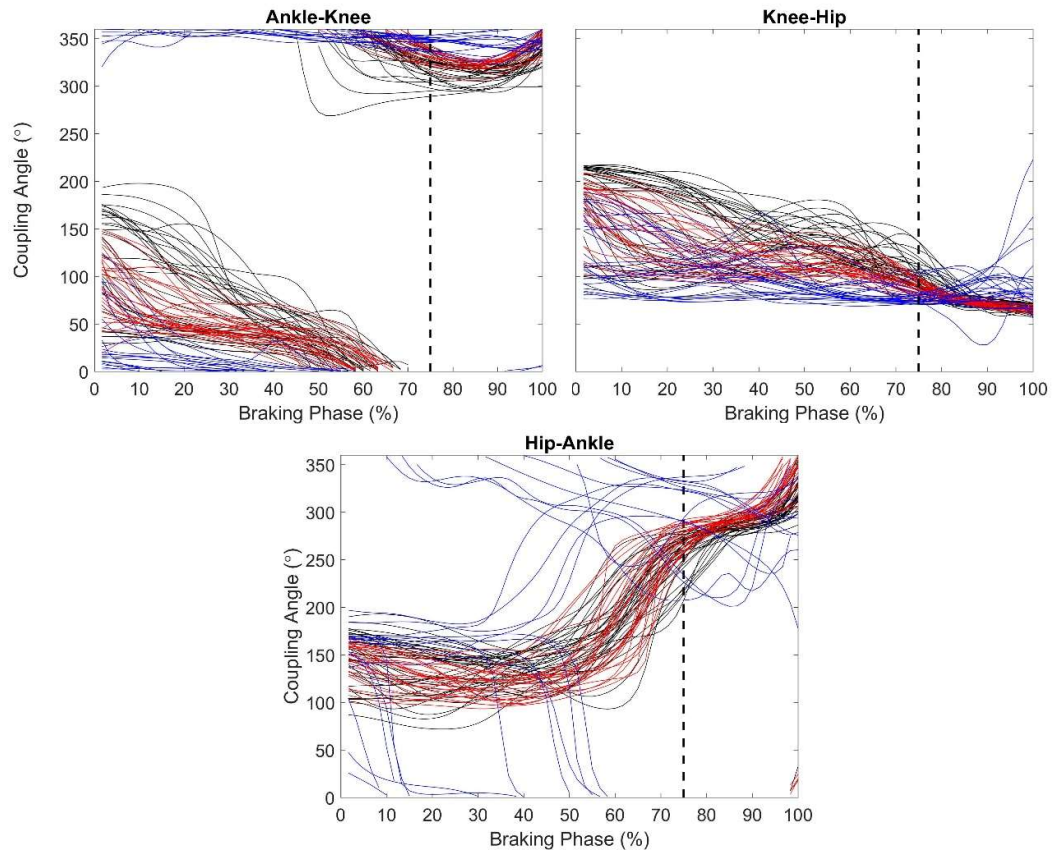


Figure 3.10. Trailing limb lower-limb joint pair coupling angle waveforms for the heel initial contact (black), toe initial contact (red), and intact limb of ITTAs (blue) groups. The vertical dashed line denotes the end of the single limb support phase. Three trials for each participant is presented.

The trailing limb had two phases of interest: single limb support (phase 1) and double limb support (phase 2). For phase 1, the coupling angles for the knee-hip and hip-ankle joint pairs were relative flat (Figure 3.10). The ankle-knee coupling angles, however, presented with a constant negative slope. This coupling angle could be reduced by calculating the difference in the coupling angle at the beginning of the phase to the end of the phase. However, the constant negative slope was only apparent for the HC group and only in the ankle-knee joint pair. Therefore, the average coupling angle was calculated for phase 1 and phase 2. As the hip-ankle joint pair does have a definite shift in coupling angle strategy from ~60-75% of the braking phase (representing the shift into the propulsion phase), this portion of the

phase was removed from the average calculation for phase 1. Both the HC and TC groups had limited ‘cliffs’ during both phases of the trailing limb for all lower-limb joint pairs. The prosthetic limb of ITTAs, however, had many ‘cliffs’ within the ankle-knee joint pair coupling angle which denotes a coupling angle around the $0^{\circ}/360^{\circ}$ point with limited changes across the single and double support trailing limb phases. This was adequately represented by the reduction utilised above.

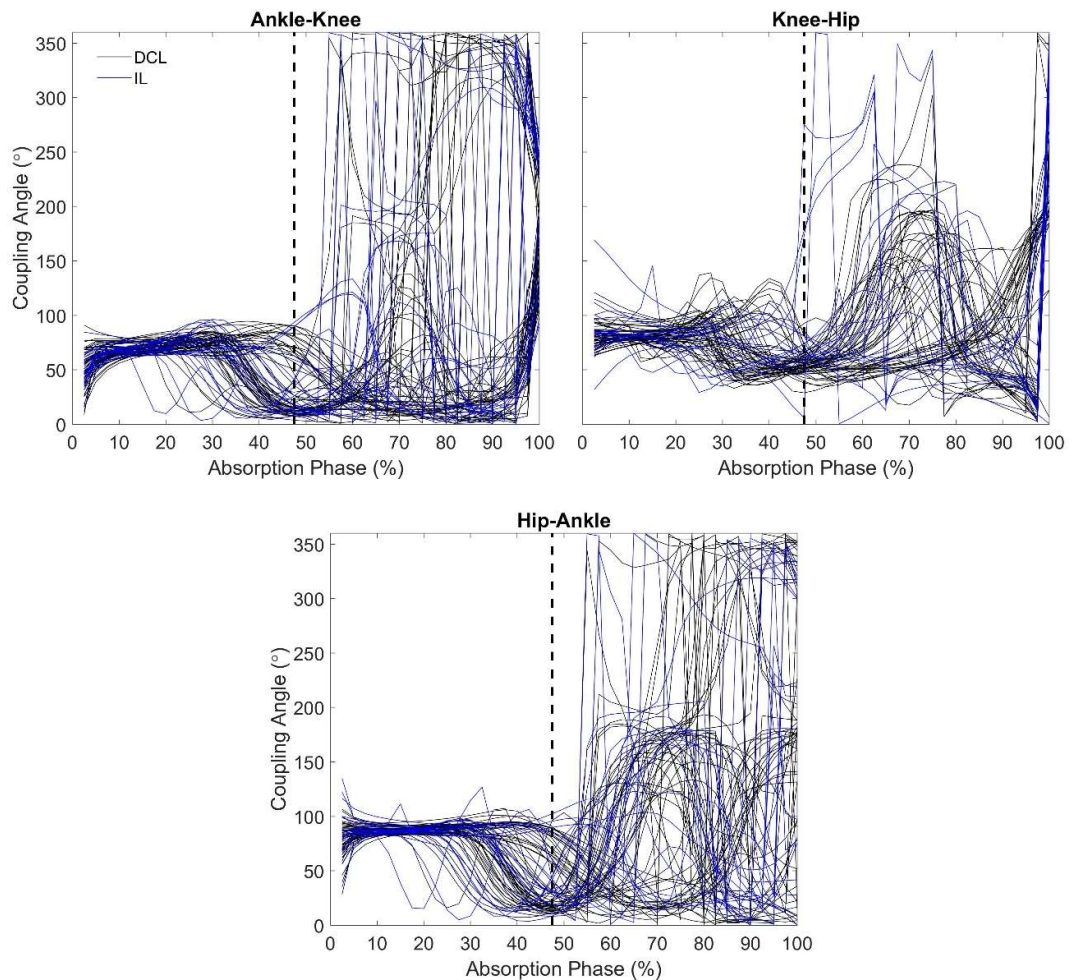


Figure 3.11. Unilateral drop landing joint pair coupling angle waveforms for the intact limb (IL) of ITTAs (blue) and dominant control limbs (DCL; black). The black vertical dashed line denotes the average time point at which peak vGRF occurred. All trials are presented for each participant.

During drop landings, the average coupling angle was calculated for the initial loading response phase when landing due to the many ‘cliffs’ occurring after peak vGRF occurred. Peak vGRF was used as the point indicating the end of the initial loading

response phase as peak magnitude from the other loading waveforms occurred at a similar time point. Figure 3.11 and Figure 3.12 depict the relatively flat slope of the initial loading response for all lower-limb joint pairs (Hughes & Watkins, 2008) indicating this reduction is appropriate.

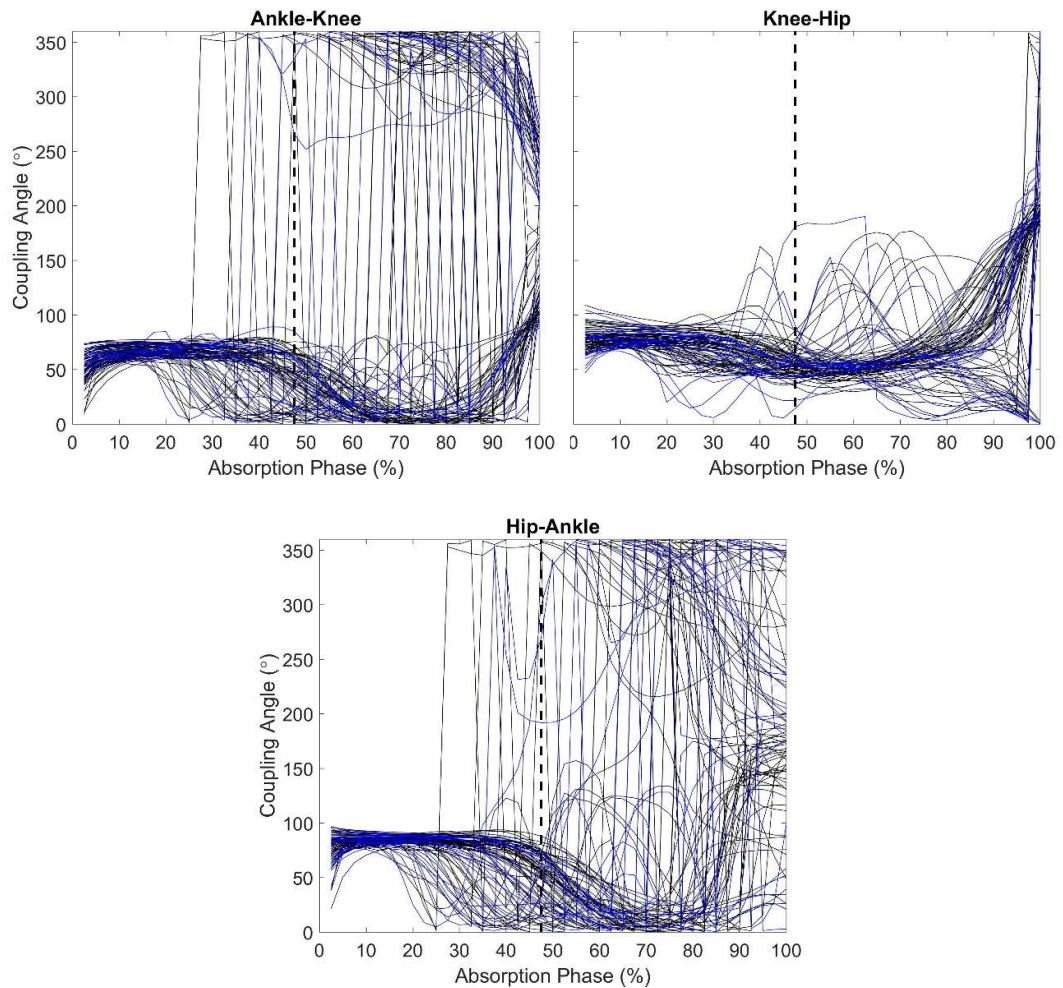


Figure 3.12. Bilateral drop landing joint pair coupling angle waveforms for the intact limb (IL) of ITTAs (blue) and dominant control limbs (DCL; black). The black vertical dashed line denotes the average time point at which peak vGRF occurred. All trials are presented for each participant.

Chapter 4.

Mechanics of a step descent in able-bodied individuals

4.1. Introduction

When stepping down from a raised surface, the leading limb must absorb increased kinetic energy, relative to level walking, while the trailing limb must safely control the lowering of the centre of mass (CoM) through increased eccentric muscular activation and subsequently propel the CoM to continue forward progression (Jones et al., 2006, van Dieën et al., 2007, Barnett et al., 2014, van Dieën et al., 2008). Yet, unlike level walking and stair descent, the biomechanical strategies adopted to achieve a step descent are not well understood. Thus, the development of load and joint mechanics of a step descent must first be established in able-bodied controls. Two step descent strategies have been identified, based on the contact area of the foot (Freedman & Kent, 1987), whereby initial contact with the leading limb is made with either the heel or toe. Factors that have been suggested to lead to the choice of descent strategy include step height (van Dieën et al., 2008, Gerstle et al., 2017), walking speed (van Dieën et al., 2008), age (van Dieën & Pijnappels, 2009), ankle joint stability (Gerstle et al., 2018), and whole body stability (van Dieën & Pijnappels, 2009). A discussion on these factors is included in Chapter 2 Section 2.4.

As there is an increased loading demand, relative to level walking gait, during step descent (Christina & Cavanagh, 2002) and stair descent (Mian et al., 2007, Paquette

et al., 2014, Novak & Brouwer, 2011), it is important to understand the role of the descent strategy in the development of load. Repetitive overloading, specifically at the knee joint, has been associated with joint cartilage degeneration (Arokoski et al., 2000) which can lead to knee pain and subsequently knee osteoarthritis (Hensor et al., 2015, Miyazaki et al., 2002). Initial loading rates, frontal plane loading, and knee joint forces are measures of load that have been linked to knee joint degeneration (Mündermann et al., 2005). van Dieën et al. (2008) examined peak vertical ground reaction force (vGRF) in the leading limb during a step descent which indicated that a toe landing reduced the vertical impact force compared to a heel landing (920 ± 265 N vs 1507 ± 360 N, respectively) due to increased ankle joint work done in the leading limb. They suggested that the increased work required to complete a toe landing was preferred at higher heights and speeds to either control momentum or to reduce impact forces. To date, only the peak vGRF has been analysed for this task and no analysis has been completed on the load at the knee joint. Given the limited research on limb and joint loading when performing a step descent, waveform analysis can determine phases of variation between descent strategies in able-bodied individuals without relying on a possibly biased discrete *a priori* approach. The loading response phase of the leading limb has been defined as the period of double support in walking and stair descent literature (Zachazewski et al., 1993). The dynamic walking theory step-to-step transition has suggested that the negative work associated with loading of the limb can occur beyond that of double support. Thus, analysis of the braking phase for the leading limb would encompass all the time points in which the limb is loading/braking. Further research is required to investigate the development of load in both descent strategies which could indicate a preferred load-avoidance approach and reduce the risk of joint degeneration.

Literature examining the role of the leading limb when performing step or stair descents have identified discrete movement features that are important for the

completion of the task (van Dieën et al., 2008, Buckley et al., 2013) and have also been shown to be important for shock absorption in other tasks to attenuate the forces acting on the body (DeVita & Skelly, 1992, Pollard et al., 2010, Blackburn & Padua, 2009, Norcross et al., 2010). Further, these discrete features (joint flexion angles, range of motion (ROM), peak joint powers, and joint work) have been found to be significantly different between individuals with knee joint degeneration and healthy able-bodied controls during stair descent (Igawa & Katsuhira, 2014). van Dieën et al. (2008) found that a toe initial contact (TC), compared to a heel initial contact (HC), had significantly greater peak power and work done at the ankle joint while there was significantly reduced peak power and work done at the knee and hip joints. The participants in the van Dieën et al. (2008) study were instructed to perform both contact strategies at a controlled speed, thus, it is unclear if these leading limb joint mechanics are consistent with 'natural' performance.

The dynamic walking theory has also demonstrated that a between-limb influence is present in the production of efficient movement (Kuo, 2007, Vanderpool et al., 2008, Morgenroth et al., 2011, Donelan et al., 2002b). Thus, it is plausible that the trailing limb mechanics of a step descent may influence the descent strategy mechanics of the leading limb and subsequently the development of load. Of the few step descent studies investigating the mechanics of the trailing limb, analysis consisted of the entire trailing limb stance phase (van Dieën et al., 2007), the single support phase to assess the lowering of the CoM (Selfe et al., 2008), or the propulsion phase features defined as the double support phase (van Dieën et al., 2008). While not well-defined, these studies suggest that there are two 'key' phases for completion of a step descent in the trailing limb: lowering of the CoM and propulsion. The only study assessing HC versus TC strategies found no significant differences in the trailing limb mechanics (van Dieën et al., 2008). It is possible that no significant differences were present in the trailing limb due to the analysis of individual joints. Inter-joint coordination

strategies can provide additional information on the relative motion of one joint on another in the performance of movement tasks (Lu et al., 2008, Nematollahi et al., 2016) which may be related to injury mechanisms (Hughes & Watkins, 2008, Doherty et al., 2014). Further, the van Dieën et al. (2008) study only assessed the propulsive phase and controlled for walking speed, suggesting similar propulsion was required to continue forward progression. As the step-to-step transition begins earlier than the double support phase (associated with the majority of propulsion), investigation into the single support phase when lowering the CoM could provide additional insight on the effect of the trailing limb mechanics on the leading limb descent strategy and subsequent development of lead limb loading.

Therefore, the purpose of this study was to determine if the load experienced is different for young healthy participants completing either a TC or HC descent strategy during a step descent from 14 cm (the height about which the strategy preference appears to be less clear). A secondary aim of this study was to determine differences in the lower-limb joint mechanics in the leading and trailing limbs between descent strategies. It is hypothesised that a TC performed at a self-selected pace, compared to a HC, will result in 1) reduced vertical forces and significantly different knee joint loading in the leading limb, 2) altered joint mechanics in the leading limb, beyond that of the ankle joint, and 3) significantly different trailing limb mechanics in both sub-phases between descent strategies.

4.2. Methods

Comprehensive methods on data collection are outlined in Section 3.4.4 and the data processing undertaken is presented in Section 3.5. of the Methods chapter. Data from able-bodied controls only were utilised in the analysis for this chapter. The leading limb was chosen by the participant and defined as the limb that first made initial contact with the ground in front of the step platform (Figure 4.1A). Participants were not instructed to perform a specific descent strategy. Descent strategies were

determined by the ankle flexion angle at initial contact.

4.2.1. Features Extracted

The loading waveforms extracted are detailed in Chapter 3, Section 3.6.1. In brief, GRFs, knee moments, and intersegmental knee forces (KF) in all three dimensions were extracted for the duration of the braking phase in the leading limb. The braking phase (i.e. leading limb phase) was defined from initial contact to the first positive point in the leading limb anterior-posterior GRF (Figure 4.1B). Loading values are presented as follows, with the positive direction denoted first: GRFx = lateral-medial, GRFy = anterior-posterior, vGRF = vertical, knee external flexor moment (KFM) = flexion-extension, knee external adduction moment (KAM) = adductor-abductor, knee external rotational moment (KMz) = internal-external, KF_x = anterior-posterior, KF_y = lateral-medial, and KF_z = compression.

To account for the inherent waveform variability between and within participants, landmark registration was applied to each loading waveform and each participant's respective time-domain (i.e., the time, in seconds, spent in the braking phase). The landmark utilised was defined as the average time point at which peak magnitude occurred across all participants in each individual loading waveform. This landmark position was selected based on the results from the study by Moudy et al. (2018) suggesting that a landmark event within the waveform of interest increases the prediction power to a performance feature after aligning to distinct whole-body phases (i.e., braking phase). See Chapter 2, Section 2.9. for additional information regarding the process and application of landmark registration. Landmark registration was not performed on the KMz waveform as there was no discernible landmark. This has been discussed in the literature as an issue with waveform analysis (Kneip & Ramsay, 2008, Ramsay, 2006).

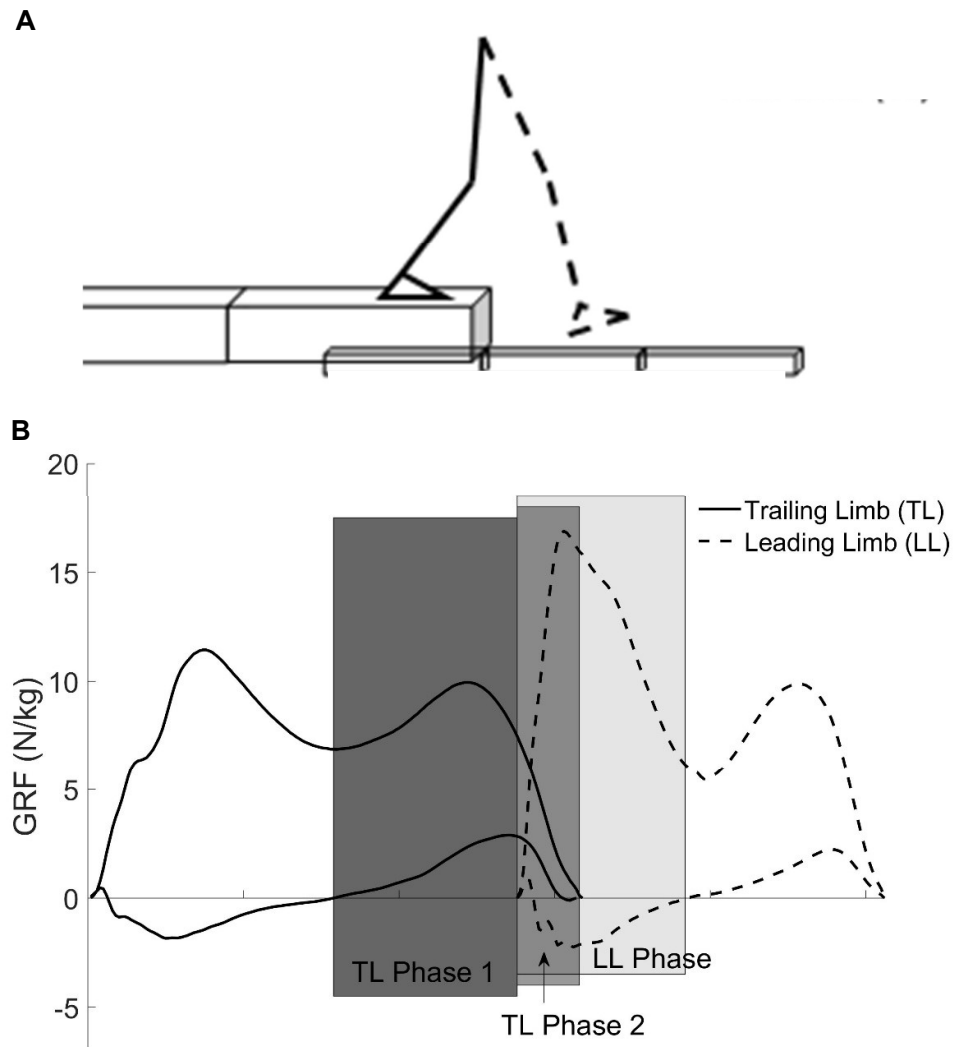


Figure 4.1. A) Depiction of the performance of a step descent with force platform placements noted and B) definition of step descent sub-phases for the leading limb (LL; dashed lines) and trailing limb (TL; solid lines) based on the $vGRF$ and anterior-posterior GRF.

Figure 4.1B presents the phase definitions for the leading limb and trailing limb. Leading limb discrete movement features were extracted from the braking phase. Trailing limb movement features were extracted for the sub-phases representative of lowering the CoM (Phase 1) and the phase in which much of propulsion occurs to continue forward progression (Phase 2). Trailing limb phase 1 was defined as the single support phase from the first positive value in the trailing limb anterior-posterior

GRF to leading limb initial contact, as measured by a 20N threshold in the vGRF. Phase 2 for the trailing limb was defined as the double support phase from leading limb initial contact to trailing limb toe-off.

The temporal-spatial parameters extracted were stepping speed, step length, double support phase duration, and the braking phase duration. Stepping speed was calculated based on the displacement over time of the CoM from initial contact of the trailing limb on the step platform to toe-off of the leading limb on the ground in front of the step platform. Step length was defined as the distance taken by the leading limb during descent, measured from the trailing limb toe marker to the leading limb toe marker at initial contact.

To aid in the definition of trailing limb sub-phases and understand the relative importance of vertical and horizontal movement between descent strategies, the following movement features were extracted: 1) vertical and horizontal CoM velocity at initial contact in the leading limb, 2) vertical and horizontal CoM displacement during both trailing limb sub-phases, and 3) vGRF and anterior-posterior GRF impulses for both trailing limb sub-phases. The CoM displacement was calculated as the maximum distance travelled by the CoM. vGRF and anterior-posterior GRF impulses were calculated as the area under the force-time curve using the trapezoidal rule.

To understand the shock absorption mechanics of the leading limb between descent strategies, the joint angles at initial contact, joint ROM, peak joint powers and joint work were extracted in the sagittal plane for the ankle, knee, and hip joints. Frontal plane knee joint angle at initial contact and ROM were additionally extracted for the leading limb. During trailing limb phase 1, sagittal plane ankle, knee, and hip joint ROM, peak joint absorption powers, and joint work were extracted to determine the single limb support approach to lowering the CoM. As minimal power absorption at the knee joint occurs in phase 1, the average value was calculated for knee power

(see Figure D1.2 in Appendix D1). Trailing limb phase 2 features included the joint angle at toe-off, peak joint propulsive powers, and joint work for all lower-limb joints. These features were extracted to understand the propulsive mechanics. Joint ROM and peak power definitions are presented in Appendix D1 for the leading and trailing limbs. Positive ROM values indicates joint flexion is occurring, whereas negative values indicate joint extension. Individual joint work was calculated as the area under the power-time curve for the leading limb and trailing limb phases of interest. For the leading limb and trailing limb phase 1, total joint work was calculated as the sum of the negative work performed at each joint. Trailing limb phase 2 total joint work was calculated as the sum of the positive work from the ankle and hip joint, and subsequently summed with the absolute negative work from the knee joint.

In addition to individual joint motion, joint coordination strategies were calculated as coupling angles for both the leading limb and trailing limb. See Section 3.6.4.1 in Chapter 3 for a full explanation on the calculation process of the coupling angle. The average coupling angle during their respective phases for each lower-limb joint pair (ankle-knee, knee-hip, and hip-ankle) were calculated.

4.2.2. Statistical Analysis

After reviewing the data, twelve participants performed a HC, and ten performed a TC. Independent *t*-tests were performed to determine differences between groups for both the loading waveforms and discrete movement features. Waveforms were analysed using statistical parametric mapping (Pataky, 2012). Section 2.7. in Chapter 2 and Section 3.6.2 in Chapter 3 provide detailed explanations on the functionality and implementation of statistical parametric mapping. Additionally, to account for possible differences in stepping speed, analyses of covariances (ANCOVA) were performed with stepping speed as the covariant for both movement features and loading waveforms. Point-by-point ANCOVAs were performed on the non-landmark registered loading waveforms.

4.3. Results

There were no significant differences between groups for age, height, or mass (Table 4.1). Additionally, stepping speed was not significantly different between groups.

Table 4.1. Participant demographics and stepping speed presented as the mean \pm SD for the initial heel contact (HC) and initial toe contact (TC) groups

	HC	TC	<i>p</i> -value
<i>Age (years)</i>	32.5 \pm 6.4	35.7 \pm 6.4	0.257
<i>Mass (kg)</i>	79.3 \pm 15	88.4 \pm 8.9	0.098
<i>Height (cm)</i>	179 \pm 6.6	180 \pm 6.2	0.669
<i>Stepping Speed (m/s)</i>	1.54 \pm 0.3	1.37 \pm 0.1	0.124

4.3.1. Loading Differences

The landmark registered loading waveform data presented with similar results to the non-landmarked registered waveform data, therefore, only the non-landmark registered data are presented in Figure 4.2. Any differences present from the landmark registered results are noted within the text. Landmark registered magnitude-domain, time-domain and warping function waveforms are presented in Appendix C1. All significant phases of difference in the loading waveforms remained significant after covarying for speed. Additional phases in the loading waveforms that became significant after covarying for speed are highlighted in red (Figure 4.2).

Waveform analysis identified significant differences between HC and TC groups during the initial loading response phase (~1-32% of the braking phase), which ended at an equivalent time to the end of the double support phase, for all loading waveforms (Figure 4.2). Additionally, waveform analysis identified a secondary phase of interest, sustained midstance loading phase (~55-96% of the braking phase), in vGRF, compressive knee force (KFz) and anterior knee force (KFx) waveforms, and, after

covarying for speed, in KAM and anterior-posterior GRF waveforms.

Within the initial loading phase, vGRF and compressive KFz (Figure 4.2C&I) were significantly reduced in the TC group ($p < 0.001$) from ~2-18% of the braking phase. After landmark registration was applied, there were no differences between groups at peak vGRF or peak KFz, however, the loading rate to peak vGRF was significantly lower for the TC group based on significant differences in the warping function ($p < 0.001$; Appendix C1). In the medial-lateral direction, the TC group experienced a medial GRFx ($p < 0.001$; Figure 4.2A) from 1-17% while the HC group experienced a lateral GRFx. This phase corresponded to a significantly greater medial KFy ($p = 0.045$; Figure 4.2G) from 10-13% in the TC group. The second significant GRFx phase from 26-29% of the braking phase was no longer present after aligning to the peak magnitude. The GRFx time-domain, however, was significantly different indicating a lower loading rate in the TC group ($p < 0.001$) with no significant difference at peak minimum magnitude. A significantly reduced KAM was experienced from ~20-36% in the TC group ($p < 0.001$; Figure 4.2D). After landmark registration, peak KAM magnitude was not significantly different between groups, however, significant differences in the KAM time-domain suggested that the KAM loading rate was significantly lower in the TC group ($p < 0.001$).

In the anterior-posterior direction, the HC group experienced an initial anterior GRFy that was not present in the TC group from ~1-8% of the braking phase ($p = 0.008$; Figure 4.2B). The greater posterior GRFy in the TC group was coupled with a significantly greater anterior KFx ($p = 0.034$; Figure 4.2H) and KFM ($p = 0.043$; Figure 4.2E). The KFM for the TC group exhibited a significantly reduced magnitude from 10-30% of the braking phase ($p < 0.001$). After registering to peak KFM, there was no difference at peak magnitude. Lastly, there was a significantly greater internal rotation (Figure 4.2F) in the TC group from 1-5% ($p = 0.036$) and 7-15% ($p = 0.017$). Peak internal rotation was also significantly greater in the TC group ($p = 0.001$).

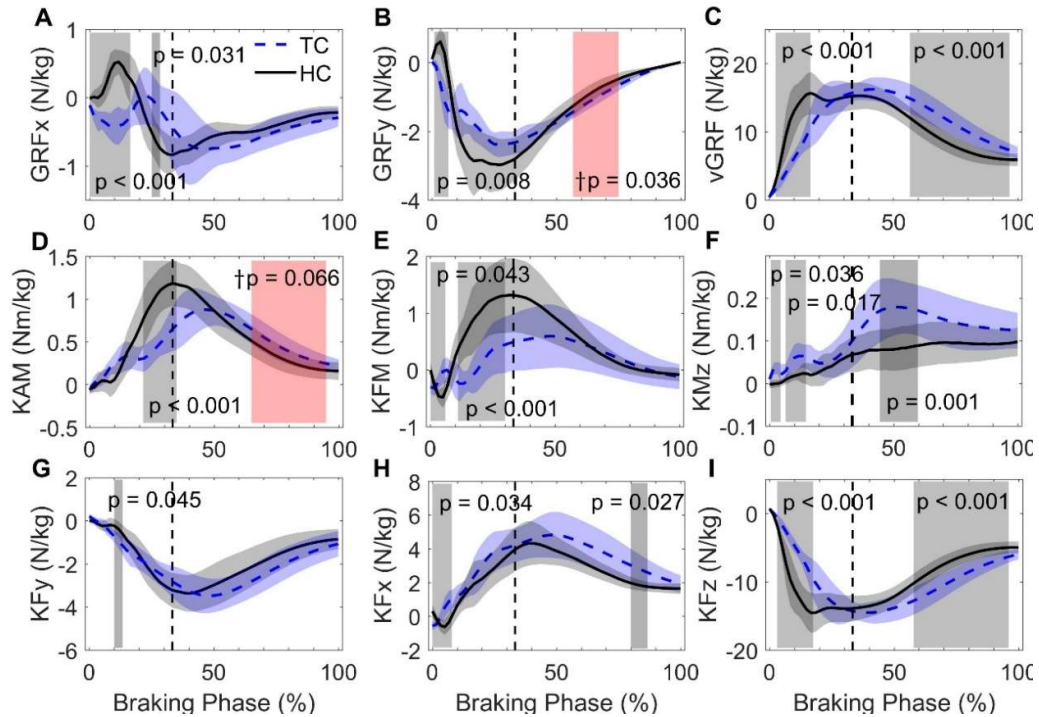


Figure 4.2. Leading limb A-C) GRF, D-F) knee moment, and G-I) intersegmental knee force waveforms for the initial heel contact group (HC; black solid line) and the initial toe contact group (TC; blue dashed line). The phases of significant difference are highlighted in grey with p -values noted. \dagger Red highlighted areas represent phases that became significant or trended towards significance after covarying for speed. The black vertical dashed line represents the average time point at which the end of the double support phase occurred across all participant trials.

The sustained loading phase magnitude in the vGRF and compressive KFz was significantly greater in the TC group from ~56-96% of the braking phase ($p < 0.001$). The anterior KFx was also significantly greater in the TC group from 80-86% of the braking phase ($p = 0.027$) and, after covarying for speed, the significant phase was maintained and grew to encompass 52-96% of the braking phase ($p = 0.015$). After covarying for differences in speed between groups, the TC group was additionally found to have maintained a significantly greater posterior GRFy from 57-75% ($p = 0.036$) and tended to maintain a significantly greater KAM from 57-95% ($p = 0.066$).

4.3.2. Movement Differences

To perform the step descent, the TC group utilised a shorter step length and spent less time in the braking phase. Additionally, the horizontal velocity at initial contact was significantly lower compared to the HC group (Table 4.2). These differences were maintained after covarying for speed ($p \leq 0.021$).

Table 4.2. Whole-body features (mean \pm SD) presented for the heel initial contact (HC) and toe initial contact (TC) groups

	HC Group	TC Group	<i>p</i> -value
<i>Step Length (m)</i>	0.86 \pm 0.12 [†]	0.72 \pm 0.07	0.002
<i>Double Support Duration (s)</i>	0.10 \pm 0.02	0.10 \pm 0.01	0.813
<i>Braking Phase Duration (s)</i>	0.31 \pm 0.03 [†]	0.27 \pm 0.03	0.002
<i>Vertical VIC (m/s)</i>	-0.34 \pm 0.05	-0.32 \pm 0.03	0.421
<i>Horizontal VIC (m/s)</i>	0.87 \pm 0.15 [†]	0.74 \pm 0.06	0.012
Trailing Limb Phase 1			
<i>CoM Vertical Displacement (m)</i>	-0.13 \pm 0.01 [†]	-0.11 \pm 0.01	< 0.001
<i>CoM Horizontal Displacement (m)</i>	0.45 \pm 0.06 [†]	0.37 \pm 0.03	0.002
<i>Vertical Impulse (N/kg/s)</i>	2.12 \pm 0.38	1.80 \pm 0.20	0.025
<i>Horizontal Impulse (N/kg/s)</i>	0.37 \pm 0.10 [†]	0.24 \pm 0.04	0.001
Trailing Limb Phase 2			
<i>CoM Vertical Displacement (m)</i>	-0.04 \pm 0.01 [†]	-0.05 \pm 0.01	< 0.001
<i>CoM Horizontal Displacement (m)</i>	0.17 \pm 0.04	0.18 \pm 0.02	0.736
<i>Vertical Impulse (N/kg/s)</i>	0.40 \pm 0.16	0.38 \pm 0.11	0.750
<i>Horizontal Impulse (N/kg/s)</i>	0.17 \pm 0.04	0.14 \pm 0.04	0.095

[†] $p < 0.05$ significant differences after covarying for speed. VIC = velocity at initial contact

The CoM vertical displacement in phase 1 was significantly less in the TC group, whereas in phase 2 the displacement was significantly greater than the HC group. For phase 1, the horizontal CoM displacement in the TC trailing limb was significantly less and the horizontal impulse was significantly lower than the HC group (Table 4.2). These differences remained significant after accounting for the effect of speed ($p \leq 0.023$). The vertical impulse during phase 1 was significantly lower in the TC group and this tended to remain significant after covarying for speed ($p = 0.068$).

4.3.2.1. Leading Limb Features

Appendix D1 presents the joint angles and powers waveform data in the leading and trailing limbs. The TC group underwent a significantly greater ankle ROM than the HC group ($p < 0.001$, ANCOVA: $p < 0.001$; Figure 4.3A). No significant differences in joint angular motion were present between groups at the knee (initial contact: $p = 0.920$, ROM: $p = 0.182$) or hip (initial contact: $p = 0.651$, ROM: $p = 0.089$) joints (ANCOVA: $p \geq 0.222$). Frontal plane movement features were not significantly different between groups (knee angle at initial contact: $p = 0.111$, HC: $1.04 \pm 3.1^\circ$, TC: $3.68 \pm 4.3^\circ$; knee ROM: $p = 0.845$, HC: $5.69 \pm 4.3^\circ$, TC: $5.27 \pm 5.5^\circ$; ANCOVA: $p \geq 0.424$).

Joint coordination, as measured by the coupling angle, was significantly different between groups for all lower-limb joint pairs ($p \leq 0.030$, ANCOVA: $p \leq 0.032$; Figure 4.3B) during initial loading. The TC group ankle-knee coupling angle of $60 \pm 8^\circ$ denotes an in-phase flexion strategy whereas the HC group performed a knee flexion strategy with some ankle plantarflexion ($348 \pm 15^\circ$; $p < 0.001$, ANCOVA: $p < 0.001$). The knee-hip coupling strategy performed by both groups represents a primarily knee flexion only strategy, however, the TC group extended the hip while flexing the knee ($103 \pm 13^\circ$; $p = 0.030$, ANCOVA: $p = 0.032$). The hip-ankle coupling strategy performed by the TC group was an ankle dorsiflexion only strategy ($95 \pm 8^\circ$), while the HC group performed primarily a hip flexion strategy with some ankle plantarflexion ($343 \pm 33^\circ$; $p < 0.001$, ANCOVA: $p < 0.001$). It should be noted that all HC participants

performed an initial hip flexion before extending the hip which was absent in the TC group (Figure D1.1 in Appendix D1).

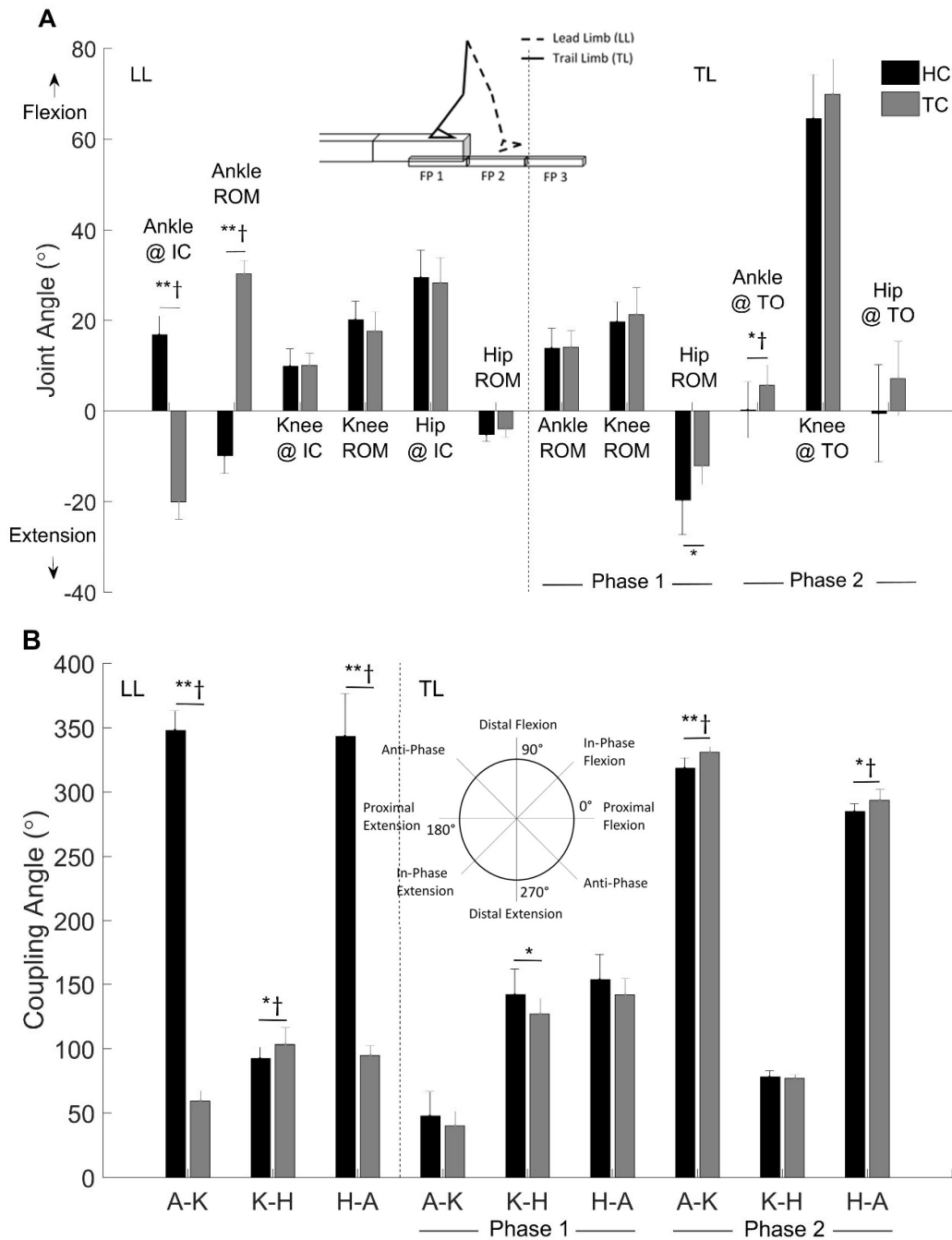


Figure 4.3. Leading limb (LL) and trailing limb (TL) A) individual joint features and B) coupling angles for all lower-limb joint pairs in the initial heel contact (HC; black) and initial toe contact (TC; grey) groups. * $p < 0.05$, ** $p < 0.001$ between groups, † $p < 0.05$ differences that remained significant after covarying for speed. IC = initial contact, TO = toe-off, ROM = range of motion, A-K = ankle-knee, K-H = knee-hip, H-A = hip-ankle.

Leading limb joint power absorption (Figure 4.4) in the TC group indicated significantly greater ankle joint ($p < 0.001$), and significantly lower knee ($p = 0.012$) and hip ($p = 0.028$) joint negative peak powers. Only the ankle joint peak absorption power remained significant after covarying for speed ($p < 0.001$), however, there was a trend towards differences being maintained after speed covariation at the knee ($p = 0.052$) and hip ($p = 0.069$) joints. Overall, the TC group performed 33% greater total joint work than the HC group in the leading limb ($p = 0.091$; Figure 4.5A). The TC group performed significantly more work at the ankle joint ($p < 0.001$, ANCOVA: $p < 0.001$) and significantly less work at the knee joint ($p = 0.003$, ANCOVA: $p = 0.014$). The work completed at the hip joint was not significantly different between groups ($p = 0.176$, ANCOVA: $p = 0.346$). The TC ankle joint performed 79% of the total lower-limb joint work, and the HC group utilised the knee joint as the primary shock absorber (55%; Figure 4.5B).

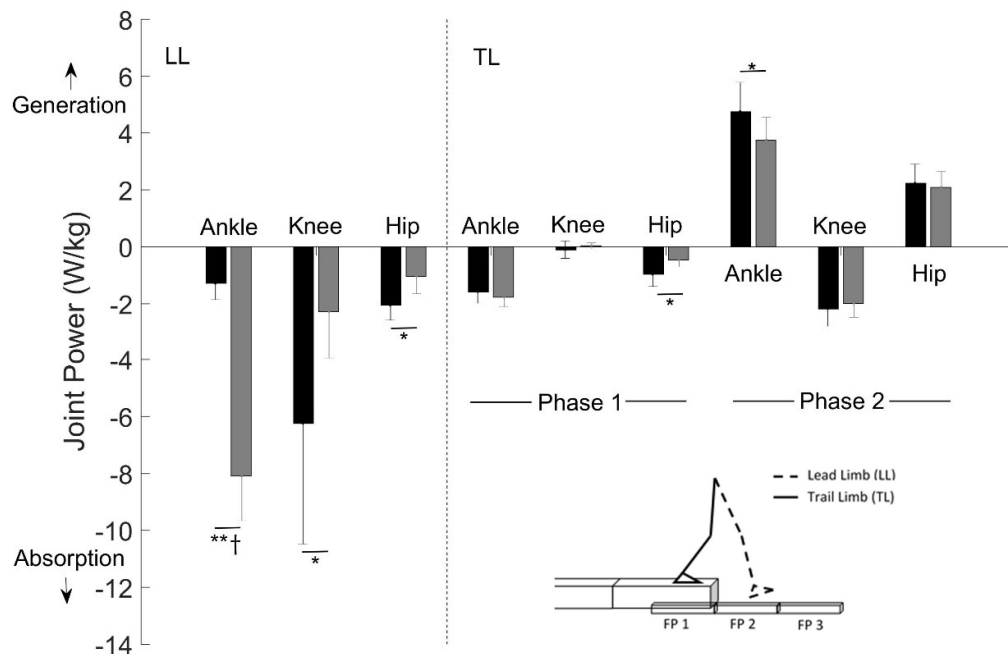


Figure 4.4. Lower-limb joint peak absorption and generation powers in the leading limb (LL) and trailing limb (TL) during their respective phases of interest in the initial heel contact (HC; black) and initial toe contact (TC; grey) groups. * $p < 0.05$, ** $p < 0.001$ between groups, † $p < 0.05$ differences that remained significant after covarying for speed.

4.3.2.2. *Trailing Limb Features – Phase 1*

The TC group trailing limb hip joint underwent a significantly reduced ROM than the HC group ($p = 0.011$) yet did not remain significant after covarying for speed ($p = 0.135$; Figure 4.3A). The trailing limb joint ROM at the ankle ($p = 0.900$; ANCOVA: $p = 0.968$) and knee ($p = 0.488$; ANCOVA: $p = 0.693$) were not significantly different between groups. Knee-hip coupling strategies were significantly different between groups ($p = 0.048$) yet did not remain significant after covarying for speed ($p = 0.392$; Figure 4.3B). Ankle-knee ($p = 0.275$; ANCOVA: $p = 0.775$) and hip-ankle ($p = 0.148$, ANCOVA: $p = 0.814$) coupling strategies were not significantly different between groups.

Hip joint peak absorption power was significantly lower in the TC group ($p = 0.004$) and tended to remain significant after covarying for speed ($p = 0.053$; Figure 4.4). The joint peak negative absorption powers at the ankle ($p = 0.262$, ANCOVA: $p = 0.585$) and knee ($p = 0.201$, ANCOVA: $p = 0.261$) were not significantly different between groups. The total negative work completed was 29% lower ($p = 0.036$) in the TC group (Figure 4.5A). The TC group completed significantly less work at the hip joint ($p = 0.013$) yet did not remain significant after covarying for speed ($p = 0.151$). The work done at the ankle ($p = 0.349$, ANCOVA: $p = 0.754$) and knee joints ($p = 0.087$, ANCOVA: $p = 0.102$) were not significantly different between groups. Both the HC and TC groups utilised the ankle joint to the greatest extent to lower the CoM (48% and 70%, respectively; Figure 4.5B).

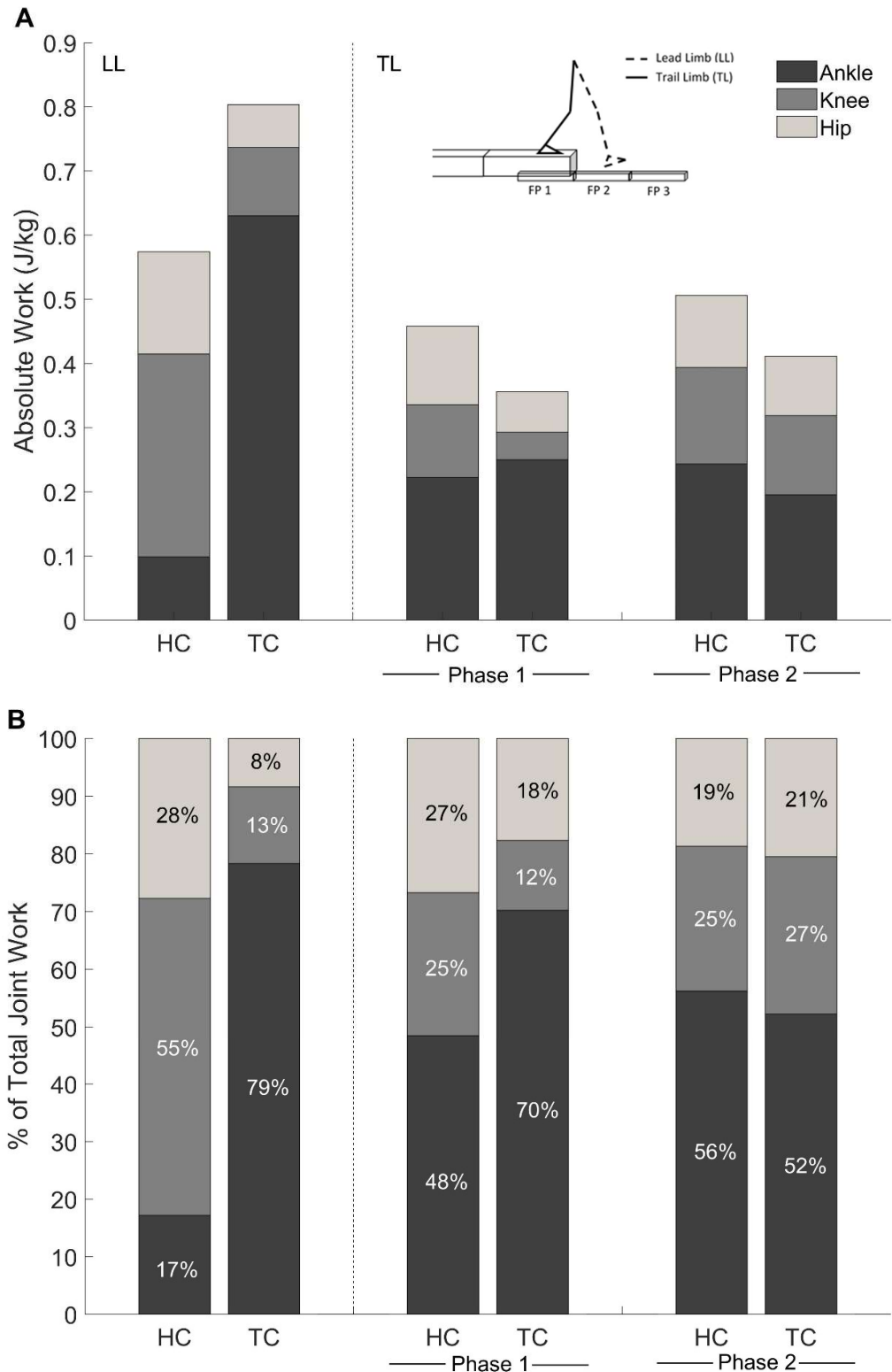


Figure 4.5. A) Absolute joint work completed and B) percentage of total negative joint work contribution at the ankle (bottom), knee (middle), and hip (top) for the leading limb (LL) and trailing limb (TL) phases for the heel initial contact (HC) and toe initial contact (TC) groups.

4.3.2.3. *Trailing Limb Features – Phase 2*

Propulsive joint mechanics were different between groups mainly at the ankle joint. The trailing limb ankle angle at toe-off was significantly less plantarflexed in the TC group than the HC group ($p = 0.032$, ANCOVA: $p = 0.041$; Figure 4.3A). No significant differences in the joint angles at toe-off were present for the knee ($p = 0.172$, ANCOVA: $p = 0.750$) or hip ($p = 0.080$, ANCOVA: $p = 0.725$) between groups. The ankle-knee ($p < 0.001$, ANCOVA: $p = 0.005$) and hip-ankle ($p = 0.025$, ANCOVA: $p = 0.018$) joint coupling strategies were significantly different between groups (Figure 4.3B). The ankle-knee strategy performed by the HC group ($319 \pm 8^\circ$) was an anti-phase strategy, while the TC group performed this same anti-phase strategy but with a greater contribution from the flexing knee ($331 \pm 4^\circ$). Similarly, the hip-ankle coupling angle represented synchronous anti-phase movement with the HC group performing with a significantly greater contribution of the hip flexing (HC: $282 \pm 8^\circ$, TC: $291 \pm 9^\circ$). The coupling strategies for the knee-hip joint pair were not significantly different between groups ($p = 0.611$).

A significantly reduced ankle power generation was performed in the TC group ($p = 0.020$) but was not significant after accounting for speed ($p = 0.154$; Figure 4.4). The joint peak powers for the knee ($p = 0.427$; ANCOVA: $p = 0.614$) and hip ($p = 0.596$, ANCOVA: $p = 0.114$) were not significantly different between groups. The overall absolute trailing limb work completed during propulsion by the TC group was 21% less ($p = 0.044$) than the HC group (Figure 4.5A). The negative work completed at the knee joint ($p = 0.311$; ANCOVA: $p = 0.260$) and the positive work completed at the ankle ($p = 0.104$, ANCOVA: $p = 0.202$) and hip joint ($p = 0.149$, ANCOVA: $p = 0.718$) were not significantly different between groups. To propel the CoM forward, both groups utilised the ankle joint to the greatest extent, as noted by the percentage of total work completed (52-56%; Figure 4.5B), followed by the knee (25-27%) then the hip (19-21%).

4.4. Discussion

This study aimed to investigate differences between TC and HC step descent strategies in whole-limb and joint load and underpinning joint mechanics of the lower-limbs. The main findings suggest that a TC may reduce the initial rate of load to peak magnitude for the medial GRFx, KAM, and vGRF with no significant differences at peak magnitude; increase the initial contact magnitudes in the medial (GRFx and KFy) and anterior-posterior (GRFy, KFM, and KFz) directions; and maintain a greater magnitude of sustained load for the vGRF, KFz, KAM, and posterior GRFy (Figure 4.2). These significant differences were independent of stepping speed; it is possible that the differences in load between strategies stemmed from the differences in the leading limb mechanics (i.e. the descent strategy chosen). Limited significant differences were found in the trailing limb when lowering the CoM and these significant differences were due to variation in stepping speed (no longer significant after covarying for speed). The propulsive phase trailing limb mechanics, however, maintained significant differences after covarying for speed between descent strategies. Thus, it is equally plausible that the differences in load between strategies could have stemmed from differences in the propulsive phase trailing limb mechanics in addition to the leading limb mechanics.

For level-walking, previous research has indicated that with increases in walking speed, peak vGRF increases and midstance minimum force decreases (Silverman et al., 2008, Spanjaard et al., 2009). The results from the current study found, using waveform analysis, that the HC group had increased force in early stance and a decreased force at midstance. The HC group stepping speed tended to be faster (1.37 m/s vs 1.54 m/s) and had significantly higher horizontal velocity at initial contact compared to the TC group (Table 4.2). When the vGRF data were landmark registered, no significant difference was found at peak magnitude; however, the time-domain was significantly different indicating an effect of the descent strategy on the

rate of force (Appendix C). When speed was used as a covariate, the significant difference in early stance for vGRF was still featured, indicating that the descent strategy influences the rate of force, independent of speed. Further, the ANCOVA results for all loading waveforms demonstrated that the significant differences between groups were maintained independent of speed. Additional significant phases were identified after covarying for speed during the sustained midstance load in the posterior GRFy and KAM. These additional phases possibly denote that TCs were able to reduce the magnitude of sustained posterior GRFy and KAM magnitudes by walking at slower speeds. The majority of differences in load between descent strategies in the leading limb are, most likely, due to differences in leading and trailing limb mechanics as significant differences in load were maintained independent of speed. However, reductions in walking speed may also aid in midstance load reduction and will be explored as a mechanism to reduce load in Chapter 6.

Vertical velocities at initial contact were not significantly different between groups and did not become significant after covarying for speed (Table 4.2). This suggests that the magnitude of vertical momentum was reduced by the same amount when descending the step. Despite the similar vertical velocities at initial contact, significant differences were present in the loading waveforms throughout the braking phase. The most commonly assessed measures of load are peak KAM and vGRF as these have been associated with degeneration of the knee joint cartilage (Vanwanseele et al., 2010, Zhao et al., 2007, Shelburne et al., 2006), and able-bodied stair descent literature has demonstrated that participants exhibit greater peak magnitudes in these features, compared to level walking (Paquette et al., 2014, McFadyen & Winter, 1988, Novak & Brouwer, 2011). In the current study, however, peak vGRF and peak KAM were not significantly different between the landing strategies, yet the rate of initial load was significantly reduced in the TC group based on significant differences in the time-domain (Appendix C). Loading rates provide an ability to measure how quickly

the load is delivered to the body over a certain time phase (Cheung & Rainbow, 2014), and it has been suggested that they are a more relevant measure than peak magnitudes in assessing joint loading and injury occurrence (Boyd et al., 1991, Morgenroth et al., 2014, Mündermann et al., 2005). This results from the current study suggest that a TC strategy may have been chosen in the attempt to reduce the initial loading rates in vGRF and KAM despite experiencing similar peak magnitudes.

In addition to vGRF and KAM, significant differences in magnitude immediately following initial contact were found in the medial (GRFx and KFy) and anterior-posterior (GRFy, KFM, and KFx) directions (Figure 4.2). The initial lateral GRFx in the HC group from 1-17% is consistent with that found in previous research examining level-walking gait which is typically performed with a heel strike at initial contact. The TC group, however, had an initial medial GRFx which has been found during stair descent, which utilises a TC strategy (Silverman et al., 2014), and in forefoot running gait (Nilsson & Thorstensson, 1989). Medial-lateral GRFs are highly influenced by changes in the foot contact angles (Simpson & Jiang, 1999) indicating that differences during initial medial-lateral GRF loading in the current study are most likely due to the contact strategies performed. The HC group had an initial peak anterior GRFy coinciding with an initial peak knee external extensor moment and posterior KFx which was absent in the TC group. This is consistent with previous research on level-walking gait and is thought to occur due to a backward deceleration of the heel at initial contact. While this heel strike transient is not always present, Hunt et al. (2010) found that osteoarthritic individuals who demonstrated a heel strike transient in walking gait were more likely to exhibit greater joint degeneration. It is, therefore, plausible to suggest that a toe contact strategy, when performing a step descent, may reduce early phase loading associated with a greater risk of injury.

Waveform analysis identified an additional phase of interest (sustained midstance loading) that is not typically assessed in biomechanics literature. The TC group

maintained greater vertical (vGRF and KFz), medial (KAM), and anterior knee forces (KFx). The increased magnitude during the sustained loading phase was possibly due to the shorter step length in the TC group (Table 4.2). While the reduced step length in the TC group allowed for the leading limb to lengthen to aid in the controlled lowering of the CoM, the more vertical alignment may have reduced the ability to control the horizontal momentum of the CoM. van Dieën et al. (2007) found that a shorter step length in unexpected stepping down resulted in inadequate control of forward momentum and a sustained midstance load was evident in the vGRF waveforms. This was further confirmed in a follow-up study. van Dieën et al. (2008) found a more anterior foot placement was utilised when performing a toe contact compared to a heel contact that enabled control over the CoM momentum. The van Dieën et al. (2008) results disagree with the current study in which the TC group had a shorter step length. As the van Dieën et al. (2008) study instructed participants to perform a toe contact strategy, the results from the current study may better reflect daily 'natural' performance indicating a TC strategy may induce a higher sustained magnitude of load in each plane of motion due to the reduced ability to control the forward horizontal momentum from a shorter step length.

The differences in load between descent strategies possibly stemmed from the differences in joint mechanics in the leading and trailing limb as alterations were independent of stepping speed. The limb lengthening mechanism in the leading limb of the TC group in the current study did not reduce the vertical velocity at initial contact. This occurred despite the TCs landing with a higher CoM as denoted by the significantly reduced CoM vertical displacement during single support of the trailing limb (Table 4.2). Thus, the ankle joint was utilised as the main shock absorber (79% of total work done) in the TC group compared to the HC group which utilised the knee as the main shock absorber (55% of total work done; Figure 4.5B). It is possible that the distribution in joint utilisation for shock absorption in the TC group is to avoid

reliance on the knee joint in the leading limb. This is possibly further confirmed by the significantly less work completed at the knee joint and reduced peak knee joint absorption power after covarying for speed in the TC group ($p = 0.014$ & $p = 0.052$, respectively; Figure 4.4). This finding is consistent with previous step and stair descent research which found that a TC utilises the ankle plantarflexor muscles to absorb the shock from landing (van Dieën et al., 2007, Spanjaard et al., 2009) while an HC strategy requires increased work done at the knee and hip joints (van Dieën et al., 2008). It is possible that by utilising the ankle joint as the main shock absorber, rather than the knee, a TC strategy may be more efficient at reducing the rate of vGRF and KAM and subsequently reducing the risk of developing knee joint comorbidities. This is explored further in Chapter 6.

Previous step descent research had not adequately defined sub-phases of the trailing limb which encompassed lowering of the CoM and propulsion. The current study attempted to define these two sub-phases. The CoM vertical displacement for both groups (Table 4.2) was 6-9 cm greater when lowering the CoM (phase 1) than during propulsion (phase 2) for both landing techniques suggesting that the single support phase (phase 1) was primarily used to lower the CoM. This demonstrates that the defined sub-phases adequately represent the sub-tasks required to perform a step descent. The TC group had significantly less CoM vertical displacement in phase 1 and significantly greater CoM vertical displacement in phase 2 (Table 4.2). This indicates that the TC group continued to lower the CoM during the propulsive phase to a greater extent than the HC group. In phase 1, the horizontal displacement of the CoM and horizontal impulse were also significantly reduced in the TC group (Table 4.2) suggesting that the TC group placed a greater emphasis on the vertical aspect of the step descent rather than continued forward progression. The TC group also utilised the trailing limb ankle joint to complete 70% of the total work when lowering the CoM while the HC group utilised the ankle joint to complete 48% of the work

(Figure 4.5B). It is possible that the TC group may not have required greater work from the knee and hip joints (Figure 4.5A) as the extended leading limb reduced the amount of vertical displacement required prior to initial contact. However, significant differences in the joint mechanics of the trailing limb when lowering the CoM did not remain significant after covarying for speed. This indicates that, when performing the step descent at the same speed, the TC and HC groups utilised strategies that were not significantly different to lower the CoM. However, during propulsion, significant differences between both groups were maintained in the trailing limb after covarying for speed. The ankle joint was the greatest contributor to propulsion (52-56%) in both groups yet was significantly reduced in the TC group (Figure 4.5B). Reduced propulsion from the trailing limb has been found to result in a shorter step length (Browne & Franz, 2017b) and, as exhibited in TCs, may contribute to the sustained magnitude of load. This will be further explored in Chapter 6.

Dynamic walking models have demonstrated that a between-limb influence is present in the production of efficient movement (Kuo, 2007, Vanderpool et al., 2008, Morgenroth et al., 2011). The TC group performed 29% less total work in the trailing limb when lowering the CoM, 21% less total work during propulsion, and 33% increased total work on the leading limb. The greater total work in the leading limb of TCs was required to absorb the greater kinetic energy not absorbed by the trailing limb prior to initial contact and to aid in continuing forward progression after trailing limb toe-off as reduced propulsion was performed by the trailing limb (Morgenroth et al., 2011, Adamczyk & Kuo, 2009, Houdijk et al., 2009, Donelan et al., 2002a). Thus, it is plausible that the trailing limb mechanics influenced the descent strategy of the leading limb and the subsequent magnitude and rate of whole-limb and joint load. This will be further explored in Chapter 5.

4.5. Conclusion

The foot contact strategy when stepping down during ongoing walking can affect the development of load. Independent of stepping speed, a TC strategy was associated with a significantly lower rates of initial vGRF and KAM load; altered initial contact magnitudes in the medial-lateral and anterior-posterior directions; and greater sustained midstance magnitudes in all three planes of motion. The TC group leading limb mechanics utilised the ankle joint, rather than the knee, as the primary shock absorber possibly indicating a knee-avoidance strategy. In addition to leading limb mechanics, there is some evidence to suggest that the trailing limb joint mechanics could influence the development of load. Analysis of individuals with reduced trailing limb functionality, such as individuals with unilateral transtibial amputations, could help to understand the role of the trailing limb on lead limb loading. Overall, the results from the current chapter would suggest that a TC strategy is the preferred descent strategy for reducing the magnitude and rate of initial loading of the leading limb.

4.6. Further Work

Previous research has postulated that a TC strategy is performed to ensure stability (van Dieën et al., 2008, van Dieën & Pijnappels, 2009). The current study on healthy able-bodied individuals (no known issues with stability) suggest that TC and HC descent strategies result in different loading patterns. This suggests that reductions in load may be a factor that drives the adoption of a TC or HC. As load demand increases with increases in step height, analysis of limb and joint loading patterns in healthy able-bodied individuals at different step heights could help to further determine choice of descent strategy.

Chapter 5.

Mechanics of a step descent in amputees

5.1. Introduction

The previous chapter provided good evidence to suggest that the trailing limb mechanics during a step descent may influence the descent strategy chosen and thereafter the magnitude and rate of limb and joint loading on the leading limb. In individuals with unilateral transtibial amputations (ITTAs), the ankle joint and surrounding musculature on one side are replaced by a prosthesis. ITTAs may have increased difficulty performing a step descent with the prosthetic limb trailing as the prosthesis is unable to mimic the functionality of an intact ankle joint (Schmalz et al., 2007, Powers et al., 1997). The leading intact limb of ITTAs is at an increased risk of joint degeneration, which is thought to stem from high load, however the development of load in the intact limb of ITTAs during a step descent is unknown. No research has been conducted to assess the descent strategy utilised by ITTAs or the compensatory strategies performed to complete the task and attenuate load.

Previous research in ITTA level walking gait have found strong negative correlations with prosthetic push-off work and the work demand on the intact limb during the braking phase (Morgenroth et al., 2011, Grabowski & D'Andrea, 2013). This has been postulated to result in increased intact limb and joint loading which is thought to place the intact limb of ITTAs at a 22-27% increased risk of experiencing knee pain and

subsequently developing degenerative knee joint diseases compared to able-bodied individuals (Struyf et al., 2009, Griffin & Guilak, 2005). It has been assumed that this is due to a greater load occurring in the intact limb compared to a control limb (Sanderson & Martin, 1997). Inconclusive results from previous walking gait literature have found limited to no differences in discrete limb or knee joint loading between intact and control limbs (Lloyd et al., 2010, Grabowski & D'Andrea, 2013). In a step-over-step stair ambulation study on ITTAs (Schmalz et al., 2007), it was found that the intact limb experienced a significantly greater peak vertical ground reaction force (vGRF) compared to a control limb. Additionally, a faster rate of load was evident as the peak magnitude occurred earlier in the intact limb. It is, therefore, possible that during a single step descent, the intact limb will experience a greater load compared to a control limb. However, no measures of limb or joint loading have been assessed when comparing the intact limb of ITTAs to an able-bodied control limb. Thus, analysis of the loading waveforms could provide indications on the important phases of interest related to joint degeneration (Pataky, 2012) rather than utilising a possibly biased discrete *a priori* approach.

When the prosthetic limb is trailing during a step descent, the reduced capacity to perform work and reduced range of motion (ROM) at the ankle joint must be compensated for by increased work at other joints in the prosthetic limb and/or the leading intact limb. This is necessary to efficiently reduce the vertical centre of mass (CoM) momentum and continue forward progression at a consistent pace. The previous chapter found that individuals who performed a toe initial contact (TC), compared to a heel initial contact (HC), completed 29% less total work in the trailing limb when lowering the CoM, 21% less work during propulsion, and 33% more work in the leading limb when loading. The trailing limb ankle joint was utilised to the greatest extent to lower the CoM (48-70%) and provide propulsion (52-56%). It is possible that ITTAs may utilise a TC as reduced work is required from the trailing

limb; however, ITTAs may compensate through increased work done at the knee and hip joints in the trailing prosthetic limb and utilise a longer leading limb. Increased prosthetic limb hip joint flexion and ‘pull-off’ power during propulsion has been demonstrated as a compensatory mechanism in ITTAs during level walking gait to accommodate for the reduced joint motion at the prosthetic ankle joint (Sanderson & Martin, 1997). Previous stair descent research in ITTAs, which utilises similar mechanics to step descent when loading, found increased ankle plantarflexion in the leading intact limb during late swing just prior to initial contact (Schmalz et al., 2007). Of the limited research conducted on step negotiation in ITTAs, there was only one study that examined the leading and trailing limb mechanics when the intact limb led during descent (Barnett et al., 2014). However, this study examined the adaptations in the first 6-months post-discharge when movement strategies are not fully established. As rehabilitation progressed, the research found no preference in descent strategy (TC or HC). The study postulated that leading with the intact limb during descent may have been used to exploit the functionality of this limb given the reduced capacity of the prosthetic limb. It is currently unknown if these compensations could influence the descent strategy approach or the development of load in the leading intact limb.

If compensatory mechanisms elsewhere in the kinematic chain are unable to accommodate for the reduced capacity of the prosthetic ankle joint, reduced forward progression will result as the vertical component is set during a step descent. Stepping speed has been found to decrease when performing an initial toe contact strategy (van Dieën et al., 2008) and reductions in walking speed have been demonstrated to improve dynamic stability (Browne & Franz, 2017a). Given the linear relationship of speed with forces and joint mechanics, it is possible that stepping speed may be reduced to maintain limb and joint loading at a lower level rather than depend on the joint mechanics alone to reduce the load (Lelas et al., 2003, Browne

& Franz, 2017a, Donelan et al., 2002a). In a study assessing TC and HC strategies during a step descent between young and elderly populations, it was determined that, while the elderly were capable of performing a HC, there was a preference of performing initial contact with the toe (van Dieën & Pijnappels, 2009). The greater preference for the TC strategy in the elderly population was possibly to maintain the vGRF at a level below that which required greater knee strength in the leading limb, increased ROM from the trailing limb, and possibly was chosen to mediate against pain at the imposed speed. It is well documented that ITTAs walk at a slower speed compared to able-bodied individuals. Thus, it is possible that ITTAs may utilise the TC strategy.

Therefore, the purpose of this study was to determine the descent strategy chosen by ITTAs (HC or TC) when performing a step descent leading with the intact limb and trailing with the prosthetic limb. This study additionally aimed to 1) examine the development of limb and joint load in the leading intact limb, 2) assess the shock absorption approach of the leading intact limb to attenuate load and 3) determine any compensatory strategies of the trailing prosthetic limb compared to able-bodied controls. It is first hypothesised that ITTAs will perform a TC strategy. Secondly, the load experienced in the intact limb of ITTAs will be significantly greater than that of controls performing the same descent strategy. Lastly, it is hypothesised that altered joint mechanics will be exhibited in the leading and trailing limbs. In particular, it is hypothesised that the leading intact limb of ITTAs, compared to able-bodied controls, will adopt a more vertical approach through increasing the plantarflexion of the ankle joint, extending the knee and hip joints thus altering the joint coordination strategies, and performing greater peak absorption power and work. The trailing prosthetic limb will perform reduced joint motion, power, and work and performed altered joint coordination strategies when lowering the CoM and propelling the CoM forward.

5.2. Methods

Comprehensive methods on data collection are outlined in Section 3.4. and the data processing undertaken is presented in Section 3.5. of the Methods chapter. The features extracted, and phase definitions are detailed in Chapter 4 Section 4.2.1.

In brief, the leading limb and trailing limb phases are defined as noted in Figure 4.1 in Chapter 4. For the ITTA group, the intact limb was utilised as the leading limb and the prosthetic limb as the trailing limb. The control group leading limb was chosen by the participant without instruction from the investigators. Loading waveforms were extracted for the leading limb only and were landmark registered to the average time point across all participants when the peak magnitude occurred within each loading waveform (Chapter 2 Section 2.9.). Discrete movement features were extracted from both the leading limb and trailing limb phases of interest as detailed in Chapter 4 Section 4.2.1. Joint angle and power waveform data are presented in Appendix D1 for the leading limb (Figure D1.1) and trailing limb (Figure D1.2).

5.2.1. Statistical Analysis

All ITTA participants performed a toe initial contact strategy ($n = 8$), therefore, only the able-bodied controls who utilised this strategy were used for comparison (TC; $n = 10$). Independent t -tests were performed to determine differences between groups for the loading waveforms and discrete movement features. Waveforms were analysed using statistical parametric mapping (Chapter 2 Section 2.7. and Chapter 3 Section 3.6.2). To determine if any differences in loading patterns or joint mechanisms were dependent on variations in stepping speed, analyses of covariances (ANCOVA) were additionally performed with speed as a covariate. A point-by-point ANCOVA was performed on the non-landmark registered loading waveforms.

5.3. Results

There were no significant differences between groups for age, height, or mass (Table 5.1). Stepping speed was significantly slower in the ITTA group than the TC group.

Table 5.1. Participant demographics and stepping speed (mean \pm SD) for the ITTA and initial toe contact (TC) groups

	ITTA	TC	<i>p</i> -value
<i>Age (years)</i>	40.0 \pm 9.0	35.7 \pm 6.4	0.254
<i>Mass (kg)</i>	84.5 \pm 18	88.4 \pm 8.9	0.546
<i>Height (cm)</i>	177 \pm 7.4	180 \pm 6.2	0.423
<i>Stepping Speed (m/s)</i>	1.14 \pm 0.2	1.37 \pm 0.1	0.003

One ITTA participant performed an external knee abduction moment and had lateral ground and knee joint intersegmental forces. This participant also had a valgus knee angle at initial contact. The remaining loading and movement features did not present differently for this participant and the results of the analysis did not change whether this participant was included. Therefore, this participant was included, and it should be noted that part of the variability in loading patterns stem from this ITTA participant.

5.3.1. Loading Differences

Loading waveforms are presented in their original temporal-spatial format (Figure 5.1). See Appendix C2 for the landmark registered results.

The intact limb of ITTAs experienced significantly less medial GRFx at initial contact (1-3% of the braking phase, $p = 0.039$; Figure 5.1A). This significant phase was due to a difference in magnitude ($p = 0.040$), rather than timing differences between groups (no significant difference in time-domain, Appendix C2), and remained significant after covarying for speed ($p = 0.005$). After covarying for speed, from 7-8% of the braking phase, the ITTA group had a significantly more posterior GRFy ($p =$

0.029; Figure 5.1B), significantly greater knee flexor moment (KFM; $p = 0.031$; Figure 5.1E), and significantly more anterior intersegmental knee force (KFx; $p = 0.030$; Figure 5.1H) compared to the TC group. There were no significant differences between groups for the remaining loading waveforms throughout the braking phase.

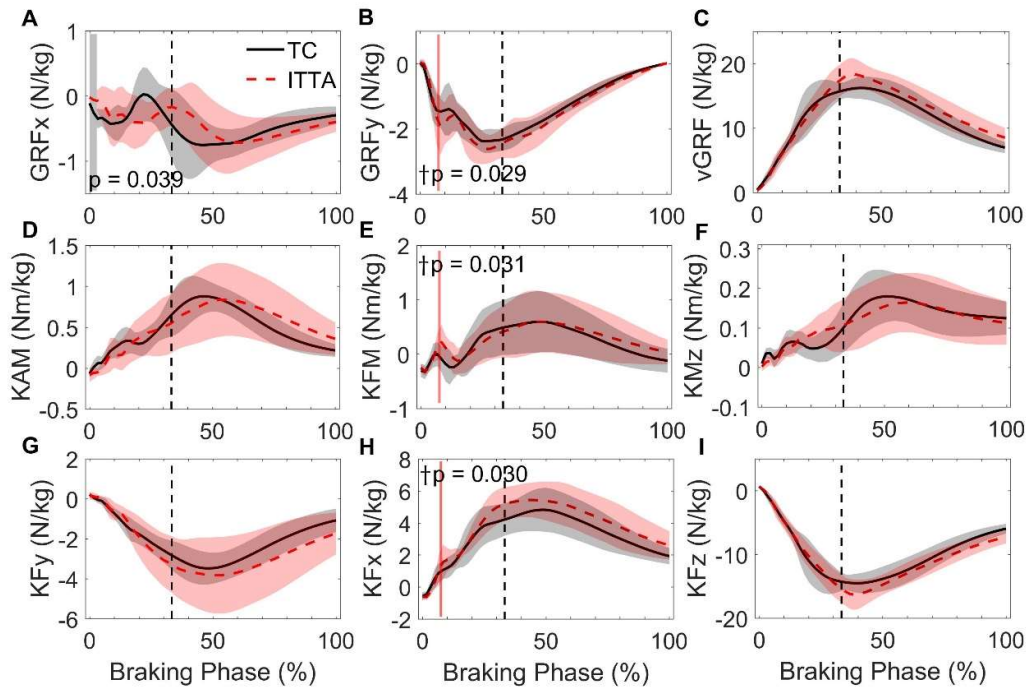


Figure 5.1. The GRF (A,B,C), knee moment (D,E,F), and intersegmental knee force (G,H,I) loading waveforms in the intact limb of ITTAs (red dashed line) and leading limb of the initial toe contact group (TC; black solid line) for the duration of the braking phase. The phase of significant difference is highlighted in grey whereas red highlighted areas represent phases that became significant after covarying for speed. The black vertical dashed line represents the average time point at which the end of the double support phase occurred across all participant trials.

5.3.2. Movement Differences

The ITTA group performed the step descent with a significantly shorter step length ($p = 0.025$, ANCOVA: $p = 0.997$; Table 4.2) and spent significantly less time in double support ($p = 0.001$, ANCOVA: $p = 0.013$). ITTAs also had significantly reduced horizontal velocity at initial contact ($p = 0.006$, ANCOVA: $p = 0.550$), CoM vertical displacement during trailing limb phase 1 ($p < 0.001$, ANCOVA: $p < 0.001$), and CoM horizontal displacement during trailing limb phase 2 ($p < 0.001$, ANCOVA: $p = 0.004$).

Additionally, the trailing limb vertical and horizontal impulse in phase 2 were significantly reduced in the ITTA group ($p < 0.001$, ANCOVA: $p \leq 0.013$).

Table 5.2. Mean \pm SD of the whole-body features for the ITTA and initial toe contact (TC) control groups

	ITTA Group	TC Group	<i>p</i> -value
<i>Step Length (m)</i>	0.63 \pm 0.09	0.72 \pm 0.07	0.025
<i>Double Support Duration (s)</i>	0.07 \pm 0.02 [†]	0.10 \pm 0.01	0.001
<i>Braking Phase Duration (s)</i>	0.26 \pm 0.02	0.27 \pm 0.03	0.707
<i>Vertical VIC (m/s)</i>	-0.32 \pm 0.08	-0.32 \pm 0.03	0.955
<i>Horizontal VIC (m/s)</i>	0.62 \pm 0.10	0.74 \pm 0.06	0.006
Trailing Limb Phase 1			
<i>CoM Vertical Displacement (m)</i>	-0.07 \pm 0.01 [†]	-0.11 \pm 0.01	<0.001
<i>CoM Horizontal Displacement (m)</i>	0.34 \pm 0.05	0.37 \pm 0.03	0.142
<i>Vertical Impulse (N/kg/s)</i>	1.59 \pm 0.34	1.80 \pm 0.20	0.128
<i>Horizontal Impulse (N/kg/s)</i>	0.21 \pm 0.05	0.24 \pm 0.04	0.117
Trailing Limb Phase 2			
<i>CoM Vertical Displacement (m)</i>	-0.06 \pm 0.02	-0.05 \pm 0.01	0.147
<i>CoM Horizontal Displacement (m)</i>	0.11 \pm 0.03 [†]	0.18 \pm 0.02	<0.001
<i>Vertical Impulse (N/kg/s)</i>	0.15 \pm 0.09 [†]	0.38 \pm 0.11	<0.001
<i>Horizontal Impulse (N/kg/s)</i>	0.05 \pm 0.04 [†]	0.14 \pm 0.04	<0.001

[†] $p < 0.05$ significant differences after covarying for speed. VIC = velocity at initial contact

5.3.2.1. Leading Limb Features

The ankle angle at initial contact was significantly more plantarflexed in the leading limb of ITTAs compared to the TC group ($p = 0.024$) and tended to remain significant after covarying for speed ($p = 0.063$; Figure 5.2A). No significant differences were found for the remaining sagittal plane joint features at any individual joint or for any joint coordination coupling angles ($p \geq 0.086$, ANCOVA: $p \geq 0.243$; Figure 5.2A&B). The frontal plane knee joint angle at initial contact ($p = 0.173$; ITTA: $1.34^\circ \pm 1.9$; TC: $3.68^\circ \pm 4.3$) and ROM ($p = 0.323$; ITTA: $3.21^\circ \pm 1.6$; TC: $5.27^\circ \pm 5.5$) were also not significantly different between groups (ANCOVA: $p \geq 0.117$).

Ankle joint peak absorption power was not significantly different between groups ($p = 0.075$), yet became significantly greater in the intact limb of ITTAs ($p = 0.017$) after covarying for speed (Figure 5.3). Peak knee ($p = 0.887$, ANCOVA: $p = 0.963$) and hip ($p = 0.744$, ANCOVA: $p = 0.457$) joint absorption powers were not significantly different between groups. The total negative work completed in the leading limb was not significantly different between groups ($p = 0.208$), however, the ITTA group performed 15% greater total work on average than the TC group (Figure 5.4A). The intact limb of ITTAs completed significantly greater work at the ankle joint ($p = 0.017$, ANCOVA: $p = 0.014$). No significant differences were present in the individual joint work at the knee ($p = 0.580$, ANCOVA: $p = 0.865$) or hip ($p = 0.519$, ANCOVA: $p = 0.437$) joints. Both the ITTA and TC groups utilised the ankle joint as the primary shock absorber (78-80%), followed by the knee (13-14%), then the hip (5-9%; Figure 5.4B).

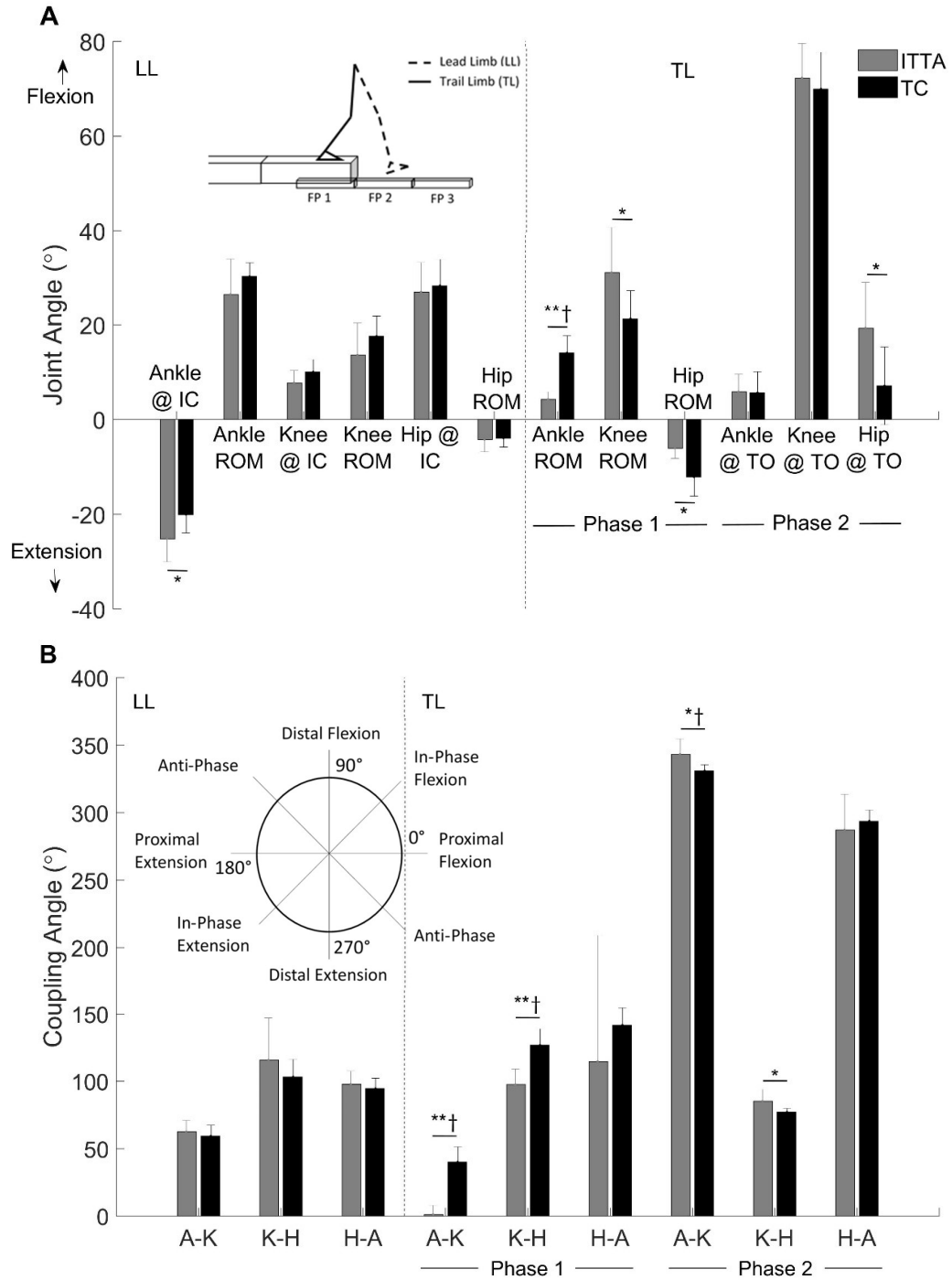


Figure 5.2. Leading limb and trailing limb A) joint angle features, and B) coupling angles for all lower-limb joint pairs. * $p < 0.05$, ** $p < 0.001$ significant differences between groups, † $p < 0.05$ significantly different after covarying for speed. IC = initial contact, ROM = range of motion, TO = toe-off, A-K = ankle-knee, K-H = knee-hip, H-A = hip-ankle.

5.3.2.2. *Trailing Limb Features – Phase 1*

When lowering the CoM, the prosthetic trailing limb performed a significantly reduced ROM at the ankle ($p < 0.001$; ANCOVA: $p < 0.001$) and hip ($p = 0.002$; ANCOVA: $p = 0.052$) joints, and significantly greater ROM was performed at the knee joint ($p = 0.016$; ANCOVA: $p = 0.154$) compared to the TC group (Figure 5.2A). The ankle-knee ($p < 0.001$, ANCOVA: $p < 0.001$) and knee-hip ($p < 0.001$, ANCOVA: $p = 0.014$) joint coordination pairs differed significantly between groups. The ITTA group ankle-knee coupling angle of $1 \pm 7^\circ$ denotes a knee flexion only strategy in the prosthetic trailing limb, while the TC group performed an in-phase flexion strategy ($40 \pm 11^\circ$; Figure 5.2B). The knee-hip joint coordination strategy for the prosthetic trailing limb also indicated a knee flexion only strategy ($98 \pm 11^\circ$). The TC group performed an anti-phase strategy ($127 \pm 12^\circ$) where the knee flexed synchronously with an extending hip. The hip-ankle coordination strategies were not significantly different between groups ($p = 0.381$, ANCOVA: $p = 0.471$).

Peak joint absorption powers were significantly reduced in the ITTA group at the ankle joint ($p < 0.001$, ANCOVA: $p < 0.001$) and significantly greater at the knee joint ($p = 0.040$, ANCOVA: $p = 0.119$) compared to the TC group (Figure 5.3). No significant difference in peak absorption power was present at the hip joint ($p = 0.891$, ANCOVA: $p = 0.875$). The total negative work completed by the trailing prosthetic limb during single support was significantly reduced ($p = 0.004$) by 58% compared to the TC group (Figure 5.4A). The negative work completed by the prosthetic limb in ITTAs was significantly lower at the ankle joint ($p < 0.001$, ANCOVA: $p < 0.001$) and hip joint ($p = 0.013$, ANCOVA: $p = 0.255$), and significantly greater at the knee joint ($p = 0.013$, ANCOVA: $p = 0.072$). The prosthetic trailing limb primarily utilised the knee joint (78%), while the TC group utilised the ankle joint (70%) to lower the CoM during single support (Figure 5.4B).

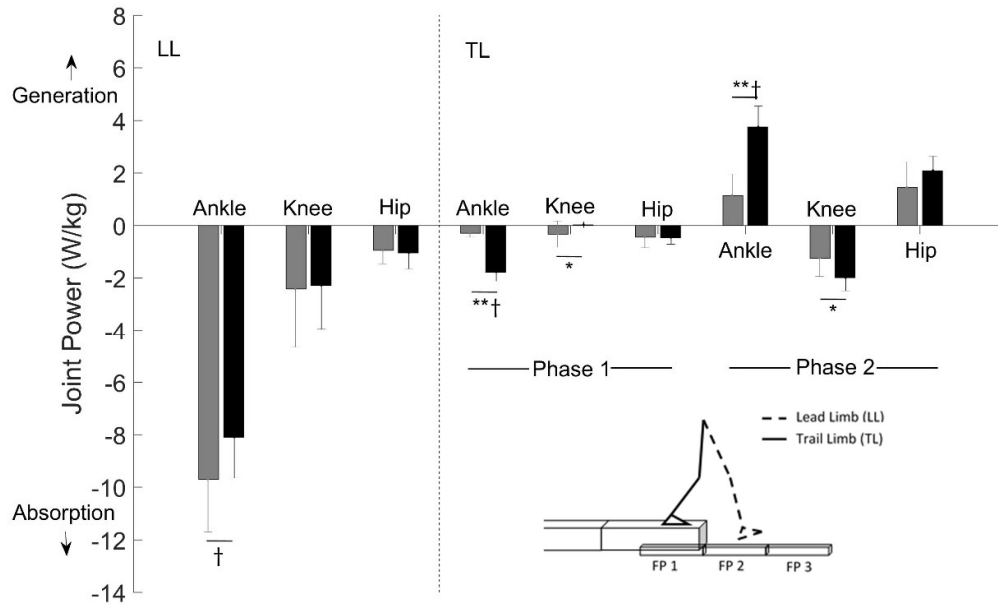


Figure 5.3. Joint peak powers in the leading limb (LL) and trailing limb (TL) phase 1 and phase 2 for the ITTA (grey) and TC (black) groups. * $p < 0.05$, ** $p < 0.001$ significant differences between groups, † $p < 0.05$ significantly different after covarying for speed

5.3.2.3. Trailing Limb Features – Phase 2

For continued forward progression, the prosthetic trailing limb of ITTAs had a significantly greater hip flexion angle at toe-off ($p = 0.011$, ANCOVA: $p = 0.553$; Figure 5.2A). The toe-off flexion angles at the ankle ($p = 0.945$, ANCOVA: $p = 0.476$) and knee ($p = 0.522$, ANCOVA: $p = 0.474$) were not significantly different between groups. However, the ankle-knee coordination strategy was significantly different between groups ($p = 0.006$, ANCOVA: $p = 0.039$; Figure 5.2B). The ITTA prosthetic limb ($343 \pm 11^\circ$) performed a knee joint flexion strategy to propel the CoM, while the TC group ($330 \pm 4^\circ$) utilised an anti-phase knee flexion strategy with ankle plantarflexion. Similarly, both groups performed an in-phase flexion strategy for the knee-hip joint pair with the ITTA group performing greater knee joint flexion ($p = 0.014$; $85 \pm 9^\circ$) than the TC group ($77 \pm 3^\circ$). This was not significant after speed covariation ($p = 0.109$). The hip-ankle coupling strategy was not significantly different between groups ($p = 0.466$, ANCOVA: $p = 0.770$).

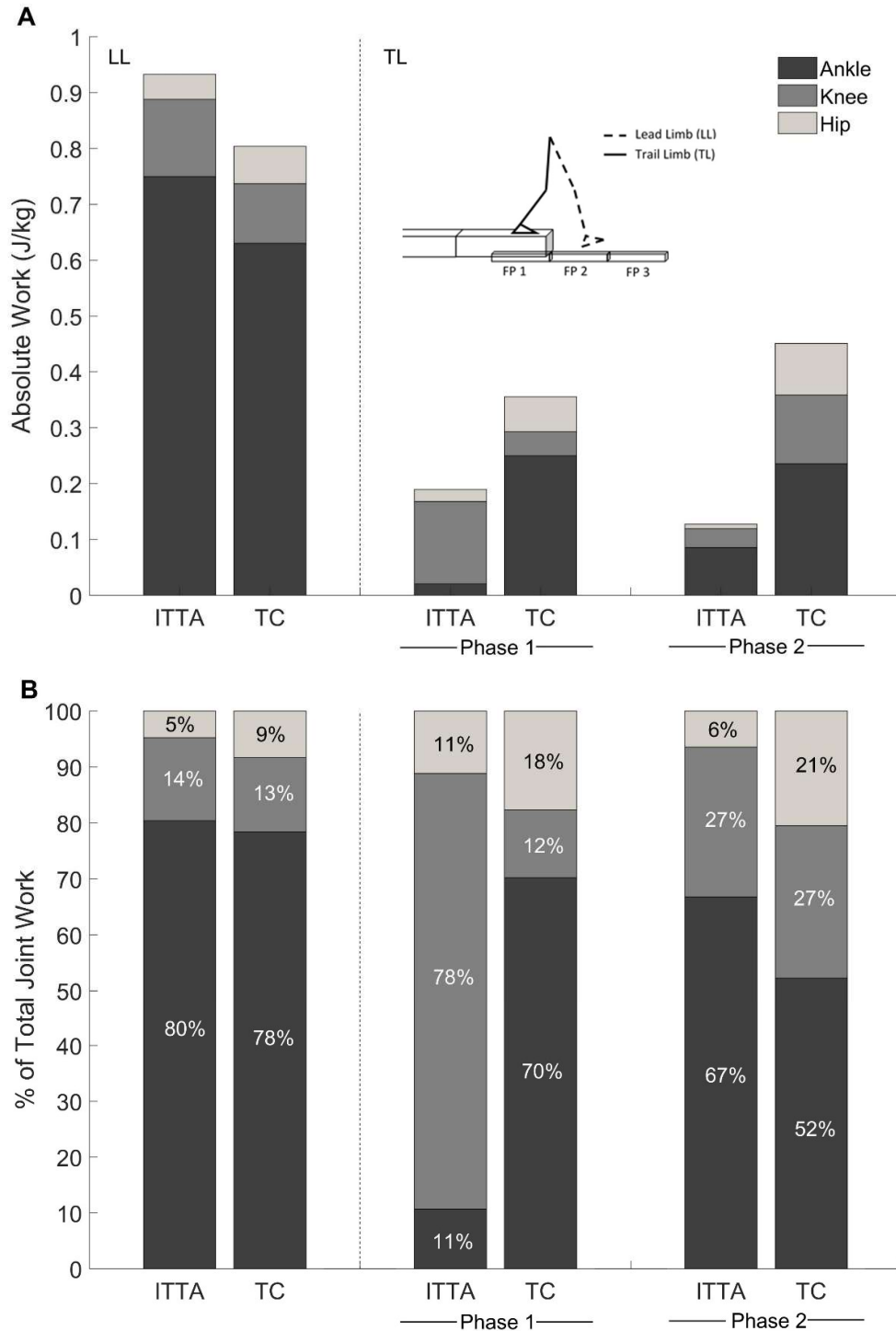


Figure 5.4. A) Absolute joint work completed and B) percentage joint contribution relative to the total joint work completed in the ankle (bottom), knee (middle), hip (top) joints during the leading limb (LL) and trailing limb (TL) phases of interest for the ITTA and toe initial contact (TC) groups.

Ankle joint peak propulsive power was significantly reduced in the trailing prosthetic limb of ITTAs ($p < 0.001$, ANCOVA: $p < 0.001$; Figure 5.3). The knee joint peak absorption power was also significantly reduced in ITTAs ($p = 0.017$) yet did not remain significant after covarying for speed ($p = 0.280$). Peak hip joint propulsive power was not significantly different between groups ($p = 0.098$, ANCOVA: $p = 0.631$). The total absolute work completed in the prosthetic trailing limb of ITTAs was significantly lower (111%, $p < 0.001$) than the TCs (Figure 5.4A). Individual joint work done in the ITTA group was significantly lower at the ankle ($p < 0.001$, ANCOVA: $p < 0.001$), knee ($p = 0.005$, ANCOVA: $p = 0.059$), and hip ($p < 0.001$, ANCOVA: $p < 0.001$) joints compared to the TC group. Both the ITTA and TC trailing limbs utilised the ankle joint to the greatest extent (52-67%) followed by the knee (27%) then the hip joint (6-21%; Figure 5.4B).

5.4. Discussion

This study aimed to investigate the descent strategy performed by ITTAs, the loading patterns in the intact leading limb, and the underlying mechanics in the leading and trailing limbs. As hypothesised, all ITTAs performed a TC strategy. In contrast with the second hypothesis, there were limited significant differences in the loading patterns between groups despite significantly reduced prosthetic limb motion and work done in both trailing limb sub-phases. The ITTAs performed the step descent at a significantly slower speed which may have influenced the development of lead limb load.

The few significant differences in load all occurred within the initial loading response. It is possible that this resulted from the shorter duration of the double support phase in the ITTA group (Table 5.2), suggesting that a quicker shift in work demand from the trailing limb to the leading limb occurred. The TC strategy may have been performed in order to utilise the functionality of the intact lead limb to accommodate for the re-distribution of work demand (Barnett et al., 2014). In agreement with the

current study, Schmalz et al. (2007), examining stair descent, found that the leading intact limb exhibited greater ankle plantarflexion immediately prior to initial contact thereby increasing the length of the limb to aid in lowering the CoM. While the Schmalz et al. (2007) study did not assess the trailing limb mechanics, the results from the current study suggest that the leading limb compensations were possibly from the reduced motion from the trailing limb. It is therefore likely that the limb lengthening mechanism was utilised in the ITTA group to aid in lowering the CoM by controlling the downward momentum and enhancing gait stability (van Dieën & Pijnappels, 2009, van Dieën et al., 2007, Barnett et al., 2014). This suggests that the descent strategy chosen was not necessarily an attempt to reduce lead limb load but could additionally be due to the reduced functionality of the prosthetic trailing limb (Buckley et al., 2013).

It is also possible that performing the step descent at a slower speed aided in gait stability and reducing limb and joint load. After speed covariation, the ITTA group experienced significant greater KFM, posterior GRF_y, and anterior KFx representing the first peak in each waveform at 7-8% of the braking phase (Figure 5.1). This denotes that if both groups had performed the step descent at the same speed, the ITTA group would have experienced a greater magnitude of load in these loading features. Given the limitations in the trailing limb, it is likely that the load experienced in the intact limb would have been greater had the step descent not been performed at a slower speed. The increased KFM and anterior KFx could suggest reduced hamstrings co-activation, which is necessary to aid in stabilising the knee joint (Paterno & Hewett, 2008). It is possible that the significantly straighter intact leading limb by ITTA participants in the current study, as denoted by the increased ankle plantarflexion at initial contact (Figure 5.2), reduced the ability of the hamstrings to activate and contributed to the increased anterior KFx. Repetitive high anterior shear forces at the knee joint can induce cartilage and ligament damage (Paterno & Hewett,

2008, Stergiou et al., 2007) and may be a factor in the increased risk of joint degeneration in ITTAs. The results from the current chapter indicate that the reduced speed in the ITTA group could be an additional approach to limit lead limb loading. This indicates that a toe landing may not be enough to reduce limb and joint loading and reductions in stepping speed may be required to limit the load experienced. This will be further explored in Chapter 6.

A possible reason for performing a toe descent strategy is to avoid reliance on the knee joint in the leading limb as this joint was only responsible for 13-14% of the total work when loading the limb for both groups (Figure 5.4B). Chapter 4 demonstrated that a heel initial contact strategy utilises the knee joint as the primary shock absorber as limited work can be done by the ankle joint given the reduced plantarflexion ROM that can be performed. Previous literature has found similar risk factors in those who develop osteoarthritis with other knee injury populations, such as anterior cruciate ligament (ACL) injuries. ACL individuals can be up to a three times greater risk of injury (including development of osteoarthritis) on the contralateral uninjured limb which is thought to stem from the compensatory asymmetrical strategies that increase the load on the contralateral limb, similar to ITTAs (Paterno et al., 2012, Wiggins et al., 2016, Goerger et al., 2015). Thus, ACL populations may aid in identifying possible load avoidance strategies. Nematollahi et al. (2016) examined segment coordination in ACL and healthy individuals when performing a step descent. The ACL individuals performed in-phase flexion strategies in the leading non-injured limb with a greater reliance on the ankle joint. The authors postulated that the knee-avoidance strategy would reduce the reliance on the knee joint and, therefore, possibly reduce the risk of developing comorbidities associated with knee joint degeneration. The ITTAs and TCs in the current study utilised similar ankle-knee in-phase flexion techniques as the ACL individuals (Figure 5.2) further suggesting that a TC strategy could be a knee load-avoidance approach.

It is well established that in elderly populations, muscular strength is lost first in the ankle joint musculature (Kerrigan et al., 1998, Judge et al., 1996) and these individuals tend to compensate through the use of the knee and hip joint musculature (Cofré et al., 2011, DeVita & Hortobagyi, 2000). It would be expected during a step descent that this population would utilise a heel contact strategy to avoid the increased ankle joint work that is accompanied with a TC strategy. However, elderly individuals tend to choose a TC strategy independent of speed or step height, further highlighting a possible knee protection priority during descent. It is additionally possible that reduced muscular strength in the trailing limb ankle joint in elderly individuals is unable to effectively lower and propel the CoM and, thus, the leading limb utilises a TC strategy as a compensatory approach (Kuo & Donelan, 2010, Adamczyk & Kuo, 2009).

The trailing limb mechanics differed significantly between groups in both sub-phases. The CoM vertical displacement, as noted in Table 5.2, was 6 cm greater in phase 1 (single support lowering the CoM) than phase 2 (double support propulsion) for the TC group. The ITTA group, however, lowered the CoM equally in both phases suggesting a different approach for task completion. During single support, the ITTA group compensated for the reduced capacity of the prosthetic ankle joint by performing greater work at the knee joint (78%; Figure 5.4B). This is in opposition of the TC group where 70% of the work to lower the CoM was done by the ankle joint. Additionally, the coordination strategies utilised in the prosthetic limb denoted a knee-flexion only strategy, rather than in combination with the hip or ankle joint (Figure 5.2B). The inability to coordinate and the reduced joint ROM from the hip and ankle joints (Figure 5.2A) in the prosthetic limb possibly resulted in the reduced vertical displacement of the CoM during single support. This is further confirmed by the extended leading limb ankle joint to aid in lowering the CoM given the limitations from the prosthetic trailing limb. The ITTA group in this study may have focused more on

the vertical displacement to lower the CoM than to continue forward progression. During the propulsive phase (phase 2), the CoM horizontal displacement and horizontal impulse were significantly reduced in the ITTA group independent of variations in stepping speed (Table 5.2). This indicates that at the same stepping speed, ITTAs would prioritise lowering the CoM over propulsion. This is further confirmed by the significantly reduced propulsive work done in the prosthetic limb at all lower-limb joints. When examining the overall contribution of each joint to the total work done, the majority of propulsion was generated by the prosthetic ankle joint in ITTAs, whereas the control group coordinated the total work done with the knee and hip joints (Figure 5.2B) which was absent in ITTAs. The trailing limb sub-phases may, therefore, not be appropriate in the ITTA population as lowering the CoM was a prominent feature in both sub-phases.

While not exhibited between ITTAs and controls performing the same descent strategy in the current study, the previous chapter found that the TC group exhibited a sustained midstance load independent of differences in speed. It was suggested that the sustained magnitude occurred due to the reduced ability to control the forward horizontal momentum stemming from a reduced step length. The ITTA group in the current study had a shorter step length (although not significant after covarying for speed; Table 5.2) and did not experience significantly different sustained load from the TC group (Figure 5.1). Therefore, the intact limb of ITTAs also presented with a sustained load. The previous chapter additionally postulated that the sustained loading phase could be due to reduced work done by the trailing limb. The ITTA group in this chapter performed 58% less total negative work in the trailing limb in phase 1, 111% less total work during phase 2, and 15% increased total work in the leading limb. While the work done in trailing limb was significantly reduced in the ITTA group, the sustained load was not significantly different. This could have been due to the slower stepping speed; however, the sustained loading phase did not become

significant after covarying for speed. Thus, it is possibly that the trailing limb mechanics may not have as much influence on the sustained midstance load as previously postulated in Chapter 4. Further research is warranted to determine the movement features in both the leading and trailing limbs that underpin the load experienced throughout the braking phase (Chapter 6).

5.5. Conclusion

Established ITTAs utilise a toe contact strategy when descending a step of 14 cm, representative of standard kerb height. There were few significant differences present in the limb and knee joint loading waveforms throughout the braking phase between groups. This occurred despite significant differences in the prosthetic trailing limb's ability to lower the CoM and propel the CoM to continue forward progression. ITTAs utilised a more vertical approach in the leading intact limb when performing the step descent compared to the controls. It is possible that ITTAs performed the TC strategy due to the limited functional capacity of the prosthetic trailing limb in both sub-phases rather than to reduce the load on the leading limb. The ITTA group performed the step descent at a slower speed which could have aided in reducing the load experienced throughout the braking phase given the limitations from the prosthetic trailing limb. When leading with the intact limb, utilisation of a TC strategy and reductions in stepping speed may be effective approaches to reduce the load experienced while compensating for limitations present in the prosthetic limb.

The results from this chapter suggest that a TC strategy, if not already currently utilised by ITTAs, should be the preferred descent strategy to mediate the magnitude and rate of initial loading of the leading limb. During rehabilitation post-amputation, it could be suggested that a TC strategy should be taught as a means of reducing load and possibly subsequent reduction of joint degenerative diseases.

5.6. Further Work

As ITTAs are at a greater risk of developing degenerative diseases, it is important to understand the joint mechanics that may aid in reducing limb and joint loading. Chapter 4 and the current chapter have suggested that trailing limb mechanics, leading limb descent strategies, and stepping speed may influence the magnitude and rate of limb and knee joint loading throughout the braking phase. No research has examined the movement features that most contribute to high load. The next chapter will attempt to determine the 'key' movement features that underpin high load.

While the focus of this thesis is on the intact limb leading during descent, trailing with the intact limb could enhance gait stability by utilising the functionality of the intact limb to lower the CoM and provide adequate propulsion. However, the load demand of the trailing limb is unknown, and it is possible that the demand when acting as a trailing limb may be greater than that when leading given the reduced ability of the prosthetic to take the load when leading. Further research should examine a step descent when leading with the prosthetic limb and trailing with the intact limb.

Chapter 6.

Lower-limb movement associated with high lead limb loading during a step descent

6.1. Introduction

Overloading of a limb during dynamic movement has been associated with the development and progression of degenerative diseases at the knee joint, such as osteoarthritis (Miyazaki et al., 2002, Vanwanseele et al., 2010, Thorp et al., 2006, Sharma et al., 2003). In injured populations, the un-injured limb is at a greater risk of developing comorbidities in the knee joint than healthy able-bodied individuals and is thought to stem from altered compensatory movement strategies resulting in high load (Paterno et al., 2012, Wiggins et al., 2016, Goerger et al., 2015). However, the movement features that contribute to high load are unclear and no research has identified these features in tasks outside of walking gait, such as step descent. Identification of these features may aid practitioners in the development of rehabilitation and exercise protocols to reduce the risk of knee loading related diseases in both able-bodied individuals and individuals with pathological gait, such as unilateral transtibial amputees (ITTAs).

In the attempt to reduce load, previous research has been conducted to examine gait modifications strategies as an alternative to invasive surgery. Modifications strategies

have included walking slower, decreasing stride length, toeing out, 'medial thrust', and use of walking canes or lateral heel wedges to reduce the first peak knee external adduction moment (KAM) (Fregly, 2012). These strategies aim to alter the magnitude of the ground reaction force (GRF) (Schmitz & Noehren, 2014) and the joint mechanics such that the lever arm of the GRF vector is minimised, thereby reducing medial knee joint loading (Hunt et al., 2006, Gerbrands et al., 2014, Schmitz & Noehren, 2014). These studies focus on reduction of medial joint loading as 60-80% of knee joint load is transmitted through the medial compartment (Erhart et al., 2010). KAM is the most commonly assessed measure of load as it has been demonstrated to be a good surrogate to assess medial knee joint compartment loading (Zhao et al., 2007) and has been associated with the severity and progression of degeneration of medial compartment joint tissue (Vanwanseele et al., 2010, Thorp et al., 2006, Miyazaki et al., 2002). Therefore, it is plausible to suggest that reductions in the vGRF and alterations of the joint mechanics to minimise the lever arm, thereby reducing KAM, could lower medial knee joint load during a step descent (Hunt et al., 2006, Creaby et al., 2013).

While slight reductions can occur at peak KAM when walking with any of the gait modifications strategies (e.g. walking slower), greater reductions in KAM were found over the rest of the stance phase (Fregly, 2012, Fregly et al., 2009, Walter et al., 2010, Astephen et al., 2008). This suggests the importance of examining features outside of peak magnitudes. Astephen & Deluzio (2005) utilised a principal component analysis on joint movement and loading waveforms to detect differences between osteoarthritic and control participants. This study demonstrated that the greatest variation between the two groups occurred during midstance where KAM was the greatest contributor in identifying participants with osteoarthritis. This study also found that the second most discriminatory feature in the identification of severe osteoarthritis was the medial knee joint force that occurred during the initial loading

response phase. Previous research has also suggested that loading rates in the initial loading response phase are more relevant measures than peak magnitudes in assessing joint loading (Morgenroth et al., 2014, Astephen & Deluzio, 2005, Radin & Paul, 1971). During step descent, Chapter 4 found no significant differences in the loading waveforms at peak magnitudes yet the time to peak was significantly lower when performing a toe initial contact strategy. The results from Astephen & Deluzio (2005) and Fregly (2012) in conjunction with the step descent results in the current thesis indicate the importance of reviewing loading features during initial loading response (loading rates) and midstance (sustained load). It is possible that different phases of loading could be related to different underlying movement features.

It has been postulated in previous research that a slower stepping speed may be an attempt to improve dynamic stability of the centre of mass (CoM) (van Dieën et al., 2008, Browne & Franz, 2017a). The previous chapters have additionally provided evidence to suggest that slower stepping speeds, in addition to alterations in the joint mechanics of the leading and trailing limbs, may be performed in the effort to maintain load at a lower level in the vertical, medial, and anterior-posterior directions during initial loading and midstance. Further, in level-walking, previous research has indicated that as walking speed decreases, peak forces decrease and minimum forces during midstance increase (Silverman et al., 2008, Spanjaard et al., 2009). In a meta-regression analysis of 19 studies examining peak KAM, Telfer et al. (2017) found that a decrease in walking speed of 0.1 m/s was estimated to decrease peak KAM by 0.18%bodyweight*height. Additionally, walking speed had the strongest effect on peak KAM over modifications in gait mechanics and footwear. However, other studies have suggested increases in the duration of load that occurs with reduced walking speeds could be detrimental (Robbins & Maly, 2009, Landry et al., 2007). It is currently unclear if speed alone can explain reductions in load or if it could also be due to the descent strategies chosen.

Step and stair descent research have currently postulated that only the underlying mechanics in the leading limb are related to reductions in load (van Dieën et al., 2008, Schmalz et al., 2007, Lythgo et al., 2007). Gait modification research also tends to only examine the limb of interest (i.e. leading limb) without modifying the mechanics performed by the contralateral limb (i.e. trailing limb). The results from chapters 4 & 5 have provided good evidence to suggest that, in the trailing limb, a reduced ability to coordinate the lower-limb joints to lower the CoM and decreased propulsive power to continue forward progression may affect the leading limb shock absorption mechanics (i.e. joint power). Subsequently, these compensatory mechanisms may influence the magnitude and rate of load in the leading limb. It is possible that a combination of leading and trailing limb joint mechanics may provide an optimal approach to performing a step descent with the notion of reducing limb and joint loading.

As repetitive high loading is related to the degeneration of joint cartilage (Arokoski et al., 2000), it is important to understand the movement strategies that underpin high load. Thus, the purpose of this study was to identify joint mechanics in the leading and trailing limbs that are related to high lead limb loading at the ground and in the knee joint in the vertical, medial, and anterior-posterior directions when performing a step descent during on-going walking. It is hypothesised that speed will be positively related to variations in limb and joint load. It is additionally hypothesised that joint mechanics in the leading and trailing limb will be significantly related to lower loading rates and reduced sustained load.

6.2. Methods

The data extraction procedures are outlined in Chapter 4 Section 4.2. . Loading waveforms and joint movement data were extracted for the leading and trailing limbs of three experimental groups: ITTAs ($n = 8$) and two able-bodied control groups that completed either a heel ($n = 12$; HC) or toe ($n = 10$; TC) initial contact descent strategy

with the leading limb. The leading limb was defined for the able-bodied controls as the first limb chosen to lead during descent, without instruction by the investigators. The intact limb of ITTAs was utilised as the leading limb and the prosthetic limb as the trailing limb.

The vGRF, KAM, and anterior-posterior intersegmental knee forces (KFx) were assessed. vGRF and KAM load were assessed as they are commonly used across the literature to assess limb and joint loading and vGRF, KAM, and KFx were all found to be significantly different between descent strategies (Chapter 4 Section 4.3.1). The vGRF, KAM, and KFx loading waveforms were reduced to discrete features based on the previous chapters results. The vGRF and KAM discrete features included loading rates and an average magnitude value of the sustained loading phase. The first impact peak in KFx (~7-8% of the braking phase; see Figure 4.2 and Figure 5.1) was extracted for further analysis. The braking phase was defined from initial contact to the last negative point in the anterior-posterior GRF. Loading rates were calculated by dividing peak magnitude by the time taken from initial contact, based on a 20N threshold, to the time of peak magnitude. This approach was utilised to avoid erroneous calculations associated with impact peaks that were present in the KAM waveforms. Additionally, the time point at which peak vGRF occurred was determined based on the force platform output due to the higher sampling rate (1000 Hz) to ensure greater accuracy in the timing of this peak time point. The average magnitude during the sustained midstance loading phase was calculated from 55-100% of the braking phase. This was based on the results from Chapter 4 (Section 4.3.1). This reduction was deemed appropriate due to the relatively flat plateau occurring within this phase. While peak magnitude is another reduction that is commonly used in the literature, the previous chapters found no significant differences at peak magnitude in the vGRF, KAM, or KFx waveforms between descent strategies or between ITTAs and able-bodied controls. Thus, peak magnitude was not included in this analysis.

Movement features were extracted from the leading limb and both trailing limb sub-phases (Section 4.2.1). To maintain power and avoid overfitting the data due to a smaller sample size ($n = 30$), the number of movement features were reduced for input into the regression model (Peduzzi et al., 1996). While there are many arbitrary rules in determining the number of predictors input into a regression analysis, Austin & Steyerberg (2015) found that as little as 2 participants per predictor variable ($30 \text{ participants} / 2 = 15 \text{ predictors maximum}$) enabled accurate estimations of regression coefficients, specifically the adjusted R^2 value, with less than 10% relative bias (systematic error). To account for all phases of interest when performing a step descent, movement features were chosen from the temporal-spatial parameters, leading limb joint mechanics associated with shock absorption, and both trailing limb phases of interest. Trailing limb phase 1 features corresponded to the controlled lowering of the CoM and phase 2 features represent the phase in which the majority of propulsion occurs to continue forward progression. The movement features chosen for further analysis were based on: 1) reducing multicollinearity, 2) significantly different features between descent strategies from Chapter 4 Section 4.3.2, and 3) significantly different features between ITTAs and controls from Chapter 5 Section 5.3.2. Multicollinearity of predictor features in a regression model can lead to unreliable estimates of regression coefficients (Alin et al., 2009) and make the interpretation of regression results difficult. Multicollinearity was assessed based on Pearson's correlation coefficients and variance inflation factors with thresholds of 0.7 and 10, respectively (O'Brien, 2007, Dormann et al., 2013). Multicollinearity results and discussion of the final features included in the regression model are presented in Table E1.1 in Appendix E. The temporal-spatial movement features selected were walking speed (m/s) and duration of the braking phase (s). Absolute ankle, knee, and hip peak absorption and propulsive powers (W/kg) were extracting from the leading limb and the trailing limb during phase 2 (see Appendix D for definition of peak powers). The movement features from trailing limb phase 1 included the ankle-knee,

knee-hip, and hip-ankle joint coordination coupling angles (°).

6.2.1. Statistical Analyses

Given that there were no significant differences in group demographics and that ITTAs did not perform differently to the toe landing control group, all three experimental groups were considered a single cohort to increase the variability and sample size of the dataset. Pearson's product moment correlations were performed to assess the bivariate relationships between discrete limb and joint loading features with each movement feature. The r -values were interpreted as no relationship = $r < 0.3$, weak = $0.3 < r < 0.5$, moderate = $0.5 < r < 0.7$, and strong = $0.7 < r < 1.0$. Forced entry multiple linear regression was performed to determine the amount of variance in the limb and joint loading features that could be explained with all movement features entered as predictor features. Features were z-score standardised prior to input into the regression model to determine the relative importance of each feature.

6.3. Results

Cohort demographics and discrete loading features are presented in Table 6.1. After examining the scatter plots for each bivariate correlation, an outlier was detected in the KAM loading features only. This outlier was the ITTA participant detected in Chapter 5 that had a knee external abduction moment and lateral ground and knee forces. As the sample size for this analysis is considered small (typically $n > 100$), an outlier would have a greater effect on the correlation coefficient. An outlier positioned away from the regression line effectively decreases the magnitude of the correlation coefficients. Therefore, this participant was removed for the analyses involving KAM.

Table 6.1. Cohort demographics and discrete loading features (mean \pm SD)

	Age (years)	35.6 \pm 7.6
Demographics	Height (cm)	179 \pm 6.5
	Mass (kg)	83.7 \pm 14
	vGRF (N/kg/s)	221 \pm 92
Loading Rate	KAM (Nm/kg/s)	9.52 \pm 3.7
	vGRF (N/kg)	10.2 \pm 2.3
Avg. Sustained Load	KAM (Nm/kg)	0.47 \pm 0.2
	KFx (N/kg)	1.04 \pm 1.8

Bivariate relationships of vGRF, KAM, and KFx loading features with speed are presented in Figure 6.1. A moderate relationship existed between increased KFx impact peak and slower stepping speeds (Table 6.2). All other loading features had weak to no relationships with stepping speed.

For brevity, only the moderate to strong bivariate relationships with joint mechanics are discussed in text (Table 6.2). Higher vGRF loading rates were moderately related to increased lead limb peak knee joint absorption powers ($p = 0.001$). KAM loading rates had weak to no relationship with any movement feature (abs. $r \leq 0.42$). Increased sustained vGRF midstance load was strongly related to reduced time spent in the braking phase ($p < 0.001$) and increased lead limb peak ankle absorption power ($p < 0.001$). A moderate relationship was also found where increased sustained vGRF load was significantly related to reduced trailing limb peak propulsive power at the ankle ($p = 0.003$). Increased sustained KAM midstance load was moderately related to reduced trailing limb peak knee joint absorption power required to propel the CoM forward ($p = 0.005$). Lastly, increased KFx impact peak was strongly related to greater lead limb peak ankle joint absorption power ($p < 0.001$) and moderately related to reduced time spent in the braking phase ($p < 0.001$).

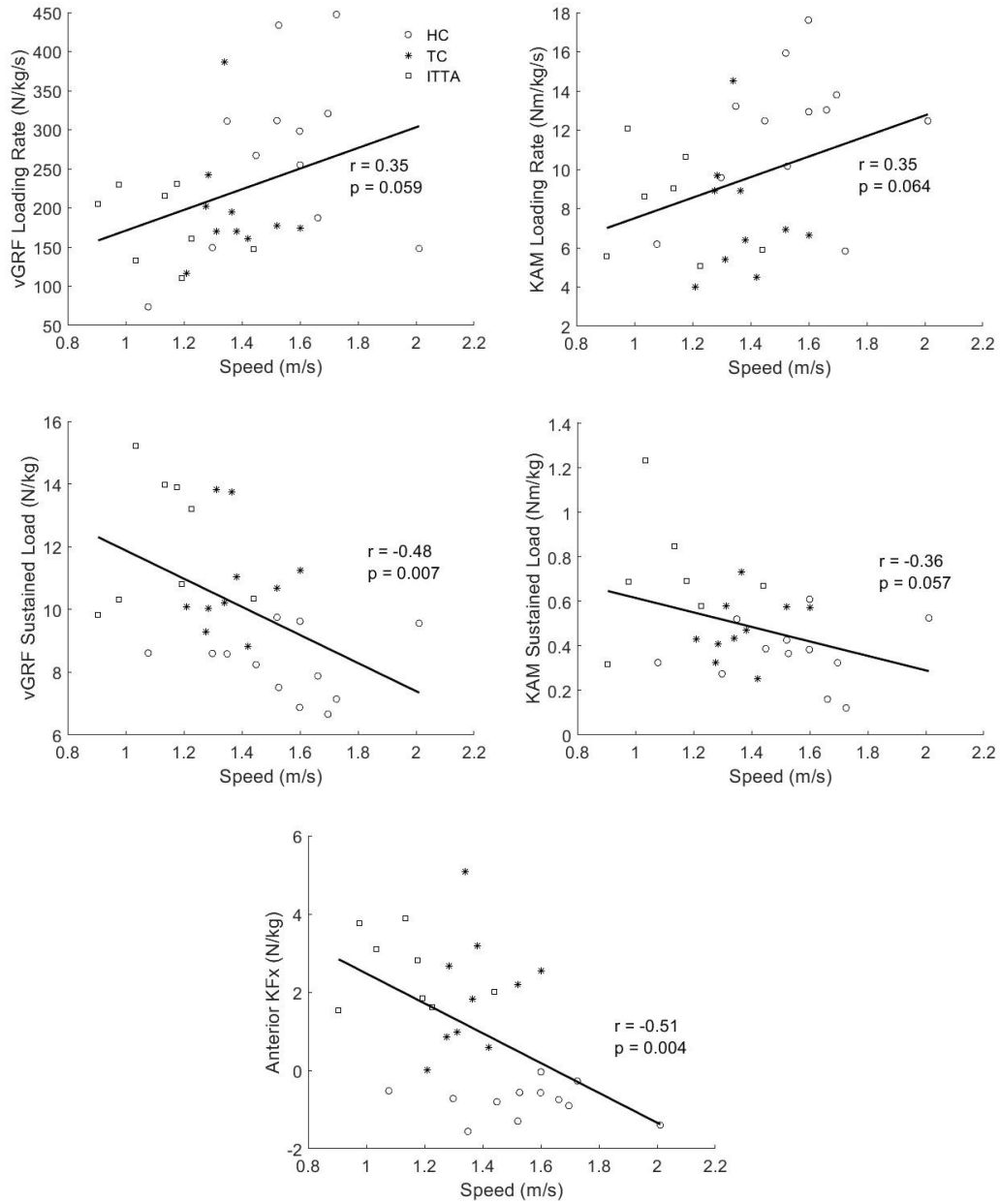


Figure 6.1. Bivariate relationships of stepping speed with vGRF and KAM loading rates and average sustained midstance magnitudes, and KFx impact peak. Experimental groups are denoted as follows: heel initial contact control (HC, circle), toe initial contact control (TC, asterisk), and intact limb of ITTAs (square).

After accounting for all other features, stepping speed was not a significant predictor in any regression model ($p \geq 0.092$; Table 6.3). Regression analyses indicated that the temporal-spatial features and joint mechanics in the leading and trailing limbs could explain 45% and 2% of the variance in the vGRF and KAM loading rates,

respectively; 75% and 36% of the variance in the vGRF and KAM sustained load, respectively; and 75% of the variance in the KFx impact peak (Table 6.3). The vGRF loading rate regression model found that the leading limb knee joint absorption power and the trailing limb knee-hip and hip-ankle joint pair coordination strategies were significant predictors. The duration of the braking phase was a significant predictor in the vGRF sustained load model. Additionally, the trailing limb hip-ankle joint pair and peak hip propulsive power tended to be significant predictors. The trailing limb knee joint propulsive power was a significant predictor that could explain the variance in the KAM sustained load. Lastly, the KFx impact peak was predominantly explained by the leading limb peak ankle joint absorption power.

Table 6.2. Pearson's product-moment bivariate correlations (*r*-values) for discrete vGRF (*n* = 30), KAM (*n* = 29), and KFx (*n* = 30) loading features with temporal-spatial, leading limb (LL) and trailing limb (TL) movement features

		LL Power						TL Phase 1 CA				TL Phase 2 Power			
		Speed	PD	Ankle	Knee	Hip	Speed	Ankle-Knee	Knee-Hip	Hip-Ankle	Ankle	Knee	Hip		
Loading Rate	<i>r</i>	0.35	0.10	-0.19	0.57	0.41	0.16	0.31	0.03	0.17	-0.01	-0.21			
	<i>p</i>	0.059	0.619	0.337	0.001	0.027	0.397	0.107	0.862	0.382	0.955	0.276			
KAM	<i>r</i>	0.35	0.20	-0.32	0.32	0.42	0.08	0.08	-0.01	0.14	0.13	0.08			
	<i>p</i>	0.064	0.301	0.096	0.094	0.025	0.700	0.689	0.963	0.467	0.517	0.687			
Sustained Load	<i>r</i>	-0.48	-0.77	0.66	-0.30	-0.37	-0.36	-0.24	0.10	-0.53	-0.46	-0.08			
	<i>p</i>	0.007	<0.001	<0.001	0.111	0.047	0.055	0.204	0.620	0.003	0.012	0.674			
Impact Peak	<i>r</i>	-0.36	-0.46	0.48	-0.14	-0.18	-0.40	-0.28	0.07	-0.45	-0.51	0.03			
	<i>p</i>	0.057	0.014	0.010	0.472	0.359	0.033	0.146	0.742	0.018	0.005	0.871			
KFX	<i>r</i>	-0.51	-0.58	0.84	0.02	-0.07	-0.27	-0.29	-0.12	-0.37	-0.11	0.10			
	<i>p</i>	0.004	<0.001	<0.001	0.914	0.708	0.159	0.126	0.542	0.049	0.582	0.610			

Bolded r-values denote p < 0.05; CA = coupling angle, PD = braking phase duration

Table 6.3. Multiple linear regression of discrete vGRF and KAM loading features with all movement features forced into the regression model. The values denoted are the β -coefficient values (standard error).

	Loading Rate			Sustained Load			Impact Peak		
	vGRF	KAM	vGRF	vGRF	KAM	KAM	KAM	KAM	KFx
	Adj. $R^2 = 0.45, p = 0.015$	Adj. $R^2 = 0.02, p = 0.456$	Adj. $R^2 = 0.75, p < 0.001$	Adj. $R^2 = 0.36, p = 0.047$	Adj. $R^2 = 0.75, p < 0.001$	Adj. $R^2 = 0.75, p < 0.001$	Adj. $R^2 = 0.75, p < 0.001$	Adj. $R^2 = 0.75, p < 0.001$	Adj. $R^2 = 0.75, p < 0.001$
	β -coefficient	p -value	β -coefficient	β -coefficient	p -value	β -coefficient	p -value	β -coefficient	p -value
Speed	-0.64 (0.4)	0.092	-0.25 (0.5)	0.612	0.434	0.12 (0.4)	0.753	-0.19 (0.2)	0.452
PD	-0.39 (0.2)	0.094	-0.26 (0.3)	0.424	0.015	0.01 (0.3)	0.960	-0.14 (0.2)	0.360
LL:									
Power									
Ankle	-0.17 (0.2)	0.503	-0.55 (0.4)	0.134	0.133	0.28 (0.3)	0.333	0.90 (0.2)	<0.001
Knee	0.60 (0.2)	0.025	0.14 (0.3)	0.680	0.473	0.05 (0.3)	0.865	0.24 (0.2)	0.174
Hip	0.10 (0.2)	0.657	0.39 (0.3)	0.216	0.913	0.04 (0.2)	0.868	0.00 (0.2)	0.991
TL Phase 1:									
CA									
Ankle-Knee	-0.38 (0.4)	0.338	-0.16 (0.5)	0.756	0.843	-0.07 (0.4)	0.860	0.17 (0.3)	0.527
Knee-Hip	1.97 (0.7)	0.011	0.20 (0.9)	0.826	0.119	-0.98 (0.7)	0.194	-0.32 (0.5)	0.508
Hip-Ankle	-1.09 (0.5)	0.029	-0.28 (0.6)	0.649	0.052	0.91 (0.5)	0.082	0.03 (0.3)	0.921
TL Phase 2:									
Power									
Ankle	0.01 (0.3)	0.965	-0.01 (0.4)	0.988	0.650	0.08 (0.3)	0.809	0.22 (0.2)	0.274
Knee	-0.07 (0.2)	0.709	-0.07 (0.3)	0.806	0.123	-0.53 (0.2)	0.023	0.07 (0.1)	0.581
Hip	0.09 (0.2)	0.722	0.41 (0.3)	0.231	0.068	0.07 (0.3)	0.805	-0.06 (0.2)	0.705

Significant features of $p < 0.05$ in each model are bolded; PD = braking phase duration; CA = coupling angle

6.4. Discussion

This chapter is the first to examine the relationships of vGRF, KAM, and anterior-posterior KFx loading with stepping speed and joint mechanics performed in the leading and trailing limbs during a step descent. In contrast to the first hypothesis, stepping speed was not a significant predictor for any loading feature when controlling for all other movement features (Table 6.3). However, the second hypothesis was confirmed indicating the importance of leading and trailing limb joint mechanics for reducing lead limb loading. The results from this study were able to identify features that may aid in reducing lead limb load which could reduce the risk of developing knee joint degenerative diseases.

When performing a step descent, van Dieën and colleagues (2008, 2007) suggested that slower stepping speeds are performed to enable greater stability during descent. In level-walking, Astephen et al. (2008) suggested that walking speed is reduced in response to pain following onset of degenerative diseases. However, Mündermann et al. (2004) found, in level-walking, that walking speed only explained 8.9% of the variance in peak KAM (a common indicator used to assess the risk of joint degeneration) in osteoarthritic patients. Despite the osteoarthritic patients walking at slower speeds, there was a wide range of peak KAM values suggesting that walking slower doesn't necessarily relate to lower peak KAM. In agreement with Mündermann et al. (2004), the current chapter found that stepping speed was not a significant predictor to explain the variance in vGRF and KAM loading rates and sustained midstance load, or KFx impact peak after considering the joint mechanics of the leading and trailing limbs. This indicates that the slower walking speeds may be a consequence of the descent strategy chosen and/or possibly performed to ensure stability and to alleviate knee pain.

Chapters 4 & 5 attempted to examine loading features independent of stepping speed by performing analysis of covariance tests. This allowed for the participants to perform

the step descent at their self-selected pace while considering variation in stepping speed. Chapter 4 demonstrated that loading features would have remained significantly different between heel contact (HC) and toe contact (TC) descent strategies independent of speed (Figure 4.2). However, chapter 4 did find that there was a trend towards an increased KAM sustained load in the TC group indicating that a slower stepping speed could reduce this load. Chapter 5 additionally found that the reduced speed in ITTAs lowered the anterior-posterior forces (Figure 5.1). While the current chapter found a moderate bivariate relationship of KFx impact peak with speed ($r = -0.51$), there were weak relationships of stepping speed with vGRF (abs. $r < 0.48$) and KAM (abs. $r < 0.36$) loading features. Further, the multiple regression results confirm that the joint mechanics, rather than speed ($p > 0.092$), are important in reducing load.

The bivariate correlation results from this study depicted a clear distinction between descent strategies which indicates that the variability in the load are based on whether a HC or TC strategy is utilised. A TC strategy utilises the ankle joint as the main shock absorber with less contribution from the knee and hip joints (van Dieën et al., 2008). This TC strategy was found to develop vGRF and KAM load at a lower rate during initial loading and maintain a greater sustained midstance load compared to a HC strategy (Chapter 4 & 5). In the current chapter, lower vGRF and KAM loading rates were moderately related to reduced lead limb peak knee joint absorption powers, consistent with TC strategy (Table 6.2). After controlling for speed and all other movement features, peak lead limb ankle joint power was not a major contributor to variations in load but rather joint mechanics beyond that of the ankle joint in both the leading and trailing limbs were important. This was unexpected given that toe and heel descent strategies are defined based on the ankle angle at initial contact in the leading limb and that it was moderately related to sustained load. Despite no relationship with the leading limb ankle joint, lower vGRF and KAM loading rates were

found to be moderately related to reduced lead limb peak knee joint absorption powers, consistent with TC strategy (Table 6.2). A reduced lead limb knee joint absorption power maintains reliance on the ankle joint as the main shock absorber, rather than the knee (Figure 4.5 & Figure 5.4; Nematollahi et al., 2016). Consistent with both HC and TC strategies, trailing limb joint coordination strategies during single support, which utilised a flexing ankle and knee joint in combination with an extending hip joint, was associated with lower vGRF loading rates (Table 6.3). ITTAs tend to utilise a knee-flexion only strategy in the trailing limb when lowering the CoM during single support. The results from this study suggest the need for the development of lower-limb joint coordination in the prosthetic limb of ITTAs. When greater kinetic energy is absorbed by the trailing limb, the kinetic energy absorbed by the leading limb is reduced (Donelan et al., 2002a) thereby lowering lead limb loading. The in-phase flexion joint coordination strategies of the trailing limb in combination with the leading limb toe initial contact strategy would possibly allow for an adequate share of the energy requirements to perform a step descent during initial loading response. Thus, this approach would lower vGRF loading rates.

KFx impact peaks were strongly associated with peak ankle joint power in the leading limb ($r = 0.84$) and, after accounting for speed and all other movement features, was maintained as the main contributor to explain the variance in KFx impact peaks ($\beta = 0.90 \pm 0.2$, $p < 0.001$). Increased peak ankle joint power, consistent with TC strategy, results in increased anterior KFx. Repetitive high anterior KFx have been suggested to induce cartilage and ligament damage (Paterno & Hewett, 2008, Stergiou et al., 2007) and, during ramp descent in healthy individuals, to be twice the magnitude of that experience in level-walking (Kuster et al., 1995, Redfern & DiPasquale, 1997, Reed-Jones & Vallis, 2008). This could suggest that a TC strategy may not provide as much benefit to load reduction as initially postulated despite reducing vGRF loading rates. However, the variation in KFx stemmed from the HC group

experiencing a posterior KFx impact peak while both TC and ITTA groups (performed a TC) had an initial anterior KFx. The posterior KFx in the HC group depicts a heel strike transient that is commonly seen in level-walking gait. Hunt et al. (2010) found that osteoarthritic individuals with heel strike transients were more likely to exhibit greater joint degeneration. Thus, it is unclear if an initial anterior KFx associated with a TC strategy is detrimental to the knee joint tissue. Despite this, there is a benefit from performing a TC strategy in reducing vGRF and KAM loading rates and is, therefore, an appropriate strategy to reduce initial lead limb loading.

Sustained load correlations were in opposition to that found during initial loading response. Decreased sustained vGRF and KAM loading were moderately related to reduced lead limb ankle joint power, consistent with a HC strategy (Table 6.2). Reduced sustained vGRF and KAM loading were also moderately correlated with increased trailing limb propulsive power at the ankle and knee joints and reduced vGRF sustained load was strongly correlated with a greater time spent in the braking phase. The sustained load correlations confirm the hypothesis from the previous two chapters which suggested that reduced propulsive power increased the magnitude of the sustained load. After accounting for other features in the model, including speed, propulsive features were maintained as important contributors to the variation in sustained load. This was evident by the association of the trailing limb knee joint absorption power with the KAM sustained load ($p = 0.023$) and the hip joint propulsive power associated with the vGRF sustained load ($p = 0.068$). For ITTAs who have limited propulsive capacity from the ankle joint, the results from the current study provide an optimal compensatory approach, by increasing propulsion from the knee and hip joints, to reduce vGRF and KAM sustained load. Additionally, while not significant, trailing limb joint coordination hip-ankle strategy to lower the CoM during single support (anti-phase strategy) tended to be an important contributor to reducing vGRF ($p = 0.052$) and KAM ($p = 0.082$) sustained load. This is consistent with the

trailing limb coordination mechanics required to lower vGRF loading rates. This suggest the importance of coordination of the trailing limb lower-limb joints prior to initial contact to both early and midstance loading in the leading limb.

The movement features selected in this chapter were only able to explain 2% of the variance in the KAM loading rate. This denotes that other contributing features that were not selected must exist. It should be noted that the features included in this chapter represented the strongest bivariate correlations with KAM loading rate amongst the remaining movement features not chosen. It is typical to assess frontal plane knee motion when examining KAM, however, no significant correlations were found for KAM loading rate with the frontal plane knee angle at initial contact ($r = -0.21$, $p = 0.279$) or ROM ($r = 0.05$, $p = 0.817$). This suggests that features beyond those discussed in this thesis may be important in explaining the variance in the KAM loading rate. These could include step width (Paquette et al., 2014, Anderson et al., 2018), forward and lateral trunk flexion (Hunt et al., 2008, Simic et al., 2012), frontal plane mechanics at the ankle and hip joints (Chang et al., 2005, Astephen et al., 2008), and internal rotation at all lower-limb joints (Astephen et al., 2008).

A limitation of the current chapter is the small sample size ($n \leq 30$). This could limit the power of the regression analysis where false negatives may have occurred. To increase the power of the analysis, the number of predictor features per dependent variable input into the regression model was reduced. Another possible limitation is the inclusion of all experimental groups in a single analysis as each group may not present with similar relationships; however, this was not apparent in this study.

6.5. Conclusion

The current study is the first to investigate the relationship between lead limb loading and underlying movement patterns when performing a step descent. Speed was not a key contributor in reducing lead limb loading during the initial loading response or sustained loading phases. By performing a TC strategy, vGRF and KAM loading rates

are lowered by reducing the knee joint absorption power. In-phase joint flexion coordination of the trailing limb when lowering the CoM may increase the percentage of total energy absorbed by the trailing limb and reduce that required by the leading limb. Joint coordination of the trailing limb is important for reducing both initial loading and sustained midstance loading. Lastly, increased propulsion from knee and hip joints in the trailing limb, consistent with a HC strategy, can be performed to reduce the magnitude of sustained load. Overall, to reduce initial loading a TC strategy should be utilised while a HC strategy should be utilised to reduce sustained load. Independent of the presence of amputation, the results from this chapter would suggest a TC strategy should be utilised to control initial loading of the leading limb for both ITTAs and controls. For ITTAs, rehabilitation or exercise protocols should focus on coordination of the trailing limb joints when lowering the CoM during single support to allow for in-phase flexion of the ankle and knee, while the hip extends.

6.6. Further Work

The results from the current chapter demonstrate that the joint mechanics, independent of speed, are important in the development of load during a step descent. However, this was determined based on covarying for different stepping speeds in which a TC strategy was performed at a slower pace. It is possible that the joint mechanics performed during a TC strategy cannot be enacted at higher stepping speeds and may, therefore, be a consequence of this approach. Further research utilising controlled stepping speed trials can investigate this theory.

Chapters 4, 5, and 6 presented evidence to suggest that the trailing limb mechanics may have influenced initial lead limb loading. The ability of the intact limb to attenuate load without the possible influence from the prosthetic limb or horizontal momentum requirements needs to be assessed. This could provide information regarding inherent deficiencies in the intact limb and mechanics performed to reduce load. This will be assessed in Chapter 7 & 8.

Chapter 7.

Mechanics of unilateral drop landings in the intact limb of amputees

7.1. Introduction

Previous research on individuals with a transtibial amputation (ITTAs) has suggested that the mechanics of the prosthetic limb may influence the intact limb mechanics, and subsequently the magnitude and rate of load experienced in walking (Morgenroth et al., 2011, Grabowski & D'Andrea, 2013), running (McGowan et al., 2012, Strike et al., 2018), step negotiation (Chapter 5), and start-stop tasks (Haber et al., 2018). This is postulated to result from the inability of the prosthesis to generate the propulsion required to continue forward progression (Morgenroth et al., 2011) or, in jump landings, from inadequate absorption of high forces through the prosthesis (Schoeman et al., 2013). These interactions between the prosthetic and intact limb may explain the altered shock absorption approach observed in the intact limb (i.e., reduced joint angles and powers) during the initial loading response phase of running, step/stair negotiation, and jump landing (Grabowski et al., 2010, Schmalz et al., 2007, Strike et al., 2018, Schoeman et al., 2013). Thus, the intact limb must perform greater work to either continue forward progression or arrest the lowering of the CoM (Donelan et al., 2002a), which results in high load compared to the prosthetic limb (Sanderson & Martin, 1997). However, no research has assessed the shock

absorption approach of the intact limb to attenuate load without the influence of the prosthetic limb and the requirement to continue forward progression. This could provide an indication of deficiencies in the intact limb following amputation, which may be useful for informing rehabilitation protocols.

A unilateral drop landing onto the intact limb can be used to further examine joint mechanics and load attenuation in response to a consistent vertical momentum. Reducing vertical momentum is required in many types of movement tasks such as walking, running, and jump landings, and is slowed through joint flexion and eccentric work to efficiently absorb rapid impact forces. Deficiencies in muscle strength of the knee extensors may also play a role in load attenuation. Decreased maximum muscle strength (maximum force/torque production) has been identified as one of the most frequent factors accompanying degenerative loading diseases (Pettersen et al., 2008) and has been suggested as an indication of increased limb loading (Egloff et al., 2012, Lloyd et al., 2010). Reduced eccentric work from the quadriceps muscles can result in the impact forces being absorbed by the surrounding tissue structures, such as cartilage and ligaments (Yeow et al., 2009b). Furthermore, frontal plane knee valgus motion can be increased 3-fold from decreased quadriceps muscle force (Hewett et al., 2005, Markolf et al., 1978) which has been identified as a risk factor associated with joint degeneration (Miyazaki et al., 2002). Increasing trunk flexion when landing has been found as a compensatory strategy to reduce the reliance on the eccentric contraction of the quadriceps. Greater trunk flexion is related to greater flexion at all lower-limb joints when landing from a jump which could aid in reducing knee joint loading (Blackburn & Padua, 2008, Blackburn & Padua, 2009). Substantial deficits in quadriceps muscle strength of 30-39% have previously been reported in the intact limb of ITTAs compared to able-bodied individuals (Lloyd et al., 2010, Pedrinelli et al., 2002); however, it is currently unknown how the intact limb may accommodate for decreased quadriceps strength when landing.

When landing from a jump, the time to develop muscular force to control joint motion is limited. Generation of rapid muscle force (i.e. explosive strength) has been shown to be important for re-stabilisation of the lower-limb joints following mechanical perturbations (Tillin et al., 2013, Andersen & Aagaard, 2006, Aagaard et al., 2002). The inability to stabilise and prevent rapid flexion of the knee joint during jump landings can lead to various acute and repetitive knee overloading injuries, e.g osteoarthritis and non-specific knee pain (Aerts et al., 2013). Explosive strength has not been examined in the intact limb of ITTAs yet could provide important information on the ability to initially stabilise the joint upon landing.

A study assessing bilateral jump landings (Schoeman et al., 2013) found that the intact limb of ITTAs underwent a smaller ROM at all lower-limb joints compared to the control population and experienced significantly greater peak vGRF (Intact limb: 25.25 ± 4.89 N/kg; Control: 22.34 ± 9.69 N/kg). This suggests that ITTAs utilise a more extended landing strategy in the intact limb. However, the ITTA study assessed a bilateral landing, thus, the restricted mechanics from the prosthesis could have influenced the results. Previous research has found that a more extended landing strategy is related to greater peak vGRF (Aerts et al., 2013). This strategy has been characterised by reduced joint flexion angles at touchdown, smaller range of motion (ROM) at each joint during load absorption, and increased joint angular velocities (Boling et al., 2009, Bisseling et al., 2008, Edwards et al., 2010, Louw et al., 2006, Bisseling et al., 2007). Previous research has consistently found the discrete movement features associated with more extended landing strategies (e.g., joint flexion, ROM, power, work) to be significantly related to various loading features (Yeow et al., 2009b, Tsai et al., 2017, Astephen & Deluzio, 2005) and significantly different between individuals with knee joint injuries (Aerts et al., 2013, Hewett et al., 2005, Boling et al., 2009, DeVita & Skelly, 1992) compared to controls. Those individuals who perform a more extended landing strategy also utilise a different joint

absorption approach as measured by joint power and work (DeVita & Skelly, 1992, Zhang et al., 2000). While the knee joint is a consistent contributor to dissipating the kinetic energy at touchdown, the percentage contribution of the ankle and hip joint work completed can shift to a more dominant ankle absorption strategy as the degree of knee flexion during landing decreases (Zhang et al., 2000, Norcross et al., 2013, DeVita & Skelly, 1992). Additionally, a more extended landing can reduce the duration of the absorption phase thus less work can be completed to dissipate impact forces. DeVita & Skelly (1992) found that a more extended landing absorbed 19% less total joint work suggesting that the kinetic energy was dissipated through other joint tissues, rather than through the large muscle groups, placing these individuals at a greater risk of tissue degeneration. These studies indicate that specific coordination strategies of the lower-limb joints, i.e. the relative motion between joints, may be related to the load experienced. It is possible that without the influence from the prosthetic limb, the intact limb may be able to adopt a more flexed landing strategy thereby reducing peak loads experienced.

In ITTAs, the intact limb is at a greater risk of experiencing knee pain, subsequent joint degeneration, and the development of comorbidities when compared to the prosthetic limb and the general population (Struyf et al., 2009, Norvell et al., 2005, Griffin & Guilak, 2005). The pathogenesis of joint degeneration is thought to stem from repetitive overloading in a limb (Arokoski et al., 2000), however, only one study has been conducted on landings in the ITTA population (Schoeman et al., 2013) where only the peak vertical ground reaction force (vGRF) was assessed. Research assessing overloading injuries has examined various discrete features within the GRF (Esposito & Wilken, 2014), knee joint moment (Morgenroth et al., 2014, Vanwanseele et al., 2010), and knee intersegmental force (Silverman & Neptune, 2014, Fey & Neptune, 2012) waveforms. There is no clear consensus on the most appropriate reduction of these loading waveforms to assess overloading associated with joint

degeneration in the ITTA population. Statistical parametric mapping is an approach which analyses a waveform in its original temporal-spatial format (Pataky, 2012) to remove the bias from an *a priori* approach when assessing limb or joint loading.

The purpose of this study was, therefore, to investigate limb and knee joint loading in the intact limb of ITTAs compared to able-bodied controls during a unilateral drop landing, independent of prosthetic limb interactions and the requirement of forward progression; and assess the mechanisms underpinning any differences, including quadriceps maximal and explosive strength and joint absorption mechanics. It is hypothesised that, compared to the control limb, the intact limb will 1) present with reduced quadriceps muscular strength and explosive strength, 2) experience a greater magnitude of load at the ground and at the knee joint throughout the absorption phase, and 3) perform altered joint mechanics in the sagittal plane for the ankle, knee, and hip joints (angles at touchdown, peak powers, and ROM, joint work, and joint coordination patterns throughout the absorption phase) and altered trunk flexion and knee joint valgus motion.

7.2. Methods

A comprehensive outline of the data collection procedures for drop landing can be found in Chapter 3 Section 3.4.5. Data processing for biomechanics data were completed as outlined in Chapter 3 Section 3.5. . One control participant was excluded from the analysis due to hip marker occlusion issues.

All strength and biomechanical features were extracted from the intact limb of ITTAs ($n = 8$) and the dominant control limb ($n = 21$). Dominance was defined as the limb that was chosen first to complete a unilateral landing.

7.2.1. Strength Data Collection

7.2.1.1. Equipment

Quadriceps isometric strength data were collected using an isokinetic dynamometer

(Humac Norm, Computer Sports Medicine Inc., Massachusetts, USA). The knee joint angle was set so that the angle during active maximal extension was 110° and the hip angle was set to 100° (full extension = 180°). Adjustable straps across the pelvis and shoulders were tightened to ensure no extraneous movement. The torque signal was sampled at 2000 Hz using an external A/D converter (16-bit signal recording resolution; Micro 1401, CED, Cambridge, UK) and interfaced with a PC using Spike 2 software (version 8; CED). All torque data were low-pass filtered using a fourth-order Butterworth filter with a cut-off frequency of 10 Hz, and were corrected for the weight of the limb by subtracting baseline resting torque.

7.2.1.2. Protocol

Participants performed a series of warm-up contractions of increasing torque values for 2-3 minutes. Following the warm-up, three maximal voluntary isometric contractions lasting ~3 s each were performed with a ~45 s rest in between each attempt. Additional attempts were required if peak force continued to increase with each subsequent effort. The only instruction provided was to 'push as hard as possible' and strong verbal encouragement was given throughout the contraction to encourage maximal effort. Real-time biofeedback of the torque-time curve and the peak torques achieved in each contraction were provided on a computer monitor in front of the participants. Maximum voluntary torque (MVT, considered a measure of maximum strength) was determined as the greatest peak torque recorded during any maximal or explosive contractions (see below), and normalised to body mass.

Explosive strength contractions were performed separate to the maximal contractions. Sahaly et al. (2001) and Dirnberger et al. (2016) examined the influence of instruction and the task goal on the measured outcome of explosive strength. They suggested that an emphasis on 'fast' during instruction without the concern for achieving maximal force production resulted in greater and more reliable explosive strength measures. Participants completed 10 explosive isometric contractions each

separated by ~20 s rest. Participants were instructed to 'push as fast and as hard as possible' for ~1 s, with an emphasis on 'fast' and aimed to achieve a minimum of 80% of MVT as quickly as possible. Real-time biofeedback was again provided to denote the participant's best explosive performance; the peak rate of torque development (RTD) was highlighted from the slope of the torque-time curve (15 ms time constant). Peak RTD calculations do not require detection of onset or peak torque and is calculated continuously prior to, during, and after each explosive contraction. The peak slope is then extracted as the measure of peak RTD. Resting torque was additionally monitored to ensure that no countermovement or pre-tension occurred before the contraction which could influence the ability to generate rapid force. Peak RTD was averaged from the three explosive voluntary contractions with the highest peak RTD's (Folland et al., 2014) and expressed relative to body mass.

7.2.2. Biomechanical Features Extracted

The loading waveforms analysed are detailed in Chapter 3 Section 3.6.1. In brief, the 3-dimensions of the ground reaction forces (GRF), knee moments (KM), and intersegmental knee forces (KF) were extracted for the duration of the absorption phase. The absorption phase was defined from touchdown, based on a 20N threshold in the vGRF through to maximal knee flexion in the limb of interest (i.e. intact limb of ITTAs and control limb). The duration of the absorption phase was calculated in seconds as a measure of the time taken to absorb the impact forces from landing.

Discrete movement features were extracted from the sagittal plane ankle, knee, and hip joints including touchdown angles, ROM, peak absorption powers, and negative joint work (see Figure D2.1 in Appendix D2). ROM was determined as the difference from minimal to maximal flexion during the absorption phase. Trunk flexion angle at touchdown and ROM was additionally extracted. This ROM was calculated based on angular change of the vector defined by the shoulder and anterior superior iliac spine markers and the vertical axis from touchdown to the end of the absorption phase.

Negative joint work was calculated as the area under the negative portion of the power-time curve using the trapezoidal rule for the duration of the absorption phase. Joint coordination was represented by coupling angles for the ankle-knee, knee-hip, and hip-ankle joint pairs. Coupling angles were calculated as the average value from touchdown to peak vGRF to assess the initial loading coupling strategy. The average value for coupling angles was deemed appropriate due to the relatively flat waveform prior to any issues associated with values around $0^{\circ}/360^{\circ}$ (Hughes & Watkins, 2008). See Chapter 3 Section 3.6.4.1 for coupling angle waveforms and discussion on its' reduction to the average discrete feature. Lastly, in the frontal plane, the knee joint touchdown angle and ROM were extracted.

7.2.3. Statistical Analysis

To assess differences between the intact and control limbs, independent *t*-tests were performed for strength, loading, and movement features. Loading waveforms were assessed using statistical parametric mapping (see Chapter 2 Section 2.7. and Chapter 3 Section 3.6.2). Landmark registration was not applied in this chapter due to the relatively short phase of landing which could result in over-registration.

7.3. Results

No significant differences were found between groups for age, height, or mass, although there was a tendency for ITTAs to be older than controls (Table 7.1). Average drop landing heights for both groups was 30.7 ± 3.4 cm and was not significantly different between groups. The duration of the absorption phase was also similar between groups.

Table 7.1. Participant demographics and whole-body features (mean \pm SD) for the intact limb of ITTAs and dominant control limbs

	ITTA	Control	<i>p</i> -value
<i>Age (years)</i>	40.0 \pm 9.0	34.0 \pm 6.5	0.064
<i>Mass (kg)</i>	84.5 \pm 18	83.4 \pm 11	0.769
<i>Height (cm)</i>	177 \pm 7.4	179 \pm 6.2	0.400
<i>Drop Height (cm)</i>	31.6 \pm 3.4	30.4 \pm 3.4	0.170
<i>Absorption Duration (s)</i>	0.21 \pm 0.04	0.20 \pm 0.13	0.798

7.3.1. Strength Differences

Table 7.2 presents the isometric strength features for both groups. There were no significant differences between the intact and control limbs for isometric MVT or peak RTD, although the intact limb had ~20-25% lower MVT and peak RTD.

Table 7.2. Maximal voluntary isometric torque (MVT) and peak rate of torque development (RTD) mean \pm SD for the intact limb of ITTAs and dominant control limb

	Intact Limb	Control Limb	<i>p</i> -value
<i>MVT (Nm/kg)</i>	2.29 \pm 1.2	2.79 \pm 0.6	0.134
<i>Peak RTD (Nm/kg/s)</i>	19.6 \pm 9.9	25.3 \pm 6.7	0.084

7.3.2. Loading Differences

Figure 7.1 presents the loading waveforms for the duration of the absorption phase in the control limb (solid black line) and the intact limb of ITTAs (dashed red line). No significant differences were present between groups for any loading waveform.

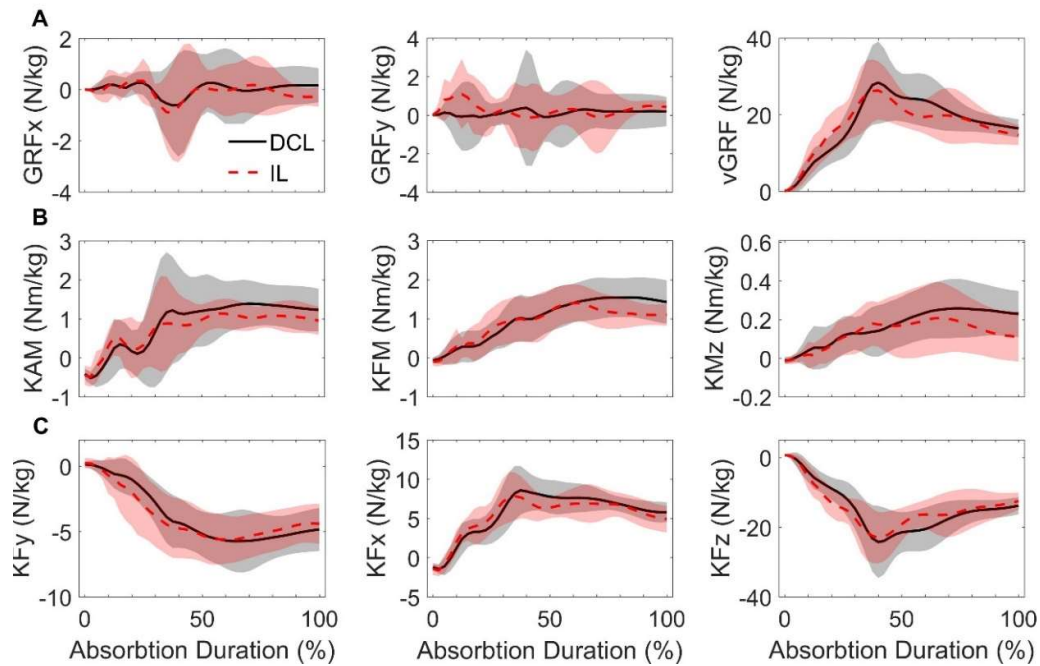


Figure 7.1. Each row presents the 3-dimensional loading waveforms for the A) GRFs, B) knee moments, and C) intersegmental knee forces (KF) in the intact limb (IL; red dashed) and dominant-control limb (DCL; black solid). Loading waveforms are presented for the duration of the absorption phase.

GRFx = lateral-medial, GRFy = anterior-posterior, vGRF = vertical, external knee flexor moment (KFM) = flexor-extensor, external knee adduction moment (KAM) = adduction-abduction, external rotational knee moment (KMz) = internal-external, KFx = anterior-posterior, KFy = lateral-medial, and KFz = compression

7.3.3. Movement Differences

The intact and control limbs did not differ significantly at any lower-limb joints or at the trunk for the touchdown angles ($p \geq 0.312$) or ROM ($p \geq 0.339$) in the sagittal and frontal planes (Figure 7.2A). Joint coordination strategies were not significantly different between groups for any lower-limb joint pair ($p \geq 0.385$; Figure 7.2B). Peak negative absorption powers were also not significantly different between groups at any joint ($p \geq 0.318$; Figure 7.2C).

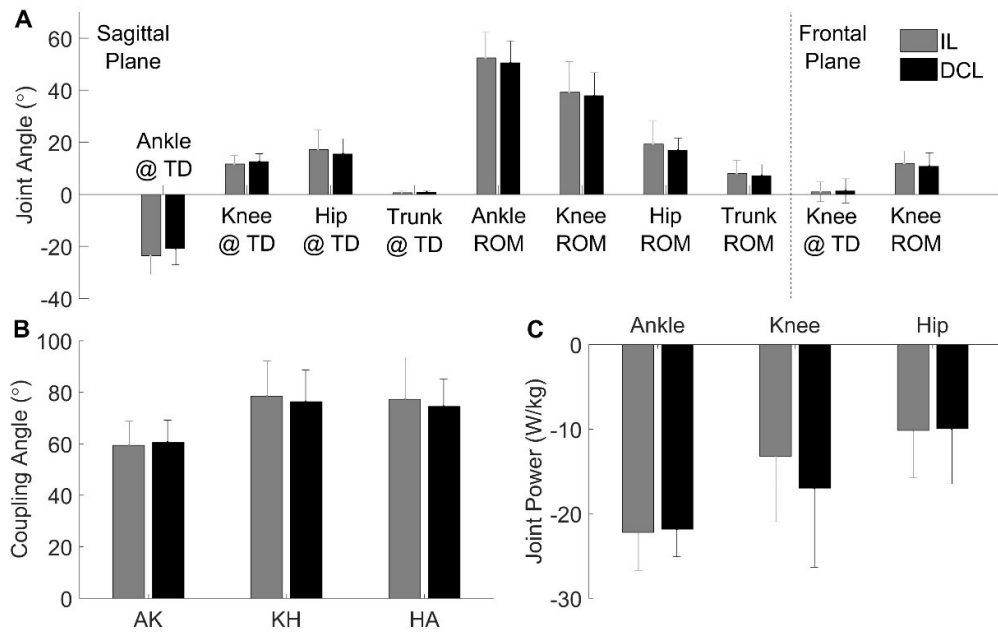


Figure 7.2. A) Joint angular position at touchdown (TD) and joint range of motion (ROM) in the sagittal and frontal plane, B) joint coordination coupling angle for the ankle-knee (AK), knee-hip (KH) and hip-ankle (HA), and C) peak joint absorption powers when landing at the ankle, knee, and hip joints in the intact limb (IL) and dominant control limb (DCL).

The individual joint work completed (Figure 7.3A) was not significantly different between groups at the ankle ($p = .950$; Intact limb: -1.23 ± 0.35 J/kg, Control limb: -1.22 ± 0.28 J/kg), knee ($p = .457$; Intact limb: -0.57 ± 0.28 J/kg, Control limb: -0.67 ± 0.36 J/kg) or hip joints ($p = .406$; Intact limb: -0.34 ± 0.25 J/kg, Control limb: -0.27 ± 0.20 J/kg). Both the intact and control limbs utilised the ankle joint as the primary joint to perform the negative work to reduce the momentum of the CoM (56-58%; Figure 7.3B).

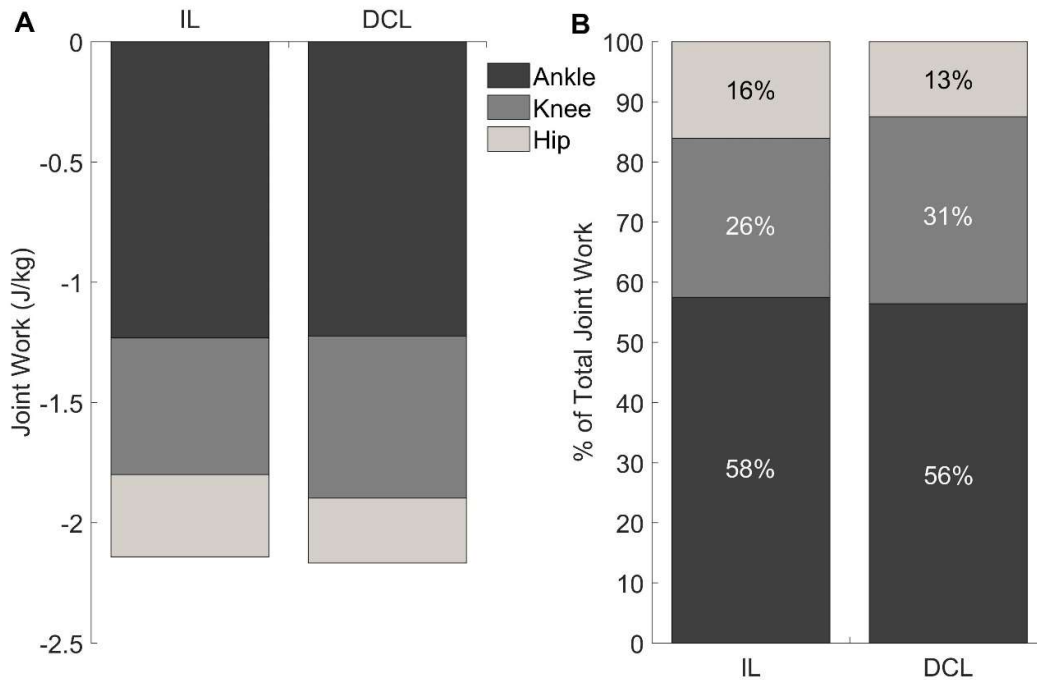


Figure 7.3. A) Individual joint work and B) joint percentage contribution of the total negative joint work performed in the ankle, knee, and hip joints for the intact limb (IL) and dominant control limb (DCL) during the absorption phase of landing

7.3.4. Waveform Variability Sub-Analysis

As noted in Figure 7.1, there was a large standard deviation in the loading features, specifically the vGRF and KAM, for both ITTAs and controls. This chapter postulated that a reduction in quadriceps strength or differences in the joint shock absorption approach of the intact limb would indicate between-group differences when all other influences were considered (i.e. landing height, prosthetic limb, forward progression). As no significant differences were found, the variance in the development of the vGRF and KAM loading waveforms are not explained by the absence or presence of an amputation. Thus, this sub-analysis aimed to examine the source of the variability and the underpinning mechanics that may have influenced the development of load.

7.3.4.1. vGRF

Upon investigation, the vGRF waveform patterns suggested a variation in the timing to peak magnitude (Figure 7.4; Ortega et al., 2010). These two patterns were evident

in both the controls and ITTAs suggesting that the pattern chosen was not group specific. To explore the variation, the ITTA and control data were combined ($n = 29$) and further split into two new groups based on the percentage of time to peak vGRF relative to the duration of the absorption phase. This approach was taken as the waveform analysis was conducted on time-normalised data. The average time to peak vGRF ($46 \pm 13\%$) was calculated and those participants with values above the average were deemed the 'late' group whilst those with values below the average were in the 'early' group (Table 7.3). Appendix F1 evaluates the group classification based on the time to peak vGRF as a percentage of the absorption phase (T%) compared to classifying based on the time to peak vGRF in seconds (Ts). Seven participants differed indicating a classification error of 24% using the T% to separate early and late groups. One participant differed due to an over-manipulation of the time-domain when linearly time-normalising the loading waveforms despite taking precautions to avoid this issue (i.e. time-normalising to the average length of the absorption phase across all participants). After removal of the outlier, the classification error reduced to 21%. The remaining six participants who differed between classification approaches had values within 0.01 s of the mean Ts and 13% from the T% mean across all participants indicating a middle peak group (Figure F1.1). These participants were removed from further analysis to ensure that comparisons were made on divergent groups (total left: $n = 22$).

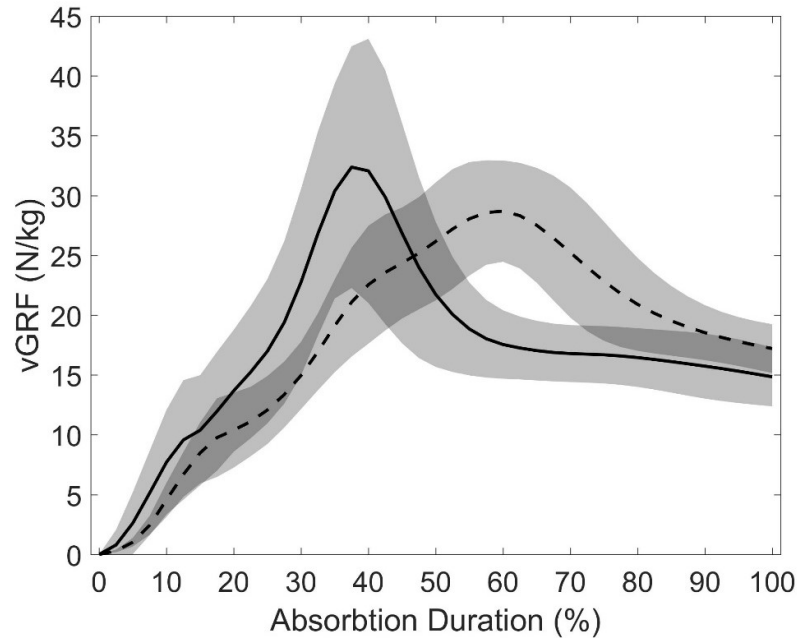


Figure 7.4. vGRF waveforms for participants with a longer time to peak magnitude (dashed line) and shorter time to peak magnitude (solid line) based on splitting the dataset by the time to peak vGRF as a percentage of the absorption phase. ITTA and control participants are present in both groups.

It can be seen in Figure 7.4 that much of the variability in the waveform could be explained by the variance in the time to peak magnitude. Both the $T\%$ ($p < 0.001$) and the T_s ($p = 0.034$) were significantly different between groups (Table 7.3). As there was a difference in the time to peak, waveform analysis did not directly compare peak magnitudes. Peak vGRF was found to be significantly higher in the early group ($p = 0.005$). Group composition consisted of equivalent numbers of controls and ITTAs, relative to their independent group size, in each group confirming that the variance in the vGRF waveform was not group specific (Table 7.3). The presence or absence of the first impact transient peak (see Figure F1.2 in Appendix F1) in each group was also identified. Impact peaks are caused by a brief inertial change of the body typically thought to occur due to the mechanics of the ankle joint (Hunt et al., 2010, Addison & Lieberman, 2015). According to Table 7.3, 83% of the participants in the early group had impact peaks present while an impact peak occurred in only 50% of the participants in the late group. Differences in the joint mechanics between groups may

explain the presence or absence of the impact peak and is explored below. Lastly, it was of interest to examine the control participant group composition in the early and late groupings compared to the group compositions in chapter 4 that was based on the initial contact step descent strategy. This could suggest that certain shock absorption mechanics are maintained across movement tasks, however, this was not present.

Table 7.3. Early and late group temporal features and group composition characteristics

	Early ($n = 12$)	Late ($n = 10$)
<i>Time to Peak (%)</i>	$37.6 \pm 6.7^{**}$	57.8 ± 8.3
<i>Time to Peak (s)</i>	$0.07 \pm 0.01^{**}$	0.09 ± 0.01
<i>Absorption Duration (s)</i>	$0.20 \pm 0.05^*$	0.17 ± 0.02
<i>Peak vGRF (N/kg)</i>	$41.3 \pm 7.1^*$	33.4 ± 3.9
Group Composition		
<i>Controls Present</i>	9	8
<i>ITTAs Present</i>	3	2
<i>Impact Peak Present</i>	10	5
<i>Step Descent: Control Heel Contact</i>	4	5
<i>Step Descent: Control Toe Contact</i>	5	3

* $p < 0.05$, ** $p < 0.001$

Comparison of the data in the new groupings found significant differences in the KFx and KFz loading waveforms ($p \leq 0.018$; in addition to the vGRF) and mechanics of the trunk and at the knee and hip joints ($p \leq 0.045$). Differences in the loading waveforms (vGRF, KFx, and KFz) occurred from ~32-38% ($p \leq 0.038$) and ~54-75% ($p < 0.001$) representing the phases in which peak magnitude occurred in the early and late groups, respectively. Those participants in the late group also had longer

times to peak magnitude in seconds in the KFx and KFz waveforms suggesting that the timing to peak is similar across multiple planes of motion.

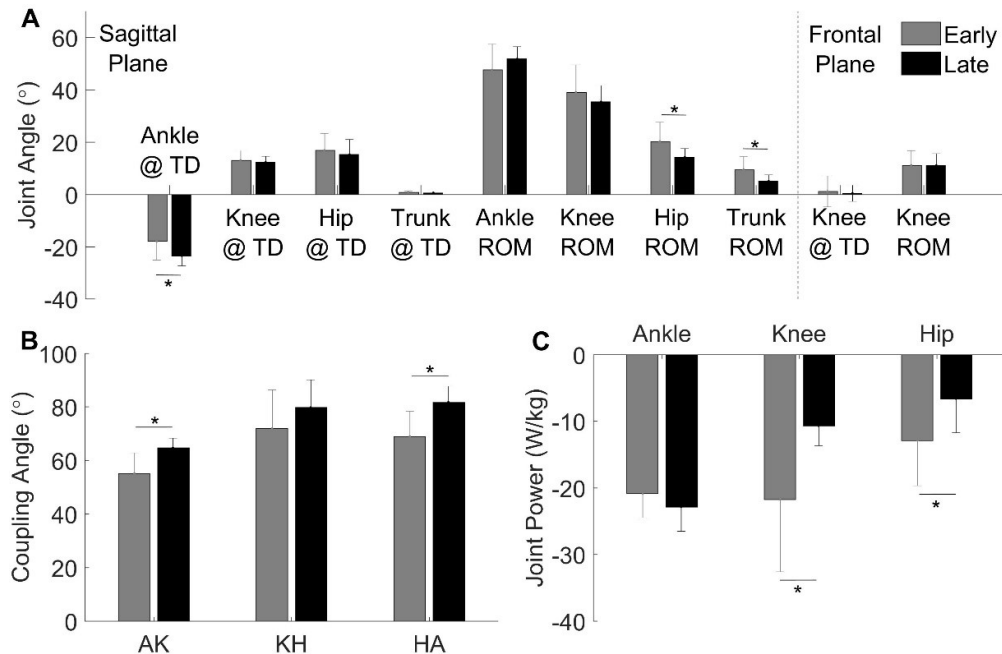


Figure 7.5. Early (grey) and late (black) groups A) Joint angular positions at touchdown (TD) and joint range of motion (ROM) in the sagittal and frontal plane, B) joint coordination coupling angle for the ankle-knee (AK), knee-hip (KH) and hip-ankle (HA), and C) peak joint absorption powers when landing at the ankle, knee, and hip joints.

Significant differences were present in the joint mechanics indicating that the shock absorption approaches could, at least in part, explain the variance in vGRF (Figure 7.5 & Figure 7.6). No significant differences were found in the strength features (MVT and peak RTD; $p \geq 0.660$). The late group exhibited significantly greater ankle plantarflexion angle at touchdown ($p = 0.041$) and significantly reduced hip ROM ($p = 0.030$) and trunk ROM ($p = 0.020$); significantly less peak joint absorption power at the knee ($p = 0.005$) and hip ($p = 0.026$) joints; significantly greater work done at the ankle joint ($p = 0.012$); and significantly less work at the knee ($p = 0.038$) and hip ($p = 0.020$) joints. Additionally, joint coordination for the ankle-knee ($p = 0.002$) and hip-ankle ($p = 0.001$) joint pairs were significantly different between groups. The late group performed an ankle dominant-strategy with less utilisation of the knee and hip joints to absorb the load through the limb. These results possibly stem from the late

group spending a shorter amount of time in the absorption phase ($p = 0.028$; Figure F1.2 in Appendix F1).

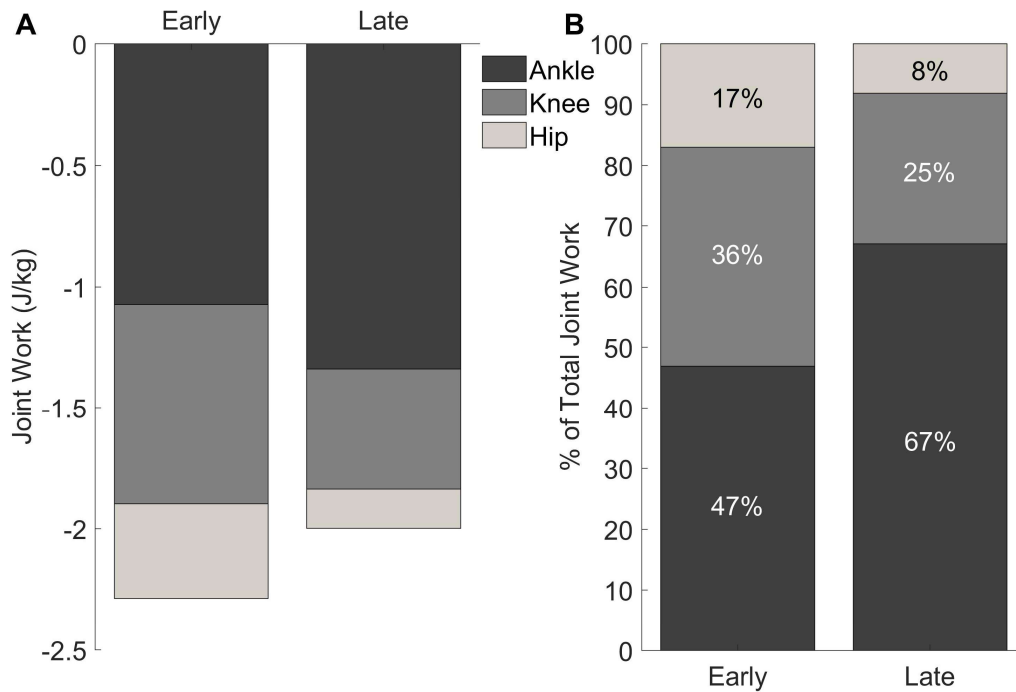


Figure 7.6. Early and late group A) individual joint work and B) joint percentage contribution of the total negative joint work performed in the ankle, knee, and hip joints during the absorption phase.

Ortega et al. (2010), assessing vertical jump landings, found similar results to that of the current sub-analysis in which a longer time to peak vGRF was significantly related to a reduced duration of the absorption phase ($r = -0.44$, $p = 0.014$) and a smaller peak vGRF ($r = -0.41$, $p = 0.026$). It was suggested that increasing the time to peak vGRF was optimal in reducing the risk of injury (by lowering the rate at which load is developed) while making the jump landing faster which is an important aspect of sport performance. The study, however, did not assess any joint mechanics and differs from other research (DeVita & Skelly, 1992, Zhang et al., 2000) which suggests that with a reduced absorption phase duration, a more extended landing strategy is performed and is associated with increased peak forces. The results from the current study demonstrate that with reduced landing duration, as exhibited by the late group,

a more extended landing strategy is performed (Figure 7.5 and Figure 7.6) yet elicits a lower peak vGRF (and possibly loading rate; Figure 7.4).

7.3.4.2. KAM

KAM is a commonly assessed loading feature that has been related to the onset and progression of joint degeneration (Zhao et al., 2007, Vanwanseele et al., 2010, Morgenroth et al., 2014). Therefore, the variability present in the KAM waveform (Figure 7.1B) was also examined. Figure 7.7A presents the combined ITTA and control KAM waveform dataset split into the early and late groupings defined by the time to peak vGRF (T%) as above. It can be seen that at least some of the variability in KAM can be explained by the variability in the time to peak vGRF suggesting that the time to peak KAM occurs at a similar time to the peak vGRF. However, there is still variability present specifically from ~25-50% of the absorption phase when the second peak in the KAM waveform occurred. Therefore, the time to peak KAM as a percentage of the absorption phase was calculated to split the combined ITTA and control dataset into new groupings. For the early_k group ($n = 10$), peak KAM occurred at $41 \pm 8.3\%$ of the absorption phase while the late_k group ($n = 12$) peak KAM occurred at $70 \pm 12\%$ ($p < 0.001$). The time to peak in seconds was also significantly different ($p < 0.001$; late_k: 0.12 ± 0.01 s, early_k: 0.08 ± 0.01 s). The time to peak KAM groupings reduced the variability further (Figure 7.7B). This suggests that the joint mechanics may have additionally influenced the development of KAM. In comparison of the participant classifications between the time to peak vGRF (Figure 7.7A) and the time to peak KAM (Figure 7.7B), only two participants differed indicating a classification error of 9.1%. Thus, as expected, differences in joint mechanics between the KAM early_k and late_k groups were similar to that of the vGRF early and late groups. This indicates that the performance of a more extended landing strategy, by utilising the ankle joint to absorb the rapid impact forces, could additionally lower the rate of KAM.

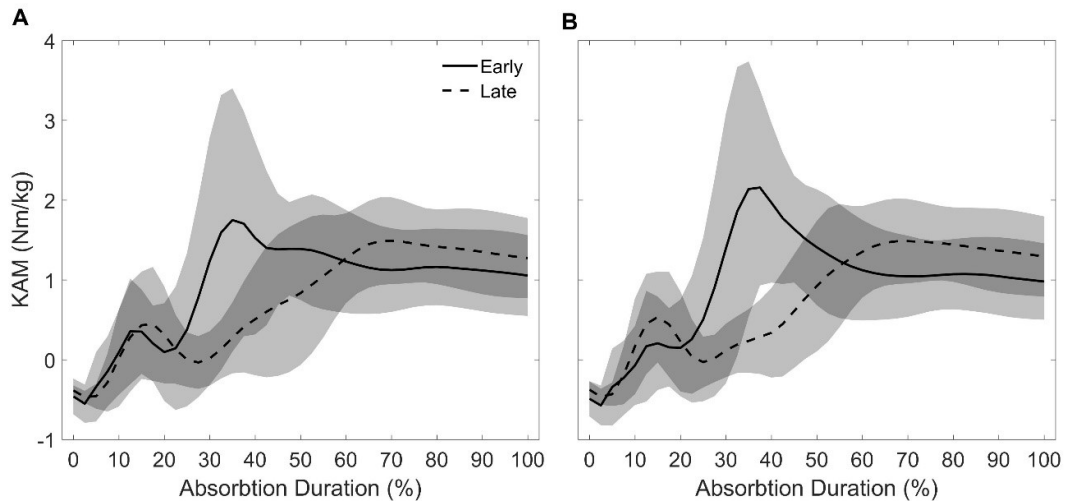


Figure 7.7. KAM waveforms (mean and SD cloud) for participants with a longer time to peak magnitude (dashed line) and shorter time to peak magnitude (solid line) based on splitting the dataset by the A) time to peak vGRF and B) time to peak KAM as a percentage of the absorption phase. TTA and control participants are present in both groups.

7.3.4.3. Stepwise Regression

Dynamic limb and joint loading is thought to be a significant risk factor in the development of injury. While movement features associated with a more extended landing strategy have been suggested as important risk factors, the relative importance of these features in relation to load have received limited attention. The above sub-analysis has suggested that a more extended landing strategy may actually lower vGRF and KAM loading rates. To determine the movement features that best explain the variance in the time to peak vGRF and KAM, stepwise regressions were performed with the average loading rates as the independent variables and movement and strength features as predictor variables. Average loading rates were calculated by dividing the peak magnitude by the time to peak. The combined dataset of all participants ($n = 29$) was input into the model as both ITTAs and controls were present in both early and late groups. To maintain power and avoid overfitting the data in the regression analysis (Peduzzi et al., 1996), <15 movement features in total were selected from the data presented in Chapter 7 (29 participants/2 = 14.5 predictor maximum; Austin & Steyerberg, 2015). To account for

any multicollinearity (Alin et al., 2009), variance inflation factors were calculated. The variance inflation factors provide an overall idea of the correlation between all features that could be included in the regression model. The discrete movement features included in the regression model had variance inflation factors of less than 10 (O'brien, 2007). See Table F2.1 in Appendix F2 for results of this analysis and discussion on the final features chosen for the model. The movement predictor features input into the final model included the joint angles at touchdown, absolute joint peak absorption powers, joint-pair coupling angles, frontal plane knee joint angle at touchdown and ROM, and MVT. All data were z-score normalised prior to input into the regression analyses to provide standardised beta-coefficients.

Three predictors in each model were able to explain 71% and 95% of the variance in the vGRF and KAM average loading rates, respectively (Table 7.4). The ankle and knee angles at touchdown and hip joint peak absorption power were significant predictors in explaining the variance in the vGRF loading rate. 91% of the variance in KAM loading rate was explained by the knee joint peak absorption power. The ankle and hip angles at touchdown were able to explain an additional 2% each. These findings demonstrate that when performing a unilateral drop landing with reduced ankle plantarflexion at touchdown, increased knee and hip flexion angles at touchdown, and greater peak knee and hip absorption powers, the limb and joint loading rates are significantly higher. A more extended landing strategy efficiently lowers the rate at which vGRF and KAM are developed by utilising the ankle joint as the primary shock absorber.

Table 7.4. Stepwise linear regression in the order added into the model. Values are denoted are the β -coefficient (standard error) with their respective adjusted R^2 contribution to the total adjusted R^2 .

vGRF Loading Rate			
Full Model: <i>Adj. R²</i> = 0.71, <i>p</i> < 0.001			
	β-coefficient	<i>p</i>-value	<i>Adj. R²</i>
<i>Ankle Angle @ TD</i>	0.81 (0.12)	< 0.001	0.40
<i>Hip Power</i>	0.60 (0.11)	< 0.001	0.26
<i>Knee Angle @ TD</i>	-0.29 (0.12)	0.026	0.05
KAM Loading Rate			
Full Model: <i>Adj. R²</i> = 0.95, <i>p</i> < 0.001			
<i>Knee Power</i>	0.83 (0.05)	< 0.001	0.91
<i>Ankle Angle @ TD</i>	0.19 (0.05)	< 0.001	0.02
<i>Hip Angle @ TD</i>	-0.17 (0.05)	0.002	0.02

7.4. Discussion

By examining a unilateral drop landing, this study investigated the limb and knee joint loading in the intact limb and the mechanisms utilised to attenuate this load without the influence of the prosthetic limb or task demands. The main finding of this study was that there were no significant differences between groups for the strength features, the joint mechanics utilised to absorb the impact from landing or in the load experienced at the ground or at the knee joint. These results provide evidence to suggest that overloading in the intact limb found in other studies and tasks (e.g., walking, step negotiation) is most likely due to the influence of the mechanics from the prosthetic limb or due to the task demands. This suggests that ITTAs are not at a greater risk of injury in the intact limb when performing a unilateral landing from a

drop height of 30 cm.

MVT was 20% and peak RTD was 25% lower in the intact limb of ITTAs compared to controls. The MVT deficits are smaller than those found in other ITTA studies which have indicated that the intact limb produces 30-39% less maximum strength than an able-bodied control (Lloyd et al., 2010, Pedrinelli et al., 2002). Further, MVT was higher in the current study compared to other ITTA studies (2.29 Nm/kg vs 0.85 Nm/kg). However, these studies included individuals whose amputation occurred due to vascular diseases, thus, the greater deficiencies in muscular strength may be due to the effects of the disease that are not present in traumatic amputations. These studies also made no reference to the activity level of their participants and Pedrinelli et al. (2002) included participants who used walking aids (20% of total participants). Those participants included in the current chapter were recreationally active (participation in sport or exercise a minimum of 2 days a week) which may have attributed to the lower percentage deficits. In comparison to previous research, MVT measured in the current study for able-bodied individuals was consistent with participants in other studies with the same activity level.

Past research has found negative correlations between quadriceps strength and peak vGRF in quadriceps inhibition (Palmieri-Smith et al., 2007) and anterior cruciate ligament injury jump landing studies (Ward et al., 2018) when landing from a height of 30 cm. Additionally, it is well known that quadriceps weakness is associated with joint degenerative diseases where strength deficits from 15-18% may be present prior to disease development (Slemenda et al., 1997, Segal & Glass, 2011). Previous research has suggested that isometric MVT deficits in the quadriceps of greater than 15% can negatively impact the loading patterns and alter the joint mechanics when landing from a jump (Schmitt et al., 2015). This can result in the absorption of impact forces by the tissue structures rather than by the bigger muscle groups, increasing the incidence of developing degenerative diseases (Yeow et al., 2009b, DeVita &

Skelly, 1992). However, the current study found no differences in loading patterns between groups suggesting that the strength deficits did not influence the magnitude or rate of load experienced.

As far as the authors are aware, the current study is the first to assess explosive strength in the intact limb of ITTAs. Previous research has found that greater RTD can aid in dynamic balance recovery (Behan et al., 2018), such as that seen in sporting movements, by rapid stabilisation of the lower-limb joints. Without stabilisation, the joints could move into injurious positions (e.g. reduced knee joint flexion) placing the load demand onto the cartilage (Winters & Rudolph, 2014). However, in the current study, the intact limb did not exhibit significantly different lower-limb motion, coordination patterns, or a shift in the shock absorption approach as both groups completed the majority of energy absorption in the ankle joint (56-58%). As the ITTA population in the current study did not experience greater limb or joint load, it is possible that both groups had sufficient quadriceps strength and were able to rapidly produce muscle strength that allowed an adequate degree of joint flexion to attenuate the load during landing (Palmieri-Smith et al., 2007).

Reduced quadriceps strength can be compensated for through a number of mechanisms including frontal plane knee valgus motion (Palmieri-Smith et al., 2008) and trunk flexion (Hughes, 2014). The current study, however, found no significant differences in the frontal plane knee motion or the sagittal plane trunk and knee flexion. These results differ from previous research. Goerger et al. (2015) suggested that when vGRF is similar, frontal plane motion may be altered as a possible compensation to absorb load when deficits in quadriceps strength are present. This was also reported by Palmieri-Smith et al. (2008) in which reduced quadriceps preparatory activation prior to touchdown was associated with increased peak knee valgus angles. Healthy participants, who landed with greater peak trunk flexion, had a reduced quadriceps activity and landing forces suggesting a reduced reliance on

the eccentric contraction of the quadriceps to attenuate load (Blackburn & Padua, 2009). Greater active trunk flexion during landing is also associated with a more flexed strategy at the knee and hip joints (Blackburn & Padua, 2008) potentially contributing to the reduced landing forces. That there were no significant differences between ITTAs and controls in the current study, suggests that the 20% deficit in quadriceps maximal strength and 25% deficit in peak RTD did not elicit compensations in the landing mechanics. Additionally, these deficits did not impact the magnitude and rate of load experienced when landing from a drop height of 30 cm. Further research could examine the landing height about which compensations may occur in response to reduced quadriceps strength.

Both groups performed an ankle dominant joint absorption approach when landing (Figure 7.3). Greater utilisation of the ankle joint to attenuate load has been found to be associated with increases in peak vGRF, KFM, and anterior KFx magnitudes (DeVita & Skelly, 1992, Zhang et al., 2000, Norcross et al., 2010). Healthy individuals who performed a more extended landing strategy at all joints utilised the ankle joint to perform ~50% of the total joint work (DeVita & Skelly, 1992, Zhang et al., 2000). Rowley & Richards (2015) determined that an optimal ankle plantarflexion angle at initial contact between 20-30° would limit the peak vGRF and vGRF loading rate when landing from a jump. Additionally, within this optimal plantarflexion range, the lower-limb joints' contribution relative to the support moment were found to be relatively equal (ankle, knee and hip joints between 30-40% of total). This suggests that in-phase joint flexion coordination could potentially reduce load at the ground and at the knee joint by absorbing the load equally at the lower-limb joints (Hughes & Watkins, 2008). The ITTA and control participants in the current study landed with an 'optimal' ankle plantarflexion angle. However, there was greater utilisation of the distal joints where 56-58% of the total joint work was completed by the ankle. In comparison to unilateral drop landing research, the joint mechanics were similar to that in the current

study (Pappas et al., 2007b, Palmieri-Smith et al., 2007). It was suggested that a more extended landing strategy is performed in unilateral landings to maintain balance despite the greater risk of injury when utilising this approach (Pappas et al., 2007b). It is also possible that the extended landing strategy was performed by ITTAs in this study to limit the eccentric work required from the quadriceps. Thus, a unilateral landing did not elicit greater joint flexion in the intact limb when the prosthetic limb contribution was absent. Single-limb balance and quadriceps strength training may enable the intact limb to adopt a more flexed landing strategy which could be important in reducing load in many sporting manoeuvres.

Landing height has been shown to influence the landing joint mechanics as greater momentum is experienced as landing height increases (Seegmiller & McCaw, 2003, Yeow et al., 2009a, Yeow et al., 2010). Schoeman et al. (2013) found greater vGRF was experienced in the intact limb compared to the control limb. However, the ITTA group landed from a significantly lower jump height than the controls. This could suggest that the vGRF should have been significantly greater when ITTAs landed from the same height as the controls. However, the vGRF experienced in the intact limb in the current study was similar to the vGRF experienced in the intact limb of the Schoeman et al. (2013) study. This occurred despite landing from almost double the height (15 cm vs 30 cm). One possible reason is that the intact limb in the current study performed greater joint ROM compared to the intact limb of the ITTAs who landed from half the height (15 ± 6 cm). Further, the intact limb in the current study performed similar ROM at all lower-limb joints to the control group in the Schoeman et al. (2013) study who landed from the same height (31 cm). This shock absorption adaptation has been seen in able-bodied individuals who increase the joint flexion angles as the drop height increases thereby limiting the load experienced (Yeow et al., 2010). Therefore, the results from the current study suggest that ITTAs can adapt to the higher landing height and attenuate load without the influence from the

prosthetic limb by adopting shock absorption strategies similar to that of a control population.

7.5. Conclusion

The intact limb of ITTAs does not experience significantly different load and does not perform significantly different joint absorption mechanics compared to an able-bodied control, when landing on this limb from a drop height of 30 cm. This was despite deficits in the knee extensor isometric MVT and peak RTD in the intact limb that were greater than deficits that have previously indicated altered joint mechanics and loading patterns. It is therefore plausible that without the influence from the prosthetic limb or the requirement for continued forward progression, the intact limb of ITTAs can attenuate load when landing from a jump up to 30 cm in height similar to able-bodied controls. The sub-analysis between early and late time to peak groups found two different strategies to attenuate limb and joint loading. A more extended landing strategy, by utilising the ankle joint as the primary shock absorber, was found to be a significant predictor in decreasing the initial rate of vGRF and KAM loading. Loading rates have been suggested as an important risk factor in the development of degenerative diseases. As the ITTAs who participated in the current study were recreationally active, this would suggest that inclusion of unilateral drop landings in rehabilitation and exercise programmes for less-active or non-established ITTAs could aid in the development of strength and coordination and increase participation in sport and exercise.

7.6. Further Work

Previous research in continuous movement tasks, such as walking, have postulated the possible influence of the prosthetic trailing limb on intact limb mechanics and loading. However, in discrete tasks which require synchronous joint flexion to attenuate load, such as jump landings, this influence has not been examined. As typical landing manoeuvres during exercise and sport are performed utilising both

limbs to attenuate load, further research is warranted to determine the influence of the prosthetic limb on the intact limbs' shock absorption approach during a bilateral landing. This will be explored in the next chapter.

To determine the viability of including unilateral drop landings in rehabilitation protocols for ITTAs, analysis of landings from different heights onto the intact limb should be performed. The height about which limb and joint load is minimised while stimulating muscle activation could be optimal for rehabilitation and increase participation in sport and exercise. This approach could additionally provide increases in stability and prevent falls in the amputee population.

Chapter 8.

Mechanics of bilateral drop landings in the intact limb of amputees

8.1. Introduction

Individuals with transtibial amputations (ITTAs) are encouraged to participate in sport and exercise by health professionals as an active lifestyle can enhance psychological well-being and provide numerous health benefits. For example, it can decrease the likelihood of developing secondary conditions post-amputation such as cardiovascular disease, hypertension, and other various chronic conditions linked to sedentary lifestyles (Chapman, 2008, Sanderson & Martin, 1996). ITTAs may be discouraged from participating in sports involving jumping (e.g. volleyball, basketball) due to the perceived excessive magnitude of load experienced during landing (Bragaru et al., 2011, Deans et al., 2012). These sports are typically adapted to either sitting or wheelchair versions for ITTAs which reduces the impact loading on the lower-limbs, however, does not necessarily provide the exercise-related benefits that comes from standing participation. Repetitive high load on the lower-limb joints is thought to increase the risk of developing degenerative joint diseases, such as osteoarthritis, specifically in the intact limb of ITTAs (Norvell et al., 2005, Struyf et al., 2009). However, there is limited research to suggest that the intact limb experiences a greater load and thereafter is at a greater risk of injury compared to able-bodied

controls when landing from a jump.

Typical bilateral landings in sport and exercise require near synchronous joint flexion of both limbs to attenuate load. Eccentric control of the plantarflexors at the ankle joint is the first point of shock absorption that aids in effectively controlling the downward momentum of the centre of mass (CoM) (DeVita & Skelly, 1992). The prosthetic ankle joint has limited range of motion (ROM) and reduced shock absorption capabilities. This can result in experiencing excessive pressure at the socket-limb interface during a landing causing pain or skin breakdown (Klute & Berge, 2004, Dudek et al., 2005). When landing from a jump, ITTAs may perform a quasi-unilateral landing as a load-avoidance strategy in the prosthetic limb or in response to the restricted mechanics of the prosthesis (Schoeman et al., 2013). As far as the authors are aware, only one study has assessed jump landings in ITTAs which depicted this quasi-unilateral landing strategy (Schoeman et al., 2013). This study found that the intact limb touched down earlier than the prosthetic limb (0.04 ± 0.02 s) and this difference in timing was significantly different to the control population, who landed with both feet almost simultaneously (0.01 ± 0.00 s). Thus, the intact limb was responsible for reducing a greater percentage of the total momentum than the prosthetic limb and the control limbs.

Chapter 7, which assessed unilateral drop landings, presented evidence to suggest that the intact limb of ITTAs is capable of attenuating load from a landing height of up to 30 cm by adopting joint mechanics not significantly different to those of an able-bodied control group when the influence of the prosthetic limb is absent. Schoeman et al. (2013) examined the performance of bilateral maximal jump landings in ITTAs. Significant differences were present in the load experienced and joint mechanics performed between the intact limb and an able-bodied control limb. This would suggest that a between-limb influence is present in discrete in-phase tasks such as landings. However, the differences found in the Schoeman et al. (2013) study may

also have been the result of differences in landing height. Landing height has been found in previous research to influence the magnitude and rate of limb and joint loading and the joint mechanics performed (Seegmiller & McCaw, 2003, Yeow et al., 2009a, Yeow et al., 2010). Therefore, a bilateral drop landing will provide the most appropriate assessment of the influence from the prosthetic limb by determining differences in the shock absorption mechanics performed by the intact limb of ITTAs and able-bodied controls.

Like ITTAs, other injury populations have also demonstrated an asymmetrical landing strategy with a greater reliance placed on the uninjured limb when landing from a jump. The uninjured/intact limb has been found to experience a significantly greater peak vGRF and higher vGRF loading rates compared to the injured/prosthetic limb which has been associated with an increased risk of knee injuries (Schmitt et al., 2015, Goerger et al., 2015, Paterno et al., 2007, Schoeman et al., 2013). In addition, the intact limb may adopt movement strategies associated with increased risk of injury (i.e. more extended landing strategy) to absorb the greater percentage of the total momentum. A more extended landing strategy has been characterised by joint strategies including reduced joint flexion angles at touchdown, less joint flexion ROM during load absorption, greater knee valgus ROM, increased joint angular velocities, and reduced trunk flexion (Boling et al., 2009, Bisseling et al., 2008, Edwards et al., 2010, Louw et al., 2006, Bisseling et al., 2007, Blackburn & Padua, 2009). The coordination strategies of the lower-limb joints have also been suggested to influence the force experienced by the limb when landing from a jump (Hughes & Watkins, 2008, Zhang et al., 2000). Previous research and the results from Chapter 7 that have assessed the mechanics during unilateral drop landings, have found a more extended landing strategy is utilised in order to effectively control the rapid lowering of the CoM (Palmieri-Smith et al., 2007, Pappas et al., 2007b). It is possible that during a bilateral landing the intact limb will perform joint mechanics similar to those observed in a

unilateral drop landing.

A greater understanding of the compensatory strategies adopted by the intact limb due to the prosthetic limb influence in landings could provide important information on the risk of participating in sports involving jumping for ITTAs. Thus, the purpose of this study was to determine the ability of the intact limb to attenuate load, when the possible influence of the prosthetic limb is present, by assessing the load experienced and the joint shock absorption mechanics performed during a bilateral drop landing compared to able-bodied controls. It is hypothesised that the intact limb, in comparison to a control limb, will 1) perform a quasi-unilateral landing, 2) experience a greater magnitude of load throughout the absorption phase at the ground and at the knee joint, and 3) land with joint mechanics associated with an extended landing strategy. Specifically, the intact limb will land with reduced joint flexion at touchdown and undergo less joint flexion ROM in the ankle, knee, hip and trunk; experience increased knee joint valgus angles at touchdown and greater valgus motion; absorb greater peak joint powers; complete greater joint work; and perform in-phase flexion coordination strategies with a greater utilisation of the distal joints compared to a control limb.

8.2. Methods

Data collection procedures for drop landing can be found in Chapter 3 Section 3.4.5 and the data processing were completed as outlined in Chapter 3 Section 3.5. Chapter 7 Section 7.2.2 discusses the biomechanical features extracted. Movement and loading features were extracted from the intact limb of ITTAs ($n = 8$) and the dominant control limb ($n = 21$) where dominance was defined as the limb that would be chosen first to complete a unilateral landing. One control participant was excluded from the analysis due to hip marker occlusion issues.

In addition to the biomechanical features from Chapter 7, this chapter extracted the limb vertical impulse and the touchdown timing difference. The limb vertical impulse

was calculated for the duration of the absorption phase as the area under the vGRF-time curves for the intact limb and control limb individually. The timing difference of touchdown between limbs was calculated in seconds from touchdown of the intact limb/control limb to the touchdown of the prosthetic limb/non-dominant control limb.

8.2.1. Statistical Analysis

Independent *t*-tests were performed to assess differences between the intact and control limbs for the loading and movement features. Loading waveforms were assessed using statistical parametric mapping (see Chapter 2 Section 2.7.).

8.3. Results

Participant demographics are presented in Table 7.1 in Section 7.3. of Chapter 7.

8.3.1. Loading Differences

The vGRF and compressive KF magnitudes differed significantly between groups. The intact limb demonstrated significantly greater vGRF from 84-87% of the absorption phase ($p < 0.001$; Figure 8.1A) and in the compressive KFz from 15-27% ($p < 0.001$; Figure 8.1C) compared to the control limb. No other significant differences between the intact and control limbs were present in the loading waveforms.

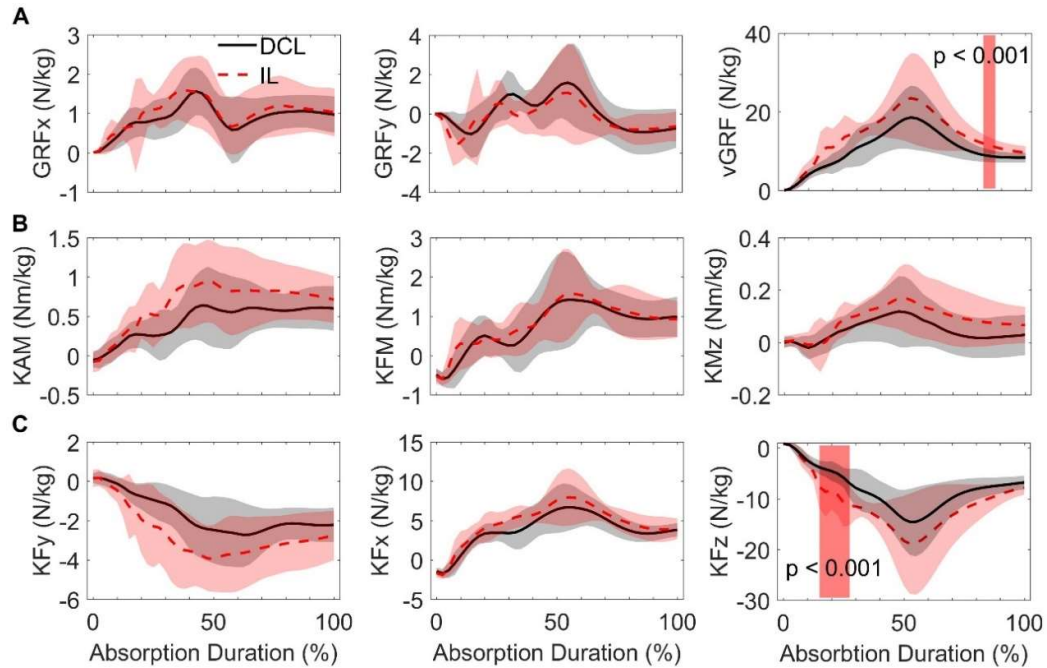


Figure 8.1. Each row presents the 3-dimensional loading waveforms for the A) GRFs, B) knee moments (KM), and C) intersegmental knee forces (KF) in the intact limb (IL; red dashed line) and dominant-control limb (DCL; black solid line). Loading waveforms are presented for the duration of the absorption phase. The highlighted red area represents the phase of significant difference between the IL and DCL with the p -value noted based on the SPM $\{t\}$ -statistic results.

GRFx = lateral-medial, GRFy = anterior-posterior, vGRF = vertical, KAM = external knee adduction moment, KFM = external knee flexor moment, KMz = internal-external, KFy = lateral-medial, KFx = anterior-posterior, and KFz = compression

8.3.2. Movement Differences

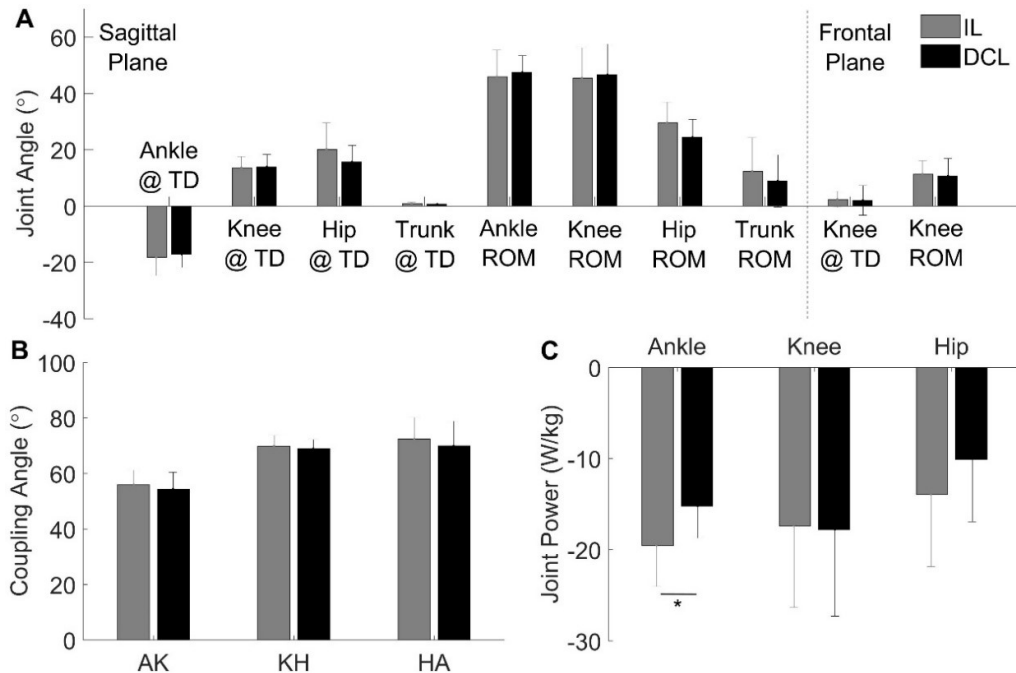
Joint angle and power waveform data are presented in Appendix D2. The vertical impulse experienced in the intact limb was significantly greater than that experienced by the control limb (Table 8.1). The touchdown timing difference was significantly greater in the ITTA group where the intact limb contacted the ground earlier than the prosthetic limb. The absorption duration was not significantly different between groups.

Table 8.1. Whole-body features (mean \pm SD) for the ITTA and control groups

	ITTA	Control	<i>p</i> -value
<i>Limb Impulse (N/kg/s)</i>	2.25 \pm 0.65	1.65 \pm 0.48	0.011
<i>Absorption Duration (s)</i>	0.18 \pm 0.07	0.17 \pm 0.08	0.801
<i>Touchdown Timing (s)</i>	0.07 \pm 0.04	0.03 \pm 0.01	<0.001

No significant differences were found between the intact and control limbs for any of the joint kinematic features in the sagittal plane during landing ($p \geq 0.131$; Figure 8.2A). Additionally, no significant differences were found in the frontal plane for the knee joint angle at touchdown ($p = 0.854$) or ROM ($p = 0.795$). No significant differences were found in the joint coordination strategies as represented by the coupling angle in any of the lower-limb joint pairs ($p \geq 0.499$; Figure 8.2B). All joint pair coupling angles represented in-phase flexion strategies, with the knee-hip and hip-ankle joint pairs utilising greater flexion from the knee and ankle, respectively.

The peak ankle joint absorption power was significantly greater in the intact limb compared to the control limb ($p = 0.011$; Figure 8.2C). Knee and hip joint peak absorption powers were not significantly different between the intact and control limbs ($p \geq 0.204$).



*Figure 8.2. A) Joint angular position at touchdown (TD) and joint range of motion (ROM) in the sagittal and frontal plane, B) joint coordination coupling angle for the ankle-knee (AK), knee-hip (KH) and hip-ankle (HA) joint pairs, and C) peak joint absorption powers when landing at the ankle, knee, and hip joints in the intact limb (IL) and dominant control limb (DCL). * $p < 0.05$ between groups*

No significant differences in the total joint work or the work completed at any individual joints were found between the intact and control limbs ($p \geq 0.104$; Figure 8.3A). The total negative joint work performed was 14% greater in the intact limb ($p = 0.117$). There were no significant differences between groups for the work done at the ankle joint ($p = 0.104$; intact limb: -0.84 ± 0.27 J/kg, control limb: -0.71 ± 0.14 J/kg), knee joint ($p = 0.808$; intact limb: -0.68 ± 0.24 J/kg, control limb: -0.66 ± 0.25 J/kg), or hip joint ($p = 0.222$; intact limb: -0.37 ± 0.19 J/kg, control limb: -0.26 ± 0.23 J/kg). Both the intact and control limbs performed the greatest negative work at the ankle joint (44%; Figure 8.3B).

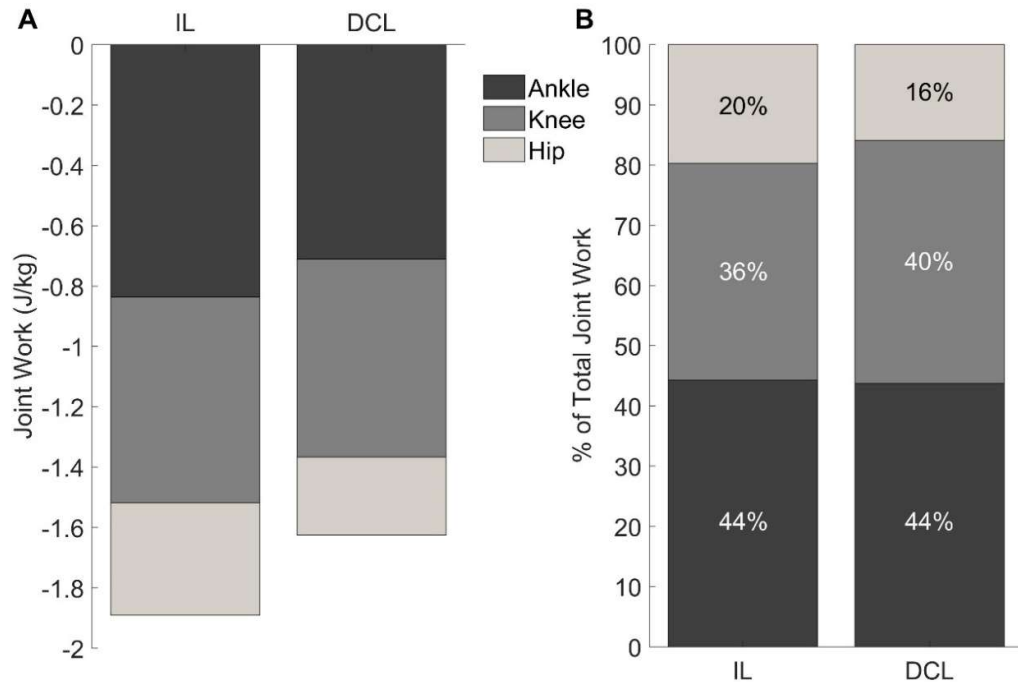


Figure 8.3. A) The individual joint work completed and B) the percentage contribution of each joint relative to the total negative joint work performed in the ankle, knee, and hip joints for the intact limb (IL) and dominant control limb (DCL) during the absorption phase of landing

8.3.3. Variability Sub-Analysis

The greater impulse experienced in the intact limb was only evident by an increased vGRF when nearing maximum knee flexion and compressive KF within the initial loading response. It is possible that significant phases of difference elsewhere in the vertical forces and within other loading waveforms were not present due to the large standard deviation in the ITTA cohort (Figure 8.1). Thus, this sub-analysis aimed to determine the source of the loading waveform variability, if the variability was group specific (i.e. ITTA vs control), and any joint mechanics that may mediate the development of load.

When reviewing the data, peak vGRF was significantly higher in the intact limb of three ITTAs compared to the other five ITTAs ($p < 0.001$; High_{ITTA}: 38.4 ± 3 N/kg, Low_{ITTA}: 19.5 ± 4 N/kg; Figure 8.4). ITTAs were split into high_{ITTA} and low_{ITTA} peak magnitude groups using a threshold based on the mean peak vGRF magnitude.

Figure 8.4 shows the reduction in variability in the vGRF waveform when splitting the ITTA cohort based on this threshold.

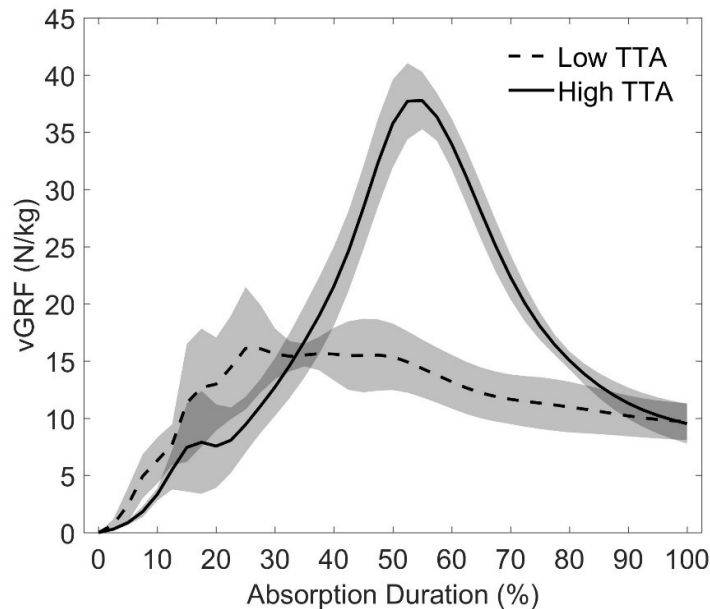


Figure 8.4. vGRF waveforms (mean and SD cloud) for the intact limb of ITTA participants with a higher peak magnitude (solid line) and lower peak magnitude (dashed line).

SPM analysis of the loading waveforms between high_{ITTA} and low_{ITTA} groups found significant differences in the vGRF and KFz waveforms from ~47-74% of the absorption phase ($p < 0.001$) representing differences in peak magnitude and possibly loading rates. No other significant differences were found in the other limb and knee joint loading waveforms. The high_{ITTA} group spent less time in the absorption phase ($p = 0.015$; High_{ITTA}: 0.11 ± 0.02 s, Low_{ITTA}: 0.22 ± 0.05 s). Therefore, there was no significant difference in the vertical impulse experienced between high_{ITTA} and low_{ITTA} groups ($p = 0.148$). The timing to peak vGRF in seconds was not different between low_{ITTA} and high_{ITTA} groups ($p = 0.209$) suggesting a lower loading rate was experienced in the low_{ITTA} group. Previous research has demonstrated that excessive vertical forces and higher loading rates can damage the articular cartilage in the joint (Tsai et al., 2017, Vanwanseele et al., 2010) and increase the risk of injury occurrence

(Radin & Paul, 1971, Aerts et al., 2013). As lower vertical forces are present in the low_{ITTA}, the joint mechanics utilised could indicate a load-avoidance strategy. Those in the high_{ITTA} group also exhibited a significantly greater peak knee absorption power ($p = 0.025$; high_{ITTA}: -25.7 ± 9.1 W/kg, low_{ITTA}: -12.4 ± 3.9 W/kg) and significantly less trunk flexion ($p = 0.018$; high_{ITTA}: 5.35 ± 2.0 , low_{ITTA}: 16.6 ± 5.7). This suggests that increasing the duration of the absorption phase, by performing greater trunk flexion and decreasing peak knee joint absorption power, could reduce the peak magnitude and loading rates of the vGRF and KFz.

An additional examination was performed to assess the variability in the vGRF waveforms from 20-30% (Figure 8.4). In the high_{ITTA} group, the variability occurred due to differences in the impact peak (Figure 8.5A). The low_{ITTA} group variability from 20-30% occurred due to differences in the timing to peak vGRF as a percentage of the absorption phase (Figure 8.5B). Two participants had an earlier peak vGRF (early-low_{ITTA}; dashed line) and three participants had a later peak vGRF (late-low_{ITTA}; solid line). No difference was present in the time to peak vGRF in seconds between the early-low_{ITTA} and late-low_{ITTA} groups. Further, the early-low_{ITTA} group had a longer duration of the absorption phase ($p = 0.015$; early-low_{ITTA}: 0.27 ± 0.04 s, late-low_{ITTA}: 0.18 ± 0.03 s). These results suggest that the variability depicted in the time-normalised vGRF waveforms for the two early-low_{ITTA} participants may be due to the time-normalisation process. This indicates the importance of examining the duration of the absorption phase (i.e. the time-domain) when analysing waveforms to aid in the interpretation of the results.

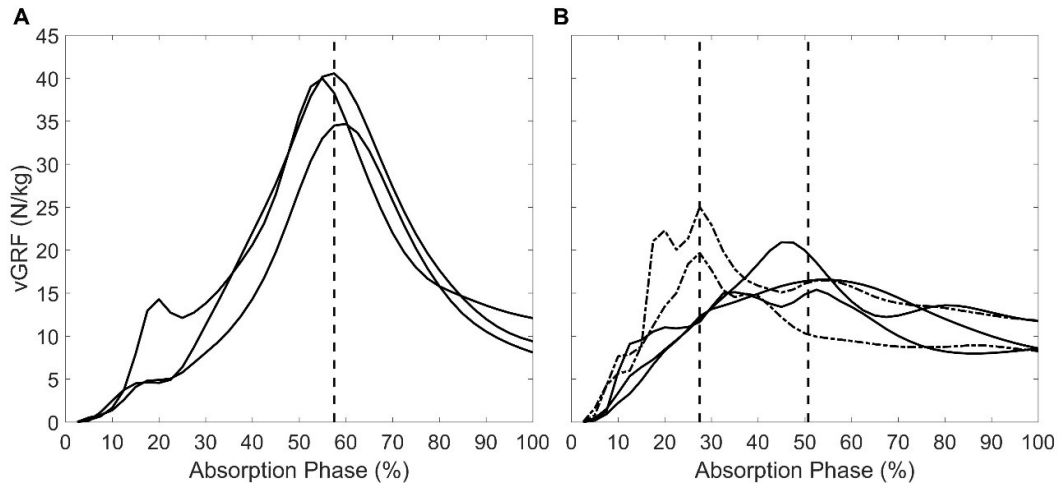


Figure 8.5. Individual mean trials for the A) high and B) low peak vGRF ITTA groups to illustrate variability in the vGRF waveform from ~20-30% of the absorption phase. Vertical black dashed lines indicate the average time at which peak vGRF occurred. The two dot-dashed lines in the low peak vGRF sub-group indicates the early peak participants.

Based on Table 8.1, the duration of the absorption phase was not significantly different between the ITTAs and controls yet both groups had high variability for this feature based on the standard deviation. The above analysis demonstrated that the ITTA sub-groups ($high_{ITTA}$ and low_{ITTA}) were able to explain the variability in the duration of the absorption phase. Therefore, the control cohort was additionally separated into $high_c$ and low_c peak vGRF sub-groups. The sub-groupings for the control limb were not as distinct as the ITTA sub-groups due to the presence of a 'middle' group ($n = 3$). The 'middle' group was identified by examining those participants who were within $\pm 10\%$ of the average peak vGRF. The number of participants included in the 'middle' group did not change if a 5% or 15% threshold was used indicating no issues with group classifications. The 'middle' group participants were excluded from further analysis to ensure that comparisons were made on divergent groups (total left: $n = 18$; $High_c$: $n = 8$ and Low_c : $n = 10$).

Figure 8.6A presents the vGRF waveforms for the $high_c$ and low_c control sub-groups. While this sub-grouping did explain some of the variability, there is still variability present throughout. Figure 8.6B and Figure 8.6C show the individual trials for the

high_c and low_c sub-groups, respectively. These figures highlight that the variability is occurring due to differences in the time to peak vGRF as a percentage of the absorption phase. Regardless of the high_c or low_c sub-groups, the time to peak vGRF in seconds was not significantly different between the individuals represented by dashed lines in Figure 8.6B&C ($p = 0.884$; 0.07 ± 0.02 s) and those presented by black solid lines (0.07 ± 0.01 s). Therefore, the variability in the vGRF waveforms was also due to differences in the duration of the absorption phase similar to that of the ITTA low sub-group.

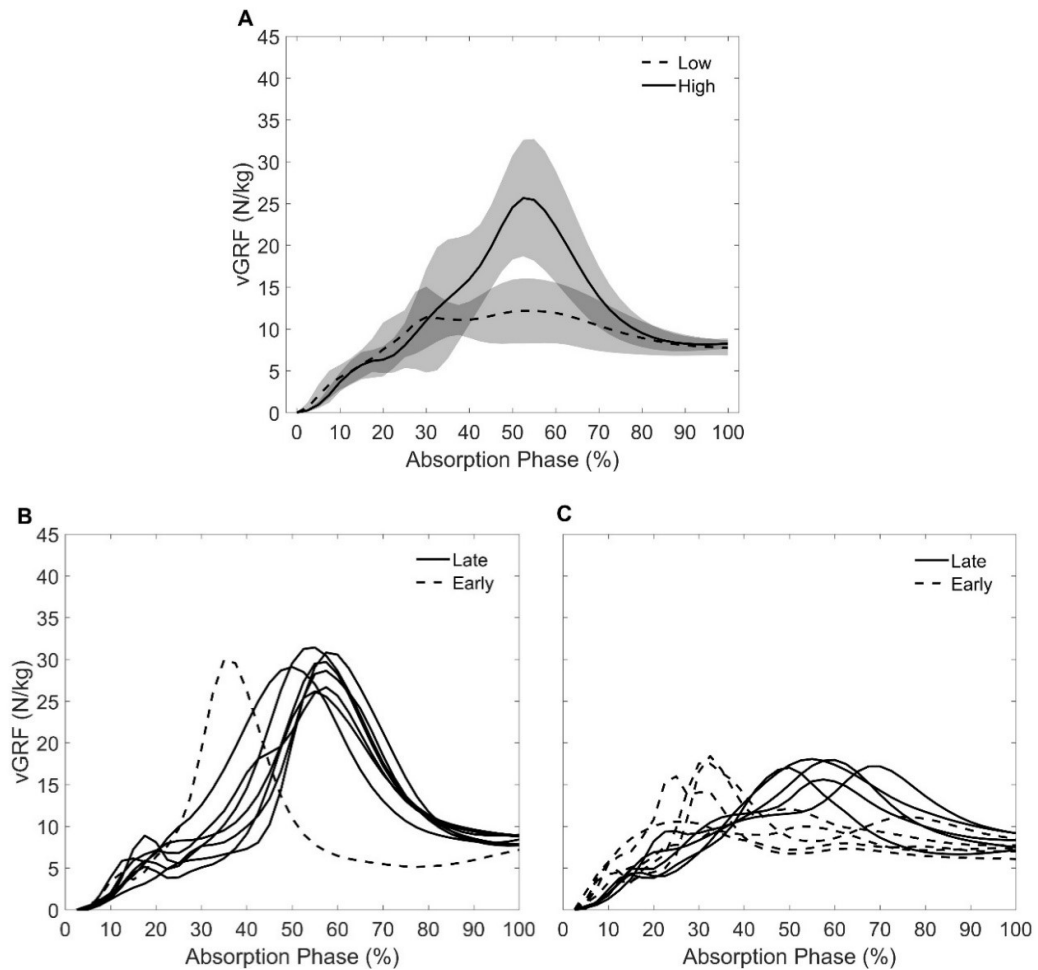


Figure 8.6. A) Control low_c (dashed line) and high_c (solid line) sub-groups mean and standard deviation clouds. Individual trials for B) high_c and C) low_c sub-group and participants with the earlier time to peak vGRF represented by a dashed line.

Comparisons of the joint mechanics between high_c and low_c sub-groups were similar to those found between the high_{ITTA} and low_{ITTA} sub-groups. The high_c group exhibited significantly reduced ankle ROM ($p = 0.013$; High_c: $43.4 \pm 4.8^\circ$, Low_c: $50.6 \pm 5.8^\circ$) and knee flexion angles at touchdown ($p = 0.036$; High_c: $11.8 \pm 2.8^\circ$, Low_c: $16.2 \pm 4.8^\circ$). Additionally, the high_c group performed significantly greater peak absorption powers at the ankle ($p = 0.044$; High_c: -16.9 ± 3.2 W/kg, Low_c: -13.5 ± 3.2 W/kg) and knee joints ($p = 0.016$; High_c: -22.8 ± 11 W/kg, Low_c: -12.5 ± 4.3 W/kg). This indicates that peak vGRF can be reduced by increasing duration of the absorption phase by increasing the ankle ROM and knee flexion angle at initial contact and decreasing the ankle and knee joint absorption powers (i.e. reducing angular velocity). The results from the sub-analysis suggest that the intact limb of ITTAs behaves similar to that of able-bodied controls.

The variability in the vGRF waveforms was unable to explain the variability in the KAM and KFy waveforms. Further investigation determined that the variability in the ITTA intact limb was due to two outliers. A single outlier was identified for KAM due to a valgus knee angle at initial contact that was not present in the other ITTA participants. After initial contact, the knee joint moved past the neutral frontal plane and into a varus position throughout the absorption phase. A different ITTA participant was identified as an outlier for KFy as they experienced greater medial knee joint forces compared to the other ITTA participants. This participant landed with the greatest knee varus angle at initial contact. In comparison to the control limbs, the results from the KAM and KFy waveform analyses did not change after the outliers were removed from their respective analyses. This indicates that the outliers did not impact the waveform analysis results for the KAM and KFy waveforms. It is possible with a bigger sample size a sub-group of participants could perform similar KAM and KFy loading patterns to these two outliers. This could indicate a secondary approach in the joint mechanics to land from a jump.

8.4. Discussion

This study investigated the bilateral drop landing mechanics in the intact limb of ITTAs that were utilised to control the downward momentum when the possible influence from the prosthetic limb was present. The first hypothesis was confirmed as the ITTA participant performed a quasi-unilateral landing based on the significantly different touchdown timings (Table 8.1). The second and third hypotheses were partially confirmed. The intact limb experienced significantly greater vGRF at the end of the absorption phase, significantly greater compressive KFz during initial loading, and absorbed significantly greater peak power at the ankle joint. No other differences were present in the load or movement features between groups.

The quasi-unilateral landing performed by the ITTA group denoted a significantly earlier touchdown of the intact limb compared to the prosthetic limb. On average, the intact limb experienced 39% of the total absorption phase before the prosthetic limb contacted the ground, while the control limb experienced 17% before contact with the contralateral limb. The intact limb also experienced 66% of the total vertical impulse compared to the control groups who experienced the same impulse in both limbs (50%). The touchdown timing difference for the ITTAs was greater in this study compared to the Schoeman et al. (2013) study (0.07 ± 0.04 s vs 0.04 ± 0.02 s, respectively). This difference between studies possibly occurred due to the difference in landing heights and jump task (drop landing from 30 cm vs countermovement jump landing from 15 ± 6 cm). This may indicate that at higher landing heights the quasi-unilateral landing strategy is amplified. Despite this quasi-unilateral landing, there were limited differences in the limb and joint load experienced in the intact limb compared to the control limb. Of the few differences found in late vGRF and early KFz, it is likely that these differences are due to the influence from the prosthetic limb as no differences were present between groups when performing a unilateral drop landing (Chapter 7).

The intact limb of ITTAs in the Schoeman et al. (2013) study found a peak vGRF of 25.3 ± 5 N/kg from a jump height of 15 ± 6 cm. Interestingly, this was equivalent to the peak vGRF experienced in the intact limb of the current study (26.5 ± 10 N/kg) when dropping from double the height (31.6 cm). The intact limb in the current study underwent greater ROM at all lower-limb joints compared to the Schoeman et al. (2013) participants. In a study by Yeow et al. (2010), able-bodied individuals performing bilateral drop landings from different landing heights (30 cm vs 60 cm) were found to experience the same peak vGRF. When the height increased, participants adapted their shock absorption approach by performing greater maximal knee flexion angles and greater eccentric knee joint work which subsequently resulted in limiting the peak vGRF experienced. While the Yeow et al. (2010) study focused solely on the knee joint, the results from the current study suggest that ITTAs are able to accommodate increased landing heights by increasing the joint motion and work completed at all lower-limb joints to an equivalent magnitude as control participants. This study presents some evidence to suggest that the significantly lower jump heights achieved by ITTAs compared to able-bodied individuals is less likely due to an attempt to limit the load experienced during landing but rather an inability to generate the propulsion required.

The intact limb of ITTAs experienced significantly greater limb impulse, therefore, 14% greater total negative work was completed to reduce the same overall momentum compared to the control group. This was primarily performed by the ankle joint as a significantly greater peak ankle joint absorption power was found in the intact limb (Table 8.2C). This may have contributed to the limited significant differences found in the loading patterns, yet was not an optimal shock absorption approach as the vertical forces tended to be greater in the intact limb. However, there was a large standard deviation in the loading patterns and in the knee and hip joint peak power and work done. This possibly indicates different landing techniques were

performed.

8.5. Conclusion

The limited differences in the loading patterns and the landing mechanics performed to attenuate load suggests that the ITTAs in this study were able to reduce the momentum adequately from a height double their typical jump height (~15 cm). However, there was a possible effect from the prosthetic limb due to the few instances of significantly increased vertical forces in the intact limb compared to the control limbs that was absent when performing a unilateral drop landing. Both ITTAs and control participants performed two distinct landing strategies. Increasing trunk flexion and reducing knee joint absorption power could increase the duration of the absorption phase and, therefore, possibly reduce the peak vGRF and compressive KFz and loading rates. Performance of these mechanics may enable ITTAs to participate in standing sports and gain the cardiovascular benefits of such exercise without experiencing high load.

Independent of the presence of an amputation, both ITTAs and controls can reduce peak magnitudes of vertical force when landing by increasing trunk flexion and utilising the ankle joint as the main shock absorber.

8.6. Further Work

Due to the variability in the loading waveforms for the intact limb, it is possible that the prosthetic limb may perform different strategies that elicit different responses from the intact limb. Further research is warranted to examine the joint mechanics of the prosthetic limb. One possible approach is by utilising cluster analysis techniques. Clustering of sub-group landing strategies in the prosthetic limb based on joint mechanics may indicate specific responses performed in the intact limb to accommodate for the reduced prosthetic absorption capacity.

Chapter 9.

Conclusion

The present work aimed to provide a greater understanding of the loading patterns experienced in the intact limb of ITTAs and assess the joint mechanisms underpinning any differences in limb and knee joint load. The results of this thesis have provided a base understanding of these mechanisms to aid in the advancement of rehabilitation and exercise protocols for individuals with unilateral transtibial amputations (ITTAs).

Mechanical overloading of a joint is thought to place an individual at an increased risk of developing joint degenerative diseases, such as osteoarthritis (Farrokhi et al., 2016). The intact limb of ITTAs is at a 25-28% greater risk of joint degeneration compared to the general population (Struyf et al., 2009, Norvell et al., 2005). Thus, it is important to understand the loading patterns experienced in the intact limb of ITTAs and identify those features that are associated with overloading. However, inconclusive results from walking gait research presented limited to no evidence of overloading occurring in the intact limb of ITTAs compared to controls. It was postulated that these inconsistent results were, in part, due to: 1) the discrete nature of commonly assessed loading features (discussed in Section 9.1), 2) an inappropriate selection of loading features (discussed in Section 9.2), and 3) overloading not being present in walking gait, but rather in other tasks, such as step descent. Strategies that could be utilised in step descent and drop landing tasks to reduce whole-limb and joint loading are discussed in Section 9.3.

9.1. Waveform Analysis

Waveform analysis, through statistical parametric mapping (SPM), was utilised to overcome the limitations associated with discrete point analysis, such as, the possibly biased *a priori* approach when selecting 'key' features (Pataky, 2012, Richter et al., 2014b). When applying SPM, the investigator must decide whether landmark registration of the waveforms is necessary to interpret the results correctly. Landmark registration was utilised in chapters 4 and 5 as variation in the timing of 'key' events resulted in magnitude comparisons across different physiological phases. Additionally, landmark registration warped the time-domain (i.e. the duration of the phase of interest in seconds) to gain additional information regarding the timing of events (i.e. loading rates). Chapters 7 and 8, examining drop landings, did not employ landmark registration due to the relatively short landing phase that could result in over-registration. Over-registration could remove important phases of interest as significant results and indicate other phases as important that only became significant due to time-warping too much (Moudy et al., 2018).

When applying SPM and landmark registration, findings from chapter 4 and 5 indicated two overall phases of interest: initial loading response and sustained midstance load. The initial loading response phase was indicative of the established discrete features utilised in previous research, i.e. loading rates and peak magnitudes. Analysis of the landmark registered time-domain demonstrated that a faster rate of load was experienced when performing a heel initial contact descent strategy. This result was interpreted from the time-domain as it was warped such that the time to peak magnitude was shorter for the heel contact group (Appendix C1). More commonly utilised in the literature is peak magnitude, however, this discrete point was not significantly different between groups for any loading waveform. This indicates the greater relative importance of loading rates over peak magnitudes (Morgenroth et al., 2014). Discrete point analysis of peak magnitude and loading rates

would have likely yielded similar results to that found by waveform analysis; however, given the issues of accurately calculating loading rates (e.g. impact peaks), SPM and landmark registration could remove these issues as both the magnitude and time-domains can be examined. Further, the sustained midstance loading phase is not commonly assessed in the literature, yet Chapters 4 & 5 indicated this phase to be a contributing feature associated with the presence of overloading. Thus, waveform analysis and landmark registration effectively reduced the bias in the selection of loading features.

Limited to no differences were found in the loading waveforms presented in chapters 7 & 8. However, there was large variability in the loading waveform data of both ITTAs and controls which may have masked any significant differences. It is possible that discrete point analyses of established variables could have found significant differences between groups, however, this would have concealed the variability in the waveform that indicated distinct approaches to landing. When high variability is present in the loading waveforms, this would suggest that multiple approaches to perform the task demands are present and further inspection is required. Future research should utilise waveform analysis when the literature is unclear on the appropriate discrete features to answer the research questions, yet caution should be used when interpreting SPM results.

9.2. Intact Limb Loading

In chapter 4, an analysis was performed to demonstrate the influence of descent strategies on the development of load in able-bodied controls. Indeed, a toe initial contact reduced initial vGRF and KAM loading rates to peak magnitude; had increased intersegmental knee forces in the medial and anterior directions immediately following initial contact; and maintained a greater sustained midstance vGRF, KAM, and compressive and anterior knee forces compared to a heel initial contact. As these loading differences were maintained after covarying for stepping

speed, it was postulated that the development of load stemmed from differences in the leading limb and trailing limb mechanics (discussed in Section 9.3). It is possible that medial and anterior forces at the knee joint increased immediately following initial contact as a consequence of the extended leading limb (Chapter 6; Podraza & White, 2010, Tsai et al., 2017) which could induce cartilage and ligament damage (Paterno & Hewett, 2008, Stergiou et al., 2007). However, Hunt et al. (2010) found individuals that present with a heel strike transient, associated with anterior GRF and posterior knee force, are more likely to exhibit greater joint degeneration. While a toe initial contact could reduce vGRF and KAM loading rates, a consequence may be increased medial and anterior knee joint forces. As recommended in further research (Section 9.6.), the relative contribution of each measure of load to the onset and progression of joint degeneration must be investigated.

Chapter 5 utilised ITTAs as an experimental model to further examine the role of the trailing limb on the development of lead limb loading. ITTAs performed a toe initial contact strategy when descending from a step. Few significant differences in loading patterns were found compared to able-bodied controls performing the same descent strategy (Chapter 5). This occurred despite significant reductions in the trailing limb capacity to lower the centre of mass (CoM) and propel the CoM to continue forward progression. A more extended leading limb was performed by ITTAs possibly to compensate for the trailing limb deficiencies. This indicates that the chosen descent strategy was not necessarily an attempt to reduce load but could additionally be chosen due to the reduced functionality of the prosthetic trailing limb. This may have allowed the intact limb ankle joint to act as a more efficient shock absorber than the controls and, therefore, reduce the load experienced at the ground and at the knee joint. Additionally, it was also postulated that significant reductions in stepping speed may have aided in reducing anterior-posterior ground and knee joint load as these features were only significant after covarying for speed. The significantly greater

medial GRFx that was present in the intact limb of ITTAs independent of stepping speed was, therefore, most likely due to the more plantarflexed ankle joint in the leading limb (Simpson & Jiang, 1999). However, stepping speed was not a significant contributor in the reduction of initial loading rates, sustained loading magnitudes, or anterior-posterior knee forces (KFx; Chapter 6). This indicates the importance of leading limb and trailing limb joint mechanics in the reduction of load independent of walking speed.

To limit lead limb loading throughout the braking phase, a toe contact strategy should be performed to reduce initial vGRF and KAM loading rates while a heel contact strategy should be performed to reduce vGRF and KAM sustained loading (Chapter 6). These recommendations are based on the vGRF and KAM loading only as they are commonly examined loading features associated with joint degeneration (Schmitz & Noehren, 2014, Vanwanseele et al., 2010). Chapters 4 & 5 additionally found that these two features exhibited significant differences in both the initial loading response and sustained loading phase between descent strategies and between ITTAs and control participants. However, other loading features that differed significantly between descent strategies may contribute to joint degeneration. After covarying for speed, the intact limb of ITTAs experienced a greater anterior knee force (Chapter 5). Initial peak anterior-posterior KFx was additionally assessed suggesting that a greater anterior KFx was strongly related to increased peak ankle joint absorption power in the leading limb, consistent with a toe contact strategy. As discussed above, the literature is currently unclear as to the extent to which anterior KFx may contribute to joint degeneration.

9.3. Joint Mechanics

The intact limb of ITTAs can attenuate increased loading demand in higher impact activities by performing joint mechanics that are not significantly different from able-bodied controls (Chapter 5 & 7). This could suggest that no inherent deficiencies in

the intact limb are present post-amputation. The few instances of overloading in the intact limb that were found in Chapter 5, 7, & 8 are, therefore, most likely due to other influences that could alter the intact limb mechanics. These influences could be the task demand (i.e. vertical displacement during horizontal progression) or prosthetic limb contributions that results in inappropriate compensatory strategies in the intact limb contributing to high load. Thus, it is plausible that altering the joint mechanics in both the intact and prosthetic limbs could provide optimal strategies to reduce load (Chapter 6).

The dynamic walking theory has demonstrated between-limb influences are present during level-walking in both able-bodied (Kuo, 2007) and ITTA populations (Morgenroth et al., 2011). This between-limb influence has previously only been assessed by examining the GRF impulse under each limb and the propulsive work from the ankle joint alone. The results from chapter 6 & 8 indicate that between-limb influences can occur in other continuous anti-phase movement tasks, such as step descent, and possibly when performing discrete in-phase tasks, such as drop landings. Significant bivariate correlations were found between trailing limb joint coordination and propulsive mechanics and lead limb vGRF, KAM, and anterior KFx loading during step descent (abs. $r = 0.37-0.53$, $p < 0.05$). After accounting for all other features, including stepping speed, trailing limb mechanics remained significant or tended to be significant predictors for vGRF loading rates and vGRF and KAM sustained midstance load ($p \leq 0.068$). Joint coordination of the trailing limb when lowering the CoM reflected flexing ankle and knee joints, while the hip extended. This approach was significantly related to reduced vGRF loading rates and reduced vGRF and KAM sustained load. Increased propulsion from the knee and hip joints was also associated with reduced vGRF and KAM sustained load (Chapter 6). This indicates that joint mechanics, beyond that of the ankle joint, are important in reducing contralateral limb loading. Further, when performing a bilateral landing, the intact limb

of ITTAs experienced significantly greater vGRF and compressive knee forces (Chapter 8). These differences were not present when performing a unilateral landing (Chapter 7). This could suggest an influence from the prosthetic limb contributions as all other variables were kept consistent. The results from both tasks suggest that changes in limb loading can occur due the mechanics from both the ipsilateral and contralateral limbs.

Joint coordination is the ability of a system to functionally control joints in time and in sequence to produce a functional movement pattern (Byrne et al., 2002). Much of joint coordination research has been qualitative in nature and limited research has investigated the possible relationship between coordination strategies and injury (Hughes & Watkins, 2008, Doherty et al., 2014). Trailing limb joint coordination to lower the CoM, during single support on the step platform, was found to be a significant predictor in reducing early and midstance lead limb loading (Chapter 6). Additionally, coordination strategies were significantly different between descent strategies even when limited to no significant differences were present in the individual joint motion (Chapter 4 & 5). This confirms the importance of examining the relative influence of one joint on another in the production of movement and its importance in reducing load.

9.4. Application for ITTAs

Based on the previously discussed step descent strategies (Section 9.3), it is possible that introduction of these gait modifications prior as soon as possible after amputations could reduce the risk of injury occurrence and possibly delay or prevent the onset of degenerative diseases. Regression models suggested that increased trailing limb propulsion from the hip joint and absorption power from the knee joint could reduce sustained load. This provides a possible solution for ITTAs to increase propulsive capacity that is lost at the prosthetic ankle joint.

In addition to the step descent strategies, inclusion of drop landings in rehabilitation and exercise protocols could aid in the development of strength and coordination of the joints. Dropping from a height of 30 cm was associated with limb and joint loading that had limited to no significant differences from able-bodied controls (Chapter 7 & 8). This could suggest that unilateral and bilateral drop landings do not place the intact limb at a greater risk of joint degeneration. Bilateral drop landings provide an added benefit of stimulating osteogenesis of the bone in the prosthetic limb that is commonly unloaded (Gailey et al., 2008). Landing on both limbs from a height of up to 30 cm may provide the loading required to reduce the risk of osteoporosis in the prosthetic limb while promoting stimulation of the quadriceps musculature and coordination between-limbs.

Landing during sport requires rapid deceleration of the CoM. Generation of quadriceps muscle force rapidly (i.e. explosive strength) has been suggested as an important feature in re-stabilisation of the joint following mechanical perturbations (Tillin et al., 2013, Andersen & Aagaard, 2006, Aagaard et al., 2002). Explosive strength training can provide a functional benefit in reducing the risk of falls by aiding in balance recovery after a trip (Bento et al., 2010). Including drop landings during rehabilitation could introduce explosive strength training earlier and provide functional benefits in daily life.

9.5. Limitations

Limitations of the thesis include the inability to control the prostheses worn by participants, Plug-in-Gait and inverse dynamic assumptions, and the small number of ITTAs. While not part of the inclusion criteria, all participants did wear dynamic elastic response type prostheses that allowed for participation in higher impact activity. Inverse dynamic calculations do not consider any co-contraction between agonist and antagonist muscle groups during movement (Robertson et al., 2013). Additionally, calculation of the intersegmental joint forces can underestimate the actual joint

contact forces as muscle co-contraction and compressive forces due to ligamentous structures are not included (Zajac et al., 2002). However, this approach is an easy and non-invasive alternative to *in vivo* and computationally expensive and complex modelling approaches (Silverman & Neptune, 2014, Zhao et al., 2007).

Another limitation is the process of linearly time-normalising the data for waveform analysis. To avoid over- or under-stretching the data during time-normalisation, the average duration of the phase of interest (in frames) was used as the number of frames to lengthen or shorten each waveform across all participants. The sub-analysis in chapter 8 indicated that some of the variation present in the waveform loading patterns were due to large standard deviations in the duration of the absorption phase. Due to the differences in this duration, some waveforms during linear time-normalisation indicated an earlier time to peak which was not present in its original temporal-spatial format. However, the variability in the waveform analysis identified two distinct sub-groups that utilised differing mechanics to land from the specified height (as discussed in Section 9.1). Thus, examination of the time-domain and discrete temporal measures should be examined to aid in the interpretation of the results from waveform analyses.

9.6. Further Work

This thesis provided information on the mechanics that are performed by ITTAs during step descent and drop landing tasks. This information can be utilised for further research on intervention studies. Additional suggestions for further work other than that already indicated in each chapter are as follows:

- 1) It is possible that the sustained loading phase during a step descent could be an additional indicator of the risk of developing degenerative loading diseases. Given the greater risk of joint degeneration in the ITTA population, and that the ITTAs in the current study experienced a significantly greater sustained

load, further work is warranted to determine the relationship of this loading phase to the onset and progression of joint cartilage degeneration.

- 2) Degenerative disease are thought to occur due to contributions from multiplanar limb and joint loading. However, the current research is unclear on the magnitude and extent of these contributions to joint degeneration. Further research on the percentage contribution of each loading feature assessed in the current thesis to increases in joint degeneration is needed. This information could identify which loading features should be targeted in gait modification strategies.
- 3) While not examined in this study, the asymmetry or magnitude of difference in load between the intact limb and prosthetic limb may be an additional factor in the increased risk of developing loading related diseases. Step and stair descent research on the load experienced denote that ITTAs exhibit a significantly increased peak magnitude of load and loading rate in the intact limb compared to the prosthetic limb (Buckley et al., 2013, Barnett et al., 2014, Schmalz et al., 2007). As limited differences in load were present between the intact limb and control limbs, it may be that the magnitude of asymmetry places ITTAs at a greater risk of injury.
- 4) Waveform analysis can indicate different loading patterns within and between subject populations. Differentiation of loading patterns could indicate subset populations utilising different mechanics to attenuate load. Further research could utilise the loading waveform patterns in cluster analysis techniques to aid in determining the mechanics utilised in each subset to indicate the mechanisms possibly related to injury.

Appendix A.

Participant Documentation

Appendix A1 – University of Roehampton Ethical Approval

The research for this project was submitted for ethics consideration under the reference LSC 16/176 in the Department of Life Sciences and was approved under the procedures of the University of Roehampton's Ethic Committee on 11.07.16.

Dr Neale Tillin
University of Roehampton, Department of Life Sciences
Whitelands College
Holybourne Avenue, London
SW15 4JD

Email: hra.approval@nhs.net

27 September 2017

Dear Dr Neale Tillin

Letter of HRA Approval

Study title:	Quadriceps muscular function and multijoint coordination strategies of the lower-body in transtibial amputees.
IRAS project ID:	225792
Protocol number:	n/a
REC reference:	17/NW/0566
Sponsor	University of Roehampton

I am pleased to confirm that HRA Approval has been given for the above referenced study, on the basis described in the application form, protocol, supporting documentation and any clarifications noted in this letter.

Participation of NHS Organisations in England

The sponsor should now provide a copy of this letter to all participating NHS organisations in England.

Appendix B provides important information for sponsors and participating NHS organisations in England for arranging and confirming capacity and capability. Please read *Appendix B* carefully, in particular the following sections:

- *Participating NHS organisations in England* – this clarifies the types of participating organisations in the study and whether or not all organisations will be undertaking the same activities
- *Confirmation of capacity and capability* - this confirms whether or not each type of participating NHS organisation in England is expected to give formal confirmation of capacity and capability. Where formal confirmation is not expected, the section also provides details on the time limit given to participating organisations to opt out of the study, or request additional time, before their participation is assumed.
- *Allocation of responsibilities and rights are agreed and documented (4.1 of HRA assessment criteria)* - this provides detail on the form of agreement to be used in the study to confirm capacity and capability, where applicable.

Further information on funding, HR processes, and compliance with HRA criteria and standards is also provided.

Appendix A3 – Consent to Contact Form



IRAS ID: 225792
Version 1
Last Edited: 06/08/2017

Request for more information on research project

Title of Project: Quadriceps neuromuscular function and multijoint coordination strategies of the lower-body in transtibial amputees

I confirm that I have received some information on the research project above, and I am happy to be contacted via the details below, to receive more information about this project. I understand this form does not constitute consent to participate in the study, and that my personal details will not be shared with anyone other than the listed researchers below.

Patient's name

Patient's signature

Date

Researchers: Sarah Moudy (PhD student)
Amy Sibley (PhD student)
Dr. Neale Tillin (Chief investigator)
Dr Siobhan Strike (Supervisor)

Please enter contact details here.

Daytime Phone Number (10:00 – 17:00)	
Evening Phone Number (17:00 – 20:00)	
Email Address	

You will only be contacted by telephone at the times specified above. If you prefer not to be contacted during a certain period, please leave the row blank.



PARTICIPANT INFORMATION SHEET

Title of Research Project: Quadriceps neuromuscular function and multijoint coordination strategies of the lower-body in transtibial amputees

What is the purpose of the study?

The aim of this study is to conduct a comprehensive investigation of quadriceps (thigh muscle) function and coordination of the leg joints in unilateral transtibial amputees (TTAs). This amputation is on one leg only anywhere below the knee but above the foot. The investigation will consider the association between muscle function and joint coordination in both the amputated and intact limbs compared to able-bodied people. Such insight might provide a better understanding of the atypical loading patterns commonly observed in amputees. The results will help in the design of better rehabilitation protocols, to provide a better quality of life for amputees.

How many participants will take part?

40-80 participants (at least 20 TTAs and 20 able-bodied) will be included in this study.

Are there any exclusion criteria?

Yes. Exclusion criteria include:

- Anyone under the age of 20 or over the age 50
- Participants with cardiovascular disease risk factors or musculoskeletal injuries
- Residual limb (stump) length of less than 5 cm
- Skin damage on the residual limb
- Amputation occurring from vascular related diseases
- Undergone your procedure less than six months previously

If you are an amputee, you must have a K-rating of K3/K4 indicating you are able to traverse most environmental barriers.

Can I change my mind once I take part?

Yes. If you wish to participate in this study after reading this information sheet and asking any questions that you wish to ask, you will be required to sign a consent form. However, you are entitled to withdraw from participating at any point during the study and you do not have to explain your reason for doing so, although we do ask that you inform us of your choice to withdraw by contacting one of the investigators (details below).

How many times will I visit the lab?

You will visit the biomechanics laboratory (B047) at Roehampton University on three separate occasions. The lab is on the basement level of Parkstead House. There is lift access to the lab. Each visit will last between two to three hours.

Is there anything I need to do before I visit the lab?

Please refrain from drinking alcohol for 24 hours, or undertaking any strenuous exercise for 36 hours prior to each laboratory visit. Please avoid using body lotions/ moisturisers on the day of your visit as these products make it difficult to maintain adequate contact between the measurement equipment and your skin.

Please bring a pair of loose fitting shorts with you to wear during the first two lab sessions. Running or football shorts are ideal. For females, non-underwired bras are recommended to prevent discomfort in the strength testing chair. For the third session, tight fitting shorts, training top and training shoes should be worn. Females are requested to wear sports bra where possible, as this will allow for more comfortable execution of the movements required. There are private changing rooms and showers at the lab that are available for your use.

Please try to avoid clothing with reflective markings on them as these can interfere with the cameras we'll be using during your third visit. As it is necessary for the cameras to see all of the reflective markers throughout the movement, tops/t-shirts will either need to be taped up to waist height or removed during data collection in order that the view of markers on your torso is not obstructed. When data is not being collected, you may remain fully clothed.

What will I do during the first lab visit?

The first visit will be used to familiarise yourself with the protocols and measurements that will be taken during subsequent visits. To begin, you will be verbally taken through the procedures for each of the visits. Health/activity questionnaires and consent forms will be completed during this time and are expected to take no longer than 15 minutes to complete. Amputees will also need to complete a questionnaire giving details of their amputation history. You will then perform a series of voluntary and electrically evoked involuntary isometric (static) contractions of the thigh (quadriceps) muscles in a strength testing chair, similar to a knee extension resistance exercise machine that you might find in a gym. Full information about the procedures in the strength testing chair is given below. In this initial visit, data will be collected following the protocol outlined below – this is a chance for you to get to know the measurements (including electrical stimulation) that will be taken during your second visit.

What will I do during the second lab visit?

You will be seated in the strength testing chair, and will perform a warm-up of contractions that gradually increase in force for approximately two minutes. Procedures for the lab visits are as follows:

EMG skin preparation and electrode placement: This will take place for your second session only. When you first arrive in the lab, the skin over the surface of three thigh muscles will be

Appendix A4 – Information Sheet

Version 2. Last edited: 09/02/2018

prepared for electrode placement. This involves shaving, lightly scrubbing, and cleaning three different patches of skin. Each area will be approximately 6x6 cm. EMG electrodes (which measure the electrical activity of your muscles) will then be placed over the sites that have been prepared.

Electrically Evoked Involuntary Contractions: Evoked contractions involve electrical stimulating the muscle to elicit muscle contractions which last for less than a second. The stimulation is made via an electrode placed at the top of your thigh. Both 'twitch' (one electrical impulse) and 'octet' (eight impulses) responses will be measured.

Once the optimal location for the electrical stimulation has been found at a low intensity, the current will gradually be increased, and three maximal twitch contractions will then be evoked. Each stimulation will be separated by 15-20 seconds to allow time for your muscles to recover. The current will then be decreased and we will do the same for octet contractions.

Maximal voluntary contractions and superimposed doublets: You will perform 4-6 contractions in which you are instructed to push 'as hard as possible' for around three seconds. You will have 30-60 seconds of rest between each contraction. In half the contractions, an electrical impulse (known as a doublet) will be delivered to your thigh during the contraction (using the same method as for the twitches and octets), and a further two doublets will be elicited at rest immediately after the contraction. Doublets are similar to the twitch and octet contractions only they are evoked by just two electrical impulses in a row.

Explosive voluntary contractions: These contractions are used to assess how rapidly muscles can generate force. You will perform 10-15 explosive contractions of your quadriceps muscles each lasting around one second, in which you are instructed to push 'as fast as possible'. Each contraction will be followed by at least 20 seconds of rest to allow your muscles to recover.

Ramped contractions: Ultrasound images of one of your quadriceps muscles will firstly be recorded with you at rest. You will then perform up to five contractions of the quadriceps whereby you will slowly increase the force you produce over a five second period from rest to your maximum. There will be a line displayed on a screen for you to follow. These contractions will be separated from each other by one minute.

What will I do during the third lab visit?

Upon arrival, you will first have body measurements taken including height, weight, knee and ankle width, and leg length. Next, 37 reflective markers will be placed around your whole body in order for the cameras to capture your movement. As the cameras only records the reflection from the markers placed on your legs and hips, the system will not be able to identify you other than by the number assigned to you. EMG will also be used during this visit with the same preparation as in your second lab visit. The electrodes will be placed on your thigh muscles. You will do a brief warm-up walking around the lab at a self-selected pace for five-minutes. After the warm-up, you will perform a series of different movements: walking, running, step-

descent, and jumping. You will be given sufficient time to practice each movement being examined.

Walking: For each trial, you will walk at a self-selected speed (determined by your practice walks) along a 10m walkway. In order to maintain the same pace, we will instruct you to walk either faster or slower after each pass. Around 20-30 trials will be collected.

Step-Descent: This movement will be performed on a custom-built platform that is the same height as a standard kerb. You will walk at a self-selected speed (same as your walking speed) across the platform and step down onto the ground and continue walking. The movement will be performed by both limbs stepping off the platform and you will complete around 10-15 trials for each leg.

Running: Similar to walking, you will run along the same 10 m walkway at a pace necessary to complete 5 km in 30-35 min. You will not be asked to run 5 km, only to run the length of the 10-m walkway. You will be instructed to either increase or decrease the pace after each pass. Around 20-30 trials will be collected.

Jumping: You will be performing two different types of jumps: maximal effort vertical jumps and a drop landing. The vertical jumps will be performed firstly with both limbs pushing off the floor (without using your arms), and then also using each limb singly in turn to complete the movement. The drop landings will involve you hanging from a bar by your hands, and letting go to drop to the floor. The bar will be moved so that your feet are 25 cm from the ground. You will be allowed to practice these jumps before data collection takes place. Data from three successful (full recovery after landing) maximal effort jumps and drop landings will be collected.

Are there any risks or side effects in participating?

Muscle soreness and strain: This may occur after the measurement sessions and last for up to 72 hours. The risk and severity of muscle soreness will be no greater than that experienced with physical exercise performed for recreation and health (e.g., playing a team sport or resistance exercise in the gym), and should not prevent you from performing normal daily activities.

Electromyography skin preparation: Shaving and cleaning your skin may cause soreness and redness, similar to that experienced when shaving other areas of the body, but these effects should wear off within a couple of days.

Involuntary contractions: The electrical stimulation procedures involved in the involuntary contractions can be uncomfortable at high intensities, such as those that will be used during the octet contractions of this study, but this discomfort is very short term (i.e., lasts for <1 second), and there are no known long term side-effects apart from potential muscle soreness. There is a very small risk of you experiencing nausea or dizziness/ faintness as a result of this stimulation. If this occurs, you will be withdrawn from any further stimulation aspects of the study.

Slips, Trips, and Falls: As you will be walking along a custom-built platform in order to step-down, there is an added risk of tripping or falling off the platform. The platform is of standard kerb-height (14 cm) and is at least 1 meter in width to provide no added risk than that of daily activity. During jumping, you will be asked to perform both jumps off a single limb (intact and amputated limb) and drop off a platform. You will be monitored closely to ensure safe landing techniques are being utilised. If unable to perform any of these jumps, you will be withdrawn from this aspect of the study.

Use of reflective markers: The markers will be placed directly onto your skin using double-sided tape. There is a potential risk of allergic reaction, and therefore a hypoallergenic tape will be used for marker placement.

Should you perceive excessive discomfort or injury at any point during the study, your involvement will be discontinued, and advice on rest and recovery strategies will be provided.

Benefits of participation in this study?

As compensation for your time and effort, you will receive £10 in cash per visit (£30 in total). Amputees that incur greater than £10 in travels costs can additionally be compensated up to a further £20 (£30 in total) per session upon providing a ticket receipt or details of distance driven (£0.45 /mile).

Amputees also receive a personalised report on their movement patterns and muscle strength with exercise recommendations for improving health, fitness and quality of life.

Will my taking part in this study be kept confidential?

Only the study investigators will have access to the information collected from your participation. The data will be coded numerically (rather than by name) for confidentiality purposes. Data storage will adhere to the Data Protection Act.

What will happen to the results of the study?

The results will be submitted as part of the thesis for Doctoral Studies, for publication to a peer-reviewed journal and may be presented at conferences. Information regarding all individual participants will remain confidential.

What happens if I change my mind?

You are able to decline participation in certain aspects of the study (e.g. electrical stimulation or single-limb jumps), but still continue in all other aspects without withdrawing from the study. If you change your mind and no longer wish to participate all together, please let one of the investigators know as soon as possible. You can change your mind at any time.

If you are a student at the University of Roehampton, there is no compulsion or academic pressure to take part in the project. Should you decline to participate or subsequently withdraw, your course marks will not be adversely affected.

Appendix A4 – Information Sheet

Version 2. Last edited: 09/02/2018

I have some more questions – who should I contact?

If you have any further questions please contact one of the lead investigators, Amy Sibley or Sarah Moudy. Alternatively, you may contact either the Directors of Studies for both researchers – Dr Siobhán Strike – or the Supervisor for both – Dr Neale Tillin (details below).

Amy Sibley

University of Roehampton
Whitelands College
Holybourne Avenue
London
SW15 4JD
sibleya@roehampton.ac.uk
Tel. +44 (0)20 8392 4174

Sarah Moudy

University of Roehampton
Whitelands College
Holybourne Avenue
London
SW15 4JD
moudys@roehampton.ac.uk
Tel. +44 (0)20 8392 3342

Dr Neale Tillin

University of Roehampton
Whitelands College
Holybourne Avenue
London
SW15 4JD
neale.tillin@roehampton.ac.uk
Tel. +44 (0)20 8392 3542

Dr Siobhán Strike

University of Roehampton
Whitelands College
Holybourne Avenue
London
SW15 4JD
s.strike@roehampton.ac.uk
Tel. +44 (0)20 8392 3546

What if I have any concerns and would prefer not to contact the investigator?

If you would prefer to contact someone independent to the study you should contact the head of the department of Life Sciences at Roehampton University, Dr Caroline Ross.

Dr. Caroline Ross

University of Roehampton
Whitelands College
Holybourne Avenue
London
SW15 4JD
c.ross@roehampton.ac.uk
Tel. +44 (0)20 8392 3529



PARTICIPANT CONSENT FORM

Title of Research Project: Quadriceps neuromuscular function and multijoint coordination strategies of the lower-body in transtibial amputees

Brief Description of the Study: Injury to muscles, joints and bones can lead to alterations in muscle strength and function that influence joint coordination during movement. It is conceivable that transtibial amputation, an amputation that can occur anywhere in the location below the knee but above the foot, may also influence muscle strength and function but this has not been investigated. It is also unclear whether any changes in muscle function may contribute to changes in joint coordination in amputees. The aim of this study is to provide a comprehensive investigation of quadriceps (thigh) muscle function and joint coordination of both the amputated and intact limbs in transtibial amputees (TTAs) compared to able-bodied people, and consider the association between muscle function and joint coordination. Such insight might provide a better understanding of the abnormal loading patterns commonly observed in amputees, and the physiological mechanisms underpinning these loading patterns. The results will help in the design of better rehabilitation protocols, to provide a better quality of life for amputees.

This project will consist of three visits to our facilities at Roehampton University each lasting between 2-3 hours. 40-80 participants (at least 20 able-bodied and 20 TTAs) will be included in this study. You will undergo a familiarisation session in the biomechanics (B047) laboratory to allow you to become acquainted with the environment and the measurements that will be taken in the later sessions. During the physiology sessions, you will complete a series of static contractions of the quadriceps (thigh) muscles from both legs, whilst sat in a strength testing chair. This will include voluntary maximal contractions, contractions at varying degrees of your maximum ability, and evoked contractions using an electric stimulus. You will also do some slow contractions which will be videoed using ultrasound. In the biomechanics measurement session, you will complete four dynamic movements: walking, running, step-descent, and jumping. Please refer to the participant information sheet for further details on the research project.

Lead Investigator Contact Details:

Amy Sibley
University of Roehampton
Whitelands College
Holybourne Avenue
London
SW15 4JD
sibleya@roehampton.ac.uk
Tel. +44 (0)20 8392 4174

Sarah Moudy
University of Roehampton
Whitelands College
Holybourne Avenue
London
SW15 4JD
moudys@roehampton.ac.uk
Tel. +44 (0)20 8392 3342

Appendix A5 – University of Roehampton Consent Form

Consent Statement: I agree to take part in this research, and am aware that I am free to withdraw at any point without giving a reason, although if I do so I understand that my data might still be used in a collated form. I understand that the information I provide will be treated in confidence by the investigator and that my identity will be protected in the publication of any findings, and that data will be collected and processed in accordance with the Data Protection Act 1998 and with the University's Data Protection Policy.

Name

Signature

Date

Please note: if you have a concern about any aspect of your participation or any other queries please raise this with one of the lead investigators. You can also contact the Director of Studies for both researchers – Dr Siobhan Strike – or the Supervisor for both researchers – Dr Neale Tillin. However, if you would like to contact an independent party please contact the Head of Department.

Director of Studies Contact Details: Supervisor Contact Details:

Dr Siobhán Strike
University of Roehampton
Whitelands College
Holybourne Avenue
London
SW15 4JD
s.strike@roehampton.ac.uk
Tel. +44 (0)20 8392 3546

Dr Neale Tillin
University of Roehampton
Whitelands College
Holybourne Avenue
London
SW15 4JD
neale.tillin@roehampton.ac.uk
Tel. +44 (0)20 8392 3542

Head of Department Contact Details:

Dr. Caroline Ross
University of Roehampton
Whitelands College
Holybourne Avenue
London
SW15 4JD
c.ross@roehampton.ac.uk
Tel. +44 (0)20 8392 3529

Appendix A6 – NHS Consent Form



Version 2.
Last Edited: 02/08/2017

IRAS ID: 225792

Participant ID Number:

CONSENT FORM

Title of Project: Quadriceps neuromuscular function and multijoint coordination strategies of the lower-body in transtibial amputees

Name of Researchers: Sarah Moudy and Amy Sibley

1. I confirm that I have read the information sheet dated 02/08/2017 (version 2) for the above study. I have had the opportunity to consider the information, ask questions and have had these answered satisfactorily.
2. I understand that my participation is voluntary and that I am free to withdraw at any time without giving any reason, without my medical care or legal rights being affected.
3. I understand that the information collected about me will be used to support other research in the future, and may be shared anonymously with other researchers.
4. I agree to take part in this research, and am aware that I am free to withdraw at any point without giving a reason, although if I do so I understand that my data might still be used in a collated form. I understand that the information I provide will be treated in confidence by the investigator and that my identity will be protected in the publication of any findings, and that data will be collected and processed in accordance with the Data Protection Act 1998 and with the University's Data Protection Policy

_____	_____	_____
Name of Participant	Date	Signature
_____	_____	_____
Research Name	Date	Signature

When completed: 1 for participant; 1 for researcher site file; 1 to be kept in medical notes.



PROOF OF PAYMENT FORM

I confirm that I have received the £10 per visit in cash (£30 total) for taking part in the PhD Study entitled 'Quadriceps muscular function and multijoint coordination strategies of the lower-body in transtibial amputees'.

Name:

Address:

Session	Signature	Date
Session 1 - £10		
Session 2 - £10		
Session 3 - £10		

Appendix A8 – Amputee Mileage Claim Form



**MILEAGE CLAIM
FORM**

Name: _____

Address: _____

Vehicle Type: Car/ Motorcycle (please circle)

Mileage allowance: 45p/ mile (car); 24p/ mile (motorcycle)

SESSION ONE

Date	To	From	Distance	Total Cost
TOTAL CLAIM				£
TOTAL REIMBURSED				£

SESSION TWO

Date	To	From	Distance	Total Cost
TOTAL CLAIM				£
TOTAL REIMBURSED				£

SESSION THREE

Date	To	From	Distance	Total Cost
TOTAL CLAIM				£
TOTAL REIMBURSED				£

Appendix B.

Pilot Study Results

Appendix B1 – Step Platform Validation

To test the validity of force data collected from the step platform, both static and dynamic data were collected. Static data were collected from three different masses: ~20 kg, ~30 kg, and ~40 kg. These weights were measured on three separate scales and averaged to determine known weight quantities. The variability of the force output over 2 seconds was calculated as the standard deviation and the accuracy was determined as the difference of the mean force signal from the actual mass (DfA). These data from the step platform were compared to the same force platform (FP) without the step platform attachment (Table B1.1).

Table B1.1. Static variability and accuracy measures for the standard force platform position output (FP1) and with the addition of the step platform output (step) for three different masses

	~20 kg Mass		~30 kg Mass		~40 kg Mass	
	FP1	Step	FP1	Step	FP1	Step
<i>Mean (N)</i>	190	186	308	302	426	420
<i>SD (N)</i>	1.54	1.54	1.63	1.62	1.66	1.66
<i>DfA (N)</i>	2.11	-2.38	2.60	-2.78	3.17	-2.67
<i>MAE</i>	2.26	2.45	2.69	2.81	3.21	2.72

DfA = difference from actual, MAE = mean absolute error

The overall variability of the static vertical ground reaction force (vGRF) signal ranged from 1.54 – 1.66N for all three weights and was consistent with and without the step platform. The step platform consistently underestimated each mass from 2.38 – 2.78N while FP1 consistently overestimated by 2.11 – 3.17N. The average difference between the two data collection methods was greatest as the mass increased (Table B1.2). The difference between the upper and lower LOA is between 8.6 and 9.4N suggesting an effect from the step platform. Previous research has suggested that a greater than 5N difference between FPs can result in cumulative error in higher-order calculations (Rist et al., 2014, Wong et al., 2010). To address this possible issue,

Appendix B1 – Step Platform Validation

dynamic movement was captured and analysed to assess the validity of capturing force data using the step platform.

Table B1.2. Bland-Altman 95% limits of agreement (LOA) between the standard force platform output and the step platform force output for three different masses

	Mass 1	Mass 2	Mass 3
<i>Avg. Difference (N)</i>	-4.50	-5.37	-5.84
<i>Upper 95% LOA</i>	-0.20	-0.87	-1.15
<i>Lower 95% LOA</i>	-8.79	-9.87	-10.5

Dynamic habitual walking peak vGRF, peak anterior-posterior GRF (hGRF), vertical and anterior-posterior impulse, and knee external adduction moment (KAM) data were captured from three participants as they walked across FP1 with and without the step platform. Three trials per participant ($n = 9$ per condition) with successful foot strikes were captured. To determine if any differences were present between conditions, dependent t-tests were performed with an alpha level set at 0.05. Table B1.3 presents the mean and standard deviation for both conditions with their respective p -values. Results suggest force data collected from the step platform provide accurate and reliable force platform data.

Table B1.3. Mean (SD) and p -values presented for discrete dynamic walking features for both force platform conditions

	FP1	Step	p -value
<i>Peak vGRF (N/kg)</i>	11.4 ± 0.5	11.7 ± 0.4	0.545
<i>Peak KAM (N.m/kg)</i>	0.82 ± 3.1	0.82 ± 2.8	0.995
<i>Peak hGRF (N/kg)</i>	-2.61 ± 0.3	-2.33 ± 0.5	0.283
<i>Vertical Impulse</i>	3.29 ± 0.1	3.28 ± 0.0	0.814
<i>A-P Impulse</i>	-0.28 ± 0.1	-0.36 ± 0.1	0.092

Appendix B2 – Vicon System Accuracy

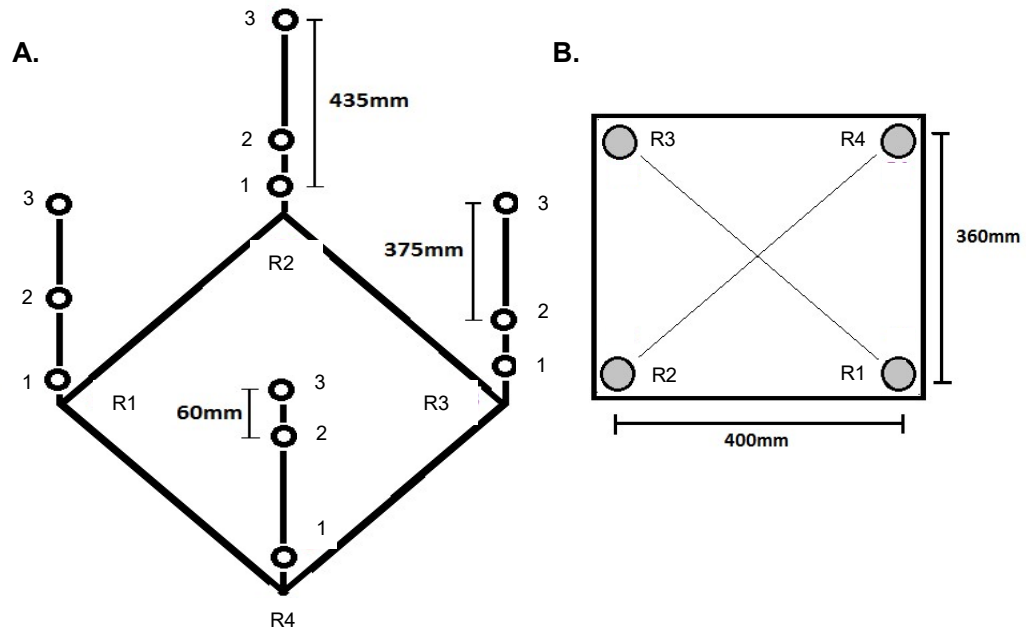


Figure B2.1. A) Configuration of the rigid frame, showing rod and marker positions. B) Base plate dimensions from rod centre to rod centre. Neither diagram to scale.

Table B2.1. Static frame variability between trials

	Mean	SD	SEM
Z: Rod 2	434.7	0.1	0.2
Z: Rod 3	376.8	0.1	0.9
Z: Rod 4	58.1	0.1	0.9
X: Rod 3&4	401.6	0.0	0.8
Y: Rod 2&3	360.6	0.0	0.3
XY: Rod 2&4	541.7	0.0	0.9
XYZ: Rod 2&4	695.0	0.0	0.5

Appendix B3 – Cross-Platform Strike Validation

The purpose of this pilot study was to determine 1. The reliability and accuracy of individual force platforms, and 2. The validity of cross-platform strikes in comparison to full-platform strikes. To assess these aims, both static and dynamic data were collected. Static data was assessed with three known weight quantities for full and cross-platform conditions. The vertical ground reaction force for the cross-platform condition was manually summed in excel.

Table B3.1. Static vertical ground reaction force (N) reliability and accuracy of both full-plate and cross-plate strikes for three different known masses

	FP1	FP2	FP1 & 2	FP3	FP2 & 3
Mass 1					
<i>Mean</i>	190.4	191.3	189.5	190.6	190.5
<i>SD</i>	1.54	1.54	1.99	1.95	2.29
<i>DfA</i>	2.11	2.96	1.17	2.33	2.17
<i>MAE</i>	2.26	2.99	1.89	2.55	2.59
Mass 2					
<i>Mean</i>	307.7	308.8	306.0	309.0	308.9
<i>SD</i>	1.63	1.59	2.09	2.07	2.40
<i>DfA</i>	2.60	3.71	0.90	3.91	3.73
<i>MAE</i>	2.69	3.72	1.84	3.96	3.87
Mass 3					
<i>Mean</i>	425.8	426.4	423.1	422.4	427.3
<i>SD</i>	1.66	1.55	2.12	1.93	2.44
<i>DfA</i>	3.17	3.69	0.44	-0.31	4.63
<i>MAE</i>	3.21	3.70	1.74	1.56	4.69

DfA = difference from actual mass; MAE = mean absolute error

Appendix B3 – Cross-Platform Strike Validation

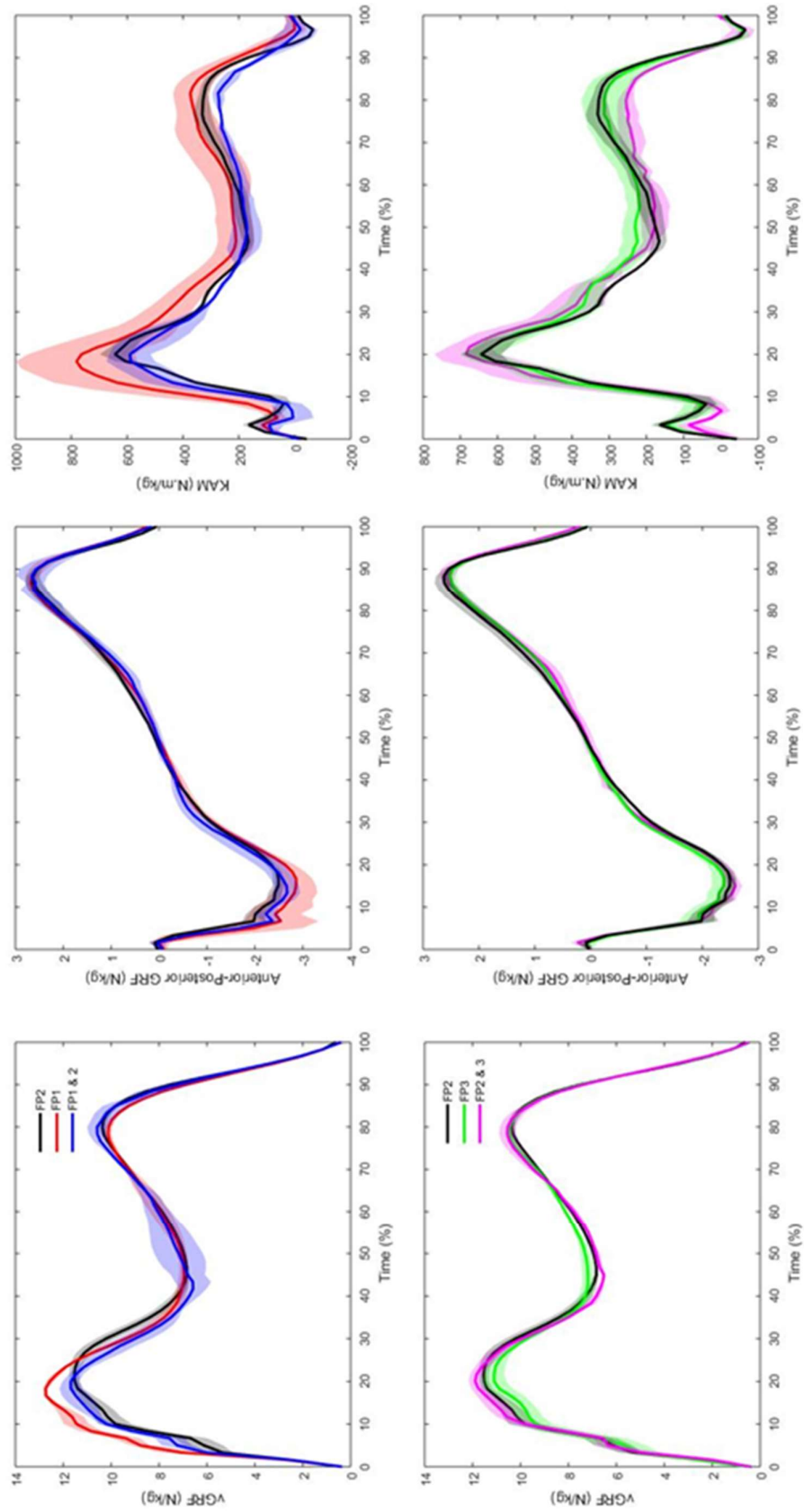


Figure B3.1. Dynamic walking gait force and knee moment waveforms for full-platform and cross-platform strikes

Appendix B3 – Cross-Platform Strike Validation

Dynamic walking trials were collected from one participant for both strike conditions ($n = 3$ trials per force platform). Force data were filtered using a 4th order Butterworth filter with a cut-off frequency of 8Hz. Data were body mass and time normalised. An SPM ANOVA was run between the full-platform strikes and corresponding cross-platform strikes. No significant differences were found between strike conditions. The results from this pilot study validate the force output and subsequent inverse dynamic calculations from a cross-platform strike. Foot strikes are still invalid for FP to floor strikes and when both feet are in contact with the same FP at the same time.

Appendix B4 – Marker Placement Accuracy and Joint Centre Calculations

This pilot study was conducted to determine the reliability of marker placement. Marker placement is crucial in the calculation of joint centre location and subsequent inverse dynamic calculations. Two participants were marked up twice on the same day and the average distance between lower body markers during a static trial was determined.

Table B4.1. Within-day repeatability of marker placement for two participants

	Participant 1			Participant 2		
	Trial 1	Trial 2	SEM	Trial 1	Trial 2	SEM
Inter ASIS	232	235	0.06	283	286	0.06
Left ASIS to Knee	444	438	0.09	465	464	0.05
Right ASIS to Knee	449	438	0.17	466	462	0.06
Left Knee to Ankle	457	456	0.02	404	402	0.03
Right Knee to Ankle	451	459	0.14	401	399	0.04

Appendix C.

Chapter 4 & 5 Landmark

Registration Results

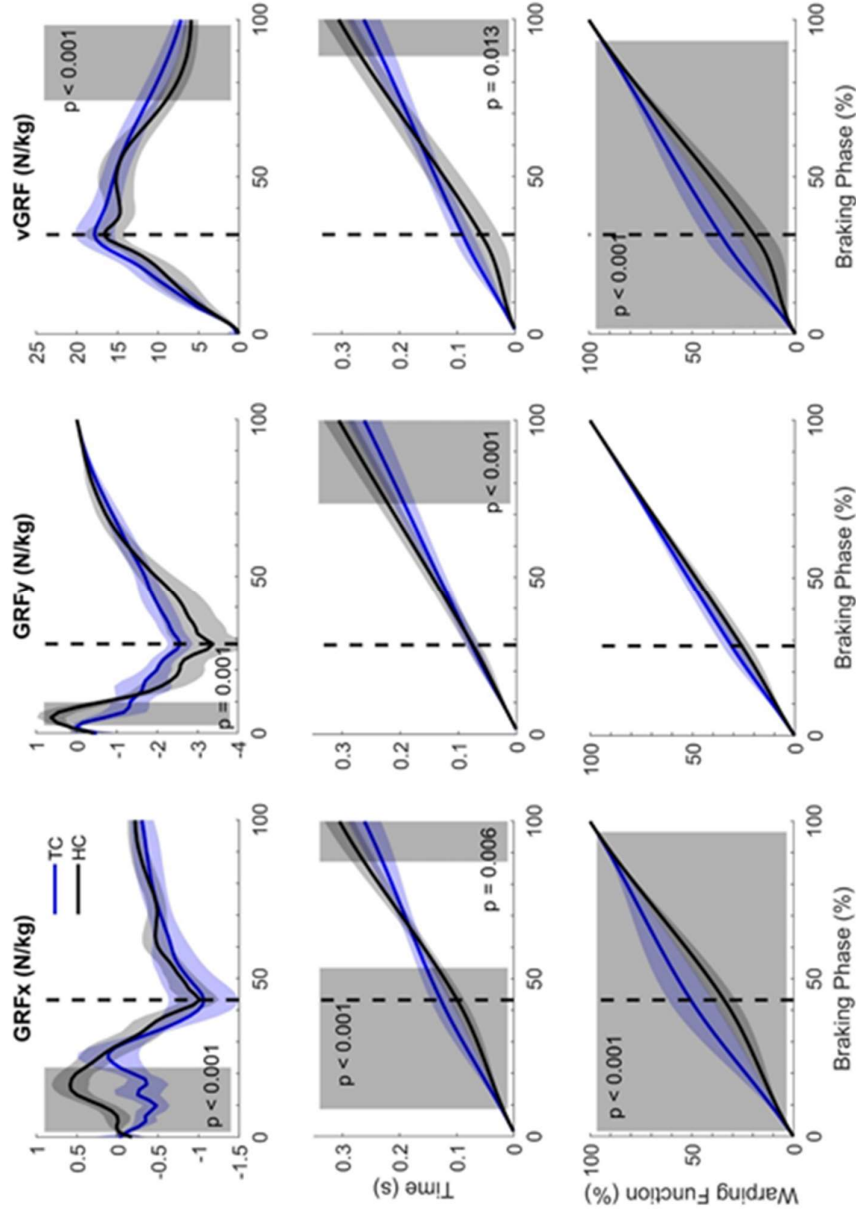


Figure C1.1. GRF landmark registered magnitude-domain (top row), time-domain (middle row), and warping function (bottom row) with significant differences highlighted in grey between heel initial contact (HC: black) and toe initial contact (TC: blue) descent strategies. The vertical dashed line represents the end of the double support phase.

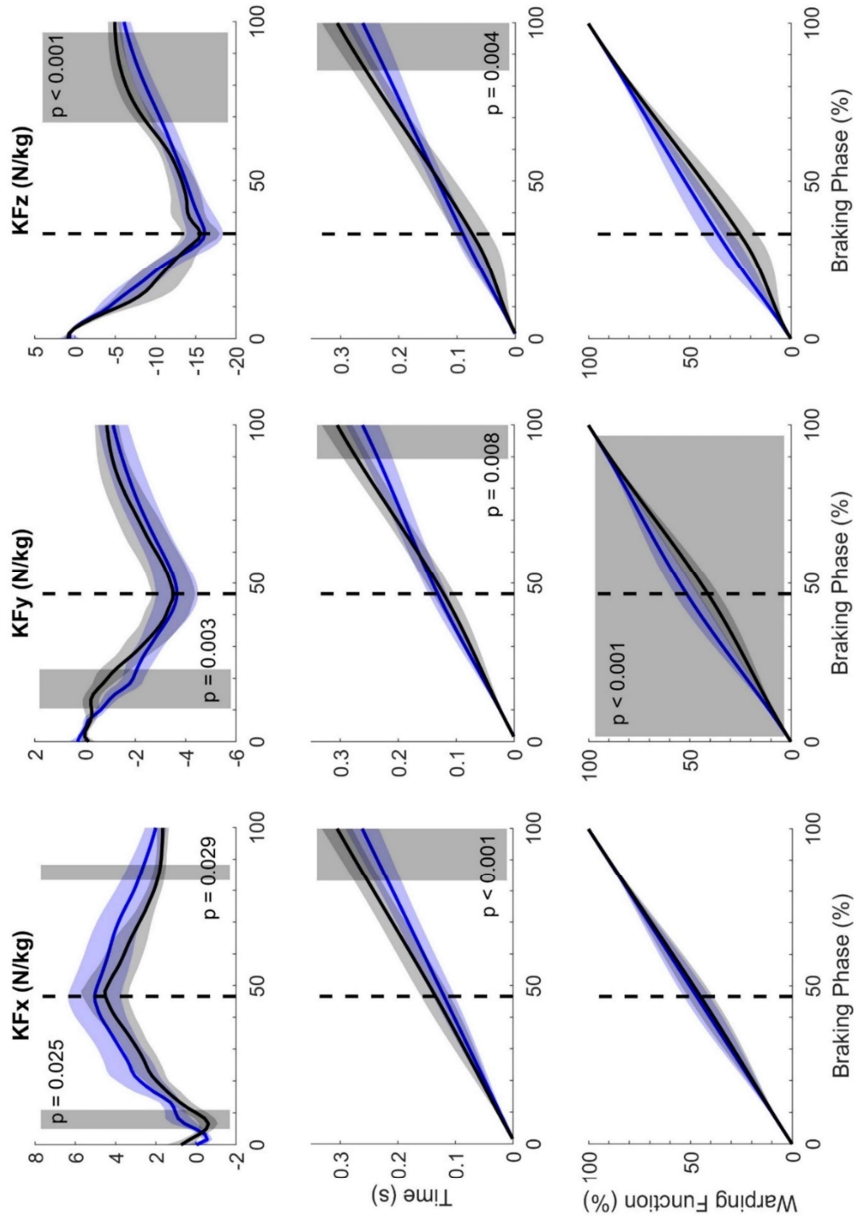


Figure C1. 2. The knee intersegmental forces (KF) landmark registered magnitude-domain (top row), time-domain (middle row), and warping function (bottom row) with significant differences highlighted in grey between heel initial contact (black) and toe initial contact (blue) descent strategies. The vertical dashed line represents the end of the double support phase.

Appendix C1 – Chapter 4 Landmark Registration Results

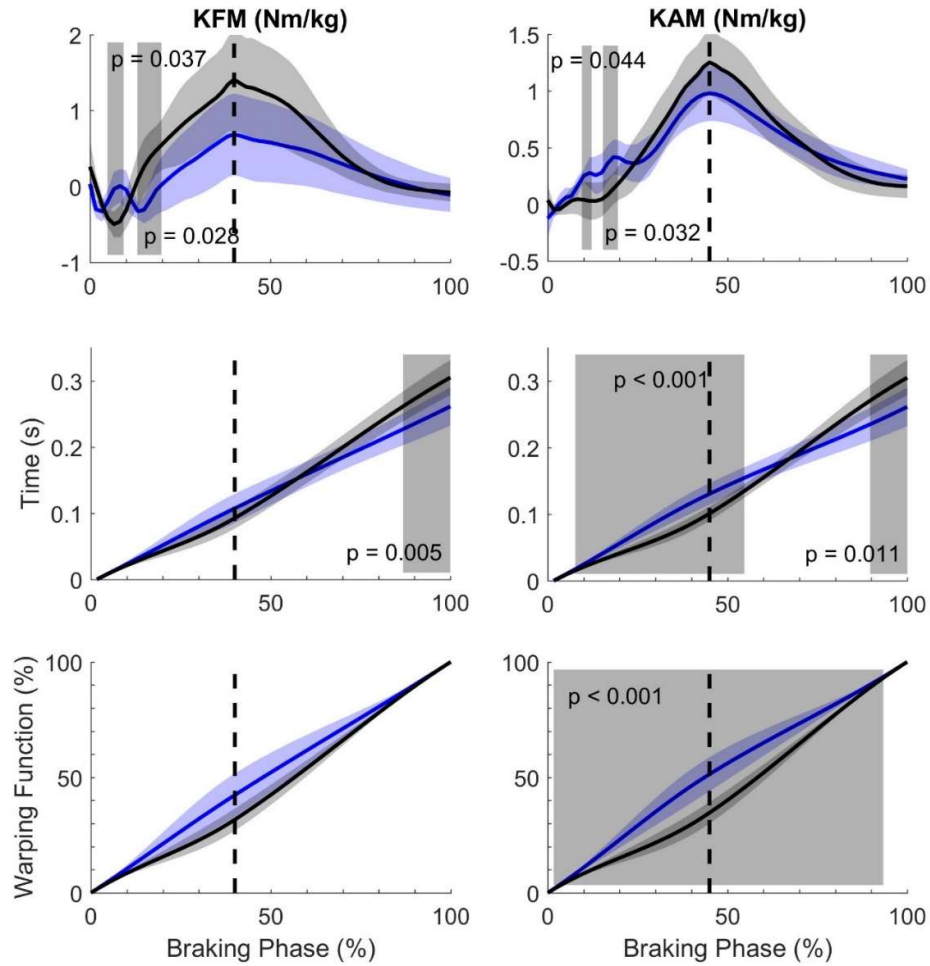


Figure C1.3. Knee moment landmark registered magnitude-domain (top row), time-domain (middle row), and warping function (bottom row) with significant differences highlighted in grey between heel initial contact (black) and toe initial contact (blue) descent strategies. The vertical dashed line represents the end of the double support phase.

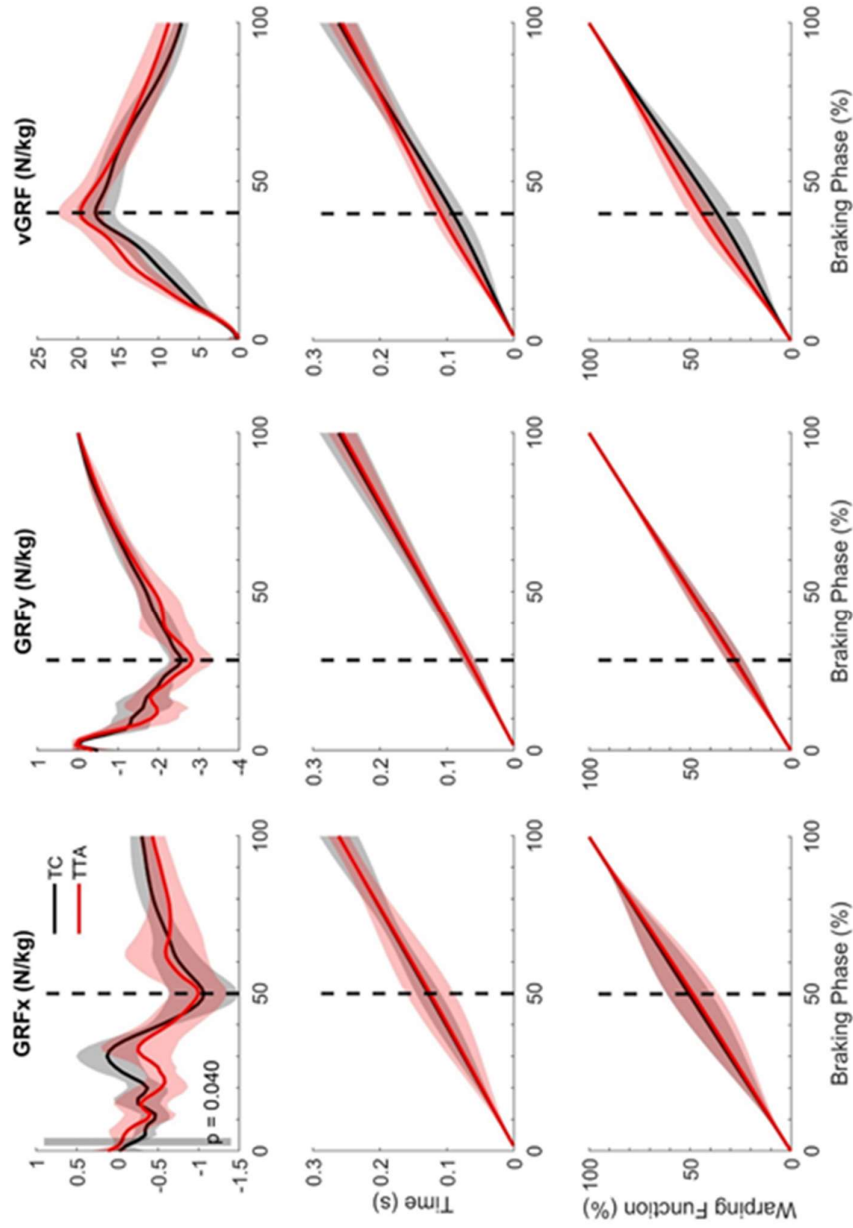


Figure C2.1. GRF landmark registered magnitude-domain (top row), time-domain (middle row), and warping function (bottom row) with significant differences highlighted in grey between the intact limb of TTAs (red) and toe initial contact (TC: black) control limb. The vertical dashed line represents the end of the double support phase.

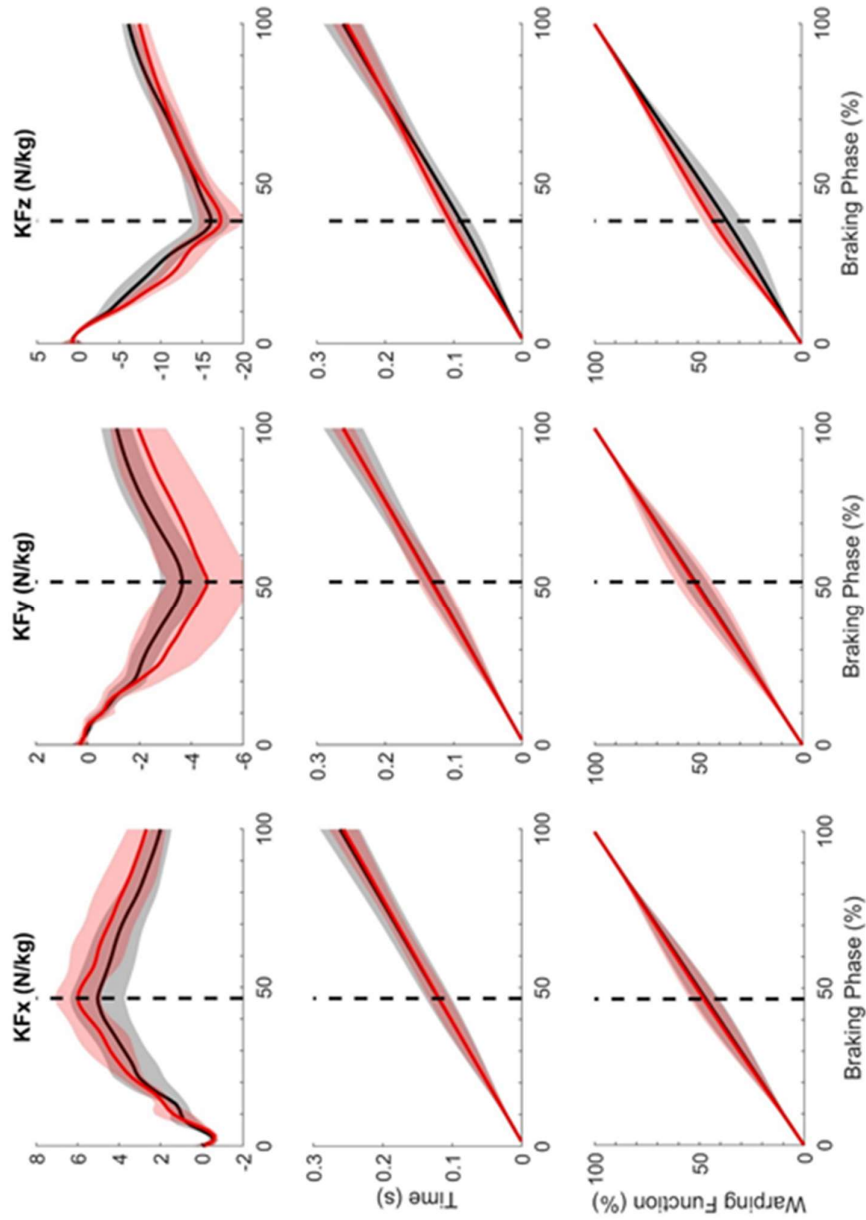


Figure C2.2. The knee intersegmental forces (KF) landmark registered magnitude-domain (top row), time-domain (middle row), and warping function (bottom row) for the intact limb of TTAs (red) and toe initial contact (black) control limb. The vertical dashed line represents the end of the double support phase.

Appendix C2 – Chapter 5 Landmark Registration Results

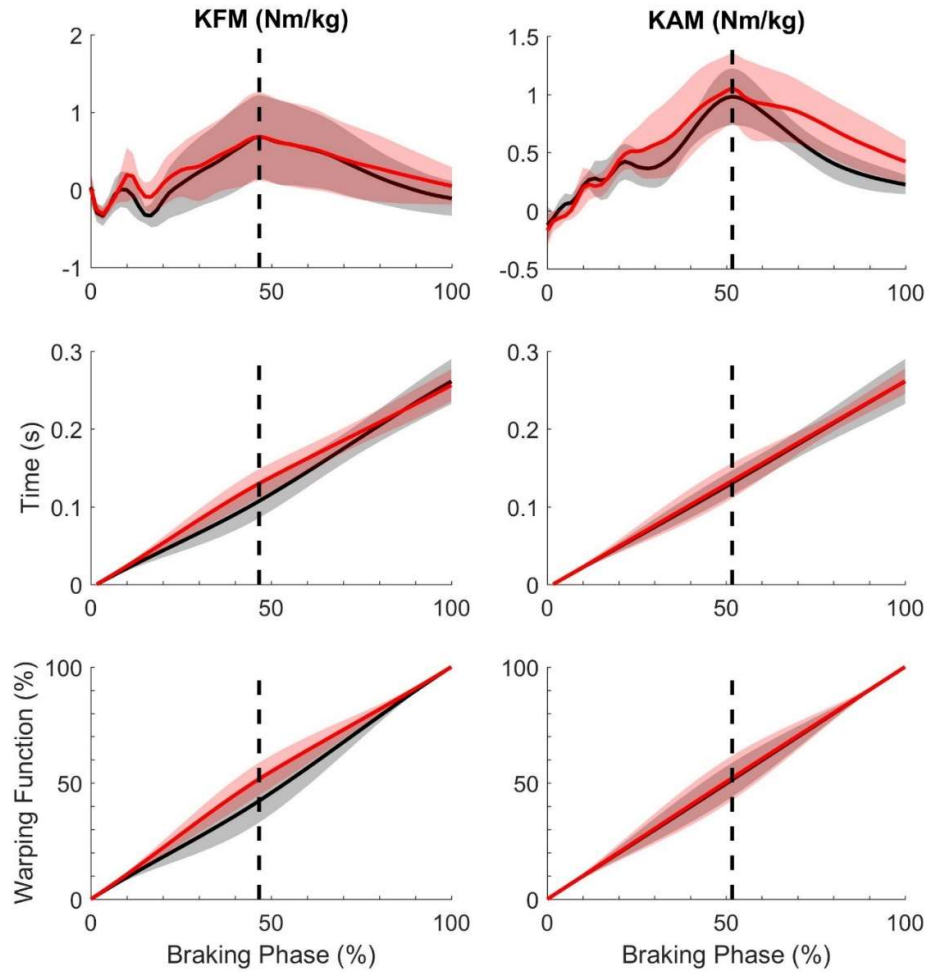


Figure C2.3. Knee moment landmark registered magnitude-domain (top row), time-domain (middle row), and warping function (bottom row) for the intact limb of ITTAs (red) and toe initial contact (black) control limb. The vertical dashed line represents the end of the double support phase.

Appendix D.

Lower-Limb Joint Angle and Power

Waveforms

Appendix D1 – Step Descent Movement Waveforms

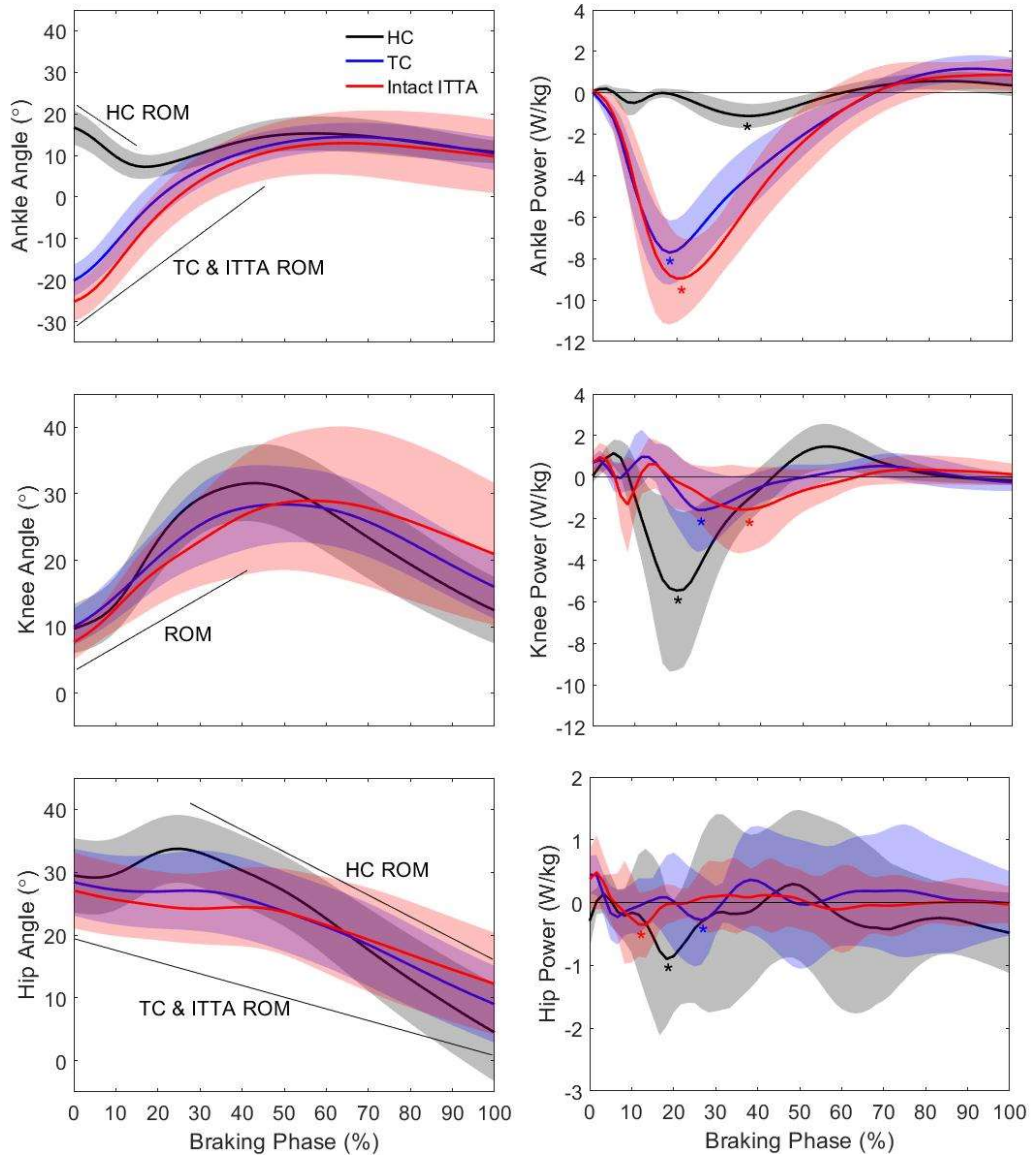


Figure D1.1. Leading limb sagittal plane joint angle and power waveforms for the ankle, knee, and hip during a step descent for the heel initial contact (HC) controls (black), toe initial contact (TC) controls (blue), and intact limb of ITTAs (red). Calculation of joint range of motion (ROM) and *peak powers are denoted on their respective figures.

Appendix D1 – Step Descent Movement Waveforms

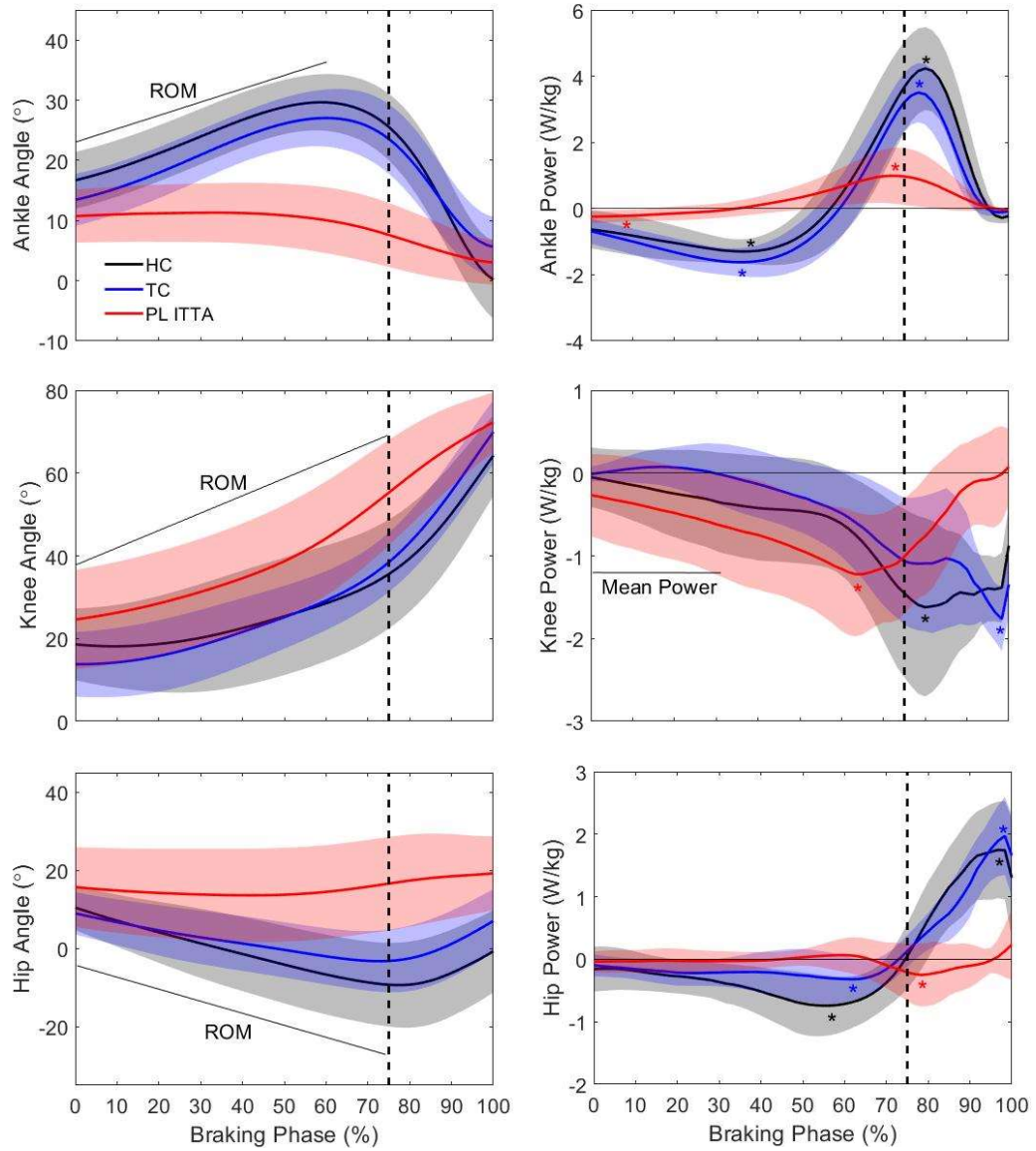


Figure D1.2. Trailing limb sagittal plane joint angle and power waveforms for the ankle, knee, and hip during a step descent for the heel initial contact (HC) controls (black), toe initial contact (TC) controls (blue), and prosthetic limb (PL) of ITTAs (red). Calculation of joint range of motion (ROM) and *peak powers are denoted on their respective figures. The vertical black dashed line represents initial contact of the leading limb.

Appendix D2 – Drop Landing Movement Waveforms

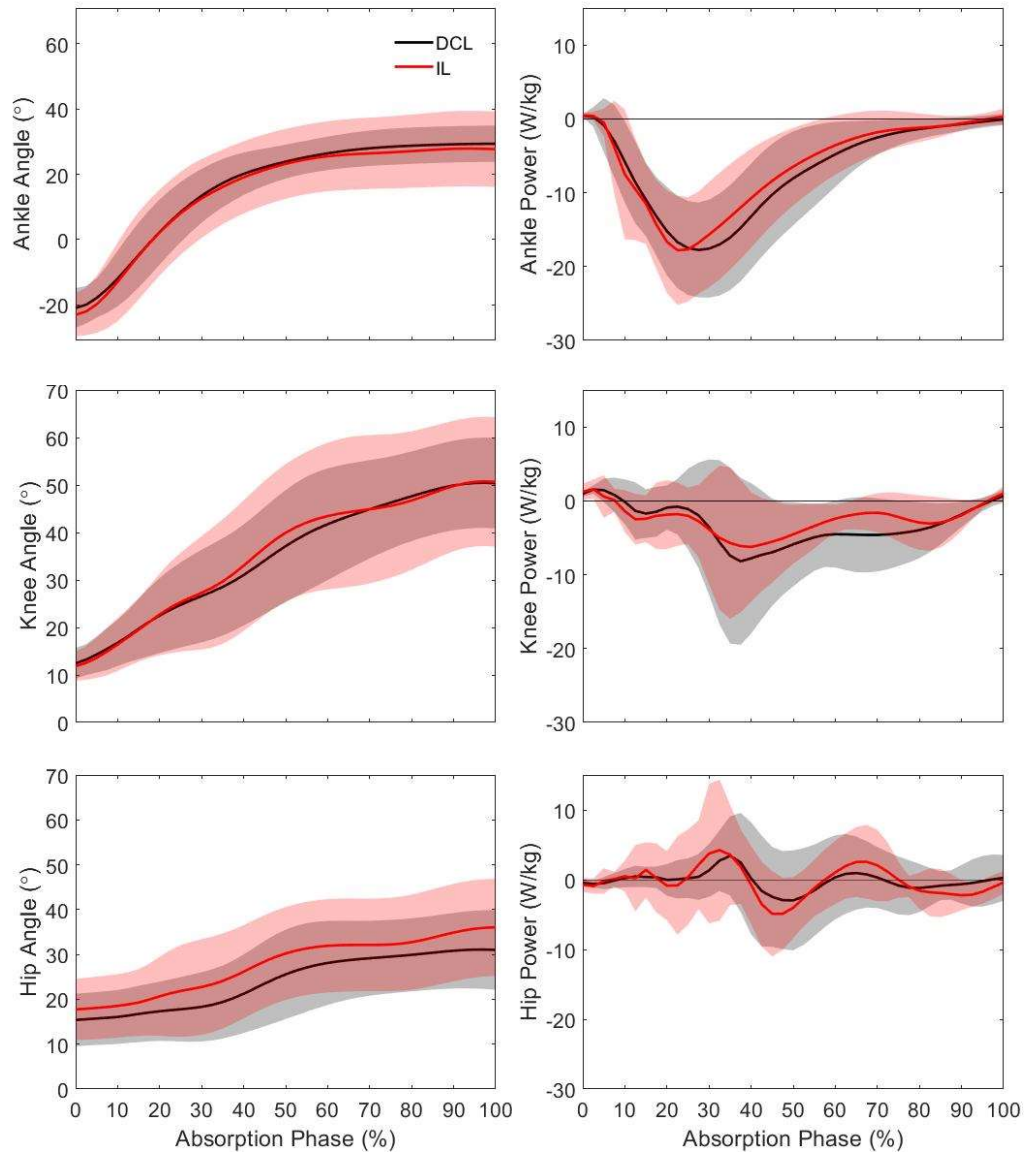


Figure D2.1. Unilateral drop landing sagittal plane joint angle and power waveforms for the ankle, knee, and hip when landing on the intact limb (IL) of ITTAs (red) and dominant control limb (DCL; black).

Appendix D2 – Drop Landing Movement Waveforms

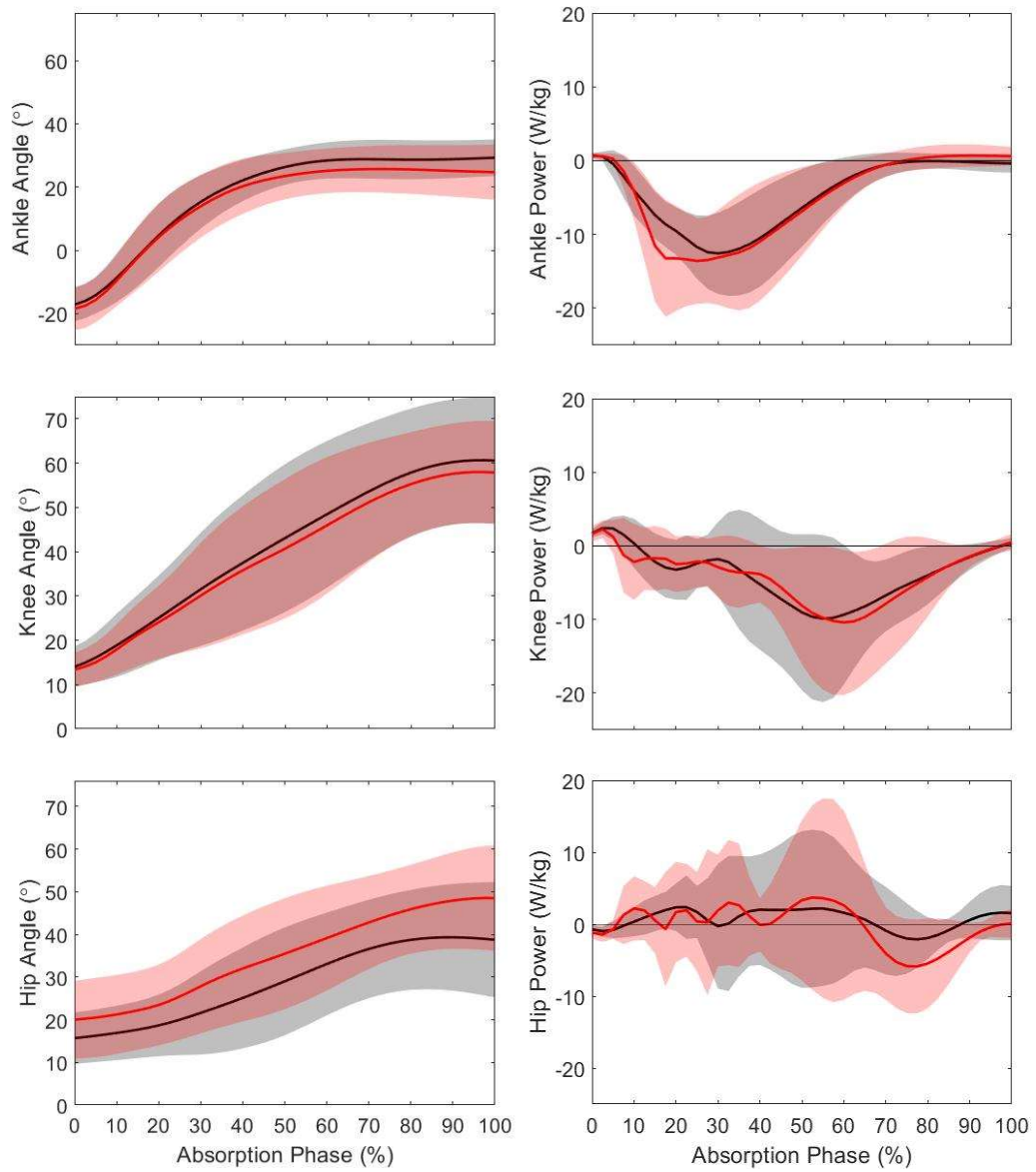


Figure D2.2. Bilateral drop landing sagittal plane joint angle and power waveforms for the ankle, knee, and hip when landing on the intact limb (IL) of ITTAs (red) and dominant control limb (DCL; black).

Appendix E.

Discussion on Feature Selection for Chapter 6

Table E1.1. Variance inflation factors (VIF) and absolute *r*-values for the movement features included in the step descent regression model

VIF	TS			LL Power				TL Phase 1 CA				TL Phase 2 Power		
	Speed	PD	H	A	K	H	AK	KH	HA	A	K	H		
Speed	2.42	1.37	1.46	1.63	1.52	1.46	1.09	2.03	1.13	1.68	1.20	1.44		
Abs. <i>r</i> -values														
Speed	1	0.16	0.48	0.52	0.56	0.48	0.02	0.82	0.31	0.68	0.53	0.69		
PD		1	0.38	0.68	0.34	0.38	0.39	0.22	0.11	0.55	0.28	0.03		
A			0.43	1	0.44	0.43	0.18	0.55	0.19	0.71	0.43	0.21		
K			0.73		1	0.73	0.11	0.45	0.07	0.43	0.36	0.17		
H			1			1	0.12	0.47	0.16	0.47	0.43	0.27		
TL Phase 1 CA							1	0.06	0.49	0.24	0.14	0.11		
AK								1	0.45	0.64	0.51	0.61		
KH									1	0.20	0.14	0.13		
HA										1	0.48	0.36		
TL Phase 2 Power											1	0.56		
A												1		
K													1	
H														1

Bolded values indicate $p < 0.05$; TS = temporal-spatial, LL = leading limb, TL = trailing limb, PD = absorption phase duration, CA = coupling angle, A = ankle, K = knee, H = hip

Appendix E1 – Chapter 6 Correlation Analysis

The features utilised in the regression model were chosen as the best representation of the significant differences between descent strategies and between ITTAs and able-bodied controls. These features reflected the shock absorption approach in the leading limb, the joint mechanics to control the lowering of the CoM, and propulsive joint mechanics required for continued forward progression. These features also represented the lowest combination of variance inflation factors (< 2.5) despite a few correlation coefficients greater than 0.7. The threshold levels for correlation coefficients present in the literature have ranged from 0.5-0.95. Variance inflation factors were, therefore, utilised as a secondary approach to determine multicollinearity.

Appendix F.

Chapter 7 Additional Information

Appendix F1 – Chapter 7 Sub-Analysis

Analysis of the threshold classification error used to separate the drop landing dataset into early and late time to peak vGRF. Seven participants from the entire dataset ($n = 29$) were classified differently depending on whether the time to peak vGRF threshold was calculated as the percentage of the absorption phase or in seconds.

Table F1.1. Individual participant time to peak vGRF difference from the mean across all participants as a percentage of the absorption phase and in seconds

	Time to Peak vGRF (%)	Time to Peak vGRF (s)	Group
<i>Participant 1</i>	0.6	0.012	ITTA
<i>Participant 2</i>	3.7	0.004	ITTA
<i>Participant 3</i>	7.1	0.005	ITTA
<i>Participant 4</i>	7.2	0.005	Control
<i>Participant 5</i>	30.5	0.035	Control
<i>Participant 6</i>	12.6	0.011	Control
<i>Participant 7</i>	11.2	0.005	Control

Bolded indicates values outside of 1 standard deviation from the mean

Table F1.1 demonstrates that six of these participants had values near the mean values across all participants indicating the presence of a middle group. One participant data indicated an over manipulation of the time-domain when linearly time-normalising the data due to an extended absorption phase. The point of maximum knee flexion, indicating the end of the absorption phase, occurred at a similar time to peak ankle and hip flexion and the point when the pelvis origin velocity reached zero. This suggests that the definition of the absorption phase was appropriate, and the participant was an outlier in how they performed their landing.

Appendix F1 – Chapter 7 Sub-Analysis

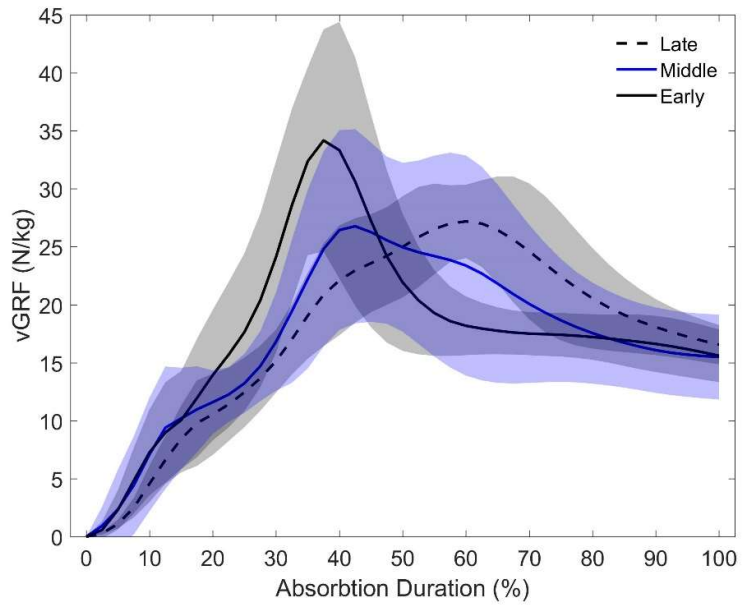


Figure F1.1. Depiction of the middle group (blue) relative to the early (solid black) and late (dashed black) groups.

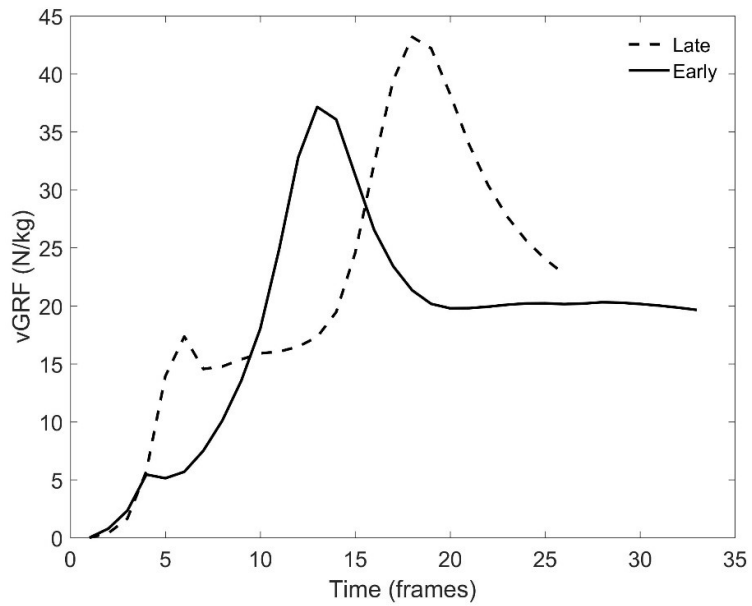


Figure F1.4. Representative trials for participants in the early and late groups in their original temporal format. The figure depicts the shorter duration of the absorption phase with a longer time to peak vGRF.

Appendix F1 – Chapter 7 Sub-Analysis

Table F2.1. Variance inflation factors (VIF) and Pearson's correlation coefficients between all movement features

	Angle @ TD			ROM			Power			Work			CA			Frontal Knee		Strength		Rel. RTD			
	A	K	H	A	K	T	A	K	H	A	K	H	AK	HA	ROM	TD	MVT	Abs. RTD					
VIF	1.5	1.2	1.1	1.2	2.2	2.5	2.7	1.5	1.6	1.9	2.2	3.0	2.4	3.5	6.3	1.5	4.8	1.1	1.2	1.5	1.7	1.2	
Abs. r-values																							
A	1	0.5	0.1	0.5	0.6	0.1	0.0	0.0	0.5	0.4	0.0	0.7	0.3	0.0	0.1	0.2	0.1	0.1	0.2	0.1	0.1	0.1	0
K		1	0.3	0.3	0.1	0.2	0.0	0.1	0.1	0.2	0.3	0.2	0.2	0.3	0.0	0.4	0.1	0.5	0.4	0.1	0.1	0.1	0.1
H			1	0.0	0.2	0.2	0.1	0.2	0.3	0.3	0.4	0.3	0.3	0.4	0.1	0.2	0.1	0.3	0.4	0.1	0.1	0.0	0.0
T				1	0.4	0.2	0.0	0.4	0.4	0.1	0.1	0.5	0.1	0.1	0.0	0.0	0.0	0.1	0.3	0.3	0.2	0.1	0.1
A					1	0.7	0.2	0.1	0.5	0.2	0.0	0.8	0.1	0.2	0.3	0.1	0.3	0.3	0.3	0.3	0.1	0.1	0.1
K						1	0.6	0.2	0.3	0.1	0.3	0.5	0.3	0.6	0.8	0.3	0.7	0.0	0.4	0.2	0.1	0.1	0.1
H							1	0.6	0.1	0.1	0.3	0.1	0.3	0.8	0.7	0.6	0.1	0.2	0.1	0.2	0.1	0.1	0.1
T								1	0.4	0.1	0.2	0.2	0.1	0.5	0.6	0.4	0.0	0.1	0.1	0.3	0.2	0.3	0.3
A									1	0.2	0.4	0.7	0.1	0.2	0.1	0.2	0.2	0.2	0.1	0.1	0.0	0.2	0.2
K										1	0.1	0.3	0.8	0.1	0.2	0.1	0.4	0.2	0.3	0.4	0.3	0.1	0.1
H											1	0.1	0.2	0.8	0.1	0.1	0.1	0.1	0.2	0.1	0.2	0.2	0.2
A												1	0.1	0.1	0.2	0.1	0.2	0.2	0.0	0.2	0.1	0.1	0.1
K													1	0.0	0.4	0.3	0.6	0.4	0.1	0.5	0.5	0.2	0.2
H														1	0.5	0.4	0.5	0.1	0.2	0.1	0.2	0.1	0.1
AK															1	0.5	0.9	0.1	0.1	0.1	0.2	0.3	0.3
KH																1	0.5	0.2	0.2	0.2	0.1	0.3	0.3
HA																	1	0.2	0.1	0.2	0.3	0.3	0.3
ROM																		1	0.4	0.2	0.1	0.1	0.1
TD																			1	0.0	0.0	0.0	0.0
MVT																				1	0.7	0.1	0.1
Abs. RTD																					1	0.6	0.6
Rel. RTD																						1	1

Bolded values indicate $p < 0.05$. A = ankle, K = knee, H = hip, T = trunk, TD = touchdown, ROM = range of motion, CA = coupling angle, AK = ankle-knee, KH = knee-hip, HA = hip-ankle, MVT = maximum voluntary torque, RTD = rate of torque development

References

- Aagaard, P., Simonsen, E.B., Andersen, J.L., Magnusson, P. & Dyhre-Poulsen, P. (2002) Increased rate of force development and neural drive of human skeletal muscle following resistance training. *Journal of Applied Physiology*. 93(4) pp.1318-1326.
- Adamczyk, P.G. & Kuo, A.D. (2009) Redirection of center-of-mass velocity during the step-to-step transition of human walking. *The Journal of Experimental Biology*. 212(Pt 16) pp.2668-2678. DOI: 10.1242/jeb.027581 [doi] .
- Addison, B.J. & Lieberman, D.E. (2015) Tradeoffs between impact loading rate, vertical impulse and effective mass for walkers and heel strike runners wearing footwear of varying stiffness. *Journal of Biomechanics*. 48(7) pp.1318-1324.
- Aerts, I., Cumps, E., Verhagen, E., Verschueren, J. & Meeusen, R. (2013) A systematic review of different jump-landing variables in relation to injuries. *The Journal of Sports Medicine and Physical Fitness*. 53(5) pp.509-519. DOI: R40Y2013N05A0509 [pii] .
- Alin, A., Kurt, S., McIntosh, A.R., Öviz, A. & Özgören, M. (2009) Partial least squares analysis in electrical brain activity. *Journal of Data Science*. 7(1) pp.99-110.
- Andersen, L.L. & Aagaard, P. (2006) Influence of maximal muscle strength and intrinsic muscle contractile properties on contractile rate of force development. *European Journal of Applied Physiology*. 96(1) pp.46-52.
- Anderson, J., King, S., Przybyla, A., Ranganath, L. & Barton, G. (2018) Reduction of frontal plane knee load caused by lateral trunk lean depends on step width. *Gait & Posture*. 61pp.483-487.
- Arokoski, J., Jurvelin, J., Väättäinen, U. & Helminen, H. (2000) Normal and pathological adaptations of articular cartilage to joint loading. *Scandinavian Journal of Medicine & Science in Sports*. 10(4) pp.186-198.
- Astephen, J.L., Deluzio, K.J., Caldwell, G.E. & Dunbar, M.J. (2008) Biomechanical changes at the hip, knee, and ankle joints during gait are associated with knee osteoarthritis severity. *Journal of Orthopaedic Research*. 26(3) pp.332-341.
- Astephen, J.L. & Deluzio, K.J. (2005a) *Changes in Frontal Plane Dynamics and the Loading Response Phase of the Gait Cycle are Characteristic of Severe Knee Osteoarthritis Application of a Multidimensional Analysis Technique*. DOI: <https://doi.org/10.1016/j.clinbiomech.2004.09.007> .
- Astephen, J.L. & Deluzio, K.J. (2005b) *Changes in Frontal Plane Dynamics and the Loading Response Phase of the Gait Cycle are Characteristic of Severe Knee Osteoarthritis Application of a Multidimensional Analysis Technique*. DOI: <https://doi.org/10.1016/j.clinbiomech.2004.09.007> .

- Austin, P.C. & Steyerberg, E.W. (2015) *The Number of Subjects Per Variable Required in Linear Regression Analyses*. DOI: <https://doi.org/10.1016/j.jclinepi.2014.12.014> .
- Barnett, C., Polman, R. & Vanicek, N. (2014) Longitudinal changes in transtibial amputee gait characteristics when negotiating a change in surface height during continuous gait. *Clinical Biomechanics*. 29(7) pp.787-793.
- Begg, R.K. & Sparrow, W.A. (2000) Gait characteristics of young and older individuals negotiating a raised surface: Implications for the prevention of falls. *The Journals of Gerontology. Series A, Biological Sciences and Medical Sciences*. 55(3) pp.M147-54.
- Behan, F.P., Pain, M.T.G. & Folland, J.P. (2018) *Explosive Voluntary Torque is Related to Whole-Body Response to Unexpected Perturbations*. DOI: <https://doi.org/10.1016/j.jbiomech.2018.09.016> .
- Bento, P.C.B., Pereira, G., Ugrinowitsch, C. & Rodacki, A.L.F. (2010) Peak torque and rate of torque development in elderly with and without fall history. *Clinical Biomechanics*. 25(5) pp.450-454.
- Bernstein, N.A. (1967) The co-ordination and regulation of movements.
- Beyaert, C., Grumillier, C., Martinet, N., Paysant, J. & André, J.-. (2008) *Compensatory Mechanism Involving the Knee Joint of the Intact Limb during Gait in Unilateral Below-Knee Amputees*. DOI: <https://doi.org/10.1016/j.gaitpost.2007.12.073> .
- Bisseling, R.W., Hof, A.L., Bredeweg, S.W., Zwerver, J. & Mulder, T. (2008) Are the take-off and landing phase dynamics of the volleyball spike jump related to patellar tendinopathy? *British Journal of Sports Medicine*. 42(6) pp.483-489. DOI: 10.1136/bjism.2007.044057 [doi] .
- Bisseling, R.W., Hof, A.L., Bredeweg, S.W., Zwerver, J. & Mulder, T. (2007) Relationship between landing strategy and patellar tendinopathy in volleyball. *British Journal of Sports Medicine*. 41(7) pp.e8. DOI: bjism.2006.032565 [pii] .
- Blackburn, J.T. & Padua, D.A. (2009) Sagittal-plane trunk position, landing forces, and quadriceps electromyographic activity. *Journal of Athletic Training*. 44(2) pp.174-179.
- Blackburn, J.T. & Padua, D.A. (2008) Influence of trunk flexion on hip and knee joint kinematics during a controlled drop landing. *Clinical Biomechanics*. 23(3) pp.313-319.
- Blickhan, R. (1989) The spring-mass model for running and hopping. *Journal of Biomechanics*. 22(11-12) pp.1217-1227.
- Boling, M.C., Padua, D.A., Marshall, S.W., Guskiewicz, K., Pyne, S. & Beutler, A. (2009) A prospective investigation of biomechanical risk factors for patellofemoral pain syndrome: The joint undertaking to monitor and prevent ACL injury (JUMP-ACL) cohort. *The American Journal of Sports Medicine*. 37(11) pp.2108-2116.

- Boyd, R., Walker, E., Wu, D., Lukoschek, M., Burr, D. & Radin, E. (1991) Morphologic and morphometric changes in synovial membrane associated with mechanically induced osteoarthritis. *Arthritis & Rheumatology*. 34(5) pp.515-524.
- Bragaru, M., Dekker, R., Geertzen, J.H. & Dijkstra, P.U. (2011) Amputees and sports. *Sports Medicine*. 41(9) pp.721-740.
- Brockett, C.L. & Chapman, G.J. (2016) *Biomechanics of the Ankle*. DOI: <https://doi.org/10.1016/j.mporth.2016.04.015> .
- Browne, M.G. & Franz, J.R. (2017a) Does dynamic stability govern propulsive force generation in human walking? *Royal Society Open Science*. 4(11) pp.171673.
- Browne, M.G. & Franz, J.R. (2017b) The independent effects of speed and propulsive force on joint power generation in walking. *Journal of Biomechanics*. 55pp.48-55.
- Buckley, J.G., Cooper, G., Maganaris, C.N. & Reeves, N.D. (2013) Is stair descent in the elderly associated with periods of high centre of mass downward accelerations? *Experimental Gerontology*. 48(2) pp.283-289.
- Buckthorpe, M. & Roi, G.S. 2017, "The time has come to incorporate a greater focus on rate of force development training in the sports injury rehabilitation process", *Muscles, ligaments and tendons journal*, 7(3) pp. 435.
- Burke, M.J., Roman, V. & Wright, V. (1978) Bone and joint changes in lower limb amputees. *Annals of the Rheumatic Diseases*. 37(3) pp.252-254.
- Butler, R.J., Crowell, H.P. & Davis, I.M. (2003) Lower extremity stiffness: Implications for performance and injury. *Clinical Biomechanics*. 18(6) pp.511-517.
- Buzzi, U.H., Stergiou, N., Kurz, M.J., Hageman, P.A. & Heidel, J. (2003) Nonlinear dynamics indicates aging affects variability during gait. *Clinical Biomechanics*. 18(5) pp.435-443.
- Byrne, J.E., Stergiou, N., Blanke, D., Houser, J.J., Kurz, M.J. & Hageman, P.A. (2002) Comparison of gait patterns between young and elderly women: An examination of coordination. *Perceptual and Motor Skills*. 94(1) pp.265-280.
- Cavagna, G.A., Thys, H. & Zamboni, A. (1976) The sources of external work in level walking and running. *The Journal of Physiology*. 262(3) pp.639-657.
- Chang, A., Hayes, K., Dunlop, D., Song, J., Hurwitz, D. & Sharma, L. (2005) Hip abduction moment and protection against medial tibiofemoral osteoarthritis progression. *Arthritis & Rheumatology*. 52(11) pp.3515-3519.
- Chang, R., Van Emmerik, R. & Hamill, J. (2008) Quantifying rearfoot–forefoot coordination in human walking. *Journal of Biomechanics*. 41(14) pp.3101-3105.
- Chapman, A.E. (2008) *Biomechanical Analysis of Fundamental Human Movements*. Human Kinetics.

Chau, T., Young, S. & Redekop, S. (2005) Managing variability in the summary and comparison of gait data. *Journal of Neuroengineering and Rehabilitation*. 2(1) pp.22.

Chaudhari, A.M. & Andriacchi, T.P. (2006) *The Mechanical Consequences of Dynamic Frontal Plane Limb Alignment for Non-Contact ACL Injury*. DOI: <https://doi.org/10.1016/j.jbiomech.2004.11.013> .

Cheung, R.T. & Rainbow, M.J. (2014) Landing pattern and vertical loading rates during first attempt of barefoot running in habitual shod runners. *Human Movement Science*. 34pp.120-127.

Chiu, S. & Chou, L. (2012) Effect of walking speed on inter-joint coordination differs between young and elderly adults. *Journal of Biomechanics*. 45(2) pp.275-280.

Christina, K.A. & Cavanagh, P.R. (2002) Ground reaction forces and frictional demands during stair descent: Effects of age and illumination. *Gait & Posture*. 15(2) pp.153-158.

Cofré, L.E., Lythgo, N., Morgan, D. & Galea, M.P. (2011) *Aging Modifies Joint Power and Work when Gait Speeds are Matched*. DOI: <https://doi.org/10.1016/j.gaitpost.2010.12.030> .

Crane, E.A., Cassidy, R.B., Rothman, E.D. & Gerstner, G.E. (2010) Effect of registration on cyclical kinematic data. *Journal of Biomechanics*. 43(12) pp.2444-2447.

Creaby, M.W. (2015) It's not all about the knee adduction moment: The role of the knee flexion moment in medial knee joint loading. *Osteoarthritis and Cartilage*. 23(7) pp.1038-1040. DOI: 10.1016/j.joca.2015.03.032 [doi] .

Creaby, M.W., Hunt, M.A., Hinman, R.S. & Bennell, K.L. (2013) *Sagittal Plane Joint Loading is Related to Knee Flexion in Osteoarthritic Gait*. DOI: <https://doi.org/10.1016/j.clinbiomech.2013.07.013> .

Davis, R.B., Ounpuu, S., Tyburski, D. & Gage, J.R. (1991) A gait analysis data collection and reduction technique. *Human Movement Science*. 10(5) pp.575-587.

de Cerqueira Soares, A., Yamaguti, E.Y., Mochizuki, L., Amadio, A.C. & Serrão, J.C. (2009) Biomechanical parameters of gait among transtibial amputees: A review. *Sao Paulo Medical Journal*. 127(5) pp.302-309.

de Oliveira Silva, D., Briani, R., Pazzinatto, M., Ferrari, D., Aragão, F. & de Azevedo, F. (2015) Vertical ground reaction forces are associated with pain and self-reported functional status in recreational athletes with patellofemoral pain. *Journal of Applied Biomechanics*. 31(6) pp.409-414.

Deans, S., Burns, D., McGarry, A., Murray, K. & Mutrie, N. (2012) Motivations and barriers to prosthesis users participation in physical activity, exercise and sport: A review of the literature. *Prosthetics and Orthotics International*. 36(3) pp.260-269.

Delbaere, K., Sturnieks, D.L., Crombez, G. & Lord, S.R. (2009) Concern about falls elicits changes in gait parameters in conditions of postural threat in older people.

The Journals of Gerontology. Series A, Biological Sciences and Medical Sciences. 64(2) pp.237-242. DOI: 10.1093/gerona/gln014 [doi] .

Deluzio, K.J. & Astephen, J.L. (2007) Biomechanical features of gait waveform data associated with knee osteoarthritis: An application of principal component analysis. *Gait & Posture.* 25(1) pp.86-93.

Deluzio, K.J., Wyss, U.P., Zee, B., Costigan, P.A. & Serbie, C. (1997) Principal component models of knee kinematics and kinetics: Normal vs. pathological gait patterns. *Human Movement Science.* 16(2-3) pp.201-217.

Department of Transport (2005) *Making Transport Accessible for Passengers and Pedestrians.* UK: gov.uk.

DeVita, P. & Hortobagyi, T. (2000) Age causes a redistribution of joint torques and powers during gait. *Journal of Applied Physiology.* 88(5) pp.1804-1811.

DeVita, P. & Skelly, W.A. (1992) Effect of landing stiffness on joint kinetics and energetics in the lower extremity. *Medicine & Science in Sports & Exercise.* 24(1) pp.108.

Dirnberger, J., Wiesinger, H., Wiemer, N., Kösters, A. & Müller, E. (2016) Explosive strength of the knee extensors: The influence of criterion trial detection methodology on measurement reproducibility. *Journal of Human Kinetics.* 50(1) pp.15-25.

Diss, C.E. (2001) The reliability of kinetic and kinematic variables used to analyse normal running gait. *Gait & Posture.* 14(2) pp.98-103.

Doherty, C., Bleakley, C., Hertel, J., Sweeney, K., Caulfield, B., Ryan, J. & Delahunty, E. (2014) *Lower Extremity Coordination and Symmetry Patterns during a Drop Vertical Jump Task Following Acute Ankle Sprain.* DOI: <http://dx.doi.org/10.1016/j.humov.2014.08.002> .

Dona, G., Preatoni, E., Cobelli, C., Rodano, R. & Harrison, A.J. (2009) Application of functional principal component analysis in race walking: An emerging methodology. *Sports Biomechanics.* 8(4) pp.284-301.

Donelan, J.M., Kram, R. & Kuo, A.D. (2002a) Simultaneous positive and negative external mechanical work in human walking. *Journal of Biomechanics.* 35(1) pp.117-124.

Donelan, J.M., Kram, R. & Kuo, A.D. (2002b) Mechanical work for step-to-step transitions is a major determinant of the metabolic cost of human walking. *The Journal of Experimental Biology.* 205(23) pp.3717-3727.

Donoghue, O.A., Harrison, A.J., Coffey, N. & Hayes, K. (2008) Functional data analysis of running kinematics in chronic achilles tendon injury. *Medicine and Science in Sports and Exercise.* 40(7) pp.1323.

Dormann, C.F., Elith, J., Bacher, S., Buchmann, C., Carl, G., Carré, G., Marquéz, J.R.G., Gruber, B., Lafourcade, B. & Leitão, P.J. (2013) Collinearity: A review of methods to deal with it and a simulation study evaluating their performance. *Ecography.* 36(1) pp.27-46.

- Dudek, N.L., Marks, M.B., Marshall, S.C. & Chardon, J.P. (2005) *Dermatologic Conditions Associated with use of a Lower-Extremity Prosthesis*. DOI: <https://doi.org/10.1016/j.apmr.2004.09.003> .
- Durall, C.J., Kernozek, T.W., Kersten, M., Nitz, M., Setz, J. & Beck, S. (2011) Associations between single-leg postural control and drop-landing mechanics in healthy women. *Journal of Sport Rehabilitation*. 20(4) pp.406-418.
- Edwards, S., Steele, J.R., McGhee, D.E., Beattie, S., Purdam, C. & Cook, J.L. (2010) Landing strategies of athletes with an asymptomatic patellar tendon abnormality. *Medicine and Science in Sports and Exercise*. 42(11) pp.2072-2080. DOI: 10.1249/MSS.0b013e3181e0550b [doi] .
- Egloff, C., Hügler, T. & Valderrabano, V. (2012) Biomechanics and pathomechanisms of osteoarthritis. *Swiss Med Wkly*. 142(0) .
- Ehrig, R.M., Taylor, W.R., Duda, G.N. & Heller, M.O. (2007) A survey of formal methods for determining functional joint axes. *Journal of Biomechanics*. 40(10) pp.2150-2157. DOI: S0021-9290(06)00415-5 [pii] .
- Ehrig, R.M., Taylor, W.R., Duda, G.N. & Heller, M.O. (2006) A survey of formal methods for determining the centre of rotation of ball joints. *Journal of Biomechanics*. 39(15) pp.2798-2809. DOI: S0021-9290(05)00446-X [pii] .
- Epifanio, I., Ávila, C., Page, Á & Atienza, C. (2008) Analysis of multiple waveforms by means of functional principal component analysis: Normal versus pathological patterns in sit-to-stand movement. *Medical & Biological Engineering & Computing*. 46(6) pp.551-561.
- Erhart, J.C., Dyrby, C.O., D'Lima, D.D., Colwell, C.W. & Andriacchi, T.P. (2010) Changes in in vivo knee loading with a variable-stiffness intervention shoe correlate with changes in the knee adduction moment. *Journal of Orthopaedic Research*. 28(12) pp.1548-1553.
- Esposito, E.R. & Wilken, J.M. (2014) Biomechanical risk factors for knee osteoarthritis when using passive and powered ankle-foot prostheses. *Clinical Biomechanics*. 29(10) pp.1186-1192.
- Exell, T.A., Gittoes, M.J., Irwin, G. & Kerwin, D.G. (2012) Considerations of force plate transitions on centre of pressure calculation for maximal velocity sprint running. *Sports Biomechanics*. 11(4) pp.532-541.
- Farley, C.T. & Morgenroth, D.C. (1999) Leg stiffness primarily depends on ankle stiffness during human hopping. *Journal of Biomechanics*. 32(3) pp.267-273.
- Farrokhi, S., Mazzone, B., Yoder, A., Grant, K. & Wyatt, M. (2016) A narrative review of the prevalence and risk factors associated with development of knee osteoarthritis after traumatic unilateral lower limb amputation. *Military Medicine*. 181(suppl_4) pp.38-44.
- Fey, N.P. & Neptune, R.R. (2012) 3D intersegmental knee loading in below-knee amputees across steady-state walking speeds. *Clinical Biomechanics*. 27(4) pp.409-414.

Folland, J., Buckthorpe, M. & Hannah, R. (2014) Human capacity for explosive force production: Neural and contractile determinants. *Scandinavian Journal of Medicine & Science in Sports*. 24(6) pp.894-906.

Ford, K.R., Myer, G.D. & Hewett, T.E. (2003) Valgus knee motion during landing in high school female and male basketball players. *Medicine and Science in Sports and Exercise*. 35(10) pp.1745-1750. DOI: 10.1249/01.MSS.0000089346.85744.D9 [doi] .

Freedman, W. & Kent, L. (1987) Selection of movement patterns during functional tasks in humans. *Journal of Motor Behavior*. 19(2) pp.214-226.

Fregly, B.J. (2012) Gait modification to treat knee osteoarthritis. *HSS Journal*. 8(1) pp.45-48.

Fregly, B.J., D'lima, D.D. & Colwell Jr, C.W. (2009) Effective gait patterns for offloading the medial compartment of the knee. *Journal of Orthopaedic Research*. 27(8) pp.1016-1021.

Friston, K.J., Frith, C., Liddle, P. & Frackowiak, R. (1991) Comparing functional (PET) images: The assessment of significant change. *Journal of Cerebral Blood Flow & Metabolism*. 11(4) pp.690-699.

Friston, K.J., Worsley, K.J., Frackowiak, R.S., Mazziotta, J.C. & Evans, A.C. (1994) Assessing the significance of focal activations using their spatial extent. *Human Brain Mapping*. 1(3) pp.210-220.

Gailey, R., Allen, K., Castles, J., Kucharik, J. & Roeder, M. (2008) Review of secondary physical conditions associated with lower-limb amputation and long-term prosthesis use. *Journal of Rehabilitation Research and Development*. 45(1) pp.15.

Gard, S.A. & Childress, D.S. (1999) The influence of stance-phase knee flexion on the vertical displacement of the trunk during normal walking. *Archives of Physical Medicine and Rehabilitation*. 80(1) pp.26-32.

Geiser, C., O'connor, K.M. & Earl, J.E. (2010) Effects of isolated hip abductor fatigue on frontal plane knee mechanics. *Medicine & Science in Sports & Exercise*.

Gerbrands, T.A., Pisters, M.F. & Vanwanseele, B. (2014) *Individual Selection of Gait Retraining Strategies is Essential to Optimally Reduce Medial Knee Load during Gait*. DOI: <https://doi.org/10.1016/j.clinbiomech.2014.05.005> .

Gerstle, E.E., Keenan, K.G., O'Connor, K. & Cobb, S.C. (2018) Lower extremity muscle activity during descent from varying step heights. *Journal of Electromyography and Kinesiology*.

Gerstle, E.E., O'Connor, K., Keenan, K.G. & Cobb, S.C. (2017) Foot and ankle kinematics during descent from varying step heights. *Journal of Applied Biomechanics*. 33(6) pp.453-459.

Godwin, A., Takahara, G., Agnew, M. & Stevenson, J. (2010) Functional data analysis as a means of evaluating kinematic and kinetic waveforms. *Theoretical Issues in Ergonomics Science*. 11(6) pp.489-503.

Goerger, B.M., Marshall, S.W., Beutler, A.I., Blackburn, J.T., Wilckens, J.H. & Padua, D.A. (2015) Anterior cruciate ligament injury alters preinjury lower extremity biomechanics in the injured and uninjured leg: The JUMP-ACL study. *British Journal of Sports Medicine*. 49(3) pp.188-195. DOI: 10.1136/bjsports-2013-092982 [doi] .

Grabowski, A.M. & D'Andrea, S. (2013) Effects of a powered ankle-foot prosthesis on kinetic loading of the unaffected leg during level-ground walking. *Journal of Neuroengineering and Rehabilitation*. 10(1) pp.49.

Grabowski, A.M., McGowan, C.P., McDermott, W.J., Beale, M.T., Kram, R. & Herr, H.M. (2010) Running-specific prostheses limit ground-force during sprinting. *Biology Letters*. 6(2) pp.201-204. DOI: 10.1098/rsbl.2009.0729 [doi] .

Griffin, T.M. & Guilak, F. (2005) The role of mechanical loading in the onset and progression of osteoarthritis. *Exercise and Sport Sciences Reviews*. 33(4) pp.195-200.

Grumillier, C., Martinet, N., Paysant, J., André, J.-. & Beyaert, C. (2008) *Compensatory Mechanism Involving the Hip Joint of the Intact Limb during Gait in Unilateral Trans-Tibial Amputees*. DOI: <https://doi.org/10.1016/j.jbiomech.2008.07.018> .

Haber, C.K., Ritchie, L.J. & Strike, S.C. (2018) *Dynamic Elastic Response Prostheses Alter Approach Angles and Ground Reaction Forces but Not Leg Stiffness during a Start-Stop Task*. DOI: <https://doi.org/10.1016/j.humov.2017.12.007> .

Hamill, J., Haddad, J.M. & McDermott, W.J. (2000) Issues in quantifying variability from a dynamical systems perspective. *Journal of Applied Biomechanics*. 16(4) pp.407-418.

Henriksen, M., Simonsen, E.B., Graven-Nielsen, T., Lund, H., Danneskiold-Samsøe, B. & Bliddal, H. (2006) Impulse-forces during walking are not increased in patients with knee osteoarthritis. *Acta Orthopaedica*. 77(4) pp.650-656.

Hensor, E., Dube, B., Kingsbury, S.R., Tennant, A. & Conaghan, P.G. (2015) Toward a clinical definition of early osteoarthritis: Onset of Patient-Reported knee pain begins on stairs. data from the osteoarthritis initiative. *Arthritis Care & Research*. 67(1) pp.40-47.

Hewett, T.E., Myer, G.D., Ford, K.R., Heidt Jr, R.S., Colosimo, A.J., McLean, S.G., Van den Bogert, Antonie J, Paterno, M.V. & Succop, P. (2005) Biomechanical measures of neuromuscular control and valgus loading of the knee predict anterior cruciate ligament injury risk in female athletes: A prospective study. *The American Journal of Sports Medicine*. 33(4) pp.492-501.

Hirokawa, S. (1989) *Normal Gait Characteristics Under Temporal and Distance Constraints*. DOI: [http://dx.doi.org/10.1016/0141-5425\(89\)90038-1](http://dx.doi.org/10.1016/0141-5425(89)90038-1) .

Houdijk, H., Pollmann, E., Groenewold, M., Wiggerts, H. & Polonski, W. (2009) The energy cost for the step-to-step transition in amputee walking. *Gait & Posture*. 30(1) pp.35-40.

Hughes, G. (2014) A review of recent perspectives on biomechanical risk factors associated with anterior cruciate ligament injury. *Research in Sports Medicine*. 22(2) pp.193-212.

Hughes, G. & Watkins, J. (2008) Lower limb coordination and stiffness during landing from volleyball block jumps. *Research in Sports Medicine*. 16(2) pp.138-154.

Hunt, M.A., Birmingham, T., Bryant, D., Jones, I., Giffin, J., Jenkyn, T. & Vandervoort, A. (2008) Lateral trunk lean explains variation in dynamic knee joint load in patients with medial compartment knee osteoarthritis. *Osteoarthritis and Cartilage*. 16(5) pp.591-599.

Hunt, M.A., Birmingham, T.B., Giffin, J.R. & Jenkyn, T.R. (2006) *Associations among Knee Adduction Moment, Frontal Plane Ground Reaction Force, and Lever Arm during Walking in Patients with Knee Osteoarthritis*. DOI: <https://doi.org/10.1016/j.jbiomech.2005.07.002> .

Hunt, M.A., Hinman, R.S., Metcalf, B.R., Lim, B., Wrigley, T.V., Bowles, K., Kemp, G. & Bennell, K.L. (2010) *Quadriceps Strength is Not Related to Gait Impact Loading in Knee Osteoarthritis*. DOI: <https://doi.org/10.1016/j.knee.2010.02.010> .

Hurley, G., McKenney, R., Robinson, M., Zadavec, M. & Pierrynowski, M. (1990) The role of the contralateral limb in below-knee amputee gait. *Prosthetics and Orthotics International*. 14(1) pp.33-42.

Igawa, T. & Katsuhira, J. (2014) Biomechanical analysis of stair descent in patients with knee osteoarthritis. *Journal of Physical Therapy Science*. 26(5) pp.629-631.

Isakov, E., Burger, H., Krajnik, J., Gregoric, M. & Marincek, C. (1996) Influence of speed on gait parameters and on symmetry in transtibial amputees. *Prosthetics and Orthotics International*. 20(3) pp.153-158.

Isakov, E., Keren, O. & Benjuya, N. (2000) Trans-tibial amputee gait: Time-distance parameters and EMG activity. *Prosthetics and Orthotics International*. 24(3) pp.216-220.

Jones, P.A., Herrington, L.C., Munro, A.G. & Graham-Smith, P. (2014) Is there a relationship between landing, cutting, and pivoting tasks in terms of the characteristics of dynamic valgus? *The American Journal of Sports Medicine*. 42(9) pp.2095-2102.

Jones, S.F., Twigg, P.C., Scally, A.J. & Buckley, J.G. (2006) The mechanics of landing when stepping down in unilateral lower-limb amputees. *Clinical Biomechanics*. 21(2) pp.184-193. DOI: <http://dx.doi.org/10.1016/j.clinbiomech.2005.09.015> .

Judge, J.O., Davis III, R. & Öunpuu, S. (1996) Step length reductions in advanced age: The role of ankle and hip kinetics. *The Journals of Gerontology Series A: Biological Sciences and Medical Sciences*. 51(6) pp.M303-M312.

Karimi, M.T., Salami, F., Esrafilian, A., Heitzmann, D.W.W., Alimusaj, M., Putz, C. & Wolf, S.I. (2017) *Sound Side Joint Contact Forces in Below Knee Amputee Gait with an ESAR Prosthetic Foot*. DOI: <https://doi.org/10.1016/j.gaitpost.2017.08.007> .

Kent, J. & Franklyn-Miller, A. (2011) Biomechanical models in the study of lower limb amputee kinematics: A review. *Prosthetics and Orthotics International*. 35(2) pp.124-139. DOI: 10.1177/0309364611407677 [doi] .

Kerrigan, D.C., Todd, M.K., Della Croce, U., Lipsitz, L.A. & Collins, J.J. (1998) Biomechanical gait alterations independent of speed in the healthy elderly: Evidence for specific limiting impairments. *Archives of Physical Medicine and Rehabilitation*. 79(3) pp.317-322.

Klute, G. & Berge, J. (2004) Modelling the effect of prosthetic feet and shoes on the heel-ground contact force in amputee gait. *Proceedings of the Institution of Mechanical Engineers, Part H: Journal of Engineering in Medicine*. 218(3) pp.173-182.

Kneip, A. & Ramsay, J.O. (2008) Combining registration and fitting for functional models. *Journal of the American Statistical Association*. 103(483) pp.1155-1165.

Kobayashi, H., Kanamura, T., Koshida, S., Miyashita, K., Okado, T., Shimizu, T. & Yokoe, K. (2013) Lower extremity biomechanics during single-leg drop jump in female basketball players with dynamic knee valgus alignment. *The Journal of Physical Fitness and Sports Medicine*. 2(4) pp.501-508.

Kovač, I., Medved, V. & Ostojić, L. (2010) Spatial, temporal and kinematic characteristics of traumatic transtibial amputees' gait. *Collegium Antropologicum*. 34(1) pp.205-213.

Kuenze, C.M., Foot, N., Saliba, S.A. & Hart, J.M. (2015) Drop-landing performance and knee-extension strength after anterior cruciate ligament reconstruction. *Journal of Athletic Training*. 50(6) pp.596-602.

Kuo, A.D., Donelan, J.M. & Ruina, A. (2005) Energetic consequences of walking like an inverted pendulum: Step-to-step transitions. *Exercise and Sport Sciences Reviews*. 33(2) pp.88-97.

Kuo, A.D. (2007) The six determinants of gait and the inverted pendulum analogy: A dynamic walking perspective. *Human Movement Science*. 26(4) pp.617-656. DOI: <http://dx.doi.org/10.1016/j.humov.2007.04.003> .

Kuo, A.D. & Donelan, J.M. (2010) Dynamic principles of gait and their clinical implications. *Physical Therapy*. 90(2) pp.157-174. Available at: <http://search.ebscohost.com/login.aspx?direct=true&db=s3h&AN=48349783&site=ehost-live> .

Landry, S.C., McKean, K.A., Hubley-Kozey, C.L., Stanish, W.D. & Deluzio, K.J. (2007) *Knee Biomechanics of Moderate OA Patients Measured during Gait at a Self-Selected and Fast Walking Speed*. DOI: <https://doi.org/10.1016/j.jbiomech.2006.08.010> .

LaStayo, P.C., Woolf, J.M., Lewek, M.D., Snyder-Mackler, L., Reich, T. & Lindstedt, S.L. (2003) Eccentric muscle contractions: Their contribution to injury, prevention, rehabilitation, and sport. *Journal of Orthopaedic & Sports Physical Therapy*. 33(10) pp.557-571.

Lasas, J.L., Merriman, G.J., Riley, P.O. & Kerrigan, D.C. (2003) Predicting peak kinematic and kinetic parameters from gait speed. *Gait & Posture*. 17(2) pp.106-112.

Levinger, P., Webster, K.E. & Feller, J. (2008) Asymmetric knee loading at heel contact during walking in patients with unilateral knee replacement. *The Knee*. 15(6) pp.456-460. DOI: 10.1016/j.knee.2008.06.002 [doi] .

Levitin, D.J., Nuzzo, R.L., Vines, B.W. & Ramsay, J. (2007) Introduction to functional data analysis. *Canadian Psychology/Psychologie Canadienne*. 48(3) pp.135.

Lloyd, C.H., Stanhope, S.J., Davis, I.S. & Royer, T.D. (2010) Strength asymmetry and osteoarthritis risk factors in unilateral trans-tibial, amputee gait. *Gait & Posture*. 32(3) pp.296-300.

Louw, Q., Grimmer, K. & Vaughan, C. (2006) Knee movement patterns of injured and uninjured adolescent basketball players when landing from a jump: A case-control study. *BMC Musculoskeletal Disorders*. 7(1) pp.22.

Lu, T., Yen, H. & Chen, H. (2008) Comparisons of the inter-joint coordination between leading and trailing limbs when crossing obstacles of different heights. *Gait & Posture*. 27(2) pp.309-315.

Lythgo, N., Begg, R. & Best, R. (2007) Stepping responses made by elderly and young female adults to approach and accommodate known surface height changes. *Gait & Posture*. 26(1) pp.82-89.

Maffiuletti, N.A., Aagaard, P., Blazevich, A.J., Folland, J., Tillin, N. & Duchateau, J. (2016) Rate of force development: Physiological and methodological considerations. *European Journal of Applied Physiology*. 116(6) pp.1091-1116.

Manal, K., Gardinier, E., Buchanan, T.S. & Snyder-Mackler, L. (2015) *A More Informed Evaluation of Medial Compartment Loading: The Combined use of the Knee Adduction and Flexor Moments*. DOI: <https://doi.org/10.1016/j.joca.2015.02.779> .

Mantovani, G., Lamontagne, M., Varin, D., Cerulli, G.G. & Beaulé, P.E. (2011) Is principal component analysis more efficient to detect differences on biomechanical variables between groups? In: *ISBS-Conference Proceedings Archive*.

Markolf, K.L., Graff-Radford, A. & Amstutz, H. (1978) In vivo knee stability. A quantitative assessment using an instrumented clinical testing apparatus. *The Journal of Bone and Joint Surgery.American Volume*. 60(5) pp.664-674.

Mattes, S.J., Martin, P.E. & Royer, T.D. (2000) Walking symmetry and energy cost in persons with unilateral transtibial amputations: Matching prosthetic and intact limb

inertial properties. *Archives of Physical Medicine and Rehabilitation*. 81(5) pp.561-568.

McFadyen, B.J. & Winter, D.A. (1988) *An Integrated Biomechanical Analysis of Normal Stair Ascent and Descent*. DOI: [https://doi.org/10.1016/0021-9290\(88\)90282-5](https://doi.org/10.1016/0021-9290(88)90282-5) .

McGowan, C.P., Grabowski, A.M., McDermott, W.J., Herr, H.M. & Kram, R. (2012) Leg stiffness of sprinters using running-specific prostheses. *Journal of the Royal Society Interface*. 9(73) pp.1975-1982.

McMahon, T.A. & Cheng, G.C. (1990) *The Mechanics of Running: How does Stiffness Couple with Speed?* DOI: [https://doi.org/10.1016/0021-9290\(90\)90042-2](https://doi.org/10.1016/0021-9290(90)90042-2) .

Melzer, I., Yekutieli, M. & Sukenik, S. (2001) Comparative study of osteoarthritis of the contralateral knee joint of male amputees who do and do not play volleyball. *The Journal of Rheumatology*. 28(1) pp.169-172.

Mian, O.S., Thom, J.M., Narici, M.V. & Baltzopoulos, V. (2007) Kinematics of stair descent in young and older adults and the impact of exercise training. *Gait & Posture*. 25(1) pp.9-17.

Miyazaki, T., Wada, M., Kawahara, H., Sato, M., Baba, H. & Shimada, S. (2002) Dynamic load at baseline can predict radiographic disease progression in medial compartment knee osteoarthritis. *Annals of the Rheumatic Diseases*. 61(7) pp.617-622.

Morgenroth, D.C., Medverd, J.R., Seyedali, M. & Czerniecki, J.M. (2014) The relationship between knee joint loading rate during walking and degenerative changes on magnetic resonance imaging. *Clinical Biomechanics*. 29(6) pp.664-670.

Morgenroth, D.C., Segal, A.D., Zelik, K.E., Czerniecki, J.M., Klute, G.K., Adamczyk, P.G., Orendurff, M.S., Hahn, M.E., Collins, S.H. & Kuo, A.D. (2011) The effect of prosthetic foot push-off on mechanical loading associated with knee osteoarthritis in lower extremity amputees. *Gait & Posture*. 34(4) pp.502-507.

Moudy, S., Richter, C. & Strike, S. (2018) Landmark registering waveform data improves the ability to predict performance measures. *Journal of Biomechanics*. 78pp.109-117.

Mündermann, A., Dyrby, C.O., Hurwitz, D.E., Sharma, L. & Andriacchi, T.P. (2004) Potential strategies to reduce medial compartment loading in patients with knee osteoarthritis of varying severity: Reduced walking speed. *Arthritis & Rheumatism: Official Journal of the American College of Rheumatology*. 50(4) pp.1172-1178.

Mündermann, A., Dyrby, C.O. & Andriacchi, T.P. (2005) Secondary gait changes in patients with medial compartment knee osteoarthritis: Increased load at the ankle, knee, and hip during walking. *Arthritis & Rheumatology*. 52(9) pp.2835-2844.

Murphy, D.F., Connolly, D.A. & Beynon, B.D. (2003) Risk factors for lower extremity injury: A review of the literature. *British Journal of Sports Medicine*. 37(1) pp.13-29.

- Murray, A.M., Gaffney, B.M., Davidson, B.S. & Christiansen, C.L. (2017) Biomechanical compensations of the trunk and lower extremities during stepping tasks after unilateral transtibial amputation. *Clinical Biomechanics*. 49pp.64-71.
- Nematollahi, M., Razeghi, M., Mehdizadeh, S., Tabatabaee, H., Piroozi, S., Shirazi, Z.R. & Rafiee, A. (2016) Inter-segmental coordination pattern in patients with anterior cruciate ligament deficiency during a single-step descent. *PLoS One*. 11(2) pp.e0149837.
- Neptune, R., Kautz, S. & Zajac, F. (2001) Contributions of the individual ankle plantar flexors to support, forward progression and swing initiation during walking. *Journal of Biomechanics*. 34(11) pp.1387-1398.
- Nilsson, J. & Thorstensson, A. (1989) Ground reaction forces at different speeds of human walking and running. *Acta Physiologica Scandinavica*. 136(2) pp.217-227.
- Nolan, L. & Lees, A. (2000) The functional demands on the intact limb during walking for active trans-femoral and trans-tibial amputees. *Prosthetics and Orthotics International*. 24(2) pp.117-125.
- Nolan, L., Wit, A., Dudziński, K., Lees, A., Lake, M. & Wychowański, M. (2003) Adjustments in gait symmetry with walking speed in trans-femoral and trans-tibial amputees. *Gait & Posture*. 17(2) pp.142-151.
- Norcross, M.F., Blackburn, J.T., Goerger, B.M. & Padua, D.A. (2010) The association between lower extremity energy absorption and biomechanical factors related to anterior cruciate ligament injury. *Clinical Biomechanics*. 25(10) pp.1031-1036.
- Norcross, M.F., Lewek, M.D., Padua, D.A., Shultz, S.J., Weinhold, P.S. & Blackburn, J.T. (2013) Lower extremity energy absorption and biomechanics during landing, part I: Sagittal-plane energy absorption analyses. *Journal of Athletic Training*. 48(6) pp.748-756.
- Norvell, D.C., Czerniecki, J.M., Reiber, G.E., Maynard, C., Pecoraro, J.A. & Weiss, N.S. (2005) The prevalence of knee pain and symptomatic knee osteoarthritis among veteran traumatic amputees and nonamputees. *Archives of Physical Medicine and Rehabilitation*. 86(3) pp.487-493.
- Novak, A.C. & Brouwer, B. (2011) *Sagittal and Frontal Lower Limb Joint Moments during Stair Ascent and Descent in Young and Older Adults*. DOI: <https://doi.org/10.1016/j.gaitpost.2010.09.024> .
- O'Brien, R.M. (2007) A caution regarding rules of thumb for variance inflation factors. *Quality & Quantity*. 41(5) pp.673-690.
- Oberg, T., Karsznia, A. & Oberg, K. (1993) Basic gait parameters: Reference data for normal subjects, 10-79 years of age. *Journal of Rehabilitation Research and Development*. 30(2) pp.210.
- Øiestad, B.E., Engebretsen, L., Storheim, K. & Risberg, M.A. (2009) Winner of the 2008 systematic review competition: Knee osteoarthritis after anterior cruciate ligament injury. *The American Journal of Sports Medicine*. 37(7) pp.1434-1443.

Orendurff, M.S., Raschke, S.U., Winder, L., Moe, D., Boone, D.A. & Kobayashi, T. (2016) Functional level assessment of individuals with transtibial limb loss: Evaluation in the clinical setting versus objective community ambulatory activity. *Journal of Rehabilitation and Assistive Technologies Engineering*. 3pp.2055668316636316.

Orishimo, K.F., Kremenic, I.J., Pappas, E., Hagins, M. & Liederbach, M. (2009) Comparison of landing biomechanics between male and female professional dancers. *The American Journal of Sports Medicine*. 37(11) pp.2187-2193.

Ortega, D.R., Rodriguez Bies, E.C. & Berral de la Rosa, F.J. (2010) Analysis of the vertical ground reaction forces and temporal factors in the landing phase of a countermovement jump. *Journal of Sports Science & Medicine*. 9(2) pp.282-287.

Page, A. & Epifanio, I. (2007) A simple model to analyze the effectiveness of linear time normalization to reduce variability in human movement analysis. *Gait & Posture*. 25(1) pp.153-156.

Page, A., Ayala, G., León, M.T., Peydro, M.F. & Prat, J.M. (2006) *Normalizing Temporal Patterns to Analyze Sit-to-Stand Movements by using Registration of Functional Data*. DOI: <https://doi.org/10.1016/j.jbiomech.2005.07.032> .

Palmieri-Smith, R.M., Kreinbrink, J., Ashton-Miller, J.A. & Wojtys, E.M. (2007) Quadriceps inhibition induced by an experimental knee joint effusion affects knee joint mechanics during a single-legged drop landing. *The American Journal of Sports Medicine*. 35(8) pp.1269-1275.

Palmieri-Smith, R.M., Wojtys, E.M. & Ashton-Miller, J.A. (2008) Association between preparatory muscle activation and peak valgus knee angle. *Journal of Electromyography and Kinesiology*. 18(6) pp.973-979.

Pappas, E., Hagins, M., Sheikhzadeh, A., Nordin, M. & Rose, D. (2007a) Biomechanical differences between unilateral and bilateral landings from a jump: Gender differences. *Clinical Journal of Sport Medicine : Official Journal of the Canadian Academy of Sport Medicine*. 17(4) pp.263-268. DOI: 10.1097/JSM.0b013e31811f415b [doi] .

Pappas, E., Hagins, M., Sheikhzadeh, A., Nordin, M. & Rose, D. (2007b) Biomechanical differences between unilateral and bilateral landings from a jump: Gender differences. *Clinical Journal of Sport Medicine : Official Journal of the Canadian Academy of Sport Medicine*. 17(4) pp.263-268. DOI: 10.1097/JSM.0b013e31811f415b [doi] .

Paquette, M.R., Zhang, S., Milner, C.E., Fairbrother, J.T. & Reinbolt, J.A. (2014) Effects of increased step width on frontal plane knee biomechanics in healthy older adults during stair descent. *The Knee*. 21(4) pp.821-826.

Pataky, T.C. (2012) One-dimensional statistical parametric mapping in python. *Computer Methods in Biomechanics and Biomedical Engineering*. 15(3) pp.295-301.

- Pataky, T.C., Robinson, M.A. & Vanrenterghem, J. (2013) Vector field statistical analysis of kinematic and force trajectories. *Journal of Biomechanics*. 46(14) pp.2394-2401.
- Pataky, T.C., Robinson, M.A., Vanrenterghem, J., Savage, R., Bates, K.T. & Crompton, R.H. (2014) Vector field statistics for objective center-of-pressure trajectory analysis during gait, with evidence of scalar sensitivity to small coordinate system rotations. *Gait & Posture*. 40(1) pp.255-258.
- Paterno, M.V., Ford, K.R., Myer, G.D., Heyl, R. & Hewett, T.E. (2007) Limb asymmetries in landing and jumping 2 years following anterior cruciate ligament reconstruction. *Clinical Journal of Sport Medicine*. 17(4) pp.258-262.
- Paterno, M.V. & Hewett, T.E. (2008) Biomechanics of multi-ligament knee injuries (MLKI) and effects on gait. *North American Journal of Sports Physical Therapy : NAJSPT*. 3(4) pp.234-241.
- Paterno, M.V., Rauh, M.J., Schmitt, L.C., Ford, K.R. & Hewett, T.E. (2012) Incidence of contralateral and ipsilateral anterior cruciate ligament (ACL) injury after primary ACL reconstruction and return to sport. *Clinical Journal of Sport Medicine : Official Journal of the Canadian Academy of Sport Medicine*. 22(2) pp.116-121. DOI: 10.1097/JSM.0b013e318246ef9e [doi] .
- Pedrinelli, A., Saito, M., Coelho, R., Fontes, R. & Guarniero, R. (2002) Comparative study of the strength of the flexor and extensor muscles of the knee through isokinetic evaluation in normal subjects and patients subjected to trans-tibial amputation. *Prosthetics and Orthotics International*. 26(3) pp.195-205.
- Peduzzi, P., Concato, J., Kemper, E., Holford, T.R. & Feinstein, A.R. (1996) A Simulation Study of the Number of Events Per Variable in Logistic Regression Analysis. DOI: [https://doi.org/10.1016/S0895-4356\(96\)00236-3](https://doi.org/10.1016/S0895-4356(96)00236-3) .
- Petterson, S.C., Barrance, P., Buchanan, T., Binder-Macleod, S. & Snyder-Mackler, L. (2008) Mechanisms underlying quadriceps weakness in knee osteoarthritis. *Medicine and Science in Sports and Exercise*. 40(3) pp.422.
- Podraza, J.T. & White, S.C. (2010) Effect of knee flexion angle on ground reaction forces, knee moments and muscle co-contraction during an impact-like deceleration landing: Implications for the non-contact mechanism of ACL injury. *The Knee*. 17(4) pp.291-295.
- Pollard, C.D., Sigward, S.M. & Powers, C.M. (2010) Limited hip and knee flexion during landing is associated with increased frontal plane knee motion and moments. *Clinical Biomechanics*. 25(2) pp.142-146.
- Powers, C.M. (2010) The influence of abnormal hip mechanics on knee injury: A biomechanical perspective. *Journal of Orthopaedic & Sports Physical Therapy*. 40(2) pp.42-51.
- Powers, C.M., Boyd, L.A., Torburn, L. & Perry, J. (1997) Stair ambulation in persons with transtibial amputation: An analysis of the seattle LightFoot. *J Rehabil Res Dev*. 34(1) pp.9-18.

- Radin, E.L. & Paul, I.L. (1971) Response of joints to impact loading. I. in vitro wear. *Arthritis & Rheumatism*. 14(3) pp.356-362.
- Ramsay, J.O. (2006) *Functional Data Analysis*. Wiley Online Library.
- Ramsay, J.O. & Silverman, B.W. (2002) *Applied Functional Data Analysis: Methods and Case Studies*. Springer New York.
- Reeves, N.D., Spanjaard, M., Mohagheghi, A.A., Baltzopoulos, V. & Maganaris, C.N. (2008) The demands of stair descent relative to maximum capacities in elderly and young adults. *Journal of Electromyography and Kinesiology*. 18(2) pp.218-227.
- Richards, R.E., Andersen, M.S., Harlaar, J. & van den Noort, J.C. (2018) *Relationship between Knee Joint Contact Forces and External Knee Joint Moments in Patients with Medial Knee Osteoarthritis: Effects of Gait Modifications*. DOI: <https://doi.org/10.1016/j.joca.2018.04.011> .
- Richter, C. (2014a) *The Search for Performance Related Factors in Biomechanics*. Dublin City University.
- Richter, C., Marshall, B. & Moran, K. (2014b) Comparison of discrete-point vs. dimensionality-reduction techniques for describing performance-related aspects of maximal vertical jumping. *Journal of Biomechanics*. 47(12) pp.3012-3017.
- Richter, C., O'Connor, N.E., Marshall, B. & Moran, K. (2014c) Analysis of characterizing phases on waveforms: An application to vertical jumps. *Journal of Applied Biomechanics*. 30(2) pp.316-321.
- Rist, H., Praxisklinik Rennbahn, A. & Kaelin, X. (2014) Reliability and validity of two measurement systems in the quantification of jump perfor. *Schweizerische Zeitschrift Für Sportmedizin Und Sporttraumatologie*. 62(1) pp.57-63.
- Robbins, S.M.K. & Maly, M.R. (2009) *The Effect of Gait Speed on the Knee Adduction Moment Depends on Waveform Summary Measures*. DOI: <https://doi.org/10.1016/j.gaitpost.2009.08.236> .
- Robertson, G., Caldwell, G., Hamill, J., Kamen, G. & Whittlesey, S. (2013) *Research Methods in Biomechanics, 2E*. Human Kinetics.
- Robinson, M.A., Vanrenterghem, J. & Pataky, T.C. (2015) Statistical parametric mapping (SPM) for alpha-based statistical analyses of multi-muscle EMG time-series. *Journal of Electromyography and Kinesiology*. 25(1) pp.14-19.
- Roewer, B.D., Ford, K.R., Myer, G.D. & Hewett, T.E. (2014) The 'impact' of force filtering cut-off frequency on the peak knee abduction moment during landing: Artefact or 'artifiction'? *British Journal of Sports Medicine*. 48(6) pp.464-468. DOI: 10.1136/bjsports-2012-091398 [doi] .
- Rowley, K.M. & Richards, J.G. (2015) Increasing plantarflexion angle during landing reduces vertical ground reaction forces, loading rates and the hip's contribution to support moment within participants. *Journal of Sports Sciences*. 33(18) pp.1922-1931.

Royer, T. & Koenig, M. (2005) Joint loading and bone mineral density in persons with unilateral, trans-tibial amputation. *Clinical Biomechanics*. 20(10) pp.1119-1125.

Rudenko, O., Tsyuryupa, S. & Sarvazyan, A. (2016) Skeletal muscle contraction in protecting joints and bones by absorbing mechanical impacts. *Acoustical Physics*. 62(5) pp.615-625.

Rueda, F.M., Diego, I.M.A., Sánchez, A.M., Tejada, M.C., Montero, F.M.R. & Page, J.C.M. (2013) Knee and hip internal moments and upper-body kinematics in the frontal plane in unilateral transtibial amputees. *Gait & Posture*. 37(3) pp.436-439.

Rusaw, D. & Ramstrand, N. (2010) Sagittal plane position of the functional joint centre of prosthetic foot/ankle mechanisms. *Clinical Biomechanics*. 25(7) pp.713-720.

Rusaw, D. & Ramstrand, N. (2011) Motion-analysis studies of transtibial prosthesis users: A systematic review. *Prosthetics and Orthotics International*. 35(1) pp.8-19. DOI: 10.1177/0309364610393060 [doi] .

Sadeghi, H., Allard, P., Shafie, K., Mathieu, P.A., Sadeghi, S., Prince, F. & Ramsay, J. (2000) Reduction of gait data variability using curve registration. *Gait & Posture*. 12(3) pp.257-264.

Sadeghi, H., Allard, P. & Duhaime, M. (1997) Functional gait asymmetry in able-bodied subjects. *Human Movement Science*. 16(2-3) pp.243-258. DOI: [http://dx.doi.org/10.1016/S0167-9457\(96\)00054-1](http://dx.doi.org/10.1016/S0167-9457(96)00054-1) .

Sahaly, R., Vandewalle, H., Driss, T. & Monod, H. (2001) Maximal voluntary force and rate of force development in humans - importance of instruction. 85(1) pp.345-350.

Sanderson, D.J. & Martin, P.E. (1997) Lower extremity kinematic and kinetic adaptations in unilateral below-knee amputees during walking. *Gait & Posture*. 6(2) pp.126-136. DOI: [http://dx.doi.org/10.1016/S0966-6362\(97\)01112-0](http://dx.doi.org/10.1016/S0966-6362(97)01112-0) .

Sanderson, D.J. & Martin, P.E. (1996) Joint kinetics in unilateral below-knee amputee patients during running. *Archives of Physical Medicine and Rehabilitation*. 77(12) pp.1279-1285. DOI: [http://dx.doi.org/10.1016/S0003-9993\(96\)90193-8](http://dx.doi.org/10.1016/S0003-9993(96)90193-8) .

Saunders, J.B., Inman, V.T. & Eberhart, H.D. (1953) The major determinants in normal and pathological gait. *The Journal of Bone and Joint Surgery.American Volume*. 35-A(3) pp.543-558.

Schmalz, T., Blumentritt, S. & Marx, B. (2007) Biomechanical analysis of stair ambulation in lower limb amputees. *Gait & Posture*. 25(2) pp.267-278.

Schmitt, L.C., Paterno, M.V., Ford, K.R., Myer, G.D. & Hewett, T.E. (2015) Strength asymmetry and landing mechanics at return to sport after anterior cruciate ligament reconstruction. *Medicine and Science in Sports and Exercise*. 47(7) pp.1426-1434. DOI: 10.1249/MSS.0000000000000560 [doi] .

Schmitz, A. & Noehren, B. (2014) What predicts the first peak of the knee adduction moment? *The Knee*. 21(6) pp.1077-1083.

- Schoeman, M., Diss, C.E. & Strike, S.C. (2013) Asymmetrical loading demands associated with vertical jump landings in people with unilateral transtibial amputation. *Journal of Rehabilitation Research & Development*. 50(10) .
- Schöllhorn, W.I., Nigg, B.M., Stefanyshyn, D.J. & Liu, W. (2002) Identification of individual walking patterns using time discrete and time continuous data sets. *Gait & Posture*. 15(2) pp.180-186. DOI: [http://dx.doi.org/10.1016/S0966-6362\(01\)00193-X](http://dx.doi.org/10.1016/S0966-6362(01)00193-X) .
- Seegmiller, J.G. & McCaw, S.T. (2003) Ground reaction forces among gymnasts and recreational athletes in drop landings. *Journal of Athletic Training*. 38(4) pp.311-314.
- Segal, N.A. & Glass, N.A. (2011) Is quadriceps muscle weakness a risk factor for incident or progressive knee osteoarthritis? *The Physician and Sportsmedicine*. 39(4) pp.44-50.
- Selfe, J., Richards, J., Thewlis, D. & Kilmurray, S. (2008) *The Biomechanics of Step Descent Under Different Treatment Modalities used in Patellofemoral Pain*. DOI: <https://doi.org/10.1016/j.gaitpost.2007.03.017> .
- Sharma, L., Song, J., Hayes, K., Pai, Y. & Dunlop, D. (2003) Physical functioning over three years in knee osteoarthritis: Role of psychosocial, local mechanical, and neuromuscular factors. *Arthritis & Rheumatism*. 48(12) pp.3359-3370.
- Shelburne, K.B., Torry, M.R. & Pandy, M.G. (2006) Contributions of muscles, ligaments, and the ground-reaction force to tibiofemoral joint loading during normal gait. *Journal of Orthopaedic Research*. 24(10) pp.1983-1990.
- Sigward, S.M., Ota, S. & Powers, C.M. (2008) Predictors of frontal plane knee excursion during a drop land in young female soccer players. *Journal of Orthopaedic & Sports Physical Therapy*. 38(11) pp.661-667.
- Sigward, S.M. & Powers, C.M. (2007) *Loading Characteristics of Females Exhibiting Excessive Valgus Moments during Cutting*. DOI: <https://doi.org/10.1016/j.clinbiomech.2007.04.003> .
- Silverman, A.K., Fey, N.P., Portillo, A., Walden, J.G., Bosker, G. & Neptune, R.R. (2008) Compensatory mechanisms in below-knee amputee gait in response to increasing steady-state walking speeds. *Gait & Posture*. 28(4) pp.602-609.
- Silverman, A.K. & Neptune, R.R. (2014) Three-dimensional knee joint contact forces during walking in unilateral transtibial amputees. *Journal of Biomechanics*. 47(11) pp.2556-2562.
- Silverman, A.K., Neptune, R.R., Sinitski, E.H. & Wilken, J.M. (2014) *Whole-Body Angular Momentum during Stair Ascent and Descent*. DOI: <https://doi.org/10.1016/j.gaitpost.2014.01.025> .
- Simic, M., Hunt, M.A., Bennell, K.L., Hinman, R.S. & Wrigley, T.V. (2012) Trunk lean gait modification and knee joint load in people with medial knee osteoarthritis: The effect of varying trunk lean angles. *Arthritis Care & Research*. 64(10) pp.1545-1553.

- Simpson, K. & Jiang, P. (1999) Foot landing position during gait influences ground reaction forces. *Clinical Biomechanics*. 14(6) pp.396-402.
- Sinclair, J., Taylor, P.J., Greenhalgh, A., Edmundson, C.J., Brooks, D. & Hobbs, S.J. (2012) The test-retest reliability of anatomical co-ordinate axes definition for the quantification of lower extremity kinematics during running. *Journal of Human Kinetics*. 35(1) pp.15-25.
- Slemenda, C., Brandt, K.D., Heilman, D.K., Mazzuca, S., Braunstein, E.M., Katz, B.P. & Wolinsky, F.D. (1997) Quadriceps weakness and osteoarthritis of the knee. *Annals of Internal Medicine*. 127(2) pp.97-104.
- Spanjaard, M., Reeves, N.D., van Dieën, J.H., Baltzopoulos, V. & Maganaris, C.N. (2009) *Influence of Gait Velocity on Gastrocnemius Muscle Fascicle Behaviour during Stair Negotiation*. DOI: <https://doi.org/10.1016/j.jelekin.2007.07.006> .
- Sparrow, W., Donovan, E., Van Emmerik, R. & Barry, E. (1987) Using relative motion plots to measure changes in intra-limb and inter-limb coordination. *Journal of Motor Behavior*. 19(1) pp.115-129.
- Stergiou, N., Ristanis, S., Moraiti, C. & Georgoulis, A.D. (2007) Tibial rotation in anterior cruciate ligament (ACL)-deficient and ACL-reconstructed knees. *Sports Medicine*. 37(7) pp.601-613.
- Strike, S.C., Arcone, D. & Orendurff, M. (2018) *Running at Submaximal Speeds, the Role of the Intact and Prosthetic Limbs for Trans-Tibial Amputees*. DOI: <https://doi.org/10.1016/j.gaitpost.2018.03.030> .
- Struyf, P.A., van Heugten, C.M., Hitters, M.W. & Smeets, R.J. (2009) The prevalence of osteoarthritis of the intact hip and knee among traumatic leg amputees. *Archives of Physical Medicine and Rehabilitation*. 90(3) pp.440-446.
- Taylor, W.R., Kornaropoulos, E.I., Duda, G.N., Kratzstein, S., Ehrig, R.M., Arampatzis, A. & Heller, M.O. (2010) Repeatability and reproducibility of OSSCA, a functional approach for assessing the kinematics of the lower limb. *Gait & Posture*. 32(2) pp.231-236. DOI: <http://dx.doi.org/10.1016/j.gaitpost.2010.05.005> .
- Telfer, S., Lange, M.J. & Sudduth, A.S. (2017) Factors influencing knee adduction moment measurement: A systematic review and meta-regression analysis. *Gait & Posture*. 58pp.333-339.
- Tepavac, D. & Field-Fote, E.C. (2001) Vector coding: A technique for quantification of intersegmental coupling in multicyclic behaviors. *Journal of Applied Biomechanics*. 17(3) pp.259-270.
- Thorp, L.E., Sumner, D.R., Block, J.A., Moio, K.C., Shott, S. & Wimmer, M.A. (2006) Knee joint loading differs in individuals with mild compared with moderate medial knee osteoarthritis. *Arthritis & Rheumatism*. 54(12) pp.3842-3849.
- Tillin, N.A., Pain, M.T.G. & Folland, J. (2013) Explosive force production during isometric squats correlates with athletic performance in rugby union players. *Journal of Sports Sciences*. 31(1) pp.66-76.

Tsai, L., Ko, Y., Hammond, K.E., Xerogeanes, J.W., Warren, G.L. & Powers, C.M. (2017) Increasing hip and knee flexion during a drop-jump task reduces tibiofemoral shear and compressive forces: Implications for ACL injury prevention training. *Journal of Sports Sciences*. 35(24) pp.2405-2411.

Tsushima, H., Morris, M. & McGinley, J. (2003) Test-retest reliability and inter-tester reliability of kinematic data from a three-dimensional gait analysis system. *Journal of Japan Physical Therapy Association*. 6(1) pp.9-17.

van Dieën, J.H. & Pijnappels, M. (2009) *Effects of Conflicting Constraints and Age on Strategy Choice in Stepping Down during Gait*. DOI: <https://doi.org/10.1016/j.gaitpost.2008.08.010> .

van Dieën, J.H., Spanjaard, M., Konemann, R., Bron, L. & Pijnappels, M. (2007) *Balance Control in Stepping Down Expected and Unexpected Level Changes*. DOI: <https://doi.org/10.1016/j.jbiomech.2007.06.009> .

van Dieën, J.H., Spanjaard, M., Könemann, R., Bron, L. & Pijnappels, M. (2008) *Mechanics of Toe and Heel Landing in Stepping Down in Ongoing Gait*. DOI: <https://doi.org/10.1016/j.jbiomech.2008.05.022> .

van Emmerik, R.E., Ducharme, S.W., Amado, A.C. & Hamill, J. (2016) Comparing dynamical systems concepts and techniques for biomechanical analysis. *Journal of Sport and Health Science*. 5(1) pp.3-13.

Vanderpool, M.T., Collins, S.H. & Kuo, A.D. (2008) Ankle fixation need not increase the energetic cost of human walking. *Gait & Posture*. 28(3) pp.427-433.

Vanwanseele, B., Eckstein, F., Smith, R.M., Lange, A.K., Foroughi, N., Baker, M.K., Shnier, R. & Fiatarone Singh, M.A. (2010) *The Relationship between Knee Adduction Moment and Cartilage and Meniscus Morphology in Women with Osteoarthritis*. DOI: <http://dx.doi.org/10.1016/j.joca.2010.04.006> .

Ventura, J.D., Klute, G.K. & Neptune, R.R. (2011) The effects of prosthetic ankle dorsiflexion and energy return on below-knee amputee leg loading. *Clinical Biomechanics*. 26(3) pp.298-303.

Walter, J.P., D'lima, D.D., Colwell Jr, C.W. & Fregly, B.J. (2010) Decreased knee adduction moment does not guarantee decreased medial contact force during gait. *Journal of Orthopaedic Research*. 28(10) pp.1348-1354.

Ward, S.H., Blackburn, J.T., Padua, D.A., Stanley, L.E., Harkey, M.S., Luc-Harkey, B.A. & Pietrosimone, B. (2018) Quadriceps neuromuscular function and jump-landing sagittal-plane knee biomechanics after anterior cruciate ligament reconstruction. *Journal of Athletic Training*. 53(2) pp.135-143.

Warmenhoven, J., Harrison, A., Robinson, M.A., Vanrenterghem, J., Bargary, N., Smith, R., Cobley, S., Draper, C., Donnelly, C. & Pataky, T. (2018) A force profile analysis comparison between functional data analysis, statistical parametric mapping and statistical non-parametric mapping in on-water single sculling. *Journal of Science and Medicine in Sport*. 21(10) pp.1100-1105. DOI: S1440-2440(18)30091-4 [pii] .

- Wiggins, A.J., Grandhi, R.K., Schneider, D.K., Stanfield, D., Webster, K.E. & Myer, G.D. (2016) Risk of secondary injury in younger athletes after anterior cruciate ligament reconstruction: A systematic review and meta-analysis. *The American Journal of Sports Medicine*. 44(7) pp.1861-1876.
- Winter, D. (2009) *Biomechanics and Motor Control of Human Movement*. John Wiley & Sons.
- Winter, D. & Sienko, S. (1988) Biomechanics of below-knee amputee gait. *Journal of Biomechanics*. 21(5) pp.361-367.
- Winter, D.A. (1983) Energy generation and absorption at the ankle and knee during fast, natural, and slow cadences. *Clinical Orthopaedics and Related Research*. (175)(175) pp.147-154.
- Winters, J.D. & Rudolph, K.S. (2014) Quadriceps rate of force development affects gait and function in people with knee osteoarthritis. *European Journal of Applied Physiology*. 114(2) pp.273-284.
- Wold, S., Esbensen, K. & Geladi, P. (1987) Principal component analysis. *Chemometrics and Intelligent Laboratory Systems*. 2(1-3) pp.37-52.
- Wong, A.Y., Sangeux, M. & Baker, R. (2010) Calculation of joint moments following foot contact across two force plates. *Gait & Posture*. 31(2) pp.292-293.
- Worsley, K.J., Taylor, J.E., Tomaiuolo, F. & Lerch, J. (2004) *Unified Univariate and Multivariate Random Field Theory*. DOI: <https://doi.org/10.1016/j.neuroimage.2004.07.026> .
- Yasuda, T., Yokoi, Y., Oyanagi, K. & Hamamoto, K. (2016) Hip rotation as a risk factor of anterior cruciate ligament injury in female athletes. *The Journal of Physical Fitness and Sports Medicine*. 5(1) pp.105-113.
- Yeow, C.H., Lee, P.V. & Goh, J.C. (2009a) Effect of landing height on frontal plane kinematics, kinetics and energy dissipation at lower extremity joints. *Journal of Biomechanics*. 42(12) pp.1967-1973. DOI: 10.1016/j.jbiomech.2009.05.017 [doi] .
- Yeow, C.H., Lee, P.V.S. & Goh, J.C.H. (2010) *Sagittal Knee Joint Kinematics and Energetics in Response to Different Landing Heights and Techniques*. DOI: <https://doi.org/10.1016/j.knee.2009.07.015> .
- Yeow, C.H., Lee, P.V.S. & Goh, J.C.H. (2009b) *Regression Relationships of Landing Height with Ground Reaction Forces, Knee Flexion Angles, Angular Velocities and Joint Powers during Double-Leg Landing*. DOI: <https://doi.org/10.1016/j.knee.2009.02.002> .
- Yu, B., Gabriel, D., Noble, L. & An, K. (1999) Estimate of the optimum cutoff frequency for the butterworth low-pass digital filter. *Journal of Applied Biomechanics*. 15pp.318-329.
- Zachazewski, J.E., Riley, P.O. & Krebs, D.E. (1993) Biomechanical analysis of body mass transfer during stair ascent and descent of healthy subjects. *Journal of Rehabilitation Research and Development*. 30pp.412-412.

Zajac, F.E., Neptune, R.R. & Kautz, S.A. (2002) *Biomechanics and Muscle Coordination of Human Walking: Part I: Introduction to Concepts, Power Transfer, Dynamics and Simulations*. DOI: [https://doi.org/10.1016/S0966-6362\(02\)00068-1](https://doi.org/10.1016/S0966-6362(02)00068-1) .

Zhang, S., Bates, B.T. & Dufek, J.S. (2000) Contributions of lower extremity joints to energy dissipation during landings. *Medicine and Science in Sports and Exercise*. 32(4) pp.812-819.

Zhao, D., Banks, S.A., Mitchell, K.H., D'Lima, D.D., Colwell Jr, C.W. & Fregly, B.J. (2007) Correlation between the knee adduction torque and medial contact force for a variety of gait patterns. *Journal of Orthopaedic Research*. 25(6) pp.789-797.